UNIVERSITY OF LIVERPOOL

INVESTIGATIONS INTO THE FUNCTIONS AND REGULATION OF THE MICROCEPHALY-ASSOCIATED *TRAPPC9* GENE.

Thesis written in accordance with the requirements of the University of Liverpool for the degree of Doctor in Philosophy

By

Michela Pulix

April 2017

DECLARATION

I hereby declare that except where specific reference is made to the work of others, the contents of this thesis are original and have not been submitted in whole or in part for consideration for any other degree or qualification in this or any other university. This dissertation is my own work and contains nothing which is the outcome of work done in collaboration with others except as specified in the text. This dissertation contains fewer than 65,000 words including bibliography, footnotes, tables and equations and has fewer than 70 figures.

Michela Pulix
April 2017

Abstract

Trafficking Protein Particle Complex 9 (Trappc9) belongs to the TRAPPII multiprotein complex involved in vesicular trafficking and tethering.

Loss-of-function mutations in the sequence of *TRAPPC9* have been shown to cause autosomal recessive non-syndromic intellectual disability. Characteristic symptoms among the affected individuals are dysmorphic facial features, speech delay and inability to feed themselves. Postnatal microcephaly is accompanied by agenesis of the corpus callosum, white matter abnormalities and reduced cerebellar volume.

It has been shown that Trappc9 promotes the activation of the NF-κB pathway and the NGF-induced neurite outgrowth in PC12 cells. Furthermore, it has been shown to interact with $p150^{glued}$ (subunit of dynactin) and its depletion causes the accumulation of aberrantly large lipid droplets.

Furthermore, this gene is located in the imprinted *Peg13*/*Kcnk9* gene cluster. Genomic imprinting regulates gene expression in a parent-of-origin specific manner through epigenetic mechanisms, thus resulting in preferential transcription from either the maternal or paternal allele. Conflicting reports have been published on the imprinting status of *Trappc9*.

This thesis investigates a number of aspects on the genetic regulation and cellular functions of Trappc9. It also provides a first characterisation of a novel knockout (KO) mouse model for Trappc9.

Chapter 3 describes the genetic structure and regulation of murine *Trappc9*. I demonstrated that only one transcript variant, with an alternatively spliced exon, is

produced from this gene in contrast to the information available on genomic databases. I also confirmed the imprinted expression of *Trappc9* in the mouse brain, where it shows a 70% preferential expression from the maternal allele, while a biallelic expression was found in peripheral tissues. Using a range of techniques, I also demonstrated a gradient of methylation within a CpG island located in the promoter region of murine *Trappc9*, which appears to be unrelated to the regulation of imprinting.

Chapter 4 is focussed on the molecular and cellular functions of Trappc9. As this protein has previously been linked with the NF-κB pathway and NGF-induced neurite outgrowth in PC12 cells, I tried to replicate some of the results found in the literature. Using siRNA gene silencing I created a transient knockdown for Trappc9 in PC12 cells. Unfortunately, as the differentiation of these cells reaches optimal results in 9 days, the design of the assay was not optimal to study the effect of neurite outgrowth in this cell line.

As an alternative to studying the role of Trappc9 in neurite elongation, I created a stable N2A knockdown cell line via shRNA lentivirus transduction, with 50-60% reduction of Trappc9 expression. N2A cells do not respond to NGF but differentiate in the presence of retinoic acid. Under such conditions I found that Trappc9-depleted cells tend to differentiate into cells with a reduced number of neurites, suggesting defects in neuronal differentiation might be the basis of *TRAPPC9*-induced microcephaly.

Chapter 5 describes the analysis of a novel Trappc9 KO mouse model. These mice carry a knock-in gene trap, containing a *LacZ* reporter gene, within an intron of *Trappc9* that causes a frameshift and premature interruption of transcription. Although the *LacZ* is not translated into a functional β-Galactosidase due to unexpected splicing events, I have confirmed that these mice have lost Trappc9 protein expression and found that they develop a mild microcephaly phenotype at 12 weeks of age. I also found an increase in body weight in female mice, similarly to what has been found in two human patients with

mutations in *TRAPPC9*. Immunohistochemical analysis of brain sections revealed KO mice possess a reduced number of cells positive for the progenitor cell marker Sox-2 in the dentate gyrus of the hippocampus. Preliminary results also highlighted a reduction in cells positive for the astrocyte marker GFAP in the corpus callosum and hypothalamus.

Finally, chapter 6 focuses on human *TRAPPC9*. I identified Variable Number Tandem Repeat (VNTR) polymorphisms within the promoter region of *TRAPPC9*, which appears to be an important regulatory region as it is a predicted G-quadruplex and is rich in CTCF binding sites. The three observed variants possess the ability to induce gene expression in a luciferase reporter gene assay in SH-SY5Y neuroblastoma cells but not in kidney-derived HEK293 cells, suggesting a cell specific function of these VNTRs.

In conclusion, Trappc9 is required for normal brain function in mice and the KO mouse model can be used to investigate the underlying molecular and cellular mechanisms relevant for the associated human neurodevelopmental disorder. Further investigations of this gene and its role in development will be beneficial in order to understand the mechanisms of microcephaly and intellectual disability.

Table of Contents

List of Figures

List of Tables

List of Abbreviations

Ago2	Argonaute 2
ASPM	Abnormal spindle microtubule assembly
CDK5RAP2	CDK5 Regulatory Subunit Associated Protein 2
CDKL5	Cyclin-dependent kinase-like 5
CEP152	Centrosomal Protein Of 152 kDa
CGI	CpG island
Chrac1	Chromatin Accessibility Complex 1
CRABPs	Retinoic Acid-Binding Proteins
CTCF	CCCTC-binding factor
D4	Dopamine receptor 4
Dlk1	Delta-like homologue 1
DMR	Differentially Methylated Region
DNMT	DNA Methyltransferase
DPPA3	Developmental Pluripotency-Associated Protein 3
EMFI	Embryonic fibroblasts
ENC	Enteric Neuronal Cell line
ENCODE	Encyclopaedia of DNA elements
ER	Endoplasmic reticulum
EUCOMM	European Conditional Mouse Mutagenesis Program
FMR1	Fragile X Mental Retardation 1
FOXG1	Forkhead box protein G1

G4	G-quadruplex
GEF	Guanine Exchange Factor
GFAP	Glial Fibrillary Acidic Protein
ICR	Imprinting Control Region
Igf2	Insulin-like Growth Factor 2
Igf2r	Insulin-like Growth Factor 2 Receptor
IKK	IκB kinase
IMPC	International Mouse Phenotyping Consortium
IκB	Inhibitor κB
KCNK9	Potassium Channel Subfamily K member 9
KD	Knockdown
KO	Knockout
LD	Lipid Droplets
MAOA	Monoamine Oxidase A
MCPH1	Microcephalin 1
MECP2	Methyl CpG Binding Protein 2
MTOC	Microtubule Organizing Centre
N2A	Neuro-2A
ncRNA	Non-coding RNA
NGF	Nerve Growth Factor
NIBP	NIK and IKKβ-Binding Protein
NIK	NF-κB Inducing Kinase
PCR	Polymerase Chain Reaction
PEG13	Paternally Expressed Gene 13
RA	Retinoic Acid

RAR	Retinoic Acid Receptor
RHR	Rel Homology Region
RISC	RNA-induced silencing complex
RNApol II	RNA polymerase II
shRNA	short-hairpin RNA
siRNA	small interference RNA
snoRNAs	small nucleolar RNAs
SNRPN	small nuclear ribonucleoprotein-associated protein N
TAD	Transactivation Domain
TASK3	TWIK-related acid-sensitive K1 channel 3
TNFR	TNF receptor 1
TNFα	Tumour Necrosis Factor α
TRAPP	Trafficking Protein Particle
Trappc9	Trafficking Protein Particle Complex 9
Ube3a	Ubiquitin-protein ligase E3A
UTR	Untranslated Region
VNTR	Variable Number Tandem Repeats
WT	Wild Type
Zfp57	Zinc finger protein homolog 57

CHAPTER 1

Introduction

1.1 Epigenetics

1.1.1 Definition and mechanisms

The term 'epigenetics' (from the Greek prefix *epi-* over, on top of) was coined in 1942 by C. H. Waddington to refer to a conceptual model of how genes interact with the environment to produce a phenotype (Waddington, 2014). Over the years, the definition has changed and it has been adapted to numerous concepts and fields, among which are biological development, embryology and developmental psychology. It was not until 2009, however, that the consensus definition of "stably heritable phenotype resulting from changes in a chromosome without alterations in the DNA sequence" was coined (Berger et al., 2009).

Epigenetics refers thus to the activation or repression of gene transcription due to changes in the microstructure of DNA or the associated chromatin proteins.

This regulation of transcription is vital for correct functioning of differentiated cells in order to express only genes necessary for their activity. Furthermore, DNA methylation takes part in disease susceptibility, responses to environmental stimuli and the biodiversity of natural populations (Elhamamsy, 2016).

Specific epigenetic processes include X-chromosome inactivation, genomic imprinting, gene silencing and maternal effects.

The main two mechanisms are covalent modifications of DNA and of histones. The methylation or hydroxylmethylation of cytosines occurs mostly at cytosine-guanine (CG)

sites located in structures called CpG islands, fragments longer than 500 bp so-called because they are rich in CG sites (above 55%) (Takai and Jones, 2002). CpG islands are scattered across the entire genome and are considered to be (or located in proximity of) important regulatory regions, such as promoters. DNA methyltransferases (DNMTs) are responsible for the methylation of DNA by recognising the hemimethylated sequence of DNA and methylating the other half (DNMT1) or by establishing *de novo* methylation in sites that have no marks (DNMT3a,b) (Elhamamsy, 2016).

Histone modifications, instead, occur throughout the entire genome, usually in the unstructured N-terminus called 'histone tail', in the form of post-translational modifications. Lysine acetylation, lysine and arginine methylation, serine and threonine phosphorylation, lysine ubiquitination and sumoylation are among the main histone modifications responsible for the rearrangement of chromatin structure around histones and thus for regulation of gene expression. The negative or positive charge of the amino acids bound to the histones can in fact loosen or tighten the folding of DNA around these structures, thus promoting or restricting the access to RNA polymerase II (RNApol II) and transcription factors to certain sequences (Choudhary et al., 2009).

DNA methylation is usually associated with repression of transcription, while histone acetylation usually leads to activation of transcription. This view, however, is quite simplified as the activation of a particular gene, as we will see in detail in the following sections, can often lead to the inactivation of another and vice versa.

1.1.2 Chromatin structure and epigenetic indicators of chromatin state

Within the nucleus the DNA is tightly packed with protein complexes to form the chromatin, whose primary functions are not only to package DNA to a more compact shape for storage or to facilitate mitosis, but also to prevent DNA damage and to regulate gene expression. The term 'heterochromatin' refers to a more compact DNA conformation which

is usually transcriptionally inactive, while 'euchromatin' refers to a more loose conformation that allows the interaction between DNA and transcription and replication machinery.

Nucleosomes are the main repeat element of chromatin and consist of ~150 bp of DNA wrapped around a histone octamer, consisting of two copies of the core histones H2A, H2B, H3 and H4 (Luger et al., 2012). Nucleosomes are usually connected to one another by fragments of linker DNA of 50-100 bp in length which bind the linker histone H1, responsible for the exit/entry of the DNA strand on the nucleosome (Woodcock et al., 2006). The nucleosome core particle, together with histone H1, is known as a chromatosome (Fig 1.1).

Nucleosome positioning and the associated epigenetic modifications are thought to play a role in development, transcriptional regulation, evolution, human diseases and disorders (Yazdi et al. 2015).

It has been shown that histone modifications may serve as docking sites for effectors that regulate chromatin structure and transcription (Zhai et al., 2009).

Among the numerous histone modifications that occur to regulate DNA accessibility, acetylation and methylation on specific lysine residues are particularly important for epigenetic gene regulation. Lysine methylation occurs by replacing hydrogen on the primary amine at three different levels: monomethylation (me1), dimethylation (me2) and trimethylation (me3).

While different levels of methylation on the same residue can affect transcription differently, acetylation is always correlated with transcriptional activation being localised to transcription start sites and/or enhancers of actively transcribed genes (Kimura, 2013).

The marker H3K4me3 is associated with actively transcribed genes, usually enriched around transcriptional start sites and for this reason it is considered a marker for

promoters. It is usually followed by HeK4me2 and by H3K4me1 located downstream of H3K4me2 (Barski et al., 2007; Guenther et al., 2007; ENCODE Project Consortium et al., 2012). It has been shown that methylated H3K4 can directly recruit the transcription complex and that acetylation can be added preferentially to H3K4me3 (Vermeulen et al., 2007; Bian et al., 2011).

The transcriptionally inactive or active chromatin state can therefore be robustly maintained through different histone modifications and DNA methylation.

H3K4me1 and H3K27ac are generally markers for active enhancers (Heintzman et al., 2007; Creyghton et al., 2010; Rada-Iglesias et al., 2011). However, they can also be associated with regions downstream or around actively transcribed genes (Spicuglia and Vanhille, 2012).

Heterochromatin is usually associated with H3K9me3 (Grewal and Jia, 2007; Bannister and Kouzarides, 2011; Probst and Almouzni, 2011), which is particularly enriched in pericentromeric heterochromatin and major satellite repeats (Almouzni and Probst, 2011). Another marker for silent chromatin is H3K27me3, which is generally localised to gene-rich regions with low DNA methylation. The distribution of H3K9me3 and H3K27me3 is mutually exclusive, as they do not exist in the same gene loci (Nestorov et al., 2013).

1.1.3 Variable Tandem Number Repeats (VNTRs) and associated disorders

Variable Number Tandem Repeats (VNTRs) consist of several repetitions of DNA sequence motifs inherited in a Mendelian fashion. These sequences are usually CG-rich and the number of repetitions for a particular VNTR varies between individuals. The term VNTR covers both micro- and minisatellites, which correspond to motifs of 1-6 bp and 6-500 bp, respectively.

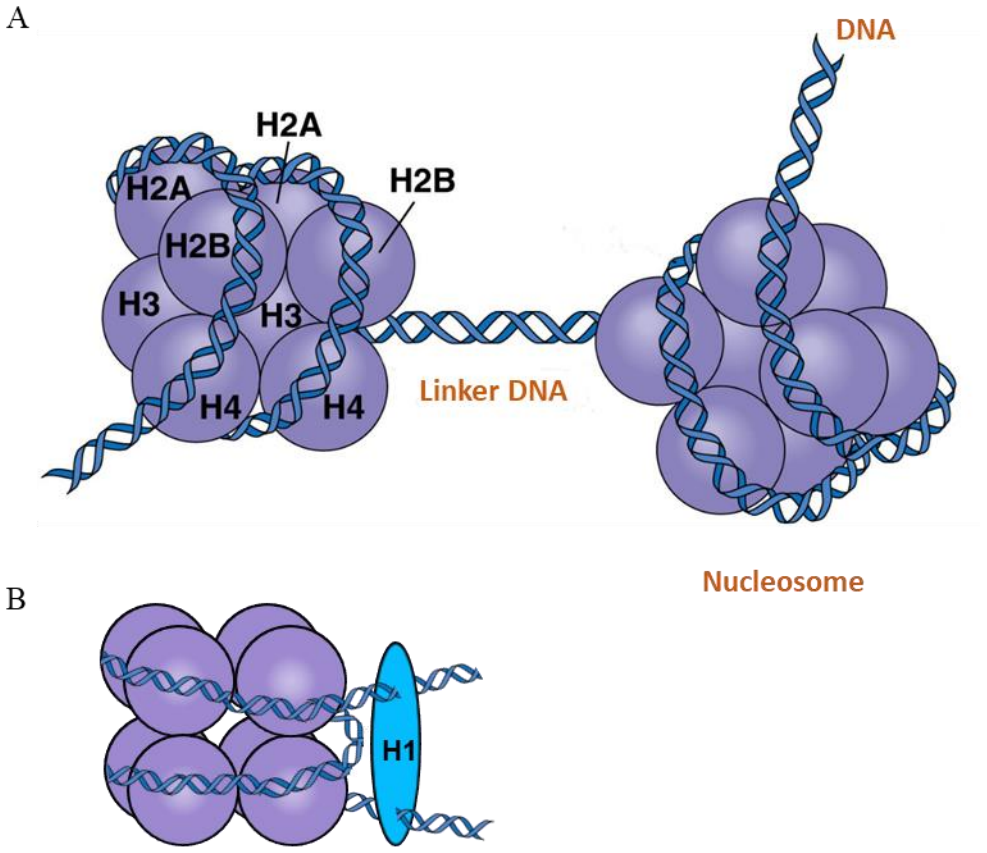

Figure 1. 1

Structure of nucleosomes. **A)** A DNA segment of around 150 bp is wrapped around a histone octamer, consisting of two copies of the core histones H2A, H2B, H3 and H4. **B)** Nucleosomes are usually connected by a fragment of linker DNA bound to histone H1. Adapted from Kim, 2014.

It has been hypothesised that VNTRs originated from slippages during DNA replication or as a consequence of unequal crossing-over, and the number of repetitions would have increased/decreased due to the repetitive nature of these sequences (Schlötterer, 2004). These sequences, estimated to be 3% of the genome are frequently found in promoters and coding regions (Lander et al., 2001; Fondon et al., 2008), have been shown to affect gene expression, transcript splicing and gene recombination (Contente et al. 2002; Lian & Garner 2005; Harding et al. 1992). For their role in multiple processes, they have also been

associated with a number of diseases and disorders, where they contribute to the aetiology, severity and progression of such conditions.

The VNTRs that lie within coding regions directly affect the protein product and therefore its functionality. Huntington's disease, for example, is caused by an increased number of repetitions of a VNTR located within an exon that leads to the misfolding and/or abnormal cleavage of huntingtin (Gusella and MacDonald, 2006).

Another example of a VNTR in coding regions is the *dopamine receptor 4*, whose third exon contains 2-11 repeats of a 48 bp unit (Ding et al., 2002). The polymorphism affects the third cytoplasmic loop of the receptor, with every repeat contributing 16 additional amino acids. In the presence of the receptor antagonist clozapine, the binding affinity is not affected by the polymorphism, but it is affected in certain conditions. In fact, in the presence of clozapine and sodium chloride, the 2- and 4-repeat alleles induced a higher binding affinity than the 7-repeats allele (Brookes, 2013).

The VNTRs located in regulatory regions such as promoters, instead, are often associated with different degrees of expression of the associated genes due to their potential to affect the binding of the transcriptional machinery. It has been shown that these repetitions present an array of recognition sequences to several proteins interacting with the DNA, among which transcription factors. Multiple binding sites have a stronger likelihood of binding a transcription factor (or multiple factors) than a single binding site (Kolesov et al., 2007). Moreover, it has also been shown that after a transcription factor dissociates from its binding site, it first slides an average of 660 bp, scanning for further binding sites before leaving the DNA strand (Kolesov et al., 2007). In this case, multiple repetitions of a binding site would prolong the permanence of the factor within the region.

A classic example of a VNTR in the promoter region can be found in the *monoamine oxidase A* (*MAOA*) gene. This gene encodes for an enzyme responsible for the turnover of serotonin,

dopamine and noradrenaline and contains two distinct VNTRs in its promoter, named 'proximal' and 'distal'. The proximal VNTR is the most studied and consists of a 30 bp motif that can be repeated 2, 3, 3.5, 4 and 5 times. The 2-, 3- and 5-repetitions have been shown to induce a low expression of the gene, while the 3.5 and 4-repetition variants have been shown to induce a high expression (Sabol et al., 1998). This VNTR has been associated with bipolar disorder, impulsivity, antisocial behaviour and panic disorder (Lim et al., 1995; Deckert et al., 1999; Samochowiec et al., 1999; Huang et al., 2004).

Interestingly, protein extractions of post-mortem brains of Alzheimer's patients with 3.5- and 4-repetition alleles showed higher levels of gene expression, while this was not the case in a control population (Wu et al., 2007). Thus, it is possible that VNTR polymorphisms may act differently in diseased and healthy tissues.

1.1.4 DNA secondary structures

DNA can adopt several conformations, in addition to the well-known double helical structure of the B-form, based on particular sequence motifs and interactions with various proteins. These alternative secondary structures, originally observed *in vitro*, have been hypothesised (and in some cases confirmed) to have functional roles *in vivo*. Non-B forms include Z-DNA, cruciform structures and G-quadruplex (G4).

Z-DNA is a left-handed helix caused by tracts of alternating purines and pyrimidines that occur once every 3000 bp in metazoans (Khuu et al., 2007) (Fig 1.2). It is stabilised by negative supercoiling and it has been hypothesised to relieve transcriptional torsional stress (Ha et al., 2005).

Cruciform structures are also stabilised by negative supercoiling and are due to a six-nucleotide inverted repeat motif that forms a four-armed shape near replication origins, breakpoint junctions and promoters (Fig 1.2). Their functional role is still unclear, but they

might be involved in chromosomal rearrangements and in stabilisation of the Y chromosome (van Holde and Zlatanova, 1994; Pearson et al., 1996; Bochman et al., 2012).

G4 structures can form within specific G-rich DNA or RNA sequences and they can adopt a variety of topologies depending on the orientation of the DNA strand, forming within one (intramolecular) or multiple (intermolecular) strands (Fig 1.3) (Bochman et al. 2012).

Intramolecular G4 structures form in specific regions that contain at least four runs of a consensus motif ($G\geq3N_{1\text{-}7}G\geq3N_{1\text{-}7}G\geq3N_{1\text{-}7}G\geq3$) arranged within two or more planar quartets, further stabilised by monovalent cations (Davis, 2004). They tend to cluster in promoters, micro- and minisatellites, near transcription factor binding sites and telomeres (Bochman et al. 2012). In humans, G4 motifs are less often found in the non-template strand, while when in the template strand they tend to cluster at the 5′ end of the 5′-UTR (Huppert et al., 2008). The function of these structures is still largely unknown but it is dependent on the location of the G4. In telomeres, it has been shown that intramolecular antiparallel G4 structures block the activity of telomerase, while intramolecular parallel G4s are instead permissive for extension by telomerase (Zahler et al., 1991; Oganesian et al., 2007).

Regarding the presence of G4 near promoter regions, instead, these structures are thought to form as a result of supercoiling-induced stress during transcription (Sun and Hurley, 2009). Furthermore, it has been hypothesised that, depending on which DNA strand encodes the G4 motif, these structures could either inhibit transcription (e.g. by blocking the transcription machinery) or enhance it (e.g. by maintaining the transcribed strand in a single-strand conformation) (Fig 1.3).

A number of G4 targeting ligands have been found to alter the expression of genes containing G4 motifs in their promoters, such as *MYC* and *KRAS* (Siddiqui-Jain et al., 2002;

Cogoi and Xodo, 2006). In addition, transcriptional enhancers or repressors bound to G4s can also affect transcription (Bochman et al. 2012).

Interestingly, bioinformatics analyses showed a higher concentration of G4 motifs in the promoter of human oncogenes than in promoters of housekeeping and tumour suppressor genes (Eddy and Maizels, 2006; Huppert and Balasubramanian, 2006).

G4s have also been implicated in cancer formation (through their function at telomeres) and in neurological disorders (Simone et al., 2015).

Expansions in the G4 sequence of the *C9orf72* gene have been linked with frontotemporal dementia and amyotrophic lateral sclerosis, while expansions in the G4 located in the 5′-UTR of *Fragile X Mental Retardation 1* (*FMR1*) have been associated with Fragile X syndrome (Simone et al. 2015).

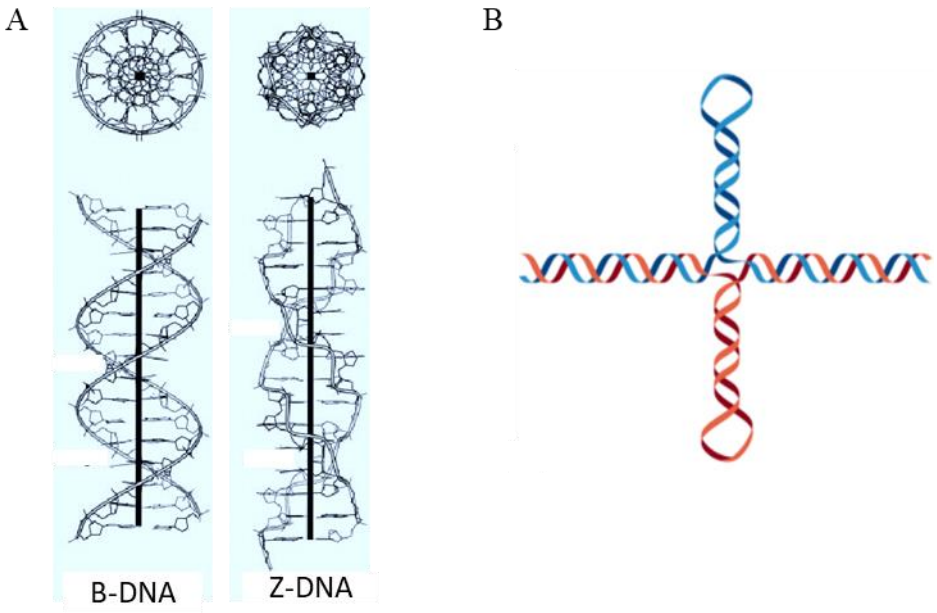

Figure 1. 2

DNA secondary structures. **A)** Structure of B-DNA and Z-DNA. **B)** Cruciform structure of DNA. Adapted from Lu and Olson 2003 and Bochman et al. 2012.

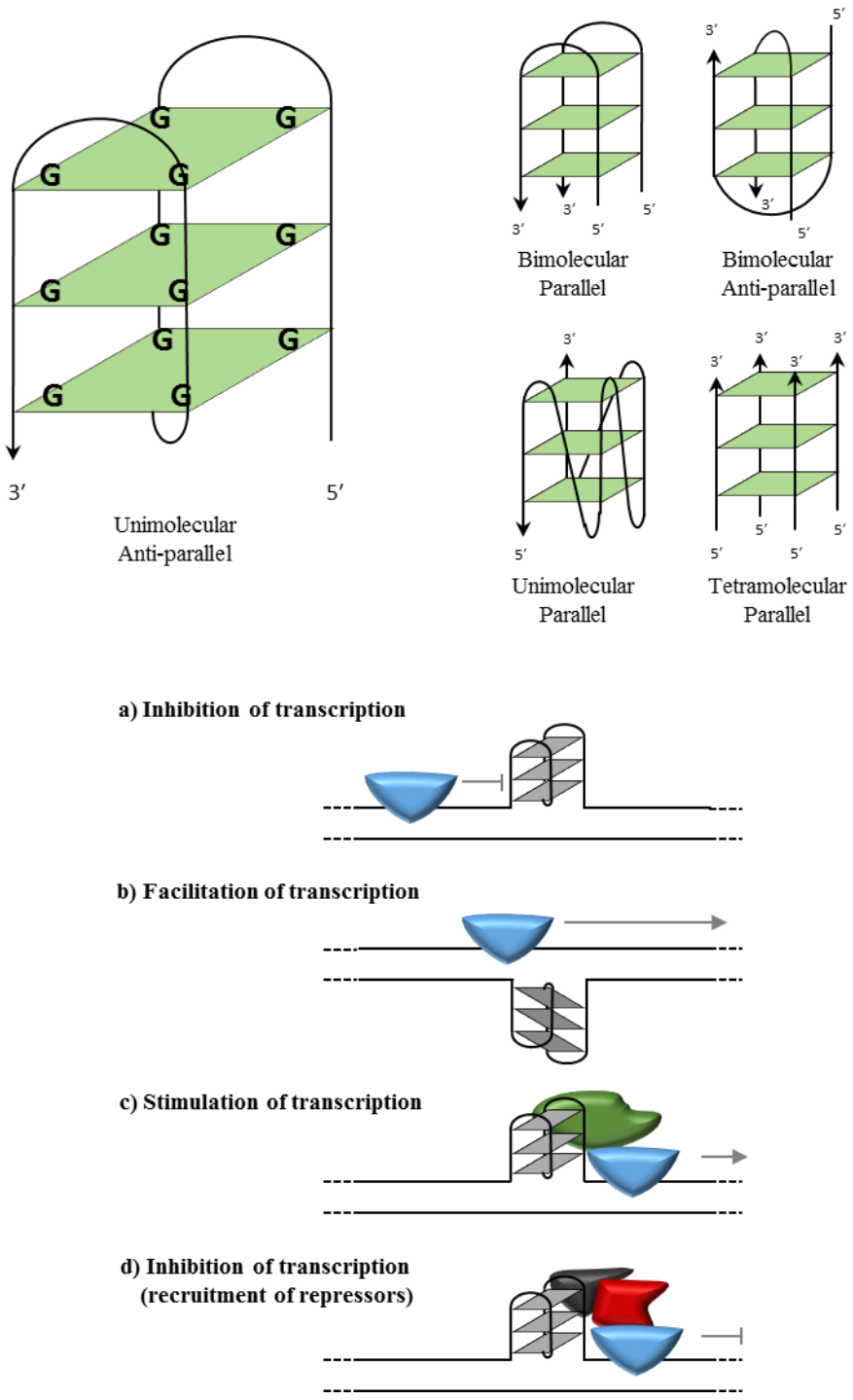

Figure 1. 3

Structures of G-Quadruplex (G4). These structures can form in different conformations depending on the DNA sequence and whether they form between one, two or more strands. Depending on their position on the sense or antisense strand they inhibit gene transcription by blocking the advancement of the RNApol II (a) and by recruiting repressors (d), or they can promote transcription by stabilising the sense strand during transcription (b) and by recruiting stimulating factors (c). Inspired by Simone et al. 2015 and Bochman et al. 2012.

1.2 Genomic imprinting

1.2.1 History and definition

Certain genes are expressed in a parent-of-origin-specific manner in an epigenetic phenomenon called 'genomic imprinting'.

The term 'imprinting' was coined in 1960 by the cytogeneticist Helen Crouse in relation to the programmed elimination of one or two paternally derived X chromosomes in *sciarid* flies. She concluded that <<the "imprint" a chromosome bears is unrelated to the genic constitution of the chromosome and is determined only by the sex of the germ line through which the chromosome has been inherited>> (Crouse, 1960).

In 1970 an imprinted gene was for the first time recognised in plants, when J. Kermicle recognised that dominant alleles related to maize kernel coloration carried by the female gametophyte may be functionally different from those carried by sperm (Kermicle, 1970).

It is during the 1970s that genetic studies in the mouse suggested the existence of imprinting in autosomes. D. R. Johnson described that a deletion in the *T-associated maternal effect* (*Tme*, later named as *insulin-like growth factor 2 receptor* (*Igf2r*) gene) locus caused *in utero* lethality when maternally but not paternally inherited (Johnson, 1974).

However, the key experiments in defining the imprinting in mammals came from studies in which newly fertilised mouse eggs that were manipulated in order to generate a diploid genetically bimaternal (parthenogenetic) or a bipaternal (androgenetic) conceptus, developed into embryos that died *in utero* and lacked embryonic and extraembryonic tissues, respectively (McGrath and Solter, 1984; Surani et al., 1984).

From these observation came the suggestion that both parental genomes are necessary during embryonic development and that certain genes carry some kind of 'mark' that distinguishes one parental allele from the other.

The first imprinted genes in the mouse were identified in the 1990s. Barlow and colleagues demonstrated that *Igf2r* was expressed only from the maternal allele and subsequent studies revealed that this gene was part of a cluster of imprinted genes in the proximal region of mouse chromosome 17 (Barlow et al., 1991; Zwart et al., 2001).

Igf2 itself was later found to be imprinted and expressed from the paternal allele (DeChiara et al., 1991), as mice with deletions in the paternal *Igf2* showed a growth deficiency phenotype. Interestingly, the adjacent *H19* gene, a non-coding RNA (ncRNA) of unknown function located 90kb downstream of the mouse *Igf2*, presents a reciprocal pattern of imprinted expression (as it is expressed from the maternal allele) and it is co-expressed with *Igf2* (Bartolomei et al., 1991; Smits et al., 2008).

In humans, the suspicion that genetic disorders could arise from parental-specific gene expression came from early observations in patients with Prader-Willi syndrome, which is characterised by hypotonia and hyperphagia in infancy and is associated with paternally derived chromosomal deletions (Knoll et al., 1989; Nicholls and Knepper, 2001).

Later studies identified several other paternally expressed genes that are likely to contribute to the diverse phenotypes of Prader-Willi syndrome, such as *SNPRN*, *NECDIN* and *HBII-85* small nucleolar RNAs (snoRNAs) (Horsthemke and Wagstaff, 2008).

According to the Medical Research Council Harwell Genomic Imprinting homepage (www.mousebook.org), to date 151 imprinted genes have been described and characterised in the mouse. Circa 100 imprinted genes have been described in humans but the imprinting is present also in other species, such as cow, dog, pig, platypus and fish (www.geneimprint.com). Furthermore, not all genes are imprinted in all mammals, with

some being imprinted in the human but not in mouse and vice versa. The mouse imprinted *Igf2r* gene in particular, has been shown to exhibit polymorphic imprinting in human, where it is imprinted in some individuals but not in others (Xu et al., 1993).

The majority (but not all) of the known imprinted genes are typically located in clusters of 3-12 genes spread over 20 kb - 3.7 Mb of DNA (Edwards and Ferguson-Smith, 2007).

These genes are usually regulated by the presence of DNA methylation in a Differentially Methylated Region (DMR), named Imprinting Control Region (ICR), but how these sequences are chosen for allele-specific methylation is poorly understood. Post-translational histone modifications also play an important role in the regulation of imprinting (Ferguson-Smith, 2011).

The processes these genes are involved in are numerous and range from foetal growth and pluripotency to differentiation and behaviour. Some imprinted genes show a tissue/cell specific imprinting but also a developmental stage specificity (Martinez et al., 2014; Perez et al., 2015).

Furthermore, imprinted genes can show specific absence of imprinting: *Delta-like homologue 1* (*Dlk1*) is a paternally expressed gene that is biallelically expressed in the postnatal neurogenic niche (Ferrón et al., 2011). Similarly, *Igf2* is biallelically expressed in the choroid plexus and leptomeninges of the brain (DeChiara et al., 1991).

In recent years, with the development of new genome wide techniques (e.g. RNA-seq), evidence has accumulated regarding the complexity of imprinting, suggesting that this epigenetic regulation might be more complicated than the 100% maternal or paternal expression described in the past.

Some genes, in fact, show a clear imprinting status, being expressed exclusively from one parental allele, while others show a preferential parental bias (Perez et al., 2015), although

whether this bias is due to cell specific imprinting and a mixture of cell types in the analysis is currently unknown.

1.2.2 Establishment and regulation of imprinting

After fertilisation, an extensive genome reprogramming and DNA demethylation process occurs, but the imprints at the maternal and paternal ICRs are maintained. *De novo* DNA methylation of the genomes occurs at the end of the preimplantation stage of development and are then maintained throughout the life of the organism in somatic cells (Fig 1.4). In the germline, instead, DNA methylation is erased during migration of primordial germ cells, which are recruited in the early embryo, into the genital ridge and re-established during gametogenesis according to the sex of the organism (Bartolomei & Ferguson-Smith 2011).

Interestingly, male and female germ cells show DNA re-methylation at different times of development, with the paternal-specific methylation of ICRs being acquired prenatally in the male germline in spermatogonia prior to the onset of meiosis and the DNA methylation in the maternal ICRs occurring postnatally in growing oocytes (Davis et al., 2000; Lucifero et al., 2004).

The DNA methylation is established in the germline by DNMT3A and the accessory protein DNMT3L (Plasschaert & Bartolomei 2014), but how the ICRs are recognised within the genome is still unknown.

Several factors contribute to the maintenance of DNA methylation in the early mouse embryo such as Developmental Pluripotency-Associated Protein 3 (DPPA3, also known as PGC7) that acts via interactions with dimethylated histone 3 (Nakamura et al., 2012). In addition, *Zinc finger protein homolog 57* (*Zfp57*) mutations are associated with defective DNA methylation at several imprinted loci (Mackay et al., 2008) and *Zfp57* null mice show loss of imprinting at many, but not all, loci (Li et al., 2008).

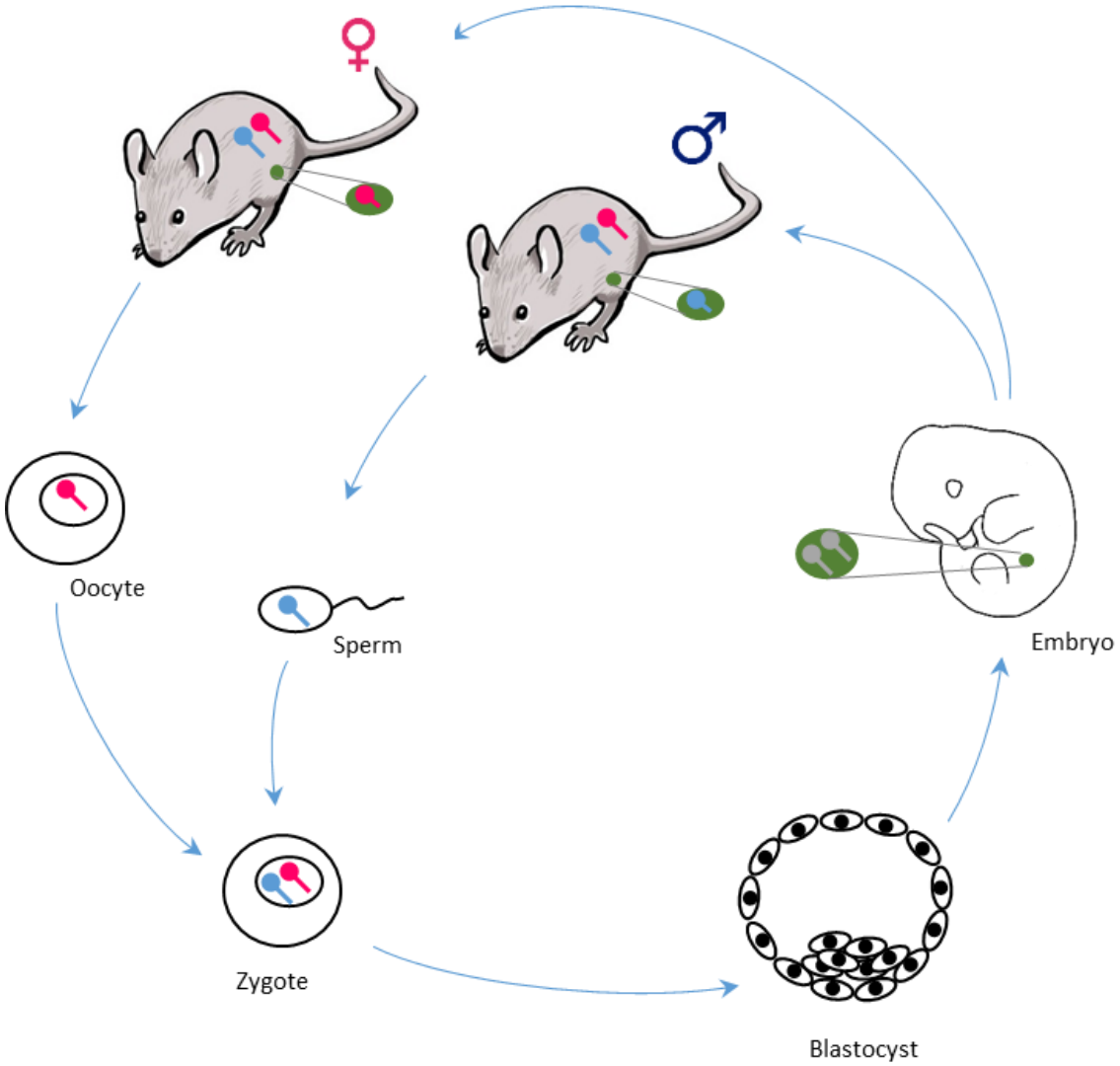

Figure 1. 4

Establishment of imprinting during development. The genomic imprints are established in the germline in a sex-specific manner and transmitted to the zygote, where they resist the reprogramming and global changes in DNA methylation that take place after fertilisation. *De novo* methylation begins at the end of the pre-implantation stage of blastocyst. While imprints are maintained in somatic cells for the whole life of the organism, imprints in the germ line are erased in primordial germ cells and re-established according to the sex of the organism, to be transmitted to the next generation. Adapted from Bartolomei and Ferguson-Smith 2011.

Interestingly, maternally methylated DMRs and ICRs are usually located at promoters while paternally methylated DMRs and ICRs are located in intergenic regions (Bartolomei and Ferguson-Smith, 2011).

The regulation of imprinted genes follows two major well defined mechanisms: the insulator model and the non-coding RNA (ncRNA) model (Fig 1.5).

An example of the insulator model is the *Igf2*/*H19* locus. *Igf2* and *H19* share a common enhancer located downstream of *H19*. On the paternal allele, where the ICR of the locus (located 2-4 kb upstream from the transcriptional start site of *H19*) is hypermethylated, this enhancer interacts with the promoter of *Ifg2*. On the maternal allele instead, the ICR is unmethylated allowing the binding of the CCCTC binding factor (CTCF), which prevents the enhancer from interacting with the *Igf2* promoter and favouring the interaction with the *H19* promoter. The methylation of the paternal ICR prevents the binding of CTCF thus promoting the expression of *Igf2* and the silencing of *H19* (Bartolomei & Ferguson-Smith 2011).

Examples for the ncRNA model, instead, are the *Igf2r*/*Airn* and *Kcnq1*/*Kcnq1ot1* loci. In these cases, the ICR coincides with the promoter of a ncRNA that is unmethylated on the paternal allele, thus allowing the expression of the ncRNA while silencing the other genes in the locus (Plasschaert & Bartolomei 2014). The methylation of the maternal ICR, instead, results in the silencing of the ncRNA and in the expression of the proximal genes (Fig 1.5).

It has been hypothesized that at the basis of this phenomenon lies either the inhibition of the recruitment of RNApol II at the promoter or the establishment of repressive chromatin marks (Nagano and Fraser, 2009; Latos et al., 2012).

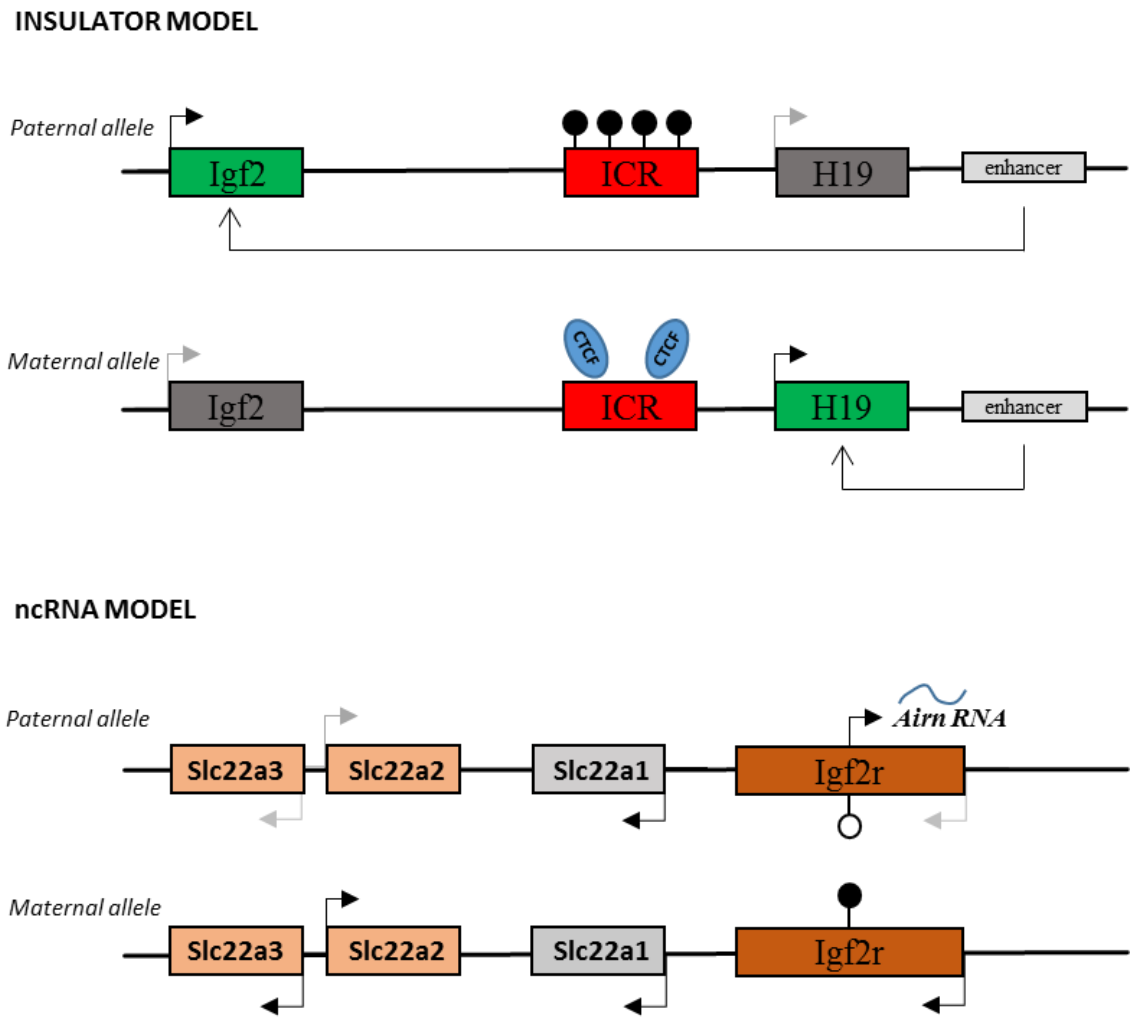

Figure 1. 5

Mechanisms of imprinting regulation. INSULATOR MODEL: the methylated (black circles) ICR on the paternal allele allows the interaction between the enhancer located downstream of *H19* with the *Igf2* promoter, thus allowing the expression of *Igf2* but not *H19*. In the maternal allele, the unmethylated ICR is a binding site for CTCF, which prevents the enhancer from interacting with *Igf2* and promotes the interaction with *H19* promoter inducing its expression. ncRNA MODEL: the methylated (black circle) ICR located in the second intron of *Igf2r* on the maternal allele causes the silencing of the gene and the expression of the ncRNA *Airn* transcribed in an antisense orientation, while *Slc22a2* and *Slc22a3* are silenced. When the ICR is methylated on the maternal chromosome *Igf2r* is transcribed along with *Slc22a2* and *Slc22a3*. *Slc22a1* is biallelically expressed despite its location in the locus. Inspired by Plasschaert et al. 2014.

1.2.3 Imprinted genes and human disorders

Imprinted genes are generally highly expressed during prenatal stages but downregulated after birth. The placenta and the brain are two main sites of expression for several imprinted genes, which correlates with the growth and neurodevelopmental defects often seen in human imprinting disorders (Coan et al., 2005; Wilkinson et al., 2007).

As more imprinted genes are being identified, recurrent themes have emerged indicating that their function relates to prenatal growth control, development of particular lineages and postnatal homeostasis. In particular, within the brain they appear to modulate metabolic axes, behaviour, learning and maternal care (Bartolomei & Ferguson-Smith 2011).

Interestingly, a number of imprinted genes have expression patterns and functions in the brain that are distinct from those seen in other tissues, such as *Ubiquitin-protein ligase E3A* (*Ube3a*) that is biallelically expressed in most tissues but maternally expressed within certain neuronal subtypes (Albrecht et al., 1997).

The best known imprinted disorders are Prader-Willi and Angelman syndromes which derive from mutations of the same domain on human chromosome 15, but that differ in the parental origin (Buiting, 2010).

Prader-Willi syndrome results from the absence of expression of a cluster of paternally expressed genes located at 15q11.2-q13 (Murrell, 2014). This syndrome is characterised by two distinct phases of clinical features. In infancy, the main symptoms are failure to thrive with muscular hypotonia, respiratory problems and feeding difficulties (Holm et al., 1993). At around two years of age an overeating behaviour, learning disability and mild developmental delay occur, followed by growth hormone deficiency and severe behavioural problems at a later stage (Holm et al., 1993; Holland et al., 1995; Murrell, 2014).

Around 70% of Prader-Willi syndrome cases derive from *de novo* deletions of the 15q-q13 region, while most of the remaining cases present as uniparental disomy of chromosome 15. The 15q.11.2-q13 region contains few protein-coding genes and multiple paternally expressed ncRNAs, several of which have been suggested to regulate alternative splicing (Kishore and Stamm, 2006; Yin et al., 2012). Among the protein-coding genes, *SNURF–SNRPN*, *NDN*, *MKRN3*, *MAGEL2* and several clusters of snoRNAs are imprinted and expressed exclusively from the paternal allele (Anderlid et al., 2014). The region also contains the paternally expressed antisense transcript to *UBE3A* located at the 3′ end of the imprinted cluster (Schaaf et al., 2013; Anderlid et al., 2014).

The sense transcript to *UBE3A* is expressed in neurons from the maternal allele and, when lost (e.g. mutations or paternal disomy), causes Angelman syndrome (Kaplan et al., 1987; Donlon, 1988; Knoll et al., 1989). Harry Angelman described this syndrome in 1965 after observing children with similar features, among which were severe learning disability, microcephaly, seizures, absent speech and a happy and sociable disposition (Buiting et al. 2016).

It is now known that the methylation and gene expression in the imprinted domain is regulated by an ICR located in the *small nuclear ribonucleoprotein-associated protein N* (*SNRPN*) upstream region (Sutcliffe et al., 1994; Buiting et al., 1995).

Imprinting disorders and syndromes can be associated with mutations or aberrations in multiple loci. A well-known example is the Beckwith–Wiedemann syndrome, a growth disorder caused by alterations in two separate imprinted domains on chromosome 11, with sporadic hypomethylation of the *KCNQ1OT1* DMR being found in the majority of cases and a gain in methylation at the *H19* intergenic DMR being observed in 5% of cases. Uniparental disomy of the 11p15 region or mutations in *CDKN1C* have also been observed (Sanchez-Delgado et al. 2016). Affected individuals exhibit macrosomia (high weight at

birth), macroglossia (unusually large tongue), visceromegaly and abdominal wall defects with an increased risk of paediatric tumours (Brioude et al., 2013).

1.2.4 *Peg13*/*KCNK9* gene cluster

Trafficking protein particle complex 9 (*Trappc9*) is located in the *Peg13*/*Kcnk9* (*Paternally expressed gene 13* and *Potassium channel subfamily K member 9,* respectively) cluster on chr 15qD3 in mice and on chr 8q24.3 in humans. The murine *Peg13* is transcribed into an intronless ncRNA (two variants of 4397 bp and 4723 bp), first described by Smith and colleagues (Smith et al., 2003). It is located in an intron of *Trappc9* in the same transcriptional orientation and, as it transpires from its name, is expressed from the paternal allele in both mouse and human brain tissue (Smith et al., 2003).

The mouse *Peg13* does not share any homology with the human *PEG13* (Smith et al., 2003), which however is located in the same intron of *TRAPPC9* and encodes for a ncRNA. Its origin might lay in the retrotransposition of another gene, although the lack of homology with other genes in the mouse genome and the lack of homology with the human gene suggest the transposition must have occurred recently in evolution (Smith et al., 2003; Suzuki et al., 2011).

All the genes in the locus (*Kcnk9*, *Trappc9*, *Chromatin accessibility complex 1* (*Chrac1)* and *Argonaute 2* (*Ago2*)) have been reported to be imprinted in the mouse, while in humans only *PEG13* and *KCNK9* have a clear imprinting status (see Fig 3.1).

The most interesting feature about this locus is that while *Peg13* is paternally expressed, *Chrac1*, *Ago2* and *Kcnk9* are maternally expressed to different degrees (Perez et al., 2015). *Chrac1* and *Ago2* in particular, have been shown to exhibit a similar pattern of maternal bias across the brain, stronger in the cortex and weaker in the olfactory bulb, hippocampus, and cerebellum (Perez et al., 2015).

Contrasting reports on the imprinting status of *Trappc9* (that I will discuss in detail in chapter 3) have been published, however, when reported as imprinted, it has been associated with expression from the maternal allele, in contrast to *Peg13*.

Methylation studies have highlighted a DMR in the promoter region of *Peg13,* which is methylated on the maternal allele, but no other hypermethylated sites were found in the locus despite the presence of several other CpG islands (Smith et al., 2003; Court et al., 2014).

AGO2 encodes for an endonuclease which acts as a major component of the RNA-induced silencing complex (RISC) in a process called RNA-interference (RNAi). This protein is known to bind microRNAs, siRNAs and *Piwi*-interacting RNAs and to mediate the loading onto RISC, where the single strand acts as a template to recognise mRNA transcripts, allowing AGO2 to cleave the mRNA and lead to inhibition of translation or transcript degradation (Meister et al., 2004; Hutvagner and Simard, 2008). This protein has proven to be crucial for mouse embryonic development as *Ago2* knockout (KO) is lethal (Morita et al., 2007; Shekar et al., 2011).

CHRAC1 encodes for a nucleosome-remodelling complex that, in conjunction with the factor NURF, open chromatin for transcription and replication by using the nucleosomal ATPase ISWI catalytic subunit, to increase the mobility of nucleosomes relative to DNA sequence (Guschin and Wolffe, 1999).

While no specific clinical disorders have been associated with both *AGO2* or *CHRAC1*, *KCNK9* is known to cause Birk-Barel syndrome when a missense mutation 770G>A in exon 2 occurs in the maternal copy of the gene (Barel et al., 2008).

KCNK9 encodes a member of the two pore-domain potassium channel named TWIK-related acid-sensitive K1 channel 3 (TASK3). The mutation causes an 80% reduction in outward current (Veale et al., 2014) and induces a distinct phenotype with delayed

development, severe feeding problems, variable clefting and intellectual disability of various degrees (Barel et al., 2008; Graham et al., 2016).

1.3 Microcephaly and TRAPPC9-related disorder

1.3.1 Definition and causes of microcephaly

Microcephaly is a significant reduction in the occipital-frontal head circumference of <−2 SD or <−3 SD, and it is usually correlated with IQ deficiency when outside the normal range of head circumference (<+3 SD to >-3 SD) (Woods & Parker 2013).

It can be distinguished into primary microcephaly, also known as congenital or developmental, and secondary or postnatal microcephaly.

Primary microcephaly is typically detected prior to 36 weeks of gestation and it is usually discernible from prenatal ultrasounds and measurements at birth. It is often caused by a failure or a reduction in neurogenesis, first trimester cytomegalovirus infections and chromosomal disorders. Rarely, it can be a very early onset of a degenerative process.

The detection of microcephaly prior to 20 weeks of gestation usually leads to severe outcomes, with extreme cases showing an occipital-frontal head circumference of <−8 SD.

Postnatal microcephaly, instead, develops after birth and its primary aetiology is usually not a failure in neurogenesis but neural migration disorders, a block to normal development or a degenerative process.

Clinically, it can be associated to a static or a progressive disorder. Static disorders usually produce a phenotype that includes dysmorphic facial features, congenital anomalies and developmental delay. In this case the two major causes are chromosome perturbations or Mendelian single gene disorders. Progressive disorders can instead be associated with metabolic diseases, although these cases are quite rare. This type of microcephaly is

associated with a high frequency of complex neurobehavioral disabilities in affected children, with a severely restricted expressive language, social impairment, repetitive thought and behavioural patterns. Epilepsy, movement disorders, abnormalities in GI motility, feeding inability or overfeeding, pain tolerance and sleep patterns can also be present (Seltzer & Paciorkowski 2014).

Due to the range of symptoms often associated with postnatal microcephalies, these have often been termed as Angelman-like and Rett-like syndromes, but through a detailed analysis it is possible to discriminate among them.

Microcephaly usually develops as part of complex disorders and the molecular and cellular basis are difficult to appoint as many genes and processed are involved.

It is known that all neurons in the cerebral cortex have completed proliferation by mid-gestation. Generally no (or very few) neurons are generated after birth but the brain volume continues to grow until adulthood thanks to development of axons, dendrites and glial cells/processes (Spalding et al., 2005). During the first year of life, in fact, a dramatic increase in brain size reflects predominantly an increase in neuronal processes and glial cells. As the head circumference continues to increase with time (until 17-18 years), children with developmental microcephaly appear to worsen with age as their head grows more slowly with often a lower number of neurons present (Herculano-Houzel et al., 2007).

A number of genes have been found responsible for the onset of microcephaly, among which the majority encode proteins associated with the centrosome or centrosomal-related activities (Gilmore & Walsh 2013).

Centrosomes are organelles that serve as the main microtubule organizing centre (MTOC) of the animal cell and are primarily responsible for the formation of the mitotic spindle via their interaction with microtubules. They are also involved in coordinating microtubules in

other processes such as cell migration and primary cilia formation (Kerjan and Gleeson, 2007; Manzini and Walsh, 2011).

Interestingly, mutations or aberrations in genes involved in lissencephaly (smooth brain) produce neuronal migration abnormalities via centrosomes and microtubules, highlighting the importance of these structures in brain development (Gilmore & Walsh 2013).

Many genes associated with microcephaly are also implicated in DNA damage responses and repair activity, with defects in the maintenance ranging from alterations of a single nucleotide to errors in chromosome segregation during mitosis (Gilmore & Walsh 2013).

For instance, mutations in *Microcephalin 1* (*MCPH1*) are associated with premature condensation of chromosomes in G2 (Neitzel et al., 2002; Trimborn et al., 2004). Furthermore, fibroblasts of patients with mutations in *Centrosomal protein of 152 kDa* (*CEP152*) develop aneuploidy in culture as a result of abnormalities in the control of chromosome segregation (Kalay et al., 2011).

A number of genes are, however, involved in the early steps of DNA repair signalling pathways (e.g. *NBS1*, *RAD50*, *MRE11A* and *ATR*) (Gilmore & Walsh 2013).

The reason why the brain is particularly sensitive to mutations in centrosomal proteins and in DNA-repair defects, or why we do not observe a strong phenotype in other tissues, is still unclear.

A hypothesis could be that neurons are more sensitive to these mutations responding with a higher apoptosis rate. KO mouse models for *CDK5RAP2* and *MCPH1*, two genes involved in the onset of primary microcephaly, show excessive cell death in the brain but whether this is the primary cause of microcephaly needs still to be confirmed (Feng and Walsh, 2004; Castiel et al., 2011).

1.3.2 Postnatal microcephaly-associated disorders

MECP2-related disorder (formerly Rett syndrome). Andreas Rett described this disorder in 1966 but it wasn't until 1999 that loss-of-function mutations in *methyl CpG binding protein 2* (*MECP2*) were associated with the phenotype (Rett, 1966; Zoghbi et al., 1999). MECP2 is a transcription factor highly expressed in the brain that recognises specifically methylated sequences. Its loss from forebrain excitatory neurons results in decreased GABAergic tone and increase excitation (Zhang et al., 2014a). The loss-of-function of *MECP2* can be caused by single base mutations, insertion or deletions. It is a dominant X-linked disorder that typically affects females with a frequency of 1 every 10000 individuals. Symptoms include severe intellectual impairment, stereotypic hand movements, growth failure and deceleration of head growth (Seltzer & Paciorkowski 2014). These symptoms occur between 6 months and 2.5 years of age but not all the affected girls experience a course of regression. Other symptoms such as breathing abnormalities, absence of speech, bruxism, abnormal sleep patterns and abnormal muscle tone are considered 'minor criteria' (Young et al., 2007). Epilepsy occurs in 60% of the affected individuals and girls with this condition have a 300-fold increased risk of sudden cardiac death. Brain abnormalities include reduced volume of white matter, corpus callosum abnormalities, ventricular dilatation and vermis hypoplasia (El Chehadeh et al., 2016). *MECP2* mutations in males are rare and they might not manifest all of the diagnostic criteria typical of female individuals, such as regression in development. They share absence of language and often exhibit a more severe phenotype that is fatal early in life (Percy, 2002).

CDKL5-related disorder (formerly Rett variant). Mutations in *Cyclin-Dependent Kinase-Like 5* (*CDKL5*) were associated with the disorder in 2004 (Weaving et al., 2004). This disorder differs from the *MECP2*-related disorder for the early onset epilepsy and common

myoclonic seizures. Affected children possess clinical features similar to *MECP2* patients but lack the regression of development and exhibit poor fine motor skills, being mostly non-ambulatory (Bahi-Buisson et al., 2008; Guerrini and Parrini, 2012).

CDKL5 is located on the X chromosome and 3% of affected individuals are males. The gene encodes for a serine-threonine kinase that regulates neuronal morphology during dendritic spine development (Ricciardi et al., 2012; Zhu et al., 2013).

More than 70 different point mutations have been described for this gene, including missense mutations within the catalytic domain, nonsense mutations, splice variants, and frameshift mutations (Bahi-Buisson and Bienvenu, 2012).

Brain MRI analyses showed non-specific abnormalities such as cortical atrophy and white matter hyperintensities (Bahi-Buisson et al., 2008).

FOXG1-related disorder (formerly Rett variant). *Forkhead box protein G1* (*FOXG1*) deletions and mutations cause severe cognitive disability, sleep dysfunctions and severe gastroesophageal reflux. Head circumference at two years of age has been noted to be low normal to borderline small and epilepsy is a common comorbidity that develops after one year of age (Seltzer and Paciorkowski, 2014). Brain abnormalities include agenesis of the corpus callosum and reduced white matter volume (Bahi-Buisson et al., 2010).

At the molecular level, FOXG1 is a transcription factor that regulates dorsal-ventral brain patterning and is important in the development of Cajal-Retzius cells in the cerebral cortex and hippocampus. It has also been shown to inhibit gliogenesis, promote neurogenesis and regulate neuronal differentiation (Hébert and Fishell, 2008; Brancaccio et al., 2010; Kumamoto et al., 2013).

1.3.3 *TRAPPC9* mutations in humans

In 2009, the American Journal of Human Genetics published reports from three separate groups regarding mutations in the sequence of *TRAPPC9* in association with recessive

autosomal non-syndromic intellectual disability (Mir et al., 2009; Mochida, 2009; Philippe et al., 2009). During the last eight years more studies were conducted and to date a total of 21 affected individuals have undergone clinical investigation. The affected individuals came from different ethnic groups, many of Arab descent, and mostly consanguineous marriages. They all presented moderate to severe intellectual disability with different degrees of microcephaly, with the head circumference ranging from -1 SD to -3 SD. Brain abnormalities included reduction of white matter volume with sulcal enlargement, subcortical T2 hyperintensity, hypoplasia/partial agenesis of the corpus callosum and cerebellar hypoplasia. The severity of the symptoms varies amongst the individuals with the most common symptoms being inability or delay of speech, late start to walk and inability to feed themselves. The majority exhibit dysmorphic facial features with short and smooth philtrum, short forehead, synophrys (unibrow) and broad nasal bridge. Epileptic seizures were reported in some cases and obesity in one female and one male (Mir et al., 2009). A happy and friendly disposition was reported in many cases, as well as stereotypic movements and hand flipping behaviour.

Pregnancies were unremarkable and head measurements at birth were available only for few patients, ranging from -0.3 SD to -2 SD and suggesting that *TRAPPC9*-associated microcephaly belongs to the postnatal category (see section 1.3.1). However, foetal head-measurements were not performed in any of the cases.

One particular case exhibited progressive cortical degeneration (Koifman et al., 2010) for the duration of the observations (up to 3.5 years of age). Unfortunately, very little is known about these patients at an adult age. Abou Jamra and colleagues reported tooth and weight loss in two female patients from the age of 20 (Abou Jamra et al., 2011), but a further progression of the disorder has not been documented.

DNA analysis revealed a range of recessive autosomally-transmitted mutations and deletions in the sequence of *TRAPPC9* that lead to the premature truncation of the protein and result in a significant degree of nonsense-mediated mRNA decay (Mir et al., 2009).

1.4 Trappc9-associated pathways and systems in the cell

1.4.1 TRAPP complexes and vesicle tethering

The Trafficking Protein Particle (TRAPP) complexes are involved in the vesicular transport of proteins and lipids between different membrane-bound compartments.

The majority of what we know about TRAPP complexes derives from studies in yeast, where these complexes are very well conserved. Three TRAPP complexes (I, II and III) have been isolated in *Saccharomyces cerevisiae* while two have been isolated in humans (II and III) (Fig 1.6). These complexes share a core structure of six polypeptides arranged into a seven subunit complex (TRAPPI), to which other subunits bind forming TRAPPII and TRAPPIII (Table 1.1). TRAPPII contains the yeast subunits tr120p and trs130p (Trappc9 and Trappc10 in mammals),

Yeast proteins	Mammalian proteins
Bet5	Trappc1
Trs20	Trappc2
Tca17	Trappc2L
Bet3	Trappc3
Trs23	Trappc4
Trs31	Trappc5
Trs33	Trappc6
Trs85	Trappc8
Trs120	Trappc9
Trs130	Trappc10
N/A	Trappc11
N/A	Trappc12
Trs65	Trappc13

Table 1. 1
TRAPP subunit homology in yeast and mammals.

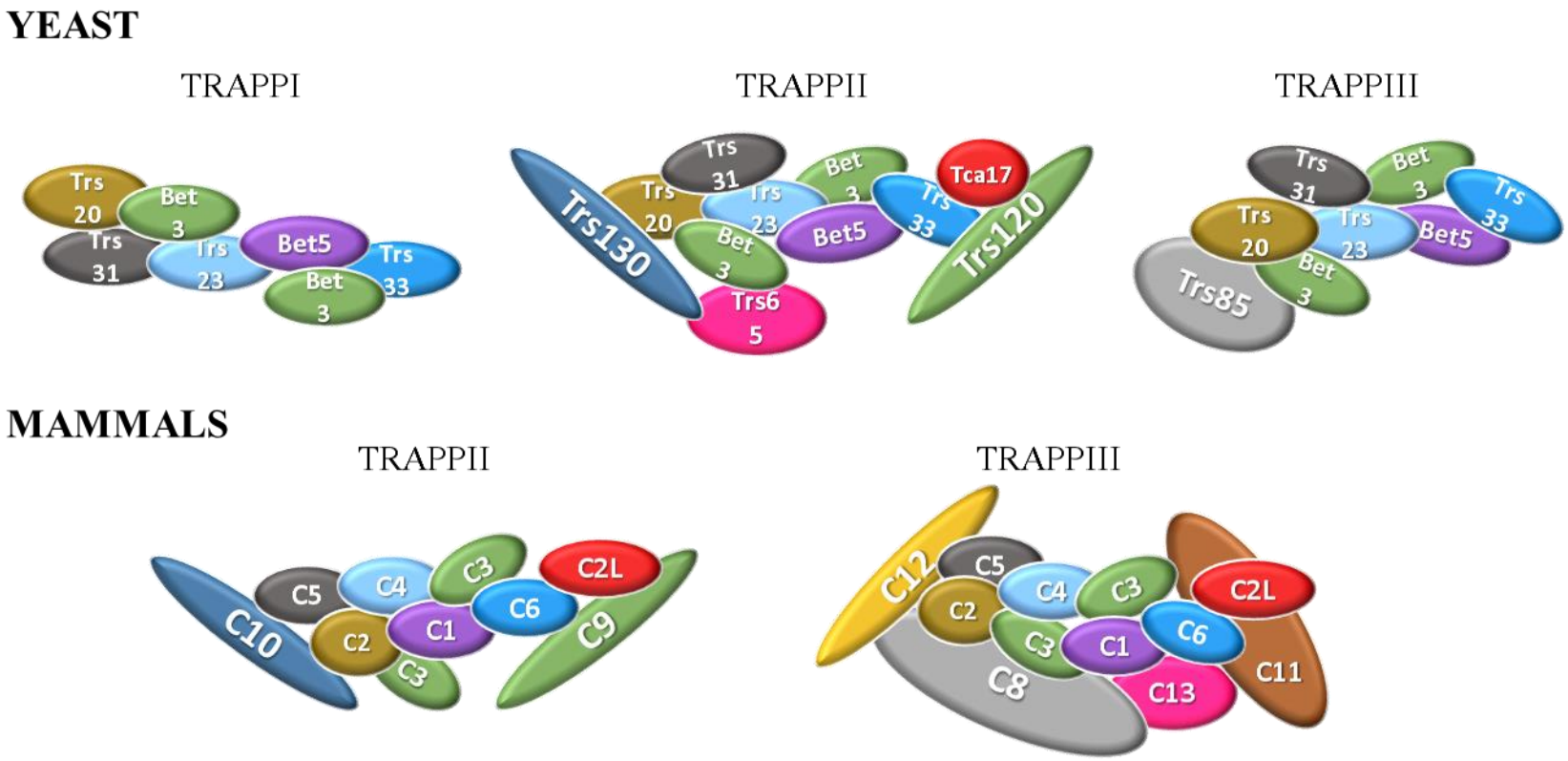

Figure 1. 6

Structures of TRAPP complexes in yeast and mammals. Adapted from Brunet et al. 2014.

while TRAPPIII contains the yeast trs85p (Trappc8) and other subunits not found in yeast (Trappc11 and Trappc12) (Barrowman et al. 2010).

Yeast TRAPPI is involved in ER-Golgi trafficking, TRAPPII in intra-Golgi and endosome-Golgi trafficking and TRAPPIII in autophagy. As a mammalian TRAPPI has not been successfully isolated, it has been hypothesised that its levels are too low to be detected or that its functions are performed by TRAPPII or by another (unknown) complex (Barrowman et al., 2010).

These complexes, along with other multisubunit complexes and long coiled-coil proteins, are involved in vesicle tethering, which refers to the initial contact between a transport vesicle and its acceptor compartment (Barrowman et al., 2010). This process precedes the fusion mediated by SNARE proteins that tightly interact to form a hairpin structure and initiate membrane mixing and fusion (Jahn and Scheller, 2006). This process is probably aided by Rab GTPases, and all three TRAPP complexes possess guanine exchange factor (GEF) activity for several Rabs (Barrowman et al. 2010).

It has been shown that Trappc1, Trappc4, Trappc5 and two Trappc3 are essential for the GEF activity of these complexes, and TRAPPII has been found to specifically possess GEF activity for Rab1 and Rab18 (Wang and Ferro-Novick, 2002; Li et al., 2017).

Trappc9 itself binds Rab1, Rab18 and Rabin 8, a GEF for Rab8 and Rab11 (Westlake et al., 2011; Homma and Fukuda, 2016; Li et al., 2017). The activation of Rab proteins by the TRAPP complexes induces the recruitment of effectors involved in the fusion of vesicle and target membrane.

Trappc9 mediates the interaction between the TRAPPII complex and COPI coated vesicles, specific to endoplasmic reticulum (ER)-Golgi and intra-Golgi trafficking (Gwynn et al., 2006; Yamasaki et al., 2009; Zong et al., 2011; Li et al., 2017).

The importance of the mammalian TRAPP complexes in development is highlighted by the fact that mutations in several of their subunits cause different disorders.

We have previously discussed mutations in *TRAPPC9* and the associated microcephaly and intellectual disability. Mutations in *TRAPPC11* have been associated with myopathy, infantile hyperkinetic movements, ataxia, and intellectual disability (Bögershausen et al., 2013; Koehler et al., 2016).

Mutations in *TRAPPC2* cause spondyloepiphyseal dysplasia tarda, a recessive disorder in bone formation which manifests in childhood with disproportionate short stature, short neck and trunk, barrel chest and absence of systemic complications (Gécz et al., 1999).

Trappc6 has been proposed to play a role in coat pigmentation in mice (Gwynn et al., 2006) and TRAPPC4 has been implicated in the tumorigenesis of colorectal cancer through the interaction with the MAP kinase ERK2 (Zhao et al., 2011; Kong et al., 2013).

Considering the trafficking function of the TRAPPII complex, a multitude of processes could be affected by its disruption and mutations in the different components of the complex could affect the interaction with specific factors, inducing the diverse conditions observed in affected individuals.

1.4.2 NF-κB pathway

Trappc9 was first identified as NIK and IKKβ binding protein (NIBP) for its ability to regulate the NF-κB pathway (Hu et al., 2005).

The NF-κB family of proteins owes its name to the interaction with an 11 bp sequence in the immunoglobulin κ-light-chain enhancer, discovered in extracts of B-cell tumours (Sen and Baltimore, 1986).

This family of transcription factors is ubiquitously expressed in mammalian cells and has been shown to regulate a number of processes, such as inflammation, immune responses, cell growth and development. The inappropriate activation of this pathway leads to

chronic inflammation, autoimmunity and various cancers (Toubi and Shoenfeld, 2004; Bassères and Baldwin, 2006; Courtois and Gilmore, 2006).

The activation of the pathway is stimulated by external stimuli, canonically cytokines, pathogens and injuries.

The family of proteins is composed of a number of factors (p65/RelA, RelB, c-Rel, p50, p52 and Relish) that, when unstimulated, are localised to the cytoplasm in the form of inactive dimers bound to the inhibitor κB (IκB). The IκB family consists of several members, among which IκBα regulates the activation and inactivation of the NF-κB pathway while its transcription is in turn regulated by NF-κB.

In the canonical pathway, the activation by external stimuli of receptors on the plasma membranes initiates a cascade of events that leads to the activation of IκB kinase (IKK) heterodimers (composed of IKKα, IKKβ and IKKγ), responsible for the phosphorylation of the inhibitory subunit of IκB. This phosphorylation leads to ubiquitination and degradation of IκB by the proteasome and releases from the inhibitory complex NF-κB proteins, which are then transported to the nucleus where they activate gene transcription (Napetschnig & Wu 2013) (Fig 1.7).

In the non-canonical pathway instead, extracellular signals induce the activation of NF-κB Inducing Kinase (NIK) that phosphorylates IKKα homodimers, which in turn phosphorylate the NF-κB precursor p100 leading to its processing to p52/RelB dimers (Fig 1.7).

All members of the family share a highly conserved DNA-binding and dimerization domain, named Rel Homology Region (RHR), that enables them to homo- or heterodimerise (Napetschnig & Wu 2013). p65, RelB and c-Rel contain a C-terminal transactivation domain (TAD) that allows them to directly activate gene expression, while

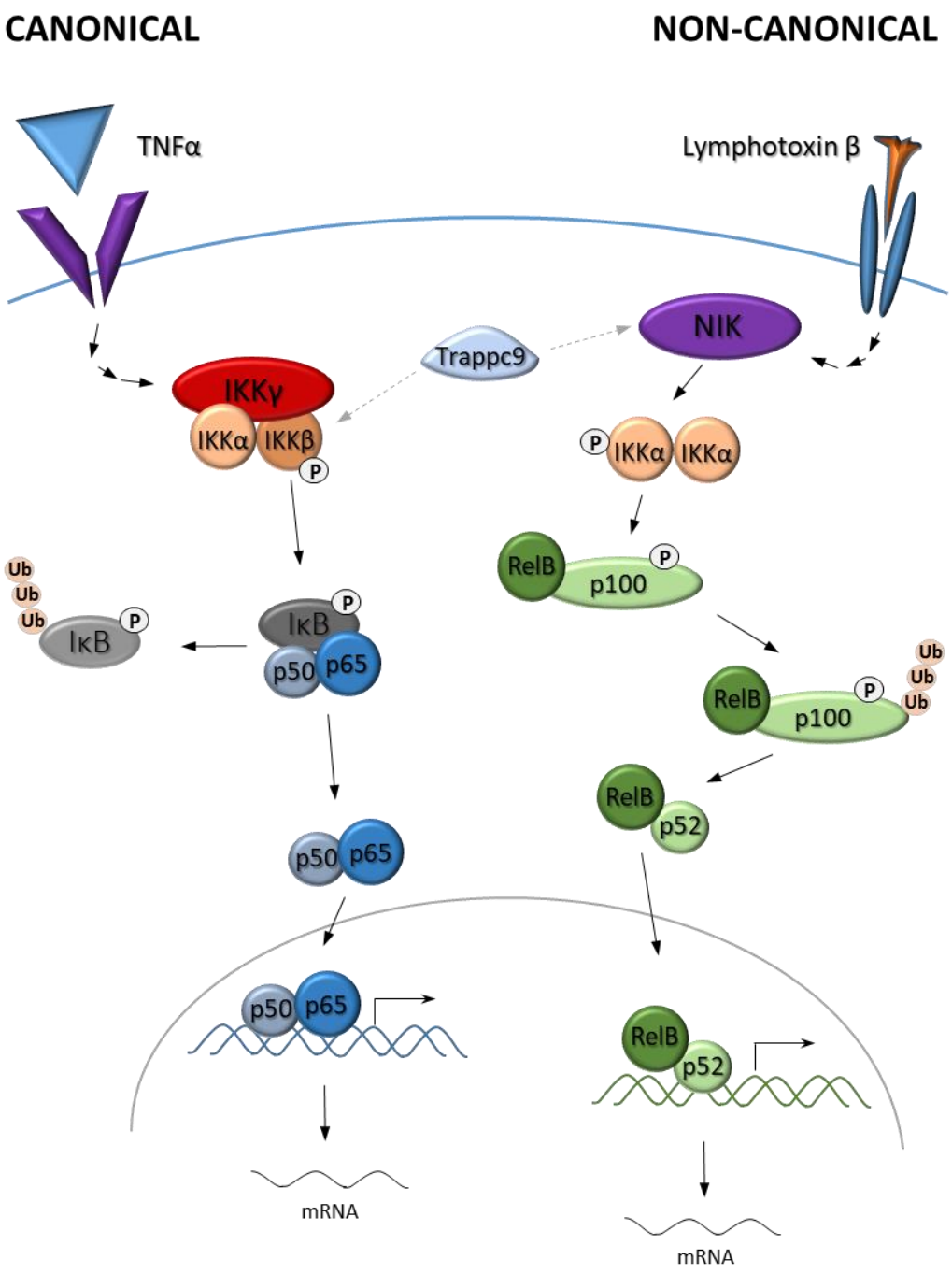

Figure 1. 7

NF-κB pathway. In the canonical activation of the pathway the extracellular signal (e.g.TNFα) activates a series of events that lead to the phosphorylation of IKKα-IKKβ heterodimers bound to a regulatory IKKγ. The phosphorylation induces the activation of IKKβ that in turn phosphorylates IκB. This phosphorylation marks IκB for ubiquitination and degradation, leaving NF-κB dimers free to translocate into the nucleus and activate gene expression. In the non-canonical activation of the pathway the extracellular signal (e.g. lymphotoxin β) induces the activation of NIK that phosphorylated and activates IKKα homodimers. The activated IKKα phosphorylates the p52-precursor p100 which is then cleaved into active p52. RelB-p52 heterodimers then translocate into the nucleus to activate gene expression. Trappc9 has been shown to interact with NIK and IKKβ. Inspired by Bonizzi and Karin 2004.

p50, p52 and Relish contain an ankyrin repeat-containing domain (repetitions of two alpha helices separated by loop) at the C-terminus instead of the TAD, which prevents them from activating gene expression as a homodimer. The active RHR domain forms when the N-terminal and C-terminal domains of two NF-κB proteins are connected by a linker to encircle the target DNA.

In addition to the originally discovered expression of NF-κB factors in lymphocytes, the presence of these proteins has also been confirmed throughout the nervous system where the most common NF-κB members are p50-p65 heterodimers and p50-p50 homodimers (Meffert & Baltimore 2005). Their presence has in fact been detected in both central and peripheral nervous system in both neurons and non-neuronal cells, such as glia and Schwann cells. Nerve Growth Factor (NGF), β-amyloid and neurotransmitters (glutamate, dopamine) can activate NF-κB pathway in addition to the classic stimuli and it has been shown that known NF-κB activators have unique roles in the central nervous system. For instance, TNFα acts as a mediator of neuronal plasticity in non-inflammatory settings in the hippocampus (Albensi and Mattson, 2000; Beattie et al., 2002) and nitric oxide regulates synaptic efficacy (Schuman and Madison, 1994).

Contribution of NF-κB in the nervous system is crucial for many processes as a number of genes is regulated by this pathway. For instance, NF-κB regulates the expression of neural cell adhesion molecule, inducible nitric oxide synthase, amyloid precursor protein, μ-opioid receptors, brain derived neurotrophic factor and Ca^{2+}/calmodulin dependent protein kinase II (Grilli et al., 1995; Simpson and Morris, 2000; Lipsky et al., 2001; Madrigal et al., 2001; Kraus et al., 2003). Furthermore, NF-κB factors have been shown to regulate cell differentiation in diverse contexts. They are known to drive the differentiation of Schwann cells and are crucial for proper myelination of peripheral axons (Nickols et al., 2003). In addition, p50-deficient mice, show 50% reduction in the number of newly born

neurons in the adult mutant hippocampus, while the net number of precursor cells is not affected (Denis-Donini et al., 2008).

Immunohistochemical studies have confirmed the localisation of NF-κB factors at synapses but only of p65-p50 heterodimers (Kaltschmidt et al., 1993; Guerrini et al., 1995; Meffert et al., 2003). Neurons from p65-deficient mice still express other NF-κB subunits but their synapses are devoid of NF-κB (Meffert et al., 2003).

It has been shown that NF-κB factors can translocate from distal sites to the nucleus in response to excitatory stimuli (Wellmann et al., 2001; Meffert et al., 2003). Trafficking within dendrites appears to be primarily in the retrograde direction (towards the nucleus) with little anterograde movement (Meffert et al., 2003). Interestingly, the ubiquitin-proteasomal system crucial for the degradation of IκB is present at dendrites and synapses and is regulated by synaptic activity (Ehlers, 2003; Patrick et al., 2003).

Evidence suggests that the NF-κB family of transcription factors has also a role in mammalian behaviour. KO mice for p65 die *in utero* from hepatocyte apoptosis, but the deletion of p65 in combination with the *TNF receptor 1* (*TNFR*) gene rescues lethality (Kaltschmidt et al., 1993; Ehlers, 2003). These mice show learning deficits in a radial eight-armed maze and p50-deficient mice show similar deficits, although to a lower degree (Meffert et al., 2003; Denis-Donini et al., 2008).

1.4.3 Cellular functions of Trappc9

In this paragraph, I provide the reader with an overview of what is currently known about Trappc9's role in the cell. Although it might appear as a series of unrelated topics, I will discuss in detail how they might be connected in chapter 4.

The first reference to Trappc9's function outside the TRAPPII complex in the cell came from Hu and colleagues, who found Trappc9 directly binding to NIK and IKKβ in HEK293 cells and in brain lysates (Hu et al., 2005). They also found that overexpression of Trappc9,

which they named NIBP (NIK and IKKβ binding protein), potentiates the TNFα-induced NF-κB DNA binding activity and induces the phosphorylation of IκBα and p65. Interestingly, the stable knockdown of Trappc9 in PC12 cells inhibited the NGF-induced neurite outgrowth and reduced the expression of the anti-apoptotic factor Bcl-XL (Hu et al., 2005).

Trappc9 has been confirmed to regulate the TNFα-induced NF-κB response in different cell lines such as enteric neuronal cell line (Zhang et al., 2014b), where it influences neuronal differentiation, and cancer cell lines (MCF7, HeLa, AGS, HCT116 and Caco-2), where it mediates tumorigenesis through NF-κB signalling (Zhang et al., 2015a).

Trappc9 also has GEF activity for Rab1, Rab18 and Rabin 8, a GEF for Rab8 and Rab11 (Westlake et al., 2011; Homma and Fukuda, 2016; Li et al., 2017). Rab18 is known to regulate lipid homeostasis and it has been found mutated in cases of Warburg micro-syndrome and Martsolf syndrome, characterised by intellectual disability, postnatal microcephaly and aberrantly large lipid droplets (LDs) (Liegel et al., 2013).

Trappc9 siRNA knockdown in HEK293 cells caused an increase in LDs accumulation and human fibroblasts isolated from individuals with mutations in *TRAPPC9* contained aberrantly large LDs. Furthermore, TRAPPII depleted cells showed a decrease in release of fatty acids (Li et al., 2017).

Trappc9 also has GEF activity toward Rabin 8, which regulates neurite outgrowth in PC12 cells and has GEF activity for Rab 11, Rab8 and Rab10 (also required for neurite outgrowth in PC12 cells) (Westlake et al., 2011; Homma and Fukuda, 2016).

Trappc9 also binds p150^{glued}, a subunit of dynactin, mediating the interaction between this and COPII vesicles, probably in order to act as tether, facilitating docking and fusion (Zong et al., 2012). Interestingly, the overexpression of all TRAPPII subunits disrupts the architecture of microtubules (Westlake et al., 2011; Zong et al., 2012) and fibroblast from a

patient with mutations in *TRAPPC9* possessed an increased number of centrosomes (Gan et al., 2014).

Lastly, Trappc9 has been associated with cell division, though the specifics of such a role are not known yet. The *drosophila* Trappc9 orthologue Brunelleschi is required for cleavage furrow ingression during cytokinesis, where mutant alleles cause the failure of male meiotic cytokinesis due to the improper localisation of Rab11 (Robinett et al., 2009). Similarly, the plant orthologue Trs120 is required for cell plate biogenesis during cell division (Rybak et al., 2014).

In summary, Trappc9 appears to have many roles in the cell, all of which could be more or less directly linked with the microcephaly phenotype observed in affected individuals.

1.5 Aims

The human microcephaly and intellectual disability disorder that develops with homozygous loss-of-function mutations of *TRAPPC9* has a severe impact on the quality of life of the affected individuals and their families. Several disorders share common traits with the *TRAPPC9*-associated condition and many of them are equally poorly understood. Microcephaly in particular is a complex condition that can derive from disruptions in a number of genes, affecting multiple pathways and systems.

A very useful tool to study the underlying mechanisms of human disorders is to generate animal models that, despite their limitations, can help understand the aetiology and progression of certain conditions. Animal models for microcephaly have been generated by creating targeted mutations in microcephaly-associated genes but, despite the emergence of certain common themes (e.g. involvement of centrosome-related genes), our knowledge

of brain development and functioning is still limited and many childhood conditions and disorders cannot be prevented.

In order to model the human disorder, I aim to analyse a newly generated KO mouse line for Trappc9 with the intention of investigating the brain abnormalities characteristic of this disorder and, using *in vitro* models, to explore the cellular basis of *TRAPPC9*-induced microcephaly.

I also aim to investigate the epigenetic regulation of *Trappc9* within the *Peg13*/*Kcnk9* imprinting locus in comparison to recently published data for both mouse and human loci.

In chapter 3 I will investigate the structure of murine *Trappc9* in the context of the *Peg13* locus, analysing the mRNA structure observed empirically against the information available on genome databases. I will also describe my investigation of *Trappc9* imprinting status via methylation analysis and allele quantification.

In chapter 4 I will discuss in depth the cellular functions of Trappc9 using cellular models of Trappc9 knockdown in immortalised cells, with particular emphasis on the role of this gene in neuronal differentiation and neurite elongation.

In chapter 5 I will describe the KO mouse model for Trappc9 and the associated microcephaly phenotype. I will also show how these mice exhibit a reduction in the number of cells positive for the progenitor cell marker Sox-2 in the hippocampus and a reduction in the number of cells positive for the glial marker Glial Fibrillary Acidic Protein (GFAP) in the corpus callosum and hypothalamus.

In chapter 6 I will move to the human *TRAPPC9*, describing a polymorphism of repetitive elements in the promoter region that might be involved in the regulation of expression of this gene with potential repercussions on brain functioning.

CHAPTER 2

Materials and methods

2.1 Animal husbandry and tissue dissection

Animal handling and experimentation were conducted in accordance with the UK Home Office under the Animal (Scientific Procedures) Act, 1986. C57BL/6N mice carrying a knock-in mutation to silence *Trappc9* (Tm1a, see chapter 5) were imported from the Sanger Institute (Cambridge, UK) and housed in ventilated environment chambers, with a 12 hr light-dark schedule and free access to food and water. Genotype-unrelated malformations (hydrocephalus, incomplete eye formation) were observed in a small number of mice in the first 2 generations and indicated background mutations in the original colony imported from the Sanger Institute. After 3 generations of breeding with C5BL/6J mice no further malformations were observed.

DNA, RNA and tissue samples were collected also from CD1 mice housed in the same conditions. RNA samples from C57BL/6J and JF1 intercrosses were kindly provided by Dr Philippe Arnaud (Université Clermont Auvergne, France).

Animals were culled by cervical dislocation or terminally anaesthetised via i.p. injection of Pentoject (Pentobarbitone Sodium 20% w/v) for intracardiac perfusion and tissue collection. The tissues were collected and processed for nucleic acid/protein extraction or fixed in Phosphate Buffered Saline (PBS - 10 mM Na_2HPO_4, 1.8 mM KH_2PO_4 137 mM NaCl, 2.7 mM KCl, pH 7.4) with 4% paraformaldehyde (PFA) for 24 hr for immunohistochemistry.

2.2 Antibodies and primers

DNA primers were designed according to target gene and application and ordered from Sigma Aldrich. Unless required by the application, the primers were designed with a CG content of 40-60%, 18-25 nucleotides in length and low potential for secondary structures. See Table 2.1 for primer sequences and target genes.

Primary and secondary antibodies were purchased from several sources. See Table 2.2 for details.

Anti-Trappc9 polyclonal custom made antibody was produced in rabbit by Dundee Cell Products Ltd (Scotland, UK) against peptides CESKRLDRATDKSG and RVESRPTNPSEGS to target amino acids 160-173 and 831-844 of murine Trappc9, respectively. The antibody was isolated from antisera by immunoaffinity chromatography using antigens coupled to agarose beads. Several purification fractions were produced and the clone R61_RVE_1.1 was selected for its proven specificity in western blot applications.

2.3 Molecular biology techniques

2.3.1 DNA and RNA extraction

DNA extraction was performed from fresh tissues by incubating the tissue of interest in Tail lysis buffer (100 mM TrisHCl pH 8.0, 5 mM EDTA, 0.2% SDS, 200 mM NaCl) supplemented with 100 μg/mL proteinase K (Sigma-Aldrich #P6556) overnight at 55˚C and by centrifuging the sample at 16000g for 2 minutes. The supernatant was diluted 1:20 in nuclease-free water and incubated at 95˚C for 10 min to inactivate the proteinase K and then used as template. DNA solutions and DNA fragments in agarose gel were purified with Wizard® SV Gel and PCR Clean-Up System (Promega #A9282).

RNA extraction was performed from frozen unfixed tissues using the RNeasy MiniElute Cleanup Kit (Qiagen #74204).

2.3.2 Polymerase chain reaction (PCR)

PCR amplification was carried out using GoTaq® G2 Hot Start Polymerase (Promega #M74408, 1.2 U per reaction) in a green master mix (Promega #M7422) or in a colourless master mix (Promega #M7432) with the addition of MgCl2 at a final concentration of 1.5 mM, primers at a final concentration of 1.25 mM and DNA/cDNA template (amount used varied between samples according to the source and application).

A thermal cycler (G-Storm GS1) performed 30-40 cycles of a 2 min 95˚C denaturation step, an annealing step at 50-60˚C (see methods in result chapters) for 30 sec and a 30-60 sec 72˚C extension step.

PCR fragments were analysed by gel electrophoresis on 0.8-2.5% molecular grade agarose (Bioline #BIO-41025) supplemented with ethidium bromide or Midori Green Direct (Geneflow #S6-0018) in Tris-acetate-EDTA (TAE) buffer (40 mM Tris pH 7.6, 20 mM acetic acid, 1mM EDTA).

2.3.3 Cloning and bacterial transformation

PCR fragments were cloned into TOPO TA Cloning® Kit (Invitrogen #45-0641) according to manufacturer's instructions and transformed into NEB® 5-alpha Competent *E. coli* (New England Biolabs #C2987). *E.coli* were grown on LB-agar plates and in LB-broth for amplification and plasmid extraction via Plasmid mini, midi and maxi kits (Qiagen #12123, #12143 and #12162).

Primer name	Sequence	Orientation	Gene	Position	Designed for
Trappc9-R1	GAACACCTTGATGCCTG CTC	Reverse	Trappc9	Exon 23	Mouse
Trappc9-F3	GAGAACTACACTGCCAA GTG	Forward	Trappc9	Exon 10	Mouse
Trappc9-R3	TGGTGGTGAGAAGCTTT GAG	Reverse	Trappc9	Exon 15	Mouse
Pr_02 Fw	TCACAGCGTGCACTCTTC AT	Forward	Trappc9	Exon 2	Rat
Pr_02 Rv	CATCACCCTGCAGCCCA AA	Reverse	Trappc9	Exon 2	Rat
Pr_04 Fw	GTTGTTGGGTCTGAAAA GAC	Forward	Trappc9	Exon 2a (mouse)	Rat
Pr_04 Rv	GGGTCAATGAGAACTTC TTGC	Reverse	Trappc9	Exon 5	Rat
Pr_05 Rv	GCTGGTGTCAGGATTTA TGC	Reverse	Trappc9	Exon 6	Rat
Pr_06 Fw	CAGACCCACAAACCCTT CT	Forward	Trappc9	Exon 17	Mouse
Pr_15 Rv	CTCTTGGTGGACATGCT CT	Reverse	Trappc9	Exon 11	Mouse
GAPDH-F1	CCTTCATTGACCTCAACT AC	Forward	GAPDH	-	Mouse
GAPDH-R1	GCCATGCCAGTGAGCTT C	Reverse	GAPDH	-	Mouse
Primer 1	TCATACACATACGATTTA GGTGACACTATAGAGCG GCCGCCTGCAGGAAA	Forward	5'- race	5'- end	-
Tr203-R2	CTTTATTCACACTGTCCC TGA	Reverse	Trappc9	203 - last exon and 3' UTR	Mouse
Tr204-R2	CTGCTAAGGAAAGACGC ACA	Reverse	Trappc9	204 - last exon and 3' UTR	Mouse
LacZ F4	TACGCCAATGTCGTTATC CA	Reverse	LacZ	-	-
LacZ R4	GCGAATACCTGTTCCGT CAT	Forward	LacZ	-	-
Pr_25 RV	GACGACAGTATCGGCCT CAG	Reverse	LacZ	-	-
Tr_VNTRexon1_Fw	CCTGCGATCCTGGAGGC	Forward	Trappc9	Variant 001 UTR	Human
Tr_VNTRexon1_Rv	GTGAAGCTCAGGGGTG GAG	Reverse	Trappc9	Variant 001 UTR	Human
Tr_VNTRintr_Fw	GAACTGGGCCTCCTTCC AG	Forward	Trappc9	intron 1	Human
Tr_VNTRintr_Rv	ATCCGTCCCGGGTTTTG C	Reverse	Trappc9	intron 1	Human
CpG1_02Fw	GGTGGTTTGGAGGTTTT AGGTTGTTTAG	Forward	Trappc9	CGI1	Mouse
CpG1_02Rv	CCAAACAACTAACAACA AAATAACAAACTATCC	Reverse	Trappc9	CGI1	Mouse
CpG1_03Fw	TTTTTTGTTAATTTATGTT TTTTTTTGTTTGTTTGG	Forward	Trappc9	CGI1	Mouse
CpG1_03Rv	AAATCTCATTCCAAATTA ACTACACATTAAAC	Reverse	Trappc9	CGI1	Mouse

CpG2_01Fw	AGAGTGTGGTATGTTTTTGTTTATTAGTGTTAATG	Forward	Trappc9	CGI2	Mouse
CpG2_01RV	AACTTCTCAAAAATCTATAACCAATCTTTAAAC	Reverse	Trappc9	CGI2	Mouse
CpG2_02Fw	TTTGTTTTGTGAGTTAGTTTAGTGTG	Forward	Trappc9	CGI2	Mouse
CpG2_02Rv	TCCAAACACTTAAACTCCAACACAATAAAAAAAAAC	Reverse	Trappc9	CGI2	Mouse
gDNA1_02_Fw	GAGGTTCCAGGCTGCTCAGT	Forward	Trappc9	CGI1	Mouse
gDNA1_02_Rv	AACGACTGGCAACAGGGTAG	Reverse	Trappc9	CGI1	Mouse
gDNA2_02_Fw	TCCGTGAGCCAGCTCAGTGTG	Forward	Trappc9	CGI2	Mouse
gDNA2_02_Rv	TCCAGGCGCTTGGACTCCAAC	Reverse	Trappc9	CGI2	Mouse
Tr_upex2n1_Fw	TGAGTTCTGCAAGGCAGAGA	Forward	Trappc9	Intron upstream of 5'-UTR	Mouse
Trappc9meth1-Fb	ATTTTGAAGAAGTTTTTTTAGAG	Forward	Trappc9	CGI2	Mouse
Trappc9meth1-R	CTCTTTTCCCTTTAAACAAAC	Reverse	Trappc9	CGI2	Mouse
Trappc9meth1-S	TTCCCTTTAAACAAACCCTC	Sequencing	Trappc9	CGI2	Mouse
Trappc9meth2-F	TGATGGTGATGAGGTTTATT	Forward	Trappc9	CGI2	Mouse
Trappc9meth2-Rb	AAACTTCTTCAAAATCTACAAAC	Reverse	Trappc9	CGI2	Mouse
Trappc9meth2-S	GGTGATGAGGTTTATTA	Sequencing	Trappc9	CGI2	Mouse
Trappc9meth3-F	GTAGGGTGATGTGGTTGAG	Forward	Trappc9	CGI2	Mouse
Trappc9meth3-Rb	ACCCTTAAACTCCAACACAAT	Reverse	Trappc9	CGI2	Mouse
Trappc9meth3-S	GGTGATGTGGTTGAGTA	Sequencing	Trappc9	CGI2	Mouse
Trappc9_SNP1-Fb	CAGCAAGTACAAGAACGCCG	Forward	Trappc9	Exon 7	Mouse
Trappc9_SNP1-R	CTCCATGCCACGCTTCTG	Reverse	Trappc9	Exon 7	Mouse
Trappc9_SNP1-S	CGCTTCTGAATCGCTAGG	Sequencing	Trappc9	Exon 7	Mouse

Table 2.1

Table of PCR primers.

2.3.4 Reverse transcription

RNA conversion to cDNA was accomplished by incubating the RNA with random hexamers (Fermentas #S0142) and dNTPs at 65˚C for 5 min and then on ice for 1 min, followed by the addition of reverse transcriptase buffer, DTT 0.1M, RiboLock RNAse inhibitor (Thermo Fisher Scietific #EO0381) and SuperScript® III Reverse Transcriptase (Invitrogen #18080-

044). The mixture was subjected to 5 min at 25˚C, 60 min at 50˚C, 15 min at 70˚C and 1 min at 4˚C. After the addition of 2.5 U of RNAse H (New England Biolabs #M0297) at 37˚C for 20 min, the samples were diluted 1:10-1:20 in nuclease-free water and used as template for PCR amplification.

2.3.5 5′- race

This method allows the tagging of 5′ ends of 5′-cap RNAs (mRNAs) by incorporating oligonucleotide sequences complementary to a primer (Primer 1, see Table 2.1) that in combination with a gene-specific primer allows the amplification of target transcripts. Using the ExactSTART™ Eukaryotic mRNA 5′&3′ RACE Kit (Epicentre #ES80910) in accordance with manufacturer's instructions, the samples were first treated with alkaline phosphatase (15 min at 37˚C) to remove the 5′-phosphate groups from 5′-mono-, di-, and triphosphorylated RNAs in the total RNA sample, leaving unaltered RNAs containing 5′-cap structures. After a step of purification (phenol:chlorophorm extraction) the samples were then treated with Tobacco Acid Pyrophosphatase (TAP) (30 min at 37˚C) to remove the 5′-cap structures, leaving an end product of mRNA with a 5′ monophosphate. A T4 RNA ligase (30 min at 37˚C) was then responsible for the ligation of 5′-RACE Acceptor Oligo. The first strand cDNA synthesis proceeded with the addition of the cDNA Synthesis Primer (1 hr at 37˚C, 10 min at 85˚C and 55˚C until next step), which consists of an oligo(dT) sequence with a PCR priming sequence (different from the PCR priming sequence of the 5′-RACE Acceptor Oligo) at its 5′ end. The last step used a PCR amplification (18-21 cycles of 95˚C for 2 sec, 60˚C for 20 sec and 72˚C for 3 min) to generate the second strand of cDNA and amplify the product, which was then used for gene-specific amplification with Trappc9 primers.

2.3.6 Bisulphite DNA conversion

This technique allows the conversion of unmethylated cytosines into uracils, leaving the methylated cytosine intact. Using the EZ DNA Methylation-Gold™ Kit (Zymo Research #D5005) in accordance with manufacturer's instructions the gDNA samples were treated with the CT conversion reagent and incubated for 10 min at 98˚C, for 2.5 hr at 64˚C and stored at 4˚C. Purification and desulphonation preceded the PCR amplification and subsequent cloning into TOPO vectors.

2.3.7 Combined Bisulphite Restriction Analysis (COBRA)

Following bisulphite conversion of DNA and PCR amplification of specific fragments (CGI1 and CGI2 in this thesis, see chapter 3), the samples were digested with restriction enzymes TaqI (Promega #R615A) and BstUI (New England Biolabs #R0518) at 65˚C and 60˚C, respectively. These enzymes recognise the restriction sites TCGA and CGCG, which in bisulphite converted gDNA remain intact only if that particular site is methylated. Therefore a digested product means the DNA fragment is methylated, while an undigested product indicates the fragment is unmethylated.

2.3.8 Pyrosequencing

The samples were PCR amplified using a set of primers (of which one was biotinylated at the 5' end) designed to obtain a product of ~100 bp. PCR samples were purified in a vacuum station in which biotinylated fragments are bound to Streptavidin-coated Sepharose beads, washed and denatured in order to generate single-strand DNA. Another set of primers (sequencing primers), designed to anneal to the opposite strand to the biotinylated primer, were then used for the pyrosequencing analysis with PyroMark Gold

Q96 SQA Reagents (Qiagen #972812) on the PyroMark Q96 ID sequencing and quantification platform.

2.3.9 Genotyping of human samples

Samples from healthy individuals and from a cohort of individuals with schizophrenia, as well as human cell line gDNA samples used in chapter 6, were kindly donated by Prof John Quinn (University of Liverpool). Subjects were all of German or central European descent and provided written informed consent. Patients with schizophrenia were selected based on diagnosis under the Diagnostic and Statistical Manual of Mental Disorders (DSM-IV) and International Classification of Disease-10 (ICD-10).

2.3.10 Sequencing

DNA samples were sequenced via Sanger sequencing externally by DBS Genomics (Durham University, UK). The samples and primers were supplied as required by the company.

2.4 Protein analysis

2.4.1 Protein extraction

Proteins were extracted from frozen tissues or fresh cell pellets washed with PBS using RIPA lysis buffer (25 mM NaPO4 buffer pH 7.5, 25 mM NaF, 25 mM β-Glycerolphosphate, 100 mM NaCl, 5 mM EGTA, 0.5% deoxycholate, 0.5% NP40, 0.1% SDS, 0.01% sodium azide) supplemented with protease/phosphatase inhibitor cocktail (Cell Signaling #5872). Lysates were centrifuged at 16000g at 4˚C to remove insoluble pellets and the supernatant passed through a 25G needle to break gDNA strings.

Protein quantification was carried out with the addition of Bradford reagent (Sigma-Aldrich #B6915). After 5 min incubation the absorbance was measured at 595 nm in a spectrophotometer. Samples were compared with a standard BSA curve made with bovine serum albumin (1-5 μg).

2.4.2 Western blot

Protein lysates were incubated for 10 min at 70˚C in NuPAGE® LDS sample buffer (Life Technologies #NP0007) with NuPAGE® reducing agent (Life Technologies #NP0009). The samples were loaded onto NuPAGE® Bis-Tris polyacrylamide 4-12% gradient gels (Life Technologies #NP0335) and run in NuPAGE® MOPS running buffer (Life Technologies #NP0001) supplemented with NuPAGE® antioxidant (Life Technologies #NP0005). Proteins were then transferred onto Immobilion® IF PDVF 0.45 μm pore membranes (Millipore #IPFL00010), previously activated in methanol, in NuPAGE® transfer buffer (Life Technologies #NP0006) supplemented with 10% methanol and antioxidant.

Blocking of the membrane was performed with Odyssey® blocking buffer (LI-COR #927-40000) followed by an overnight incubation with primary antibodies in blocking buffer. The next day the membranes were washed in PBS-T 0.1% and incubated with fluorescent antibodies (see Table 2.2) in blocking solution supplemented with 0.1% Tween® 20 (Sigma-Aldrich #1379) for 50 min, washed in PBS-T 0.1% and PBS, air dried and scanned with an Odyssey Imaging System (LI-COR).

Antibody against	Distributor and catalogue number	Source	Application and dilution	Type of antibody
Trappc9	Proteintech #16014-1-AP	Rabbit	IHC 1:1000 WB 1:1000	Primary, polyclonal
Trappc9	Dundee Cell Diagnostics, custom made R61_RVE_1.1	Rabbit	WB 1:1000	Primary, polyclonal
β-Actin	Abcam #ab13822	Chicken	WB 1:8000	Primary, polyclonal
GFAP	Dako #z0334	Rabbit	IHC 1:2000	Primary, polyclonal
IκBα	Cell Signaling #4812	Rabbit	WB 1:1000	Pimary, monoclonal
p65	Cell Signaling #8242	Rabbit	WB 1:1000 IF 1:1000	Primary, monoclonal
p-p65	Cell Signaling #3033	Rabbit	WB 1:1000	Primary, monoclonal
Sox-2	R&D Systems #AF2018	Goat	IHC 1:500	Primary, polyclonal
Alexa 488 anti-Rabbit IgG	Molecular Probes #A21206	Donkey	IF 1:800	Secondary
IRDye 680LT anti-rabbit IgG	LI-COR #92668023	Donkey	WB 1:5000	Secondary
IRDye 800CW anti-chicken IgG	LI-COR #92632218	Donkey	WB 1:10000	Secondary

Table 2.2
Table of antibodies.

2.5 Cell culture procedures

2.5.1 Cell maintenance

All cell culture procedures were carried out in a sterile environment with cell-culture grade reagents. The cells were grown at 37˚C in 5% CO2 and cultured 1-3 times a week depending on the population doubling time.

PC12 cells were grown in suspension in Dulbecco's Modified Eagle's Medium (DMEM – Sigma-Aldrich #D6171) supplemented with 2 mM L-glutamine (Sigma-Aldrich #G7513), 1 mM sodium pyruvate (Sigma-Aldrich #S8636), 100 U penicillin / 0.1 mg/L streptomycin (Sigma-Aldrich #P0781), 10% horse serum (Sigma-Aldrich #H1138) and 5% foetal bovine serum (Sigma-Aldrich #F9665). They were subcultured twice a week by gentle centrifugation and replacement of culture medium.

Neuro-2A (N2A) cells, HEK293 cells, SH-SY5Y and mouse skin embryonic fibroblasts (EMFIs) were grown at 37˚C in Dulbecco's Modified Eagle's Medium (DMEM – Sigma Aldrich #D6171) supplemented with 2 mM L-glutamine (Sigma-Aldrich #G7513), 1 mM sodium pyruvate (Sigma-Aldrich #S8636), 100 U penicillin / 0.1 mg/L streptomycin (Sigma-Aldrich #P0781), 15% foetal bovine serum (Sigma-Aldrich #F9665) and 0.1 mM non-essential amino acids (Life Technologies #11140035). N2A cells were subcultured three times a week (80-90% confluency) by a wash with PBS (Sigma-Aldrich #D8537) followed by the addition of new medium, pipetting the solution up and down on the cells.

HEK293, SH-SY5Y and EMFIs were subcultured when 80-90% confluent by being washed with PBS (Sigma-Aldrich #D8537) prior to the addition of trypsin-EDTA solution (Sigma-Aldrich #T3924), followed by the addition of fresh culture medium.

2.5.2 Cell differentiation

To induce cell differentiation PC12 cells were counted with a haemocytometer and subcultured on rat collagen (Sigma-Aldrich #C7661) coated plates at a density of $8x10^4$ cells/cm^2 and cultured in serum-free culture medium supplemented with 10 ng/mL NGF (Sigma-Aldrich #N0513) for up to 9 days.

N2A cells were counted with a haemocytometer and subcultured on cell culture plates at a density of $5x10^4$ cells/cm^2 and grown in culture medium with 2% serum supplemented with 20 μM retinoic acid (RA) (Sigma-Aldrich #R2625) for 24 hr.

2.5.3 Isolation of skin embryonic fibroblasts (EMFIs)

Mouse embryos E12.5 were dissected from the uterus into a Petri dish containing sterile PBS, the skin isolated and rinsed in PBS. The samples of skin were incubated at 37˚C in trypsin-EDTA and fragmented. DNAseI (Fermentas #EN0521) was added to a final concentration of 100 U/mL. When the tissue was fully dissolved, the cells were

resuspended in culture medium and plated onto cell culture dishes. The cells stopped dividing around the third passage.

2.5.4 Gene silencing

siRNA gene silencing was performed by transfecting PC12 cells plated on collagen coated plates with a pool of siRNA oligonucleotides (ON-TARGETplus siRNA, Dharmacon #L-080907-02-0005) (Table 2.3) combined with Lipofectamine® RNAiMAX (Thermo Fisher Scientific #1377830) in serum-free culture medium. The cells were incubated with the transfection mixture for 4 hr and then an equal volume of 2X-serum medium was added to the wells. After 72 hr the cells were harvested and processed for protein extraction and analysis. Knockdown cells were compared to cells transfected with non-targeting oligos (Dharmacon #D-001810-10-05).

shRNA gene silencing was performed by generating a lentivirus containing Mission® shRNA vectors (containing a puromycin resistance gene) specific for Trappc9 (Table 2.3) and by transducing N2A cells with this virus.

Mission® shRNA vectors were transfected into HEK293 cells in combination with packaging plasmid psPAX2 and envelope plasmid pDMD2.G in a calcium phosphate method ($CaCl_2$ + HEPES). The culture medium was changed after 24 hr and the virus-containing supernatant collected after 72 hr. The virus solution was then concentrated 10X with Lenti-X™ Concentrator (Millipore #PT4421-2).

N2A cells were plated at a density of $5x10^4$ cells/cm^2 and incubated with different concentrations of virus in culture medium supplemented with 8 μg/mL polybrene. After 24 hours the medium was replaced with fresh medium. After 72 hr the cells were subjected to selection with 3 μg/mL puromycin (Sigma-Aldrich #P8833). After 7 days in puromycin the cells were harvested and processed for protein extraction and analysis. Knockdown cells were compared to cells transfected with non-targeting vector.

2.5.5 Viability assay

Cell viability was assessed using the Prestoblue® reagent (Thermo Fisher Scientific #A13261). The cells were seeded on five 96-well cell culture plates on DAY 0 at a density of 700 cells/well. Prestoblue® was added to one plate after one hour from seeding and incubated for four hours at 37˚C in the dark. At the end of the incubation the absorbance was measured at 570 nm and the values used as DAY 0 measurements. One plate was analysed each day to a total of four days. The values were normalised to DAY 0.

2.5.6 Luciferase reporter gene assay

The cells were seeded on cell culture plastic and transfected with PGL3B, PGL3C, PGL3P or PGL3P + insert in combination with Renilla plasmid after 24 hours with TurboFect® transfection reagent (Thermo Fisher Scientific #R0531). At 48 hours after transfection, the cells were lysed and analysed with Dual-Luciferase® Reporter Assay System (Promega #E1910) in a Glomax 96 Microplate Luminometer (Promega).

RNA type	Clone	Sequence	Target
siRNA	J-080907-10	GCCAAGGACGCAUGCGGAA	Trappc9 (Rat)
	J-080907-18	AGGAGAAGUUGUACGGCGA	
	J-080907-19	CCAGUGAGUGCCAGCGAAU	
	J-080907-20	AAGCGGAUCUGCUCGGUGA	
	Non-targeting pool (control)	UGGUUUACAUGUCGACUAA UGGUUUACAUGUUGUGUGA UGGUUUACAUGUUUUCUGA UGGUUUACAUGUUUUCCUA	
shRNA	TRCN0000246674 (74kd)	CCGGGCTCGGCTTCAGTCATTTATCCTCG AGGATAAATGACTGAAGCCGAGCTTTTTG	Trappc9 (mouse)
	TRCN0000246676 (76kd)	CCGGTTCGCCAATCATCGCACATAACTCG AGTTATGTGCGATGATTGGCGAATTTTTG	
	TRCN0000246678 (78kd)	CCGGCCGAGGACATCATTGACAAATCTCG AGATTTGTCAATGATGTCCTCGGTTTTTG	
	Non-targeting (control)	No shRNA insert	

Table 2.3

Table of siRNA oligonucleotides and shRNA vector hairpin inserts used for gene silencing on PC12 and N2A cells.

2.6 Cytology and histology

2.6.1 Immunofluorescence on N2A cells

The cells were grown on glass cover slips coated with poly-L-lysine (Sigma-Aldrich #P4707) and fixed in 100% methanol at -20˚C for 20 min. After being washed in PBS, the cells were blocked in a solution containing 0.25% triton-X and 10% donkey normal serum. They were then incubated overnight at 4˚C with the blocking solution supplemented with the primary antibody. The next day they were washed in PBS and incubated with the secondary antibody (Alexa 488 anti-Rabbit IgG, see Table 2.2) plus DAPI 1:1000 (Sigma-Aldrich #D9542) for 60 min. After being washed in PBS, the coverslips were mounted on glass slides with Fluoro-Gel anti-fade mounting medium (Electron Microscopy Sciences #1798510).

2.6.2 Immunohistochemistry on brain tissue

Tissues were extracted after intracardiac perfusion of 4% PFA/PBS and fixed for at least 24 hr at 4˚C in 4% PFA/PBS. They were then dehydrated in 30% sucrose/PBS until they sank to the bottom of the container and sectioned with a cryostat onto glass slides. Antigen retrieval was achieved by incubating the slides in 10 mM sodium citrate at 65˚C for 45 sec. After 3x5 min washes in PBS, the endogenous peroxidase activity was blocked by incubating the slides in 100% methanol supplemented with 0.3% hydrogen peroxide for 5 min. The sections were blocked in a blocking solution containing 10% rabbit (goat kit, see below) or goat (rabbit kit, see below) normal serum and 0.25% triton-X for 1 hr. They were then incubated overnight in blocking solution supplemented with primary antibody. The following day the slides were washed in PBS and incubated with reagents supplied in the Vectastain Elite ABC HRP kits (Vector Laboratories, rabbit kit #PL-6101, goat kit #PK-

6105). The 1hr incubation with blocking solution containing the peroxidase-conjugated secondary antibody was followed by the formation of avidin-biotin complex (30 min) and by a 30 min incubation with 3,3′-diaminobenzidine (Sigma-Aldrich # D8001) dissolved in distilled water. The sections were then dehydrated in an ethanol series (70%, 90%, 100% and 100%) and cleared in Histo-Clear II (National Diagnostic #HS-202). The slides were mounted with Eukitt® quick-hardening mounting medium (Sigma-Aldrich #0389) or with Ecomount (Biocare #EM897L).

2.6.3 *In situ* hybridisation on brain tissue

The staining of *Trappc9* mRNA on brain tissue was carried out with the RNAscope® 2.5 HD Assay-RED (Advanced Cell Diagnostics #322350) method. Following the manufacturer's instructions, the tissues were fixed in 4% PFA/PBS for a maximum of 24 hours, dehydrated in 30% sucrose/PBS and sectioned with a cryostat. Prior to the staining procedure, the activity of endogenous peroxidases was blocked by the addition of RNAscope® Hydrogen Peroxide solution for 10 min at room temperature. Antigen retrieval was carried out by submerging the slides in a boiling RNAscope® Target Retrieval solution for 5 min. After being washed with distilled water and 100% ethanol they were air-dried. They were then treated with RNAscope® Protease Plus solution and incubated for 30 min at 40˚C.

The slides were incubated with RNAscope® Probe Mm-Trappc9-E1E2 (Advanced Cell Diagnostics #465291) and RNAscope® Negative Control Probe (Advanced Cell Diagnostics #310043) for 2 hr at 40˚C. After being washed with RNAscope® Wash Buffer they were then incubated with Hybridize AMP 1 (30 min at 40˚C), Hybridize AMP 2 (15 min at 40˚C), Hybridize AMP 3 (30 min at 40˚C), Hybridize AMP 4 (15 min at 40˚C), Hybridize AMP 5 (30 min at room temperature) and Hybridize AMP 6 (15 min at room temperature) with washes in between steps. The slides were counterstained with haematoxylin or directly

mounted with Ecomount (Biocare #EM897L) after being air-dried and quickly dipped in Histo-Clear II.

2.7 Statistical analysis

All data are generally represented as mean ± standard error of the mean (SEM), unless stated otherwise. The use of Student's T-test was based on the result of an F-test, used to determine the variance between samples. All statistical analysis was performed using Microsoft Excel or the SigmaPlot software. The statistical significance is expressed with the p-value (p), considered significant when $p<0.05$ (*), $p>0.01$ (**), $p<0.001$ (***) and $p<0.0001$ (****).

CHAPTER 3

Trappc9 gene structure and regulation

3.1 Introduction

Trappc9 is located on mouse chromosome 15qD3 in a gene cluster that comprises of the ncRNA *Peg13* (located within an intron of *Trappc9*), *Chrac1* and *Ago2* located upstream, and *Kcnk9* located downstream of *Trappc9* (Fig 3.1). *Trappc9*'s genomic sequence contains 23 exons and, according to the genomic database Ensembl, can produce four different transcript variants (Fig 3.2).

CpG islands are located within the sequences of all the genes in the cluster and only the one located within the promoter region of *Peg13* is differentially methylated (Smith et al., 2003). As no evidence has been found of other methylated sites, this differentially methylated region (DMR) has been hypothesised to be the putative imprinting control region (ICR) of the cluster. In fact, all the genes in this cluster have been reported to be imprinted, with *Peg13* being the only gene in this cluster to be expressed exclusively from the paternal allele (Smith et al., 2003), and the other genes being preferentially expressed (to different degrees) from the maternal allele (Perez et al., 2015). It is hypothesised that the methylation in *Peg13* is responsible for the imprinting of the neighbouring genes, but the mechanism is still unclear.

The imprinting status of *Trappc9* has been investigated in the past years by several research groups using a variety of techniques. The conclusions of the different reports are, however, contrasting as some reported *Trappc9* imprinted and others did not. The earliest

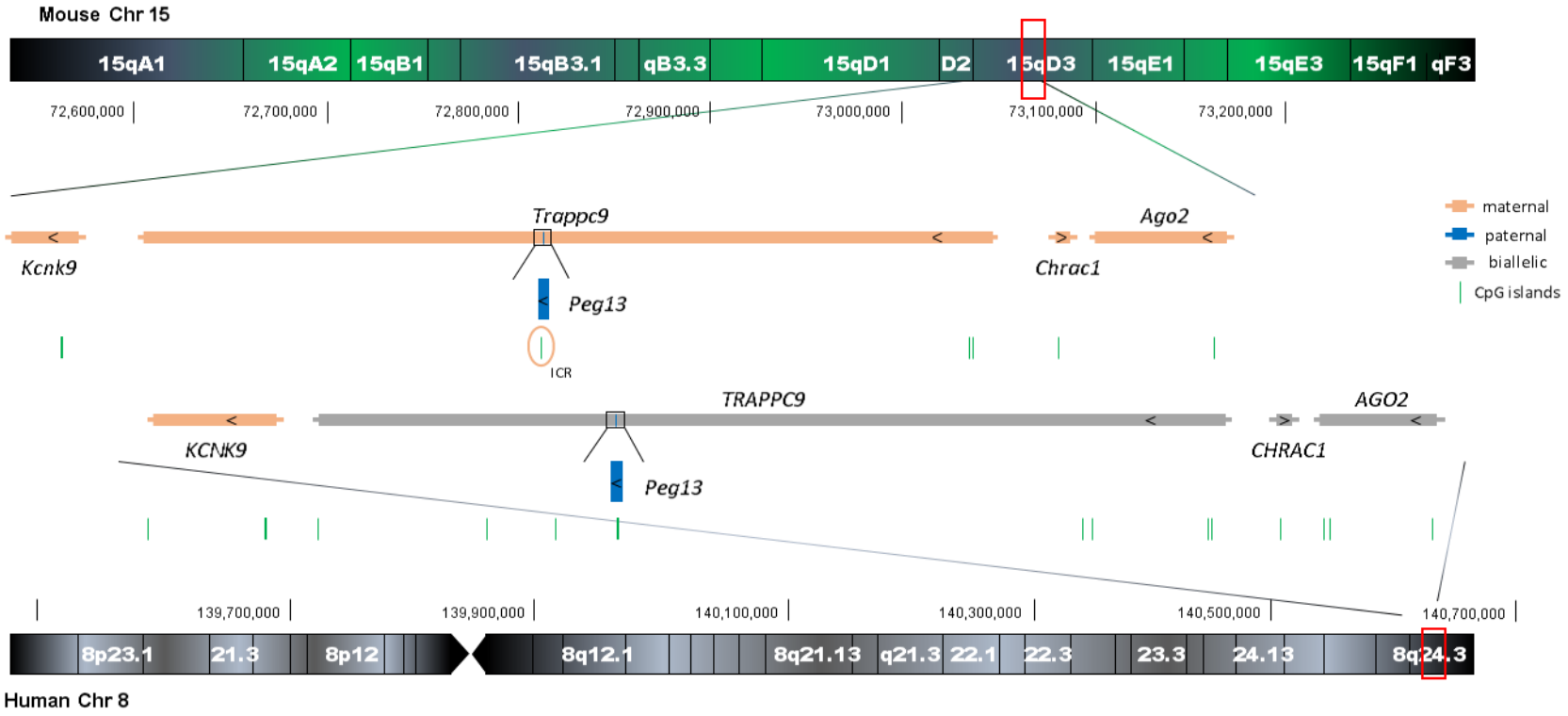

Figure 3. 1

Scheme of the mouse (top) and human (bottom) *Peg13* imprinted gene cluster. DNA methylation at *Peg13* on the maternal allele (orange circle) suppresses transcription while the unmethylated paternal allele is expressed. Further epigenetic modifications (including chromatin modifications), at the putative imprinting control region (ICR) as well as neighbouring genes, mediate the imprinted expression of the gene cluster in mouse, or *KCNK9* only in human. Trappc9 in particular shows a preferentially maternal expression in the brain and a biallelic expression in peripheral tissues. Orange bars represent expression from the maternal allele, blue ones from the paternal and grey bars represent biallelic expression. Green vertical lines represent CpG islands. Arrows indicate direction of transcription. Individual exons not shown. *Trappc9* is composed of 23 exons, with *Peg13* located between exon 17 and 18. This scheme was inspired by Court at al., 2014 and UCSC genome browser.

report on the imprinting of *Trappc9* and its neighbouring genes dates back to 2003, when for the first time a methylation in the maternal allele of *Peg13* and the gene expression from the paternal allele was described (Smith et al., 2003). The cloning and sequencing of a single nucleotide polymorphism (SNP) in *Trappc9*'s sequence from reciprocal crosses of *Mus musculus* and *Mus M. castaneus* revealed a biallelic expression of this gene (Smith et al., 2003). While cloning and sequencing are among the canonical methods for the analysis of imprinting, due to their technical limitations (e.g. false results from cloning bias; large number of sequenced clones required for statistical analysis), subsequent reports applied RNA sequencing for high throughput screenings and found *Trappc9* maternally expressed in the mouse brain and biallelically expressed in peripheral tissues (Wang et al., 2008; Gregg et al., 2010; Babak et al., 2015; Perez et al., 2015; Bouschet et al., 2016). Similarly to cloning, RNA sequencing analyses can produce false results, as the fragmentation of the RNA required by the method and the subsequent annealing of random hexamer primers can result in depletion of reads at both 5′ and 3′ ends (Hansen et al., 2010).

The work described in this chapter investigates the genetic structure and expression of *Trappc9*. As several transcript variants have been described for this gene, and given that these variants can give rise to structurally different protein isoforms, I hypothesised that different isoforms could have different functions in a tissue, region and cell specific manner. For this reason, my first aim was to successfully target and distinguish the different transcript variants, in order to apply localisation studies in different tissues and investigate the expression patterns.

In addition, in light of the contradictory literature available on the subject, I decided to investigate the imprinting status of *Trappc9* via pyrosequencing analysis of brain RNA from *Mus musculus* and *Mus M. molossinus* reciprocal crosses. Pyrosequencing is a "sequencing by synthesis" method that eliminates the biases inherent to the cloning

procedure and provides a lower cost per analysed base compared to Sanger sequencing. Using this method in combination with the bisulphite conversion of gDNA, I also aimed to shed some light into the molecular basis of this imprinting by analysing the methylation status of two CpG islands located within *Trappc9*'s sequence.

3.2 Methods

PCR. For Fig 3.2C 30 cycles were performed at an annealing temperature of 56˚C for primer combinations Pr_04Fw + Pr_04Rv, Pr_04Fw + Pr_05Rv, Pr_02Fw + Pr_04Rv, Pr_02Fw + Pr_05Rv, Pr_06Fw + Tr203Rv, Pr_06Fw + Tr204Rv. For Fig 3.5 30 cycles were performed at an annealing temperature of 58˚C for primers Primer_1 + Pr_05Rv. For Fig 3.7 40 cycles at an annealing temperature of 50˚C were performed for primers Trappc9_SNP1-Fb + Trappc9_SNP1-R. For Fig 3.11 56˚C and 30 cycles were used for primers CpG1_02Fw + CpG1_02Rv, CpG1_03Fw + CpG1_03Rv, CpG2_01Fw + CpG2_01Rv, CpG2_02Fw + CpG2_02Rv; 60˚C annealing temperature was used for primers gDNA1_02Fw + gDNA1_02Rv, gDNA2_02Fw + gDNA2_02Fw + gDNA2_02Rv. For Fig 3.12-14 an annealing temperature of 52˚C and 40 cycles were used for Trappc9meth1-Fb +Trappc9meth1-R, 50˚C annealing temperature and 40 cycles were used for Trappc9meth2-F + Trappc9meth2-Rb, Trappc9meth3-F + Trappc9meth3-Rb. For Fig 3.15 30 cycles and an annealing temperature of 56˚C were used for primers Tr_upex2n1_Fw + Pr_02Rv, GAPDH_F1 + GAPDH_R1.

Western blot. For Fig 3.6 and 3.8 anti-Trappc9 primary antibody (#16014-1-AP) was used at a 1:1000 dilution, anti-β-actin primary antibody (#ab13822) was used at a 1:8000 dilution.

3.3 Results

3.3.1 Observed transcript variants

According to the Ensembl gene database, mouse *Trappc9* has four distinct transcript variants, numbered 201-204. The variants 201 and 202 are long variants that differ in the start site and an alternatively spliced exon (exon 5), therefore comprising of 22 exons (21 and 22 coding exons, respectively). Variants 203 and 204 are instead truncated forms, differing from one another of the 5′-UTR, the last exon, and in the above mentioned alternatively spliced exon, therefore comprising of 17 and 18 exons (16 and 17 coding exons), respectively (Fig 3.2A).

As different transcript variants could have different roles in the cell or within cell types/tissues, I first aimed to identify specific regions unique for each variant.

In contrast to the information available on Ensembl, however, no evidence of an alternative start site for 201 was found. Primers were designed to target the first coding exon in variant 202, named exon 2, and the first coding exon in variant 201, named a2 (Fig 3.2). PCR amplification was performed on brain and peripheral tissue cDNA with primers targeting exon a2 and exon 2 in combination with primers for exon 5 and exon 6 (see Table 1.1 for primer sequences). The separation and visualisation on agarose gel did not reveal any products targeting exon 2a, in either newborn brain and peripheral tissues and in adult brain (Fig 3.3). The primers targeting exon 2 produced bands in both brain and periphery.

In order to investigate the existence of exon a2 and the different start sites for *Trappc9* mRNA, a 5′ race cDNA synthesis was also performed. The method consists of tagging the 5′ and 3′ ends of RNA molecules with specific sequences complementary, after the cDNA

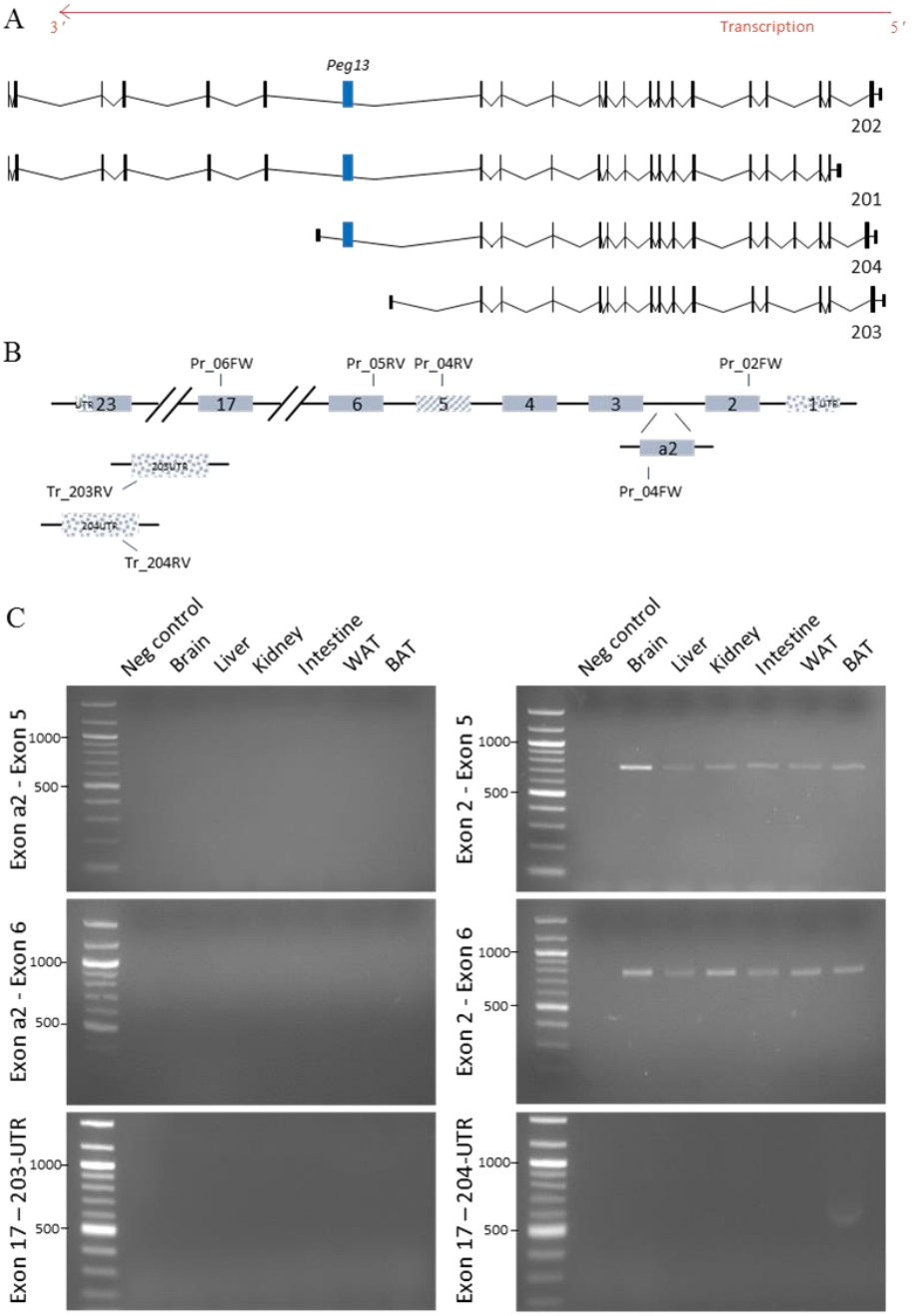

Figure 3. 2

A) Scheme of *Trappc9* transcript variants according to the Ensembl database. Exon 5 is supposed to be alternatively spliced and the variant 201 shows an alternative start site. B) Localisation of primers used in C) RT-PCR of exon a2 - exon 5/6 (expected 318 bp and 358 bp, respectively), exon 2 - exon 5/6 (expected 740 bp and 780 bp, respectively) and exon 17-UTR of variants 203 and 204 (expected 228 bp and 427 bp) in several tissues of newborn mouse. Exon a2 does not appear to be an alternative start site, exon 5 is expressed in all the tested tissues and no evidence of truncated transcript variants was found, both in the brain and in the periphery. See Table 2.1 for primer sequences and localisation. WAT: white adipose tissue; BAT: brown adipose tissue.

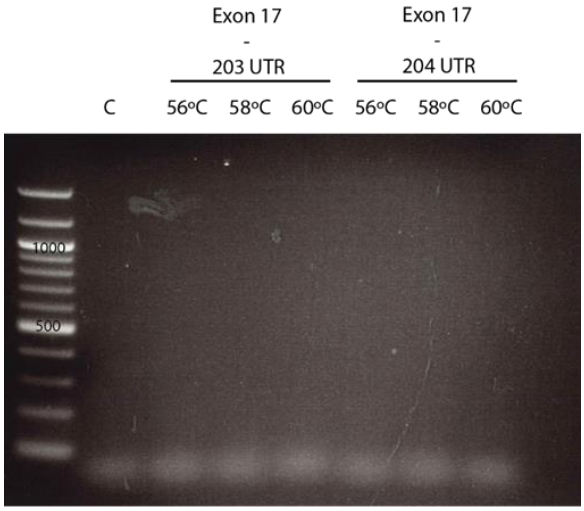

Figure 3. 3

RT-PCR of exon 17-UTR of variants 203 and 204 (expected 228 bp and 427 bp) in adult mouse brain using three different annealing temperatures. No evidence of truncated transcript variants was found.

synthesis, to a specific set of primers. These primers therefore target the 5′- and 3′-UTR and can then be used for sequencing.

The sequence of 5′-UTR - exon 6 was amplified by PCR in an adult mouse brain sample and produced three products, named Upper, Medium and Lower band (Fig 3.5). The amplified products were then re-amplified via nested PCR and sent for sequencing. The Lower band clones proved to be unspecific. Upper and Medium clones were instead specific for *Trappc9* and revealed several start sites. Medium clones started within exon 2 (first coding exon) downstream of the start codon. The lack of a close downstream methionine codon suggests these clones do not represent an alternative variant/start site, but are probably the consequence of RNA degradation or secondary structures that impair the movement of the reverse transcriptase. Upper clones started instead within the non-coding exon 1 (5′-UTR according to Ensembl), with one clone starting in the upstream intron. The sequencing results of the different clones did not show any evidence of an exon a2.

A primer was also designed to target the alternatively spliced exon 5 that, according to the information available on Ensembl, is expressed only in variants 201 and 204. No

association was found between exon 5 and exon 2a, as no evidence was ever found of an exon 2a.

As exon 5 is a small exon (27 bp), I could not distinguish between variant 202 and 204, as they differ only in the presence/absence of this exon, but sequencing of brain and peripheral tissues (Fig 3.4) revealed that exon 5 is not alternatively spliced in the brain, suggesting that variant 202 (with exon 5 spliced out) might be specific to the periphery. However, no evidence was found of any truncated variants, either in the brain or in the periphery. Specific primers were designed for variants 203 and 204 targeting the last exon and UTR sequence in association with a primer targeting exon 17, present in all variants. Despite confirming that the primers are functional (Supplementary Fig 1), no PCR product was produced for the truncated forms in the different tissues (Fig 3.2C).

3.3.2 Imprinting analysis

The expression of *Trappc9* across different tissues in humans has been documented by Hu et al. who showed via mRNA blot *Trappc9* expressed in brain, heart, muscle, kidney and placenta. Thymus, liver, intestine and lung showed a low expression while colon, spleen and leukocytes showed no expression (Hu et al., 2005).

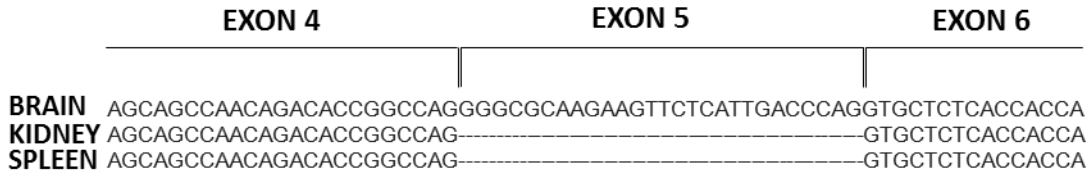

Figure 3. 4

Sequencing results for *Trappc9* exon 4-6 in adult mouse brain from RT-PCR and 5′-race, kidney and spleen. In contrast to Fig 3.2C, exon 5 appears to be alternatively spliced in kidney and spleen but not in the brain.

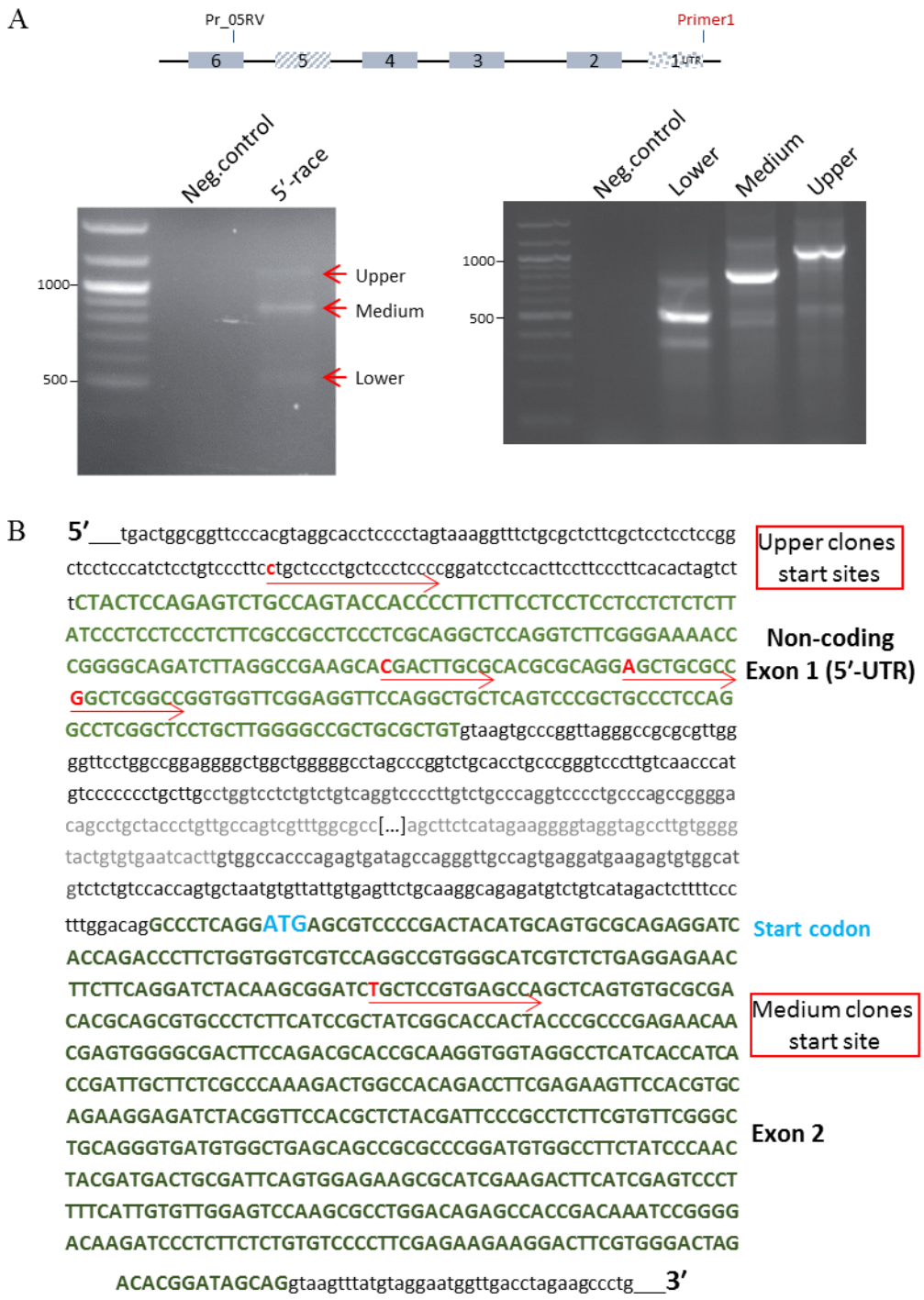

Figure 3. 5

5′-race of adult total brain mRNA. **A)** Left: PCR for *Trappc9* using 5′-race as template with Primer_1 (race specific primer) and Pr_05RV (exon 6); Right: nested PCR from A on the left (Primer_1 and Pr_05RV). Three different sized bands were produced, suggesting multiple start sites are present. **B)** Representation of *Trappc9* cDNA and sequencing results from B. Capital letters represent the exons, while lowercase letters represent the introns. The PCR products from A were cloned into Topo vector and sequenced. The clones from the lower band were found to be unspecific. The clones from the middle and the upper band were specific for *Trappc9* (start sites of these clones shown in figure).

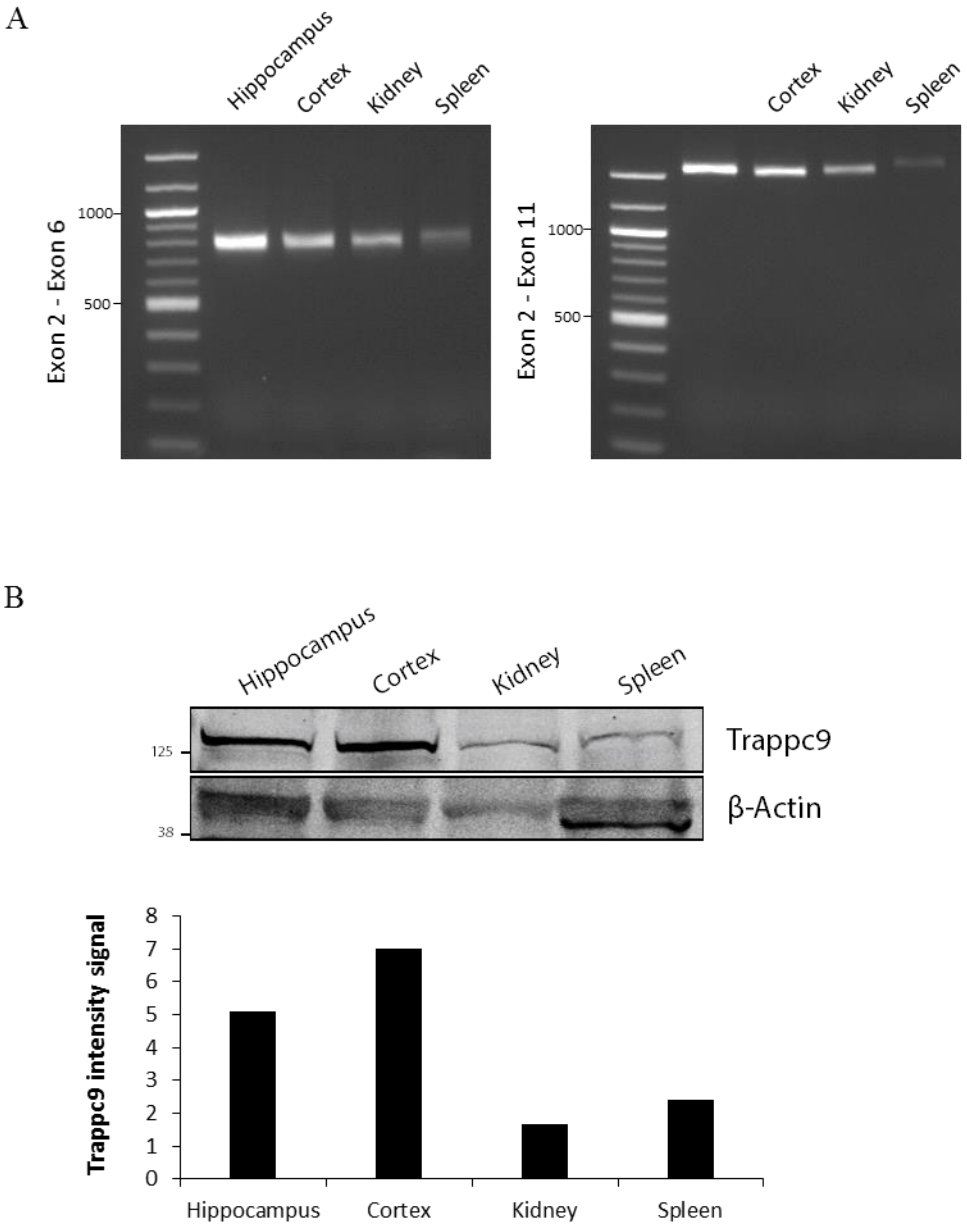

Figure 3. 6

A) RT-PCRs of adult mouse hippocampus, cerebral cortex, kidney and spleen. *Trappc9* exons 2-6 (primers Pr_02FW and Pr_05RV, expected 780 bp) and 2-11 (primers Pr_02FW and Pr_15RV, expected 1562 bp) show that Trappc9 is expressed in the brain and the periphery, although to a lower degree. B) Representative western blot for Trappc9 (primary antibody #16014-1-AP) in adult hippocampus, cerebral cortex, kidney and spleen. Trappc9 signal normalised to β-actin.

The expression patterns in the mouse brain have been investigated by Davies et al., who used in situ hybridisation to describe a general expression of Trappc9 in the brain, with hippocampus, cortex and hypothalamus being among the areas with highest expression. They also observed Trappc9 expression in the embryo, adrenal glands, heart, kidney, thymus, lung and muscle, and to a lower extent in placenta and liver (Davies et al., 2004).

In order to confirm these observations, we performed RT-PCR and western blotting in brain (hippocampus and cortex), kidney and spleen and observed a higher expression of Trappc9 in the brain than in peripheral tissues (Fig 3.6).

In the context of the imprinting status of Trappc9 in the mouse, pyrosequencing allele quantification (SNP analysis) was performed from total brain and kidney RNA from reciprocal crosses of *Mus musculus* (C57BL/6, B6) and *Mus M. molossinus* (Japanese Fancy mouse 1, JF1). A specific silent SNP located in *Trappc9* exon 7 as shown in Fig 3.7 was analysed. In the reverse cDNA orientation B6 mice carried a guanine in this position, while JF1 mice carried an adenine. Pyrosequencing results showed a 70% average expression in the adult brain from the maternal allele and a 30% from the paternal allele. In the newborn brain, a 77% average expression from the maternal allele and a 23% from the paternal were observed. Biallelic expression (49-51%) was observed in the adult kidney.

To investigate whether the parent-of-origin expression is specific to any brain areas, western blot analysis for Trappc9 was performed from 12 week-old heterozygous knockout (KO) brains (see chapter 5 for details on the animal model), using a crude dissection method and dividing the brain (including cerebellum and medulla/spinal cord) into 4 fragments (Fig 3.8). The analysis was performed on one heterozygote with the gene disruption in the maternal allele (m-/p+) and on one with the disruption in the paternal allele (m+/p-). Three technical repeats of the analysis, which showed a higher Trappc9 expression in the frontal cortex of the m-/p+ mouse than in the m+/p-, were performed.

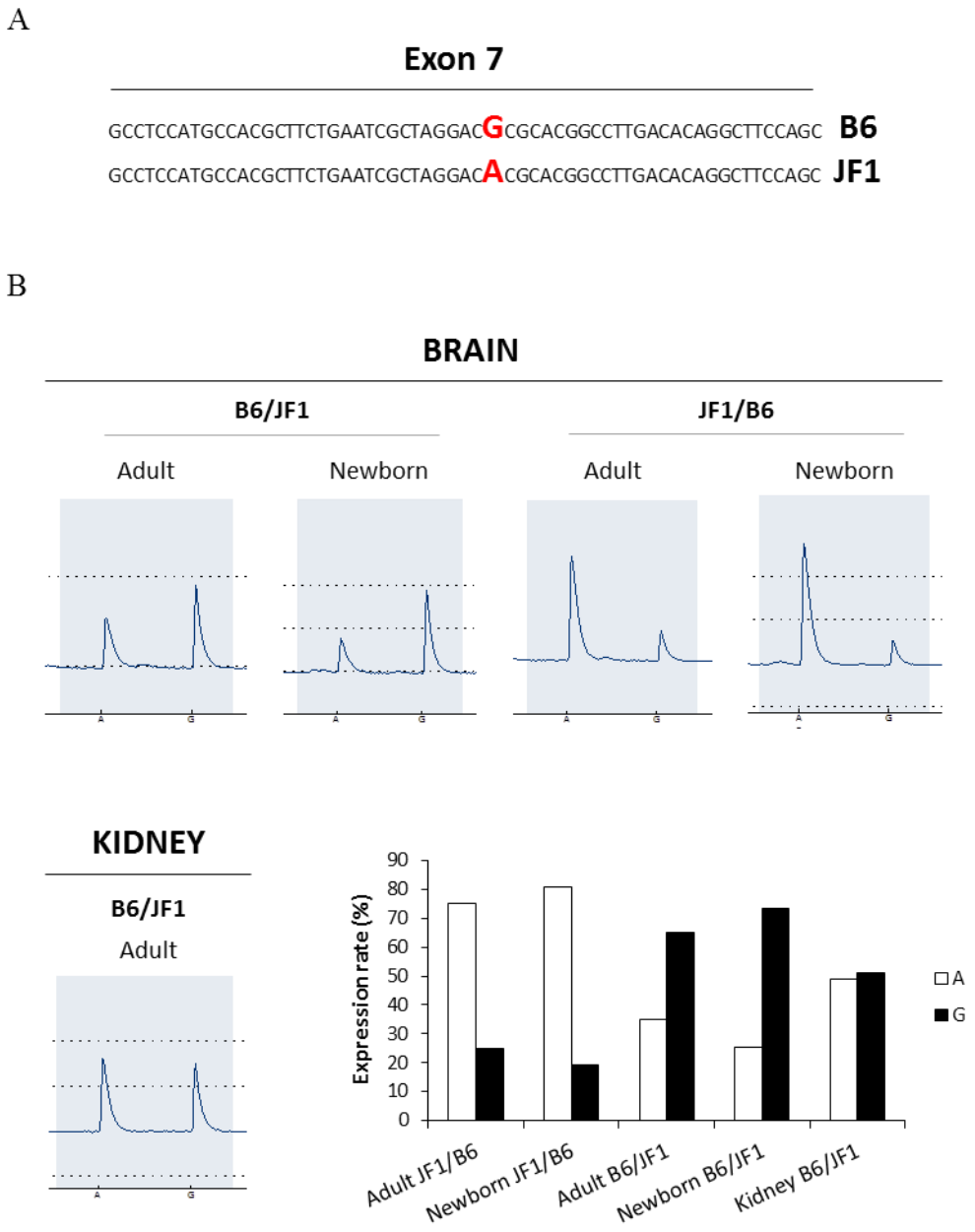

Figure 3. 7

SNP Pyrosequencing analysis for *Trappc9* allele quantification of adult and newborn total brain RNA from *Mus Musculus* (C57BL/6, B6) and *Mus M. Molossinus* (Japanese Fancy mouse 1, JF1) reciprocal crosses, where the first allele in the nomenclature represents the maternal allele. **A)** Partial sequence of exon 7 in the two strains showing the analysed SNP, which in the reverse strand corresponds to 'A' in JF1 mice and a 'G' in B6 mice. **B)** Pyrosequencing analysis of SNP in exon 7. The allele quantification revealed a preferential maternal expression of *Trappc9* in the brain (in both adult and newborn) and a biallelic expression in the kidney. For brain samples analysis n=2, for kidney n=1 (technical replicas).

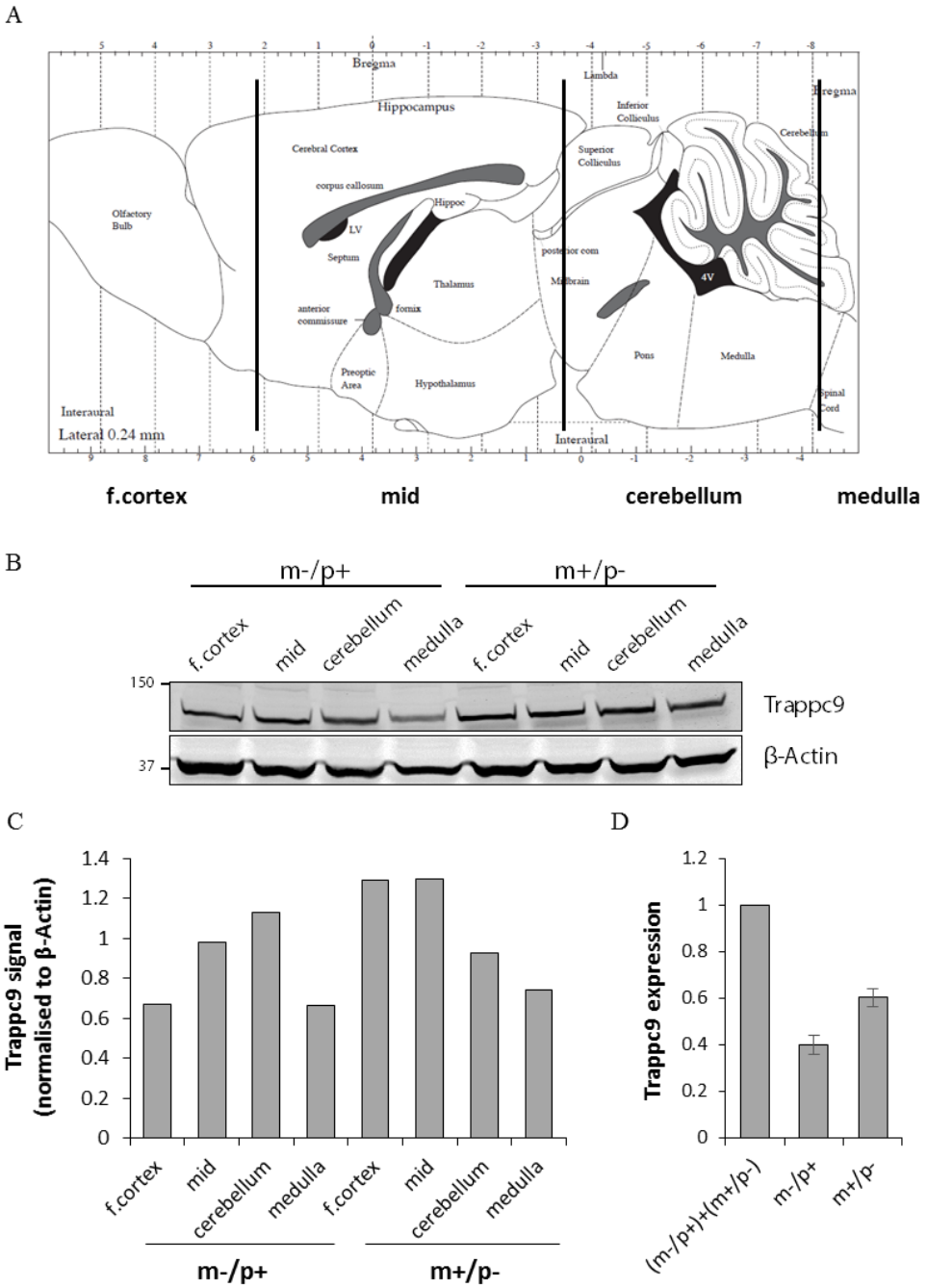

Figure 3. 8

A) Schematic representation of crude sectioning of the brain used in B) Western blot of adult heterozygous Tm1a (see chapter 5) mice for Trappc9. C) Quantification of western blot in B. Heterozygous mice show various degrees of Trappc9 expression in different parts of the brain, with mice carrying the maternal deletion (m-/p+) showing a lower expression in the frontal part of the brain compared to mice with the paternal deletion (m+/p-). D) Average degree of Trappc9 expression from the maternal (m+/p-) or paternal (m-/p+) allele (technical replicas n=3). The paternal allele contributes with an average 40% of expression while the maternal contributes with a 60% expression. Anti-Trappc9 antibody used: Proteintech #16014-1-AP. Image in A from "The Mouse Brain" atlas by G. Paxinos and K.B.J. Franklin (2001).

Other parts of the brain showed no major differences between the two genotypes. The sum of the four analysed parts reveal that overall m-/p+ mice possess a 40% expression of Trappc9, while the m+/p- show a 60%. These percentages are surprisingly similar, considering the difference in methods, to what would be expected following the pyrosequencing analysis, which showed a 30% expression in the m-/p+ mouse and a 70% in the m+/p-.

The difference in Trappc9 expression between frontal cortex and other sections in the m-/p+ brain could be an indication of regional imprinting that could not be highlighted with the pyrosequencing analysis. In fact, both pyrosequencing and western blot analyses have their limitations and might therefore produce a degree of bias. While the pyrosequencing analysis was performed on total brain RNA and could therefore not detect region-specific imprinting, the western blot analysis investigated crude sections of brain containing different areas and sub-areas that in turn could present different levels of imprinting. Furthermore, both analyses could be biased by the presence of blood in the tissues at the moment of lysis for RNA or protein extraction.

Nonetheless, the western blot results confirmed the degree of imprinting for *Trappc9* from the maternal allele observed via pyrosequencing. In addition, the reduced expression of *Trappc9* in the frontal cortex compared to other regions indicates that different levels of imprinting for this gene are present across the mouse brain.

3.3.3 Methylation analysis

The putative imprinting control region of the gene cluster to which *Trappc9* belongs might reside in *Peg13* where, it has been hypothesised, the methylation in the maternal allele drives the imprinting of the neighbouring genes. Previous reports have failed to attribute the imprinting of *Trappc9*, or any other gene in the cluster, to the methylation of specific regions outside *Peg13*.

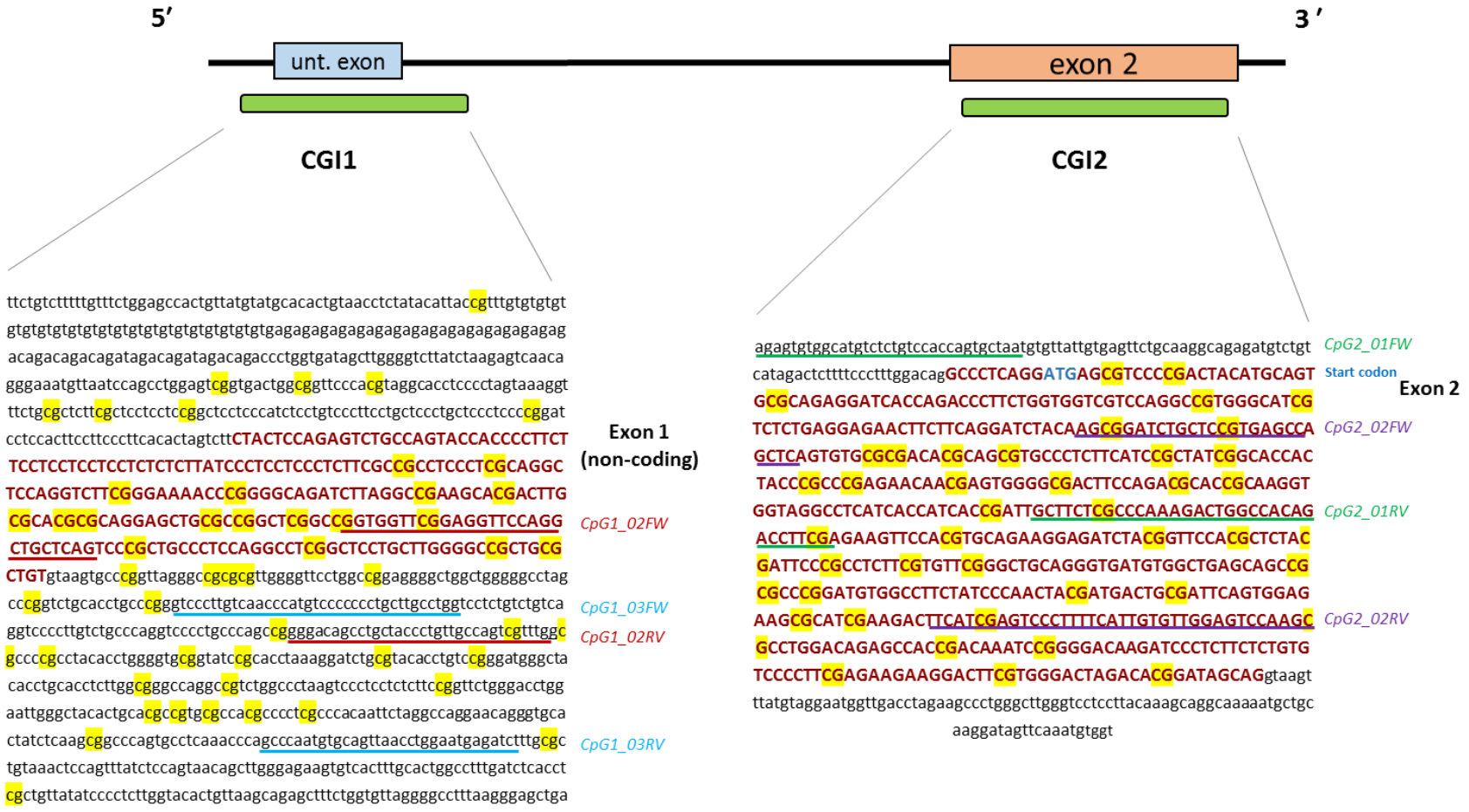

Figure 3. 9

Representation of mouse *Trappc9* **A)** CpG1 in exon 1 and **B)** CpG2 in exon 2, with location of primers used for bisulfite sequencing and COBRA analysis (Fig 9 and 10) the actual primers are complementary to the bisulfite converted gDNA sequence). Lowercase letters represent introns, capital letters exons. CG sites highlighted in yellow.

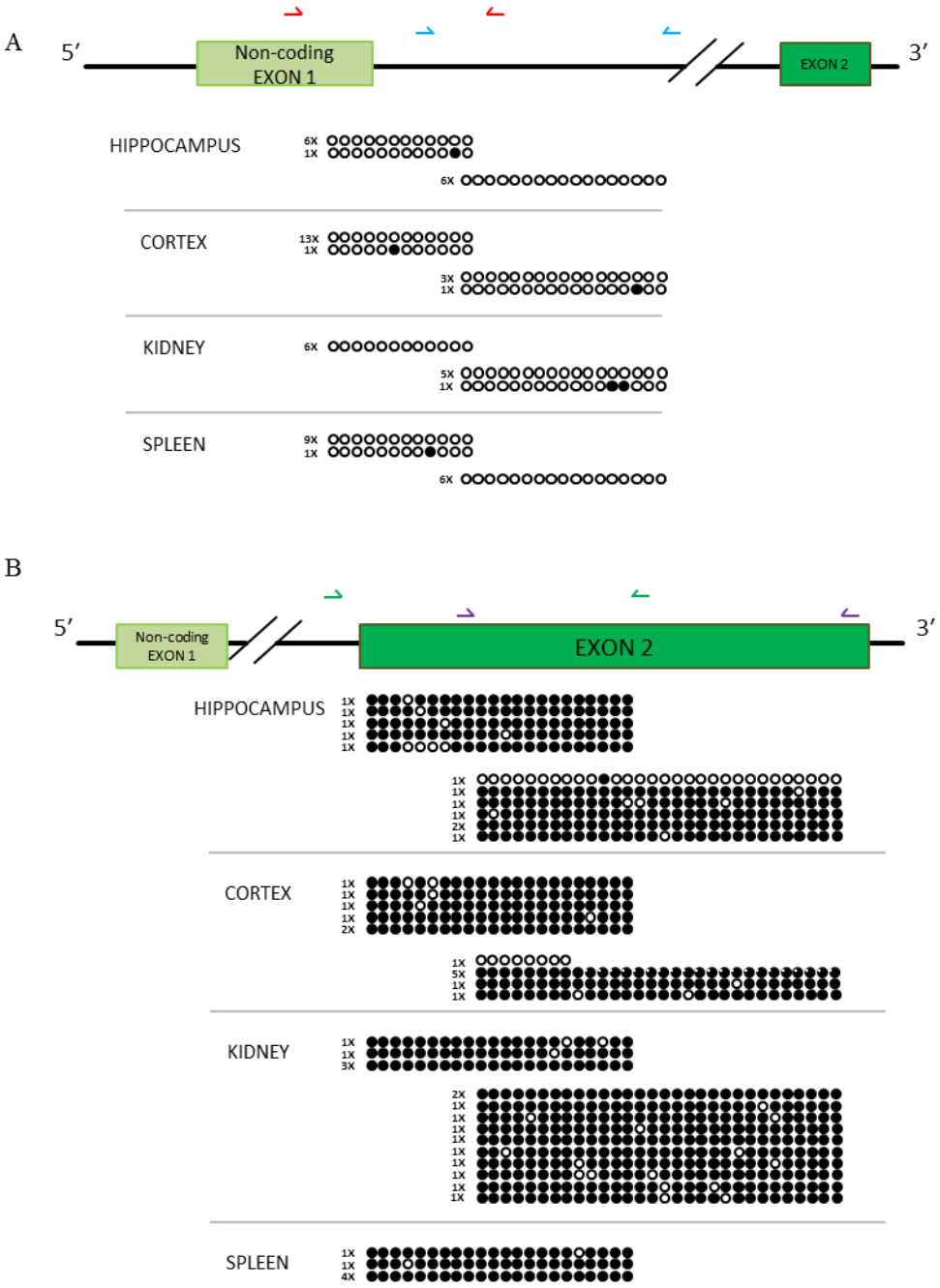

Figure 3. 10

Bisulfite sequencing of gDNA for **A)** CGI1 and **B)** CGI2 in adult mouse hippocampus, cerebral cortex, kidney and spleen. White circles represent unmethylated CG, while black circles represent methylated sites. CpG1 is predominantly unmethylated in both brain and periphery, while sequencing results for CpG2 revealed mainly methylated clones in both brain and periphery. Only one clone in the hippocampus and one in the cerebral cortex showed predominantly unmethylated sequences, suggesting there might be a cloning bias in the results. Red and blue arrows represent the location of the primers used for the PCR amplification. Numbers in front of rows indicate the number of sequenced clones characterised by that specific methylation pattern. Primers used: CpG1_02FW and CpG1_02RV (red arrows in A), CpG1_03FW and CpG1_03RV (blue arrows in A); CpG2_01FW and CpG2_01RV (green arrows in B), CpG2_02FW and CpG2_02RV (purple arrows in B).

I identified two main CpG islands located in Trappc9 exon 1 (non-coding) and exon 2 (first coding exon), which I will from now on refer to as CGI1 and CGI2, respectively (Fig 3.9).

Bisulphite sequencing of gDNA extracted from brain (hippocampus and cortex), kidney and spleen was performed using two sets of primers designed to cover the main core of each CpG island (Table 2.1).

The analysis of several clones per primer pair (Fig 3.10), revealed CGI1 to be predominantly unmethylated in both brain and peripheral tissues. CGI2 revealed mainly methylated clones in both brain and peripheral tissues, with the exception of two fully unmethylated clones found in the hippocampus and cortex.

In order to determine the reliability of this method and to confirm the methylation status of the two CpG islands, a Combined Bisulphite Restriction Analysis (COBRA) was performed. PCR-amplified fragments of CGI1 and CGI2, as analysed by bisulphite sequencing, were used for restriction digests with the enzymes BstUI (CGI1 and CGI2) and TaqI (CGI2) (Fig 3.11). These enzymes recognise specific restriction recognition sites containing CG sites, which are maintained after the bisulphite conversion only if the specific cytosines in the sequence are methylated. The restriction digest was performed with the presence of a gDNA positive control (non-bisulphite converted) that retains the intact restriction sites, and should therefore be completely digested. The analysis revealed that while CGI1 is confirmed to be unmethylated in all tissues, CGI2 shows the presence of both methylated and unmethylated alleles. This result suggests that the bisulphite sequencing was biased, probably due to the cloned sequence and its compatibility with the *E.coli* strain used for amplification. The analysis also revealed that hippocampus and cortex express the unmethylated allele (undigested product) to a higher extent, while kidney and spleen express more of the methylated allele (digested products).

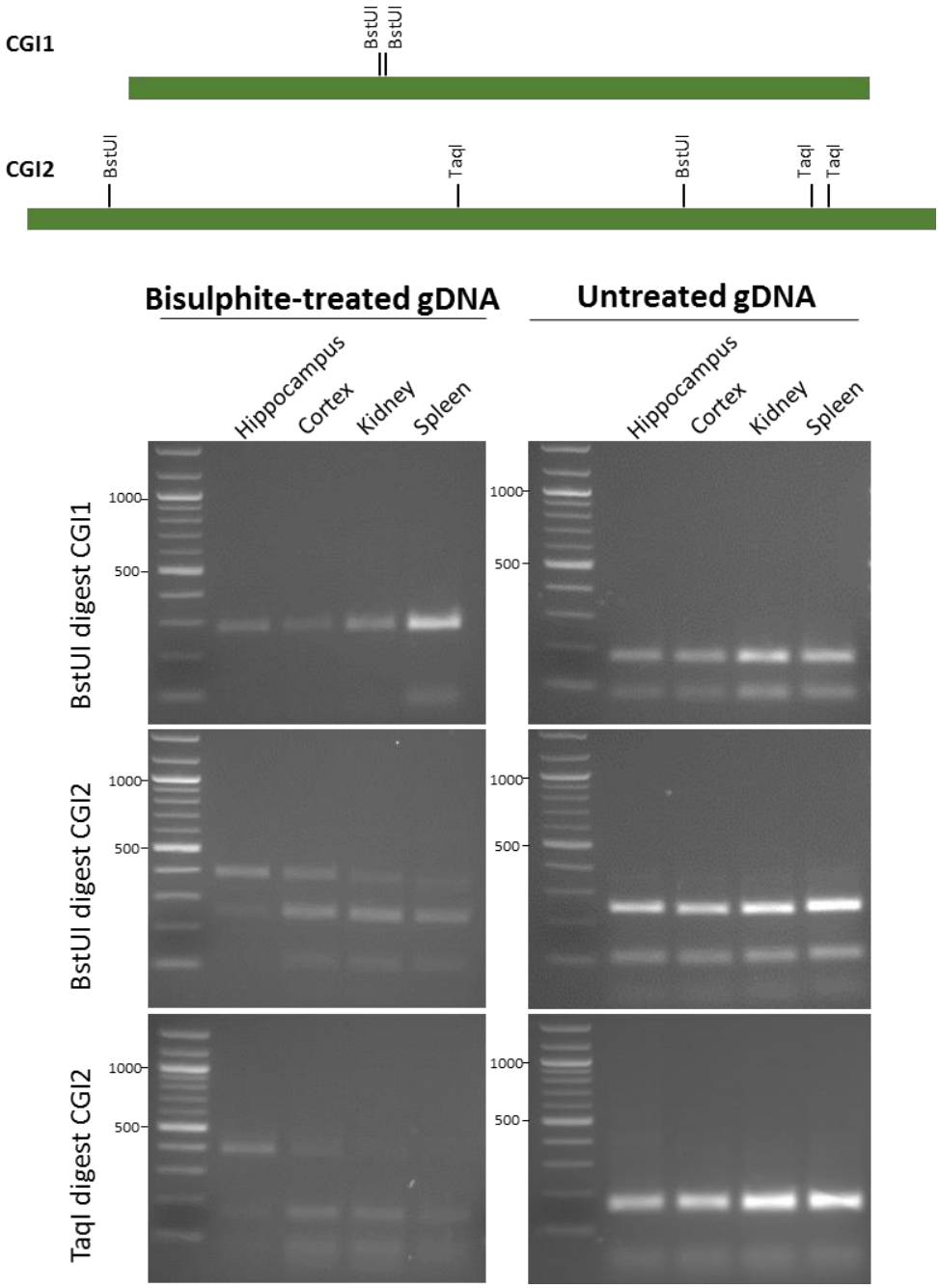

Figure 3. 11

Combined bisulphite restriction analysis (COBRA) on untreated and bisulphite treated adult mouse gDNA from hippocampus, cerebral cortex, kidney and spleen. BstUI and TaqI restriction enzymes recognise the restriction sites CGCG and TCGA, respectively. When a cytosine is unmethylated in the gDNA, it is converted to uracil during bisulphite treatment, disrupting the integrity of the restriction sites. Methylated sequences instead maintain the cytosine and the restriction enzymes are able to recognise the sites. CGI1 is confirmed to be unmethylated (100 bp band in spleen lane confirmed as primer dimer, not shown), while CGI2 shows the presence of both methylated and unmethylated alleles. For CGI1 BstUI digest the expected products are: 279 bp for the uncut, 182 bp and 97 bp for the digested sequence; for CGI2 BstUI digest: 382 bp for the uncut, 244 bp, 110 bp and 28 bp for the digested sequence; for CGI2 TaqI digest: 382 bp for the uncut, 175 bp, 156 bp, 39 bp and 12 bp for the digested sequence.

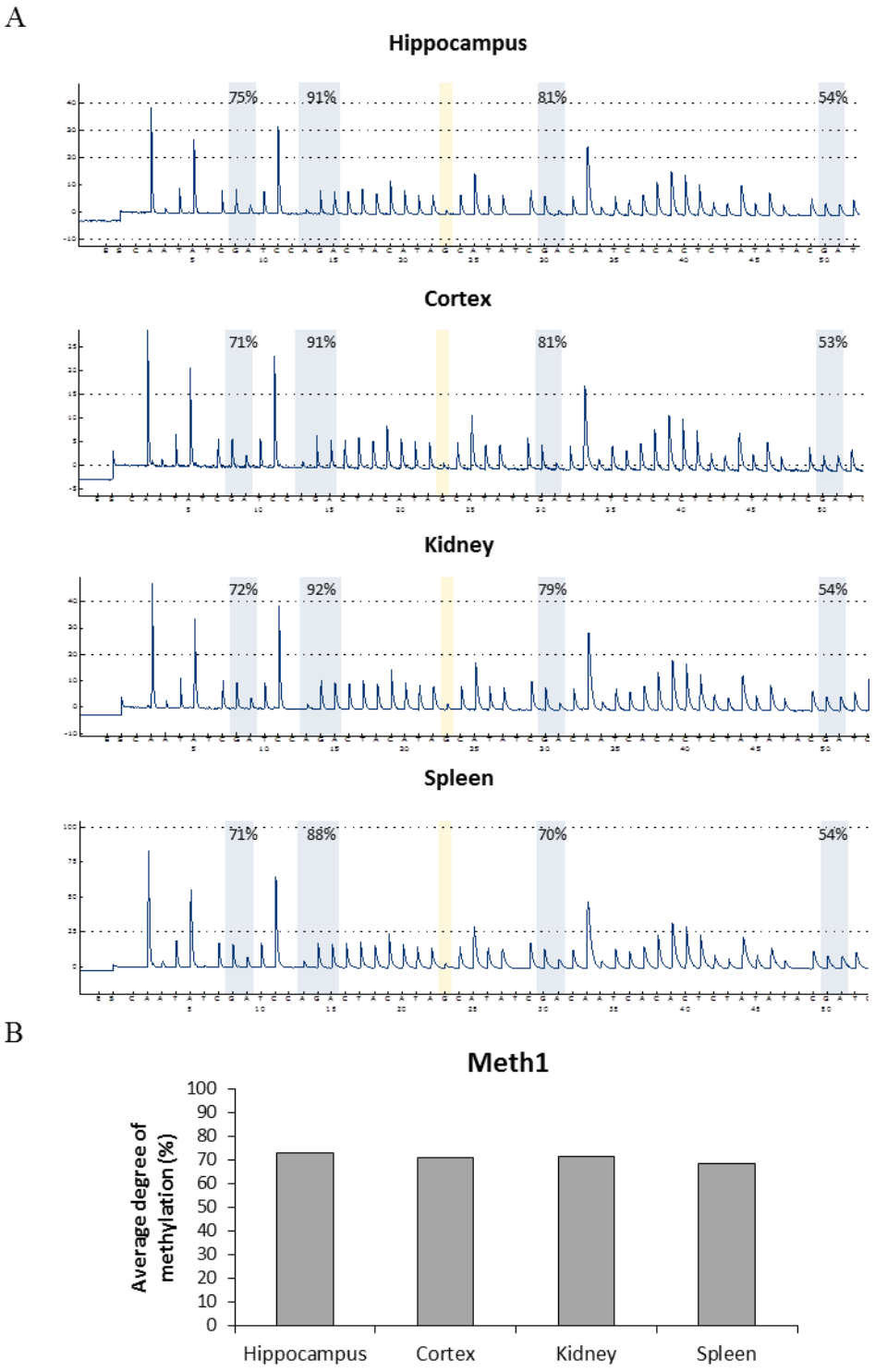

Figure 3. 12

Bisulphite pyrosequencing of gDNA at CGI2 with Meth1 primer pair in adult mouse hippocampus, cerebral cortex, kidney and spleen. **A)** Example of pyrograms obtained using the PyroMarkQ96 software (primers Trappc9meth1_Fb and Trappc9meth1_R). Percentages indicate the degree of methylation for the highlighted CG sites (light blue). **B)** Average degree of methylation for 6 CG sites (n=1).

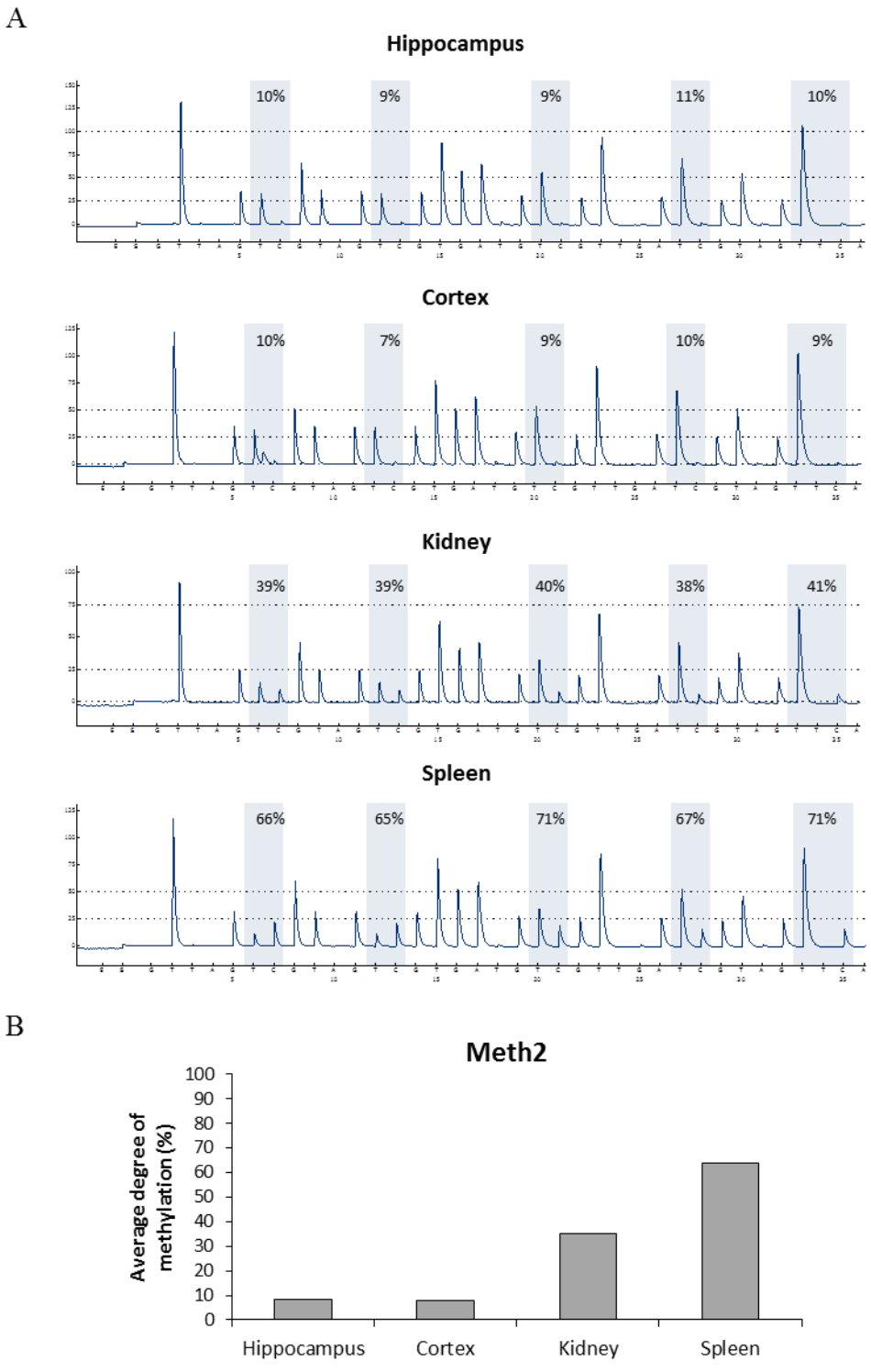

Figure 3. 13

Bisulphite pyrosequencing of gDNA at CGI2 with Meth2 primer pair in adult mouse hippocampus, cerebral cortex, kidney and spleen. **A)** Example of pyrograms obtained using the PyroMarkQ96 software (primers Trappc9meth2_F and Trappc9meth2_Rb). Percentages indicate the degree of methylation for the highlighted CG sites (light blue). **B)** Average degree of methylation for 10 CG sites (technical replicas n=2).

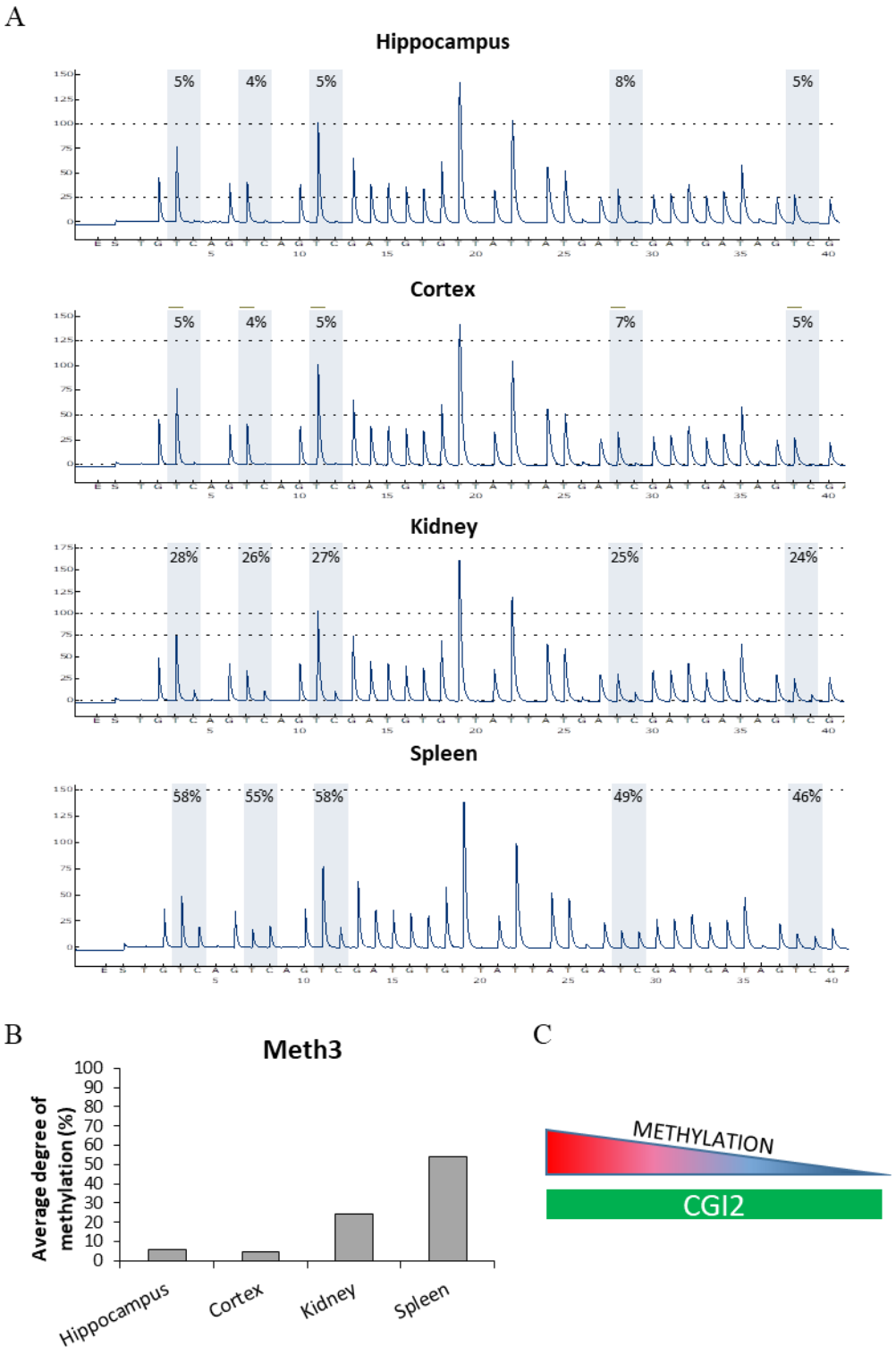

Figure 3. 14

Bisulphite pyrosequencing of gDNA at CGI2 with Meth3 primer pair in adult mouse hippocampus, cerebral cortex, kidney and spleen. **A)** Example of pyrograms obtained using the PyroMarkQ96 software (primers Trappc9meth3_F and Trappc9meth3_Rb). Percentages indicate the degree of methylation for the highlighted CG sites (light blue). **B)** Average degree of methylation for 8 CG sites (technical replicas n=2 each). **C)** Scheme of methylation across the entire CGI2.

As an alternative method of methylation analysis, pyrosequencing analysis was conducted on bisulphite treated gDNA for CGI2. Three primer pairs (meth1, meth2 and meth3) were designed to target once again the main core of CGI2 and obtain PCR products of circa 100 bp in length. Meth1 (n=1) analysed a total of 6 CG sites and showed an average methylation rate of 72.67% for hippocampus, 71% for cortex, 71.33% for kidney and 68.18% for spleen (Fig 3.12). Meth2 (n=2) comprised of 10 CG sites with an average degree of methylation of 8.35% for hippocampus, 7.85% for cortex, 34.95% for kidney and 63.85% for spleen (Fig 3.13). Meth3 (n=2) analysed a total of 8 CG sites and showed an average degree of methylation of 5.62% for hippocampus, 4.65% for cortex, 24.56% for kidney and 53.87% for spleen (Fig 3.14). Overall, these results showed a gradient of methylation across CGI2, uniform in brain and peripheral tissues for the first part of the CpG island and not uniform for the remaining part. In fact, the analysis of meth2 and meth3 combined (18 CG analysed in total) revealed an average 6.98% and 6.25% degree of methylation in hippocampus and cortex, a 29.75% in the kidney and a 58.86% in the spleen. These results are in accordance with the outcome of the COBRA analysis described above.

Considering the biallelic expression of *Trappc9* observed in peripheral tissues, and the high degree of methylation observed in the pyrosequencing analysis, it appears clear that this degree of methylation is not correlated with the imprinting status of *Trappc9*.

To investigate whether CGI2 is a regulatory sequence of an alternative (not yet observed) transcript variant of *Trappc9*, a primer to target the intron upstream to exon 2 was designed (Fig. 3.15). The validity of this primer has been confirmed on gDNA (Supplementary Fig 1). I did not, however, obtain any PCR product from cDNA in conjunction with a primer located in exon 2 (Fig 3.15), suggesting there is no alternative transcript variant starting in this region.

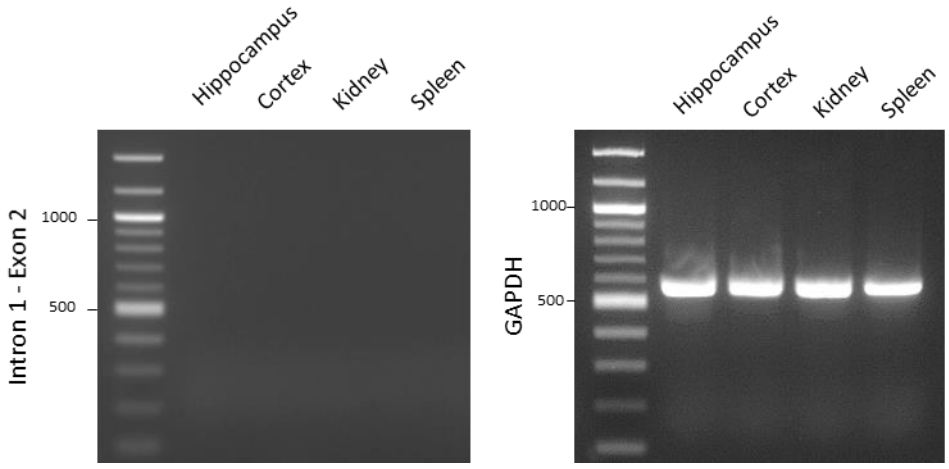

Figure 3. 15

RT-PCR of adult mouse hippocampus, cerebral cortex, kidney and spleen. In light of the tissue-specific methylation observed in exon 2, we hypothesised this might cause the transcription of an alternative isoform. Intron 1 - exon 2 (primers Tr_upex2n1_Fw and Pr_02RV, expected 431 bp) confirms that there is no alternative start site located immediately before exon 2.

3.4 Discussion

3.4.1 Transcript variants and their functional significance

The mouse genome database Ensembl is one of the most useful tools in scientific research. With the data shown in this chapter, however, I have demonstrated that the information provided by this database is not always accurate. As previously described in the introduction of this chapter, Ensembl reports four transcript variants for the murine *Trappc9* gene (see Fig 3.2). The two long variants (called 201 and 202) differ in the presence of the alternatively spliced exon 5 and an alternative start site. In Fig 3.2 I have shown that the alternative start site named exon a2 could not be detected in either mouse brain or peripheral tissues. In order to investigate the existence of an alternative start site for *Trappc9* I performed a 5′-race of adult total brain RNA (Fig 3.5). The analysis confirmed that the alternative start site called exon a2 could not be detected, and it also revealed that

the 5′-UTR sequence extends back to the upstream intron of *Trapp9*, confirming once again that the information available on Ensembl is not accurate. In addition, the alternatively spliced exon 5 was always found in correlation with exon 2, contrary to the description found in Ensembl in which variant 202 does not possess this exon. All together, these results suggest that the variant 201 does not exist.

Exon 5 should also be present in the truncated variant 204 in association with exon 2, and may be an explanation for the association between exon 2 and exon 5 we showed in Fig 3.2. However, I did not find any evidence of any truncated transcript variants for *Trappc9*, in brain or peripheral tissues (Fig 3.2-3). The only reference to the truncated forms of *Trappc9* found in the literature comes from Gregg et al., who described a paternal bias of the mRNA variant 204, having analysed a SNP in the last coding exon in reciprocal crosses of two different mouse strains (Gregg et al., 2010). This SNP, however, is located downstream of *Peg13* and it is probably part of this gene's mRNA. My analysis on the truncated forms was performed on brain and peripheral tissues of a newborn (p4) wild type (WT) mouse, but a separate analysis on adult brain cDNA (Fig 3.3) confirmed the absence of the truncated forms. Although I have not analysed any embryonic stages, I believe it to be unlikely that these forms are age-specific. This suspicion, however, needs to be confirmed.

In Fig 3.4 I show sequencing results for *Trappc9* exon 4-6 in the brain, kidney and spleen, where I observed that exon 5 is alternatively spliced in the periphery but not in the brain. The functional implications *in vivo* of this alternative splicing are not clear yet, as exon 5 contributes with 27 nucleotides and 9 amino acids (GAQEVLIDP). It is possible that this small sequence is part of a larger domain responsible for the interaction with different proteins, allowing a different function of Trappc9 in the brain.

In conclusion, I describe only two long variants of *Trappc9*, carrying 23 exons (22 coding) in the brain and peripheral tissues and 22 exons (21 coding) in peripheral tissues, with the start site located in exon 2, as described for variant 202 on Ensembl, and a 5′-UTR stretching back to the intron upstream of exon 1.

Human *TRAPPC9* shares a high homology with the mouse orthologue. According to Ensembl, the human gene is transcribed into four protein-coding transcript variants (001, 002, 003 and 016) and 12 non-coding variants (004-015). The four protein-coding variants comprise of three long variants of 23 exons (001, 23 coding), 23 exons (002, 22 coding) and 21 exons (003, 21 coding). These three long variants possess three different start sites, with variant 001 being the longest and 002 and 003 starting at the beginning and the end of exon 2, respectively. The shortest long variant, 003, does not possess exon 5.

The fourth coding variant is a truncated form of 455 bp consisting of only 2 exons, corresponding to exons 15 and 16 in variant 001. This last variant should not be considered among *TRAPPC9* variants, as it translates into a 91 amino acid peptide whose existence is yet to be confirmed.

In summary, in comparison to the mouse transcript variants, human *TRAPPC9* appears not to have functional truncated forms, suggesting a shorter protein would not be functional. In addition, the alternative splicing of exon 5, which is 27 bp long and retains 89% sequence identity with the mouse exon 5 and 100% amino acid homology, is retained in the human, hinting at a functional significance for this brief amino acid sequence. Unfortunately, no reports have been published so far on the human transcript variants so their existence and expression patterns still need to be investigated.

3.4.2 Imprinting of *Trappc9*

The earliest report of *Trappc9*'s imprinting status dates back to 2003, when Smith et al. described for the first time the paternal expression of *Peg13* in mouse brain. They analysed

brain and peripheral RNA from reciprocal crosses of *Mus musculus* and *Mus M. castaneus* via cDNA synthesis and PCR amplification, followed by cloning and sequencing, and found a biallelic expression of *Trappc9* (Smith et al., 2003).

Wang et al. in 2008 adopted Illumina sequencing and pyrosequencing analysis to investigate the imprinting status of *Trappc9*. They reported 80% expression rate from the maternal allele in the neonatal mouse brain (Wang et al., 2008).

More recently, Gregg at al. reported, using Illumina RNA sequencing of brain RNA from *Mus musculus* and *Mus M. castaneus* reciprocal crosses, a maternal expression of the different transcript variants of *Trappc9*, with the exception of the truncated form 204 which showed a paternal expression (Gregg et al., 2010). As previously described, however, a detailed analysis of the SNP analysed to target the 204 variant revealed that it is actually localised downstream of *Peg13*, and thus their analysis was most likely targeting *Peg13* mRNA and not *Trappc9*.

The maternal bias in *Trappc9* expression has been observed using RNA sequencing but the results produced with this technique can sometimes be misleading or contradictory depending on the expression threshold set for the analysis. Similarly, as we have seen earlier in this chapter, the traditional method of cloning and sequencing can result in a cloning bias and in a false-positive/negative result. For this reason, I decided to investigate the imprinting status of *Trappc9* via pyrosequencing analysis of brain and kidney RNA from reciprocal crosses of B6 and JF1 mice. I observed an average 70% expression of *Trappc9* from the maternal allele and 30% from the paternal allele in the brain, and an equal biallelic expression in the kidney (Fig 3.7). This result is in accordance with the previous reports mentioned earlier in this paragraph, and with a recent article published by Perez et al. that showed a maternal bias of *Trappc9* in mouse brain and a biallelic expression in the periphery (Perez et al., 2015).

The latest report on *Trappc9*'s imprinting status confirmed, via RNA sequencing, the maternal expression of this gene in the mouse cerebral cortex at p0 (Bouschet et al., 2016). Interestingly, this was the first group to also report a maternal bias at E13.5. The maternal expression of *Trappc9* might therefore be crucial during embryonic development, as well as in adult stages.

With the imprinting status being confirmed, I investigated whether the methylation status of *Trappc9* was responsible for the parental bias of this gene. Previous reports analysed the methylation status of *Trappc9* and found no methylated sequences in adult tissues and in E13.5 (Smith et al., 2003). Delgado and colleagues analysed the CpG island located in the promoter of human *TRAPPC9* in healthy and intellectual disability patients' blood and found no methylation in this region (Delgado et al., 2014). In accordance with these reports, I observed a low degree of methylation in the two CpG islands located within the first and second exons of *Trappc9* in mouse brain. The pyrosequencing analysis (Fig 3.12-14) also revealed a gradient of methylation within CGI2, with the first part of the island being highly methylated and the rest being methylated in the periphery but not in the brain (6.99% hippocampus, 6.25% cortex). To my knowledge, this is the first analysis of the methylation status of these regions in peripheral tissues. Although I have not analysed DNA from reciprocal crosses for this analysis, it was surprising to observe that for the majority of CGI2 there is a higher degree of methylation in kidney and spleen (29.75% and 58.86%, respectively). Therefore, I cannot report what allele carries the methylation, but the equal biallelic expression observed in these tissues (via SNP analysis) suggests that this methylation is not a driving force for the imprinting of *Trappc9*. This methylation would, in fact, repress transcription from the methylated allele and it would result in a parental bias which we did not observe.

The functional significance of the methylation of CGI2 is not yet clear, nor is the observed gradient of methylation. It is possible that this CpG island acts as a regulatory region for an alternative transcript variant of *Trappc9*, although I did not find any evidence for it.

Despite the structure of this locus hints towards the ncRNA imprinting mechanism described in chapter 1, a likely mechanism for the imprinting of the *Peg13* gene cluster, and thus of *Trappc9*, might be similar to the regulation of the *Igf2*/*H19* locus. As previously described in chapter 1, *Igf2* is expressed from the paternal allele and is located 90 kb upstream of the maternally expressed *H19*. The ICR for this cluster is located 2-4 kb upstream of the start site for *H19* and it is methylated on the paternal chromosome. An enhancer shared by the two genes is located downstream of *H19*. The absence of methylation at the ICR on the maternal allele would allow the binding of the zinc-finger insulator protein CTCF which, in turn, would block the interaction between the enhancer and the promoter of *Igf2*. As a result, the expression of *Igf2* is silenced on the maternal allele, while in the paternal allele the ICR is methylated and CTCF cannot bind (Bartolomei and Ferguson-Smith, 2011).

Similarly, analysing brain CHIP-sequencing datasets available on the Encyclopaedia of DNA Elements (ENCODE), I identified a strong brain-specific enhancer located within the intronic region downstream of exon 21 of *Trappc9*. Our hypothesis is that in the paternal allele, the putative ICR located in correspondence of *Peg13* is a binding site for the factor CTCF that in turn acts as an enhancer blocker, preventing the interaction of the above mentioned enhancer with the promoter of *Trappc9*. The lack of interaction between enhancer and promoter results in the silencing of *Trappc9*. In contrast, on the maternal allele the methylation of the ICR in *Peg13* prevents the binding of CTCF and leaves the enhancer free to interact with *Trappc9*'s promoter (Fig 3.16).

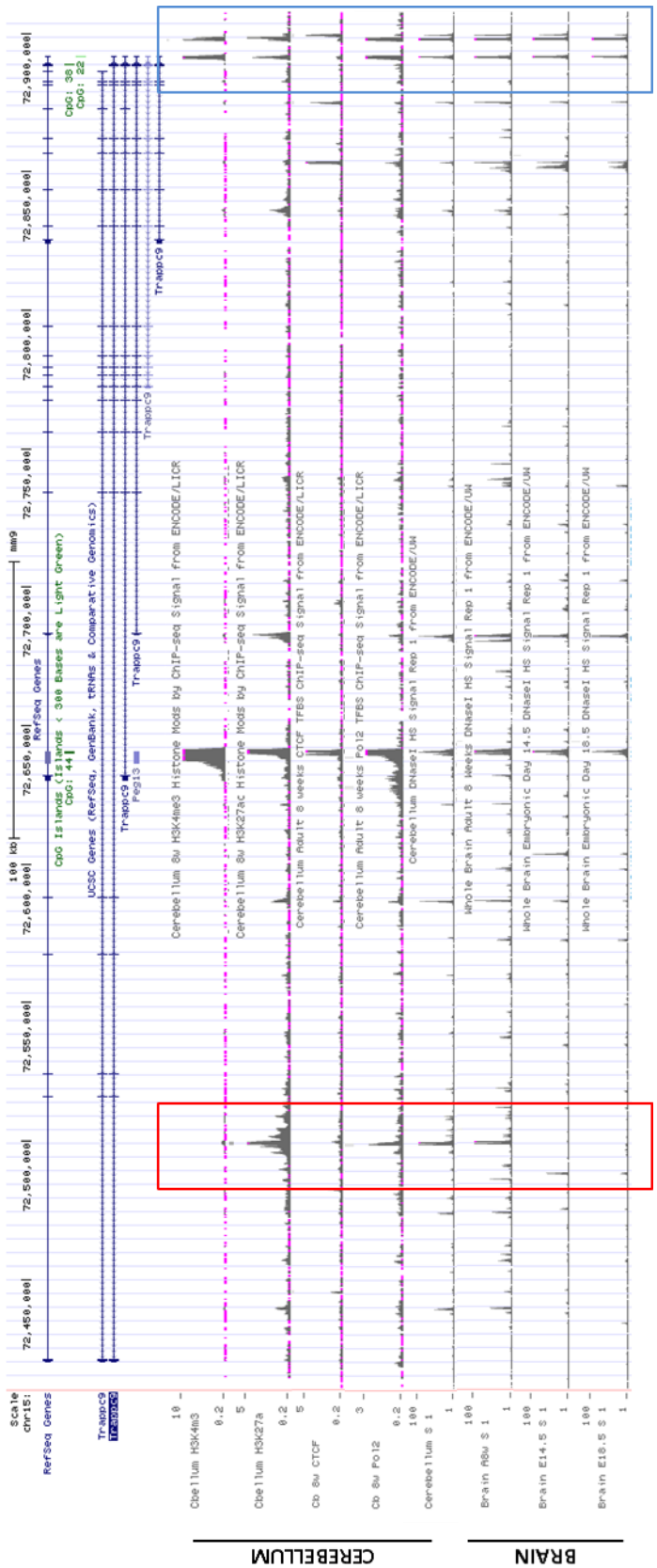

Figure 3. 16 a

CHIP sequencing data extracted from the publicly available ENCODE database. The top part represents the position on mouse chromosome 15 followed by the four previously described coding transcript variants for *Trappc9* plus two predicted peptides. Traces for cerebellum of H3K4m3 (promoter marker), H3K27a (enhancer marker), CTCF (enhancer blocker), RNApol II and DNAseI hypersentive sites (HS – enhancer marker). The red region highlights the presence of an enhancer downstream of *Trappc9* exon21 that would interact with Trappc9's promoter (blue region). Interestingly, this enhancer is present in 8 week-old brain (lower part of image) but not in embryos of E14.4 or E18.5.

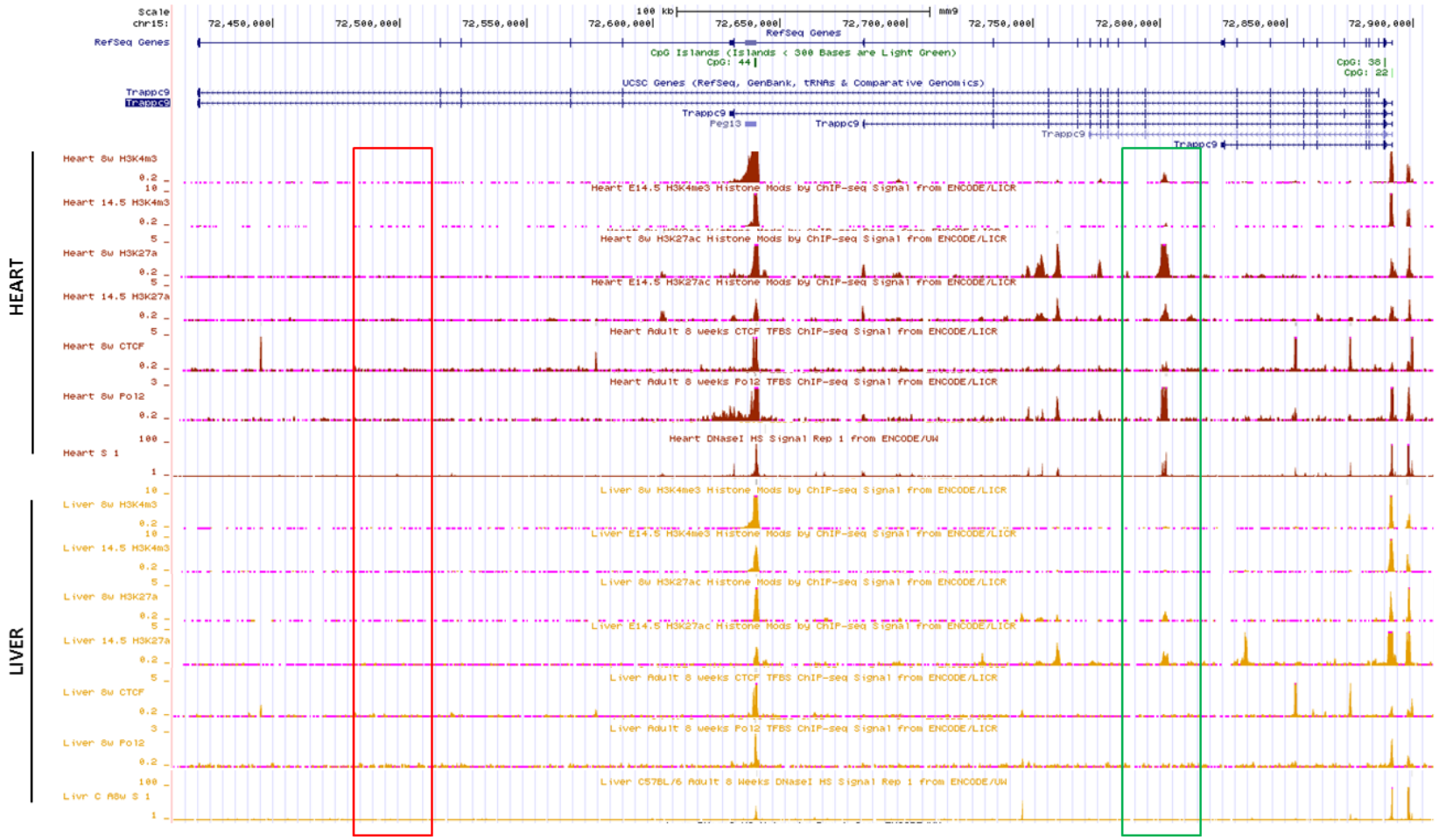

Figure 3. 16 b

CHIP sequencing data extracted from the publicly available ENCODE database for H3K4m3 (promoter marker), H3K27a (enhancer marker), CTCF (enhancer blocker), RNApol II and DNAseI hypersentive sites (HS – enhancer marker) in heart and liver. The top part represents the position on mouse chromosome 15 followed by the four previously described coding transcript variants for *Trappc9* plus two predicted peptides. The enhancer described in A is not present in the periphery. Interestingly, a heart-specific enhancer appears to be located downstream of exon 9 (green region).

Interestingly, the strong enhancer observed in the brain is not present in peripheral tissues and it would therefore explain the imprinting observed in the brain and the biallelic expression observed in the periphery.

A similar enhancer, located upstream of PEG13 and downstream of TRAPPC9 exon 17, has been described in humans. According to Court and colleagues, a CTCF-cohesin complex, bound to the paternal (unmethylated) allele of PEG13, orchestrates higher order chromatin loops. These structures prevent the interaction of the enhancer with the promoter of KCNK9, resulting in the imprinted expression of this gene (Court et al., 2014).

In the human, however, this enhancer is not disturbed by the methylation in PEG13 as, being located upstream of the ncRNA, it is able to interact with TRAPPC9 undisturbed.

The human TRAPPC9 has, similar to the mouse orthologue, a contradictory history of reports on its imprinting status. In 2012, Garg and colleagues observed an exclusive maternal expression analysing HapMap phase II data for trios (father/mother/child) (Garg et al., 2012). In contrast, Court et al. (2014) performed a SNP analysis in leukocytes, brain and placenta and found that only PEG13 and KCNK9 to be imprinted.

The latest report highlights a preferential maternal expression (stronger in the central nervous system than in peripheral tissues) in the mouse, which appears to be conserved in humans as well (Babak et al., 2015). We know by experience that SNPs found in genome databases such as Ensembl and UCSC are not always present. For example, the SNP pyrosequencing analysis described in this thesis was performed also on another SNP located in Trappc9 exon 9 (Fig 3.17) and found that different individuals of the same intercross genotype did not possess the same polymorphism. As DNA is dynamic and mutable, it is often the case that the SNPs analysed by different groups, in both mouse and human, might lead to biased analysis and thus to contradictory results. However, irrespective of the actual imprinting status of *TRAPPC9* in humans, its functional

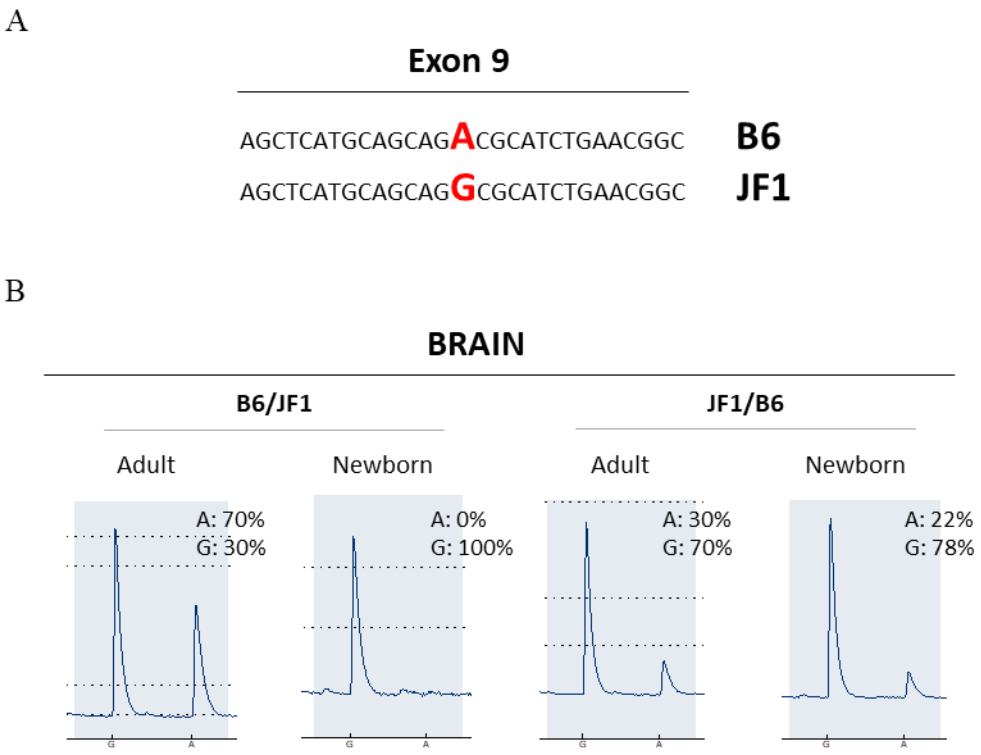

Figure 3. 17

SNP Pyrosequencing analysis for *Trappc9* allele quantification of adult and newborn total brain RNA from *Mus Musculus* (C57BL/6, B6) and *Mus M. Molossinus* (Japanese Fancy mouse 1, JF1) reciprocal crosses. **A)** Partial sequence of exon 9 in the two strains showing the analysed SNP, which corresponds to 'G' in JF1 mice and a 'A' in B6 mice. **B)** Pyrosequencing analysis of SNP in exon 9. The allele quantification revealed a preferential maternal expression of Trappc9 in the brain in adult and newborn JF1/B6 and in adult B6/JF1. Newborn B6/JF1 does not present a SNP in this position. n=1.

significance is still to be investigated. The intellectual disability and microcephaly phenotype caused by loss of TRAPPC9 is given by autosomal recessive mutations, and no dramatic phenotype has been reported for heterozygous individuals. This, however, does not preclude a role for TRAPPC9 in brain function, as the effects might be more subtle but still important.

The imprinting of *Trappc9* might have a physiological relevance in the context of its cellular functions. As we will see in chapter 4, Trappc9 regulates the NF-κB pathway and the NFG-induced Bcl-xL expression in PC12 cells (Hu et al., 2005). Bcl-xL is a long transcript variant of the Bcl-x gene (a member of the Bcl-2 family) and it acts as anti-apoptotic factor by preventing the release of mitochondrial content (Boise et al., 1993).

This protein has a fundamental role in neuronal survival, as it is the Bcl-x predominant form in neurons (González-García et al., 1995) and Bcl-x-null mice die around E13, exhibiting pronounced cell death in both peripheral tissues and central nervous system (Motoyama et al., 1995).

The programmed cell death pathway is a prominent feature in imprinting, with a number of the maternally-biased genes (Cdkn1c, Kcnk9, Blcap, Bmf) promoting apoptosis, and a number of the paternally-biased genes (Ndn, Peg3, Peg10, Plagl1, Megel2) inhibiting apoptosis. Bcl-xL exhibits a paternally-biased expression in the brain and a biallelic expression in the periphery (Perez et al., 2015). This parental bias decreases between P0 and P60, and is also region specific (Perez et al., 2015). Hu et al. demonstrated that Trappc9 is required for the NGF-induced Bcl-xL expression in Pc12 cells (Hu et al., 2005). An interesting theory is that the dynamic relationship between Trappc9 and Bcl-xL might be the foundation of the microcephaly and intellectual disability phenotype observed in humans.

CHAPTER 4

Cellular models of Trappc9 silencing

4.1 Introduction

Trappc9 is part of the TRAPPII multiprotein complex, which belongs to the TRAPP family of complexes involved in ER-Golgi, intra-Golgi, endosome-Golgi vesicle trafficking and autophagy (Brunet & Sacher 2014). It is expressed in both the brain, specifically in neurons, but also in peripheral tissues (Hu et al., 2005), although its functions are still not fully understood.

The majority of what is known about the TRAPP complexes comes from studies in yeast, where structure and function are very well conserved. The three TRAPP complexes (TRAPPI, TRAPPII and TRAPPIII) share a core of six polypeptides arranged into a seven subunit complex (TRAPPI), to which other subunits bind forming TRAPPII and TRAPPIII. TRAPPII contains the yeast subunits tr120 and trs130 (Trappc9 and Trappc10 in mammals), while TRAPPIII contains yeast trs85 (Trappc8) and some proteins not found in yeast (Trappc11 and Trappc12) (Fig 1.6, Table 1.1). These complexes are involved in a process named tethering, which refers to the initial loose physical connection between the vesicle and the target membrane that precedes the fusion mediated by SNARE proteins. This process is probably aided by Rab GTPases and, in fact, the TRAPP complexes possess guanine exchange factor (GEF) activity for several Rabs.

Trappc1, Trappc4, Trappc5 and two Trappc3 are essential for the GEF activity, and the TRAPPII complex has been found to specifically possess GEF activity for Rab1 and Rab18 (Wang and Ferro-Novick, 2002; Li et al., 2017). Trappc9 itself binds Rab1, Rab18 and Rabin

8, a GEF for Rab8 and Rab11 (Westlake et al., 2011; Homma and Fukuda, 2016; Li et al., 2017). The activation of Rab proteins by the TRAPP complexes induces the recruitment of effectors involved in the fusion of vesicle and target membrane. The mammalian TRAPPII complex specifically interacts via Trappc9 with COPI coated vesicles, specific to ER-Golgi and intra-Golgi trafficking (Gwynn et al., 2006; Yamasaki et al., 2009; Zong et al., 2011; Li et al., 2017) and depletion of Trappc10 causes disruption of the Golgi and accumulation of vesicles and cargo transport blockade at the early Golgi (Gwynn et al., 2006).

Trappc9 has been reported to localise at the ER exit sites, ER-Golgi intermediate compartment (ERGIC) and cis-Golgi (Yamasaki et al., 2009; Zahoor et al., 2010; Zong et al., 2012). It has been shown that mutations in yeast trs120/Trappc9 cause defects in trafficking within the Golgi and in the retrograde pathway from early endosomes to the late Golgi (Cai et al., 2005). This interaction has important repercussions in neuronal signaling. In fact, signaling endosomes with the characteristics of early endosomes convey NGF signals across the axons of nociceptive neurons to their cell bodies (Delcroix et al., 2003). Trappc9 has been shown to regulate the nerve growth factor (NFG)-induced neurite outgrowth in PC12 cells and it also regulates the NF-κB pathway, binding to NF-κB inducing kinase (NIK) and IκBα inducing kinase β (IKKβ) (Hu et al., 2005).

It also interacts with the cargo domain of $p150^{glued}$, a subunit of dynactin, competing with COPII-coated vesicles and disrupting, when overexpressed, the localization of $p150^{glued}$ at the microtubule organizing center (MTOC) (Zong et al., 2012).

Loss-of-function mutations in human *TRAPPC9* cause postnatal microcephaly and brain abnormalities such as thinning of the corpus callosum and cerebellar hypoplasia (Mir et al., 2009; Mochida et al., 2009).

The scientific community has only recently turned its attention to this gene and its role in brain development and neuronal function is still unclear. In this chapter, I will try to

elucidate the role of this protein within the cell in the context of neuronal differentiation and maintenance. Analysing several Trappc9-depleted cellular models generated in our lab, I will investigate the role of this protein in neurite elongation and differentiation, but I will also try to confirm its involvement in the regulation of the NF-κB pathway which has been previously reported.

4.2 Methods

Western blot. Anti-Trappc9 primary antibody (Proteintech #16014-1-AP) used in Fig 4.1 and Fig 4.4 was used at 1:1000 dilution. Anti-p65 (Cell Signaling #8242) and p-p65 (Cell Signaling #3033) in Fig 4.6 were used at a 1:1000 dilution. Anti-IκB (Cell Signaling #4812) in Fig 4.8 was used at a dilution of 1:1000. Secondary antibodies IRDye 680LT anti-rabbit IgG (LICOR #92668023) and IRDye 800CW anti-chicken IgG (LICOR #92632218) were used at a 1:5000 and 1:10000 dilution, respectively.

Immunofluorescence. Anti-p65 primary antibody in Fig 4.7 was used at a 1:1000 dilution. Secondary antibody Alexa 488 anti-Rabbit IgG (Molecular Probes #A21206) was used at a 1:800 dilution.

4.3 Results

4.3.1 siRNA knockdown in PC12 cells

The role of Trappc9 in regulating neurite outgrowth has been documented in PC12 cells (Hu et al., 2005), which are derived from a pheochromocytoma of the rat adrenal medulla. This non-adherent cell line has the ability to differentiate into neuronal-like cells in the

presence of NGF 100 ng/mL in collagen IV coated culture plates (Fig 4.1), and it has been reported that in Trappc9-depleted cells the average neurite length following differentiation is lower than in control cells (Hu et al., 2005). My first aim was to establish a temporary Trappc9 knockdown (Trappc9 kd) cell line via siRNA silencing, and to recapitulate the effects observed by Hu et al., (2005) via shRNA lentivirus knockdown.

A pool of siRNA oligonucleotides was adopted to target different parts of Trappc9's mRNA and transfected into cells with a transfection reagent. Trappc9 levels were measured via western blot analysis and resulted in an average knockdown rate of 46% compared to cells treated with non-targeting (Non-targ) oligos (Fig 4.1). The average neurite length was measured after 72 hr treatment with 100 ng/mL NGF, comparing Trappc9 kd and Non-targ data for each cell category (cells with 1, 2, 3 or 4 neurites), as cells with a high number of neurites tend to have shorter lengths (for example see Fig. 4.5D). In contrast to what had been previously observed in Hu et al. (2005), no difference was found between the two groups. I hypothesised that the temporary depletion of Trappc9 obtained with the siRNA knockdown is not suitable for this type of analysis. Firstly, the average degree of knockdown obtained might have been too low to observe a direct effect on neurite outgrowth, as large amounts of Trappc9 are still present within the cell. Secondly, the differentiation of PC12 cells reaches its optimal level, with neurites being fully formed and outstretched, around the ninth day of treatment with 100 ng/mL NGF. For this reason the 72 hr treatment used in this analysis might not have been long enough to produce observable differences between the two groups. Longer treatments, however, allowed a complete restoration of Trappc9 levels after the knockdown (Fig 4.2) and could not, therefore, be used in this analysis.

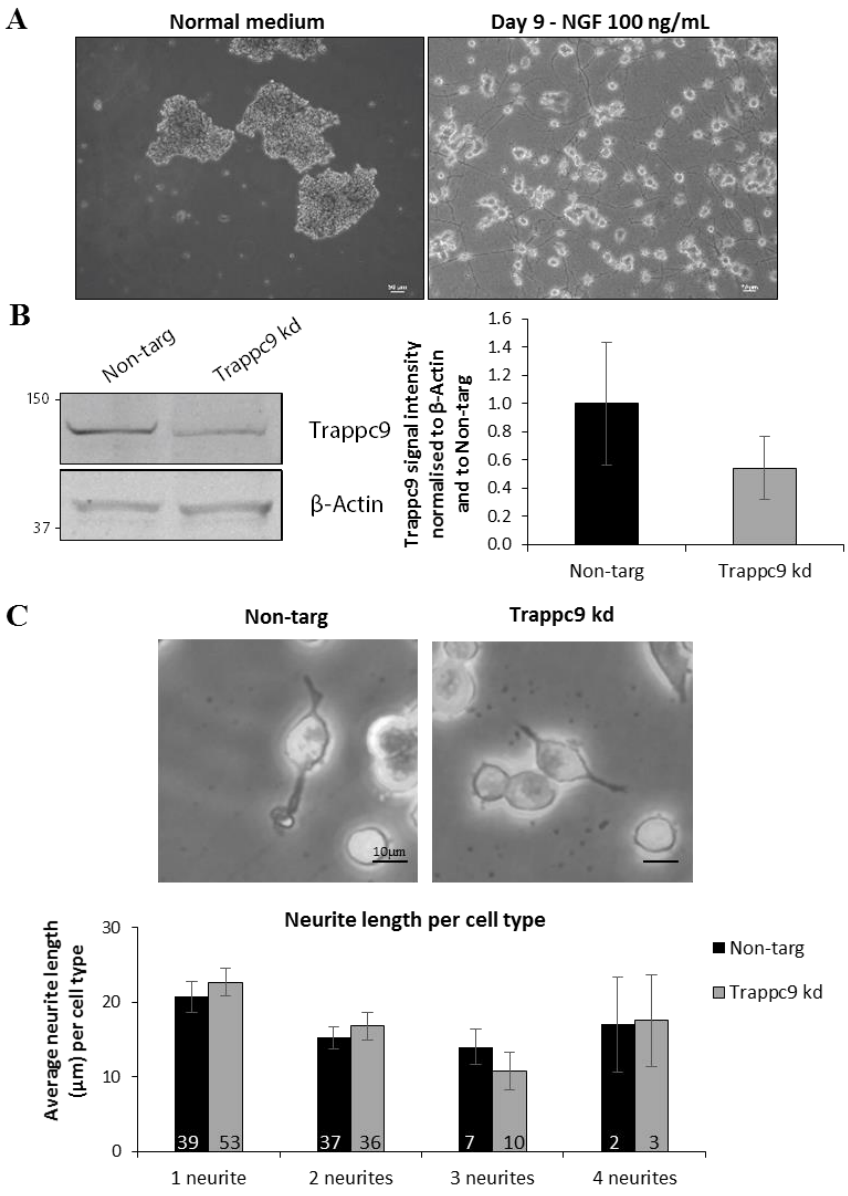

Figure 4. 1

siRNA knockdown of Trappc9 in PC12 cells. **A)** Differentiation of PC12 cells on collagen-coated tissue culture plastic with 100 ng/mL NGF. **B)** Transfection of PC12 cells with a pool of siRNA oligos targeting Trappc9. The Trappc9 knockdown (kd) cells show an average of 46% reduction in Trappc9 expression compared to the cells treated with non-targeting (Non-targ) oligos. n=4 **C)** Neurite length analysis of Trappc9 kd cells. The neurite outgrowth induced by the treatment with 100 ng/mL NGF for 72 hr was not affected by the reduction in Trappc9 expression. The graph represents the average neurite length per cells with 1-4 neurites, as cells with a high number of neurites tend to show a shorter neurite length. Numbers on graph bars represent the number of cells analysed. Total number of analysed cells: Non-targ: 85, Trappc9 kd: 102. Error bars show standard error. Scale bars: 10 µm.

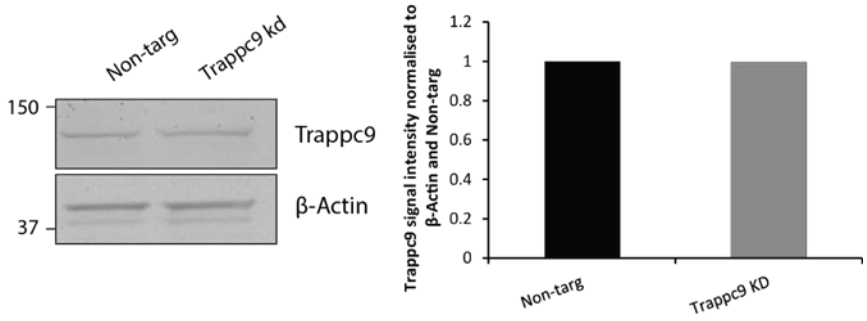

Figure 4. 2

Analysis of knockdown of Trappc9 in PC12 cells after 5 days from transfection with siRNA oligos. The expression levels of Trappc9 are restored to normal levels, rendering this protocol not suitable to study NGF-induced differentiation in a Trappc9-depleted background.

4.3.2 shRNA knockdown in N2A cells

In order to investigate the role of Trappc9 in neurite outgrowth, a stable knockdown via shRNA lentivirus transduction was performed on a different cellular model. Mouse neuroblastoma-derived Neuro-2A (N2A) cells (Fig 4.3) were selected as more directly comparable to brain cells than PC12 cells, and for their extensive use in neurite outgrowth studies, due to their ability to differentiate into neuron-like cells following treatment with retinoic acid (RA). Three different shRNA lentiviral clones were used, of which one (74kd) gave a ~70% knockdown that was not stable, and one (78kd) gave a ~30% knockdown. The third clone, named 76kd in this thesis, gave an average 63% reduction in expression, which remained around 50% at higher passages (Fig 4.4). In general, the lowest amount of viral supernatant that produced the best knockdown was selected for the gene silencing; 30-75-100 μL generated similar degrees of knockdown, and for this reason 75 μL was selected as middle ground. Control cells were transduced with a non-targeting shRNA lentiviral clone (see methods).

The morphology of 76kd does not appear different from control cells. The viability of these cells was analysed using the Prestoblue® viability reagent, as a correlation to proliferation, and measuring the absorbance at 595 nm for four days. No significant difference between

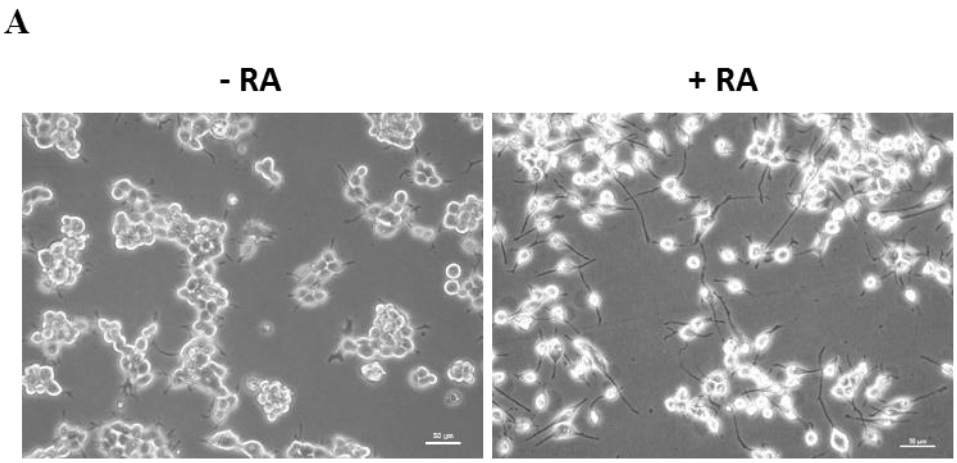

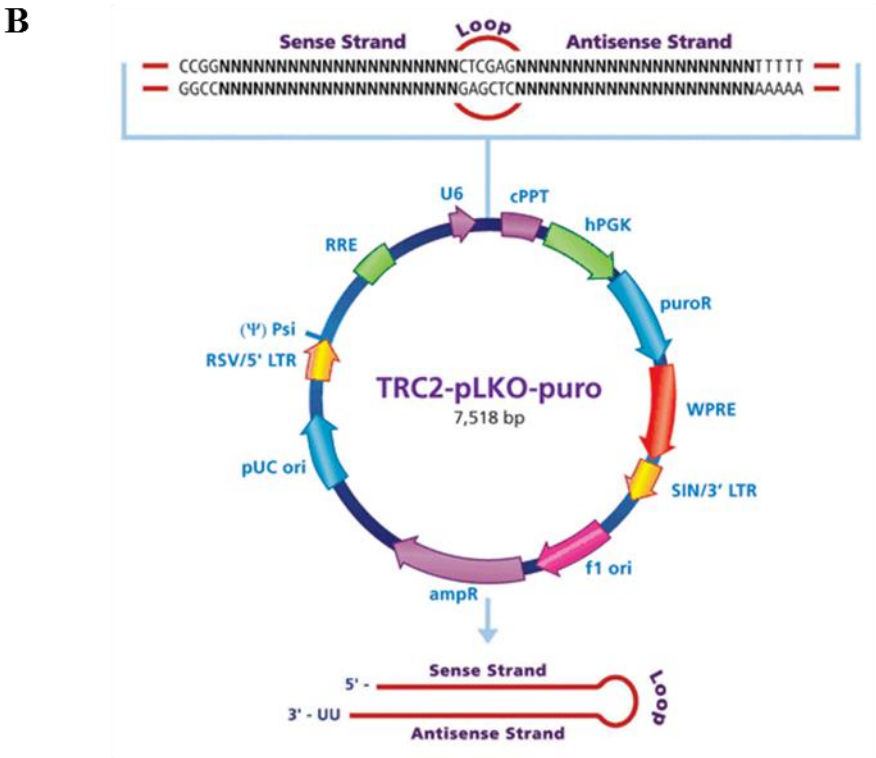

cppt	Central polypurine tract	**f1 ori**	f1 origin of replication
hPGK	Human phosphoglycerate kinase eukaryotic promoter	**ampR**	Ampicillin resistance gene for bacterial selection
puroR	Puromycin resistance gene for mammalian selection	**pUC ori**	pUC origin of replication
SIN/LTR	3' self inactivating long terminal repeat	**5' LTR**	5' long terminal repeat
		Psi	RNA packaging signal
		RRE	Rev response element

Figure 4. 3

Differentiation and Trappc9 knockdown in N2A cells. **A)** Differentiation of N2A cells with 20 µM Retinoic Acid (RA) for 24h. Scale bars: 50 µm. **B)** Mission® shRNA vector series backbone used for lentivirus knockdown of murine *Trappc9*. Scheme from www.sigmaaldrich.com; key features explained below scheme.

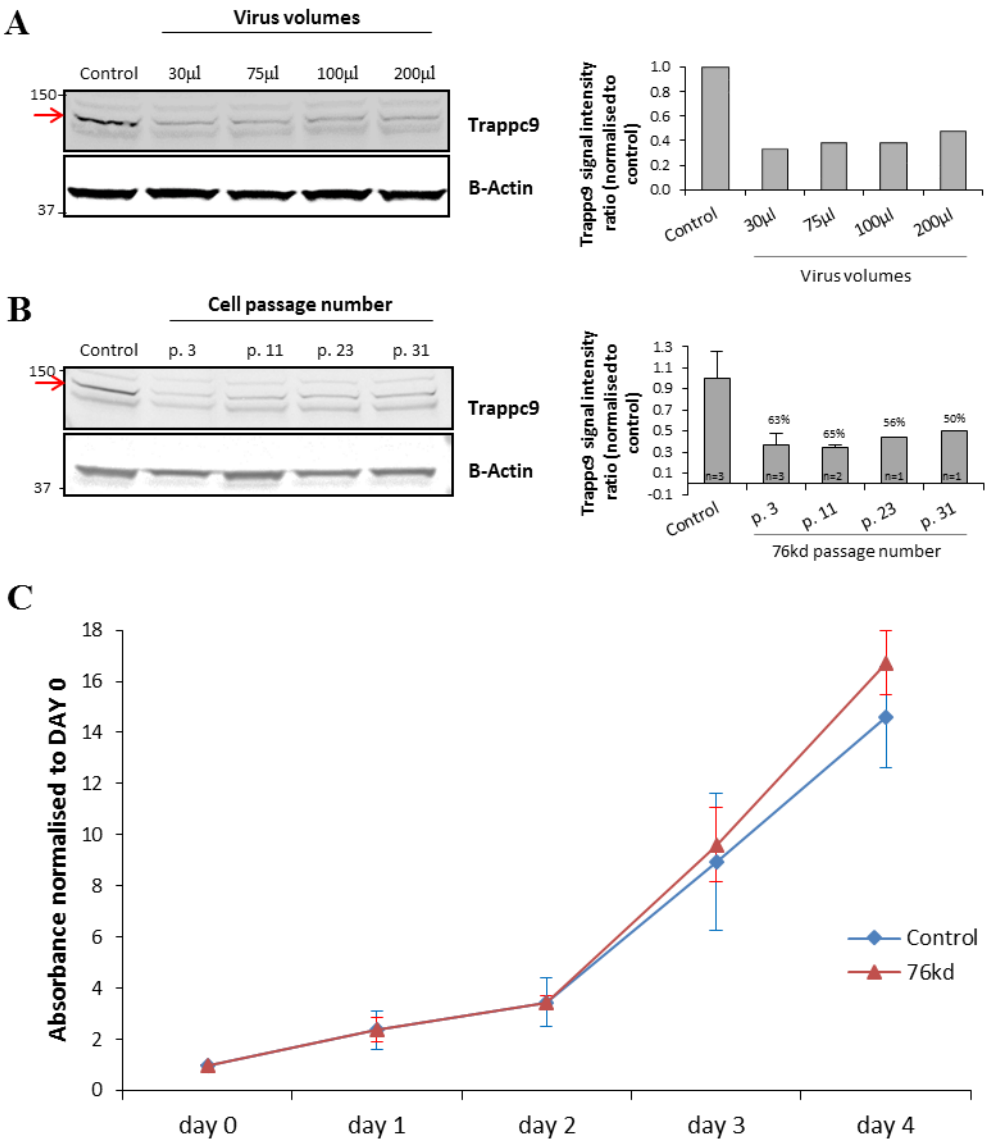

Figure 4. 4

Establishment of a N2A Trappc9 knockdown (kd) cell line via shRNA silencing. **A)** N2A cells were transduced with different amounts of shRNA clone 76 lentivirus and the Trappc9 knockdown efficiency was determined via western blotting. The clone transduced with 75µl of lentivirus (named 76kd) was selected for downstream experiments. Control cells were transduced with non-targeting shRNA lentivirus. **B)** Clone 76kd was lysed at different passage numbers and Trappc9 levels tested via western blotting to assess the stability of the knockdown. The numbers at the base of the columns represent the number of biological replicas; the percentage above the columns represent the degree of knockdown of Trappc9; the western blot image is a representative picture. **C)** As preliminary characterisation of this cell line, the viability of clone 76kd was assessed daily in comparison to control cells, using the Prestoblue® viability reagent over a 4-day period. Western blots quantification: Trappc9 signal intensity was normalised to β-actin signal intensity and then normalised to control. Red arrows indicate Trappc9. Viability assay: n=3, day 1-4 normalised to day 0. Error bars show standard error.

the two cell lines was observed (Fig 4.4), however, it was my personal impression that in culture 76kd cells might be proliferating slightly faster.

As previously mentioned, these cells assume a neuron-like phenotype when treated with RA, and a much milder differentiation in a serum-deprived environment. The cells were incubated with 20 μM RA in 2% serum medium, as higher concentrations are toxic and impair cell survival, for 24 hr and analysed their differentiation ability (Fig.4.5). Neurite length was quantified and the measurements compared among cells with the same number of neurites (1-4 neurites), as cells with a higher number of neurites tend to have shorter lengths (Fig. 4.5D). No statistical difference was found between the two cell lines for any of the analysed groups. However, a reduction of cells with four or more neurites in 76kd was observed (3.61% of the total, against the 17.65% of the control cells). This reduction is specific to the treatment with RA and does not occur in the mild differentiation observed in the serum-deprived environment (2% serum only).

4.3.3 Alterations in the NF-κB pathway

Overexpression of Trappc9 in HEK293 cells enhanced the TNFα-induced phosphorylation of p65 (Hu et al., 2005). We investigated whether our N2A 76kd cells exhibited a defect in p65 phosphorylation by treating them with 10 ng/mL TNFα for 0-30 min and analysing cell lysates with a monoclonal antibody for p-p65 (Fig 4.6). Baseline levels of p65 were not affected by the TNFα treatment in both control and 76kd cells. The levels of p-p65 increased after 20-30 min of treatment but did not show any statistical difference between control and 76kd cells.

I investigated the TNFα-induced p65 nuclear translocation efficiency in 76kd cells (Fig 4.67). p65 translocated from the cytoplasm to the nucleus after 30 mins of treatment and Trappc9 has been shown to interact with $p150^{glued}$, a subunit of dynactin.

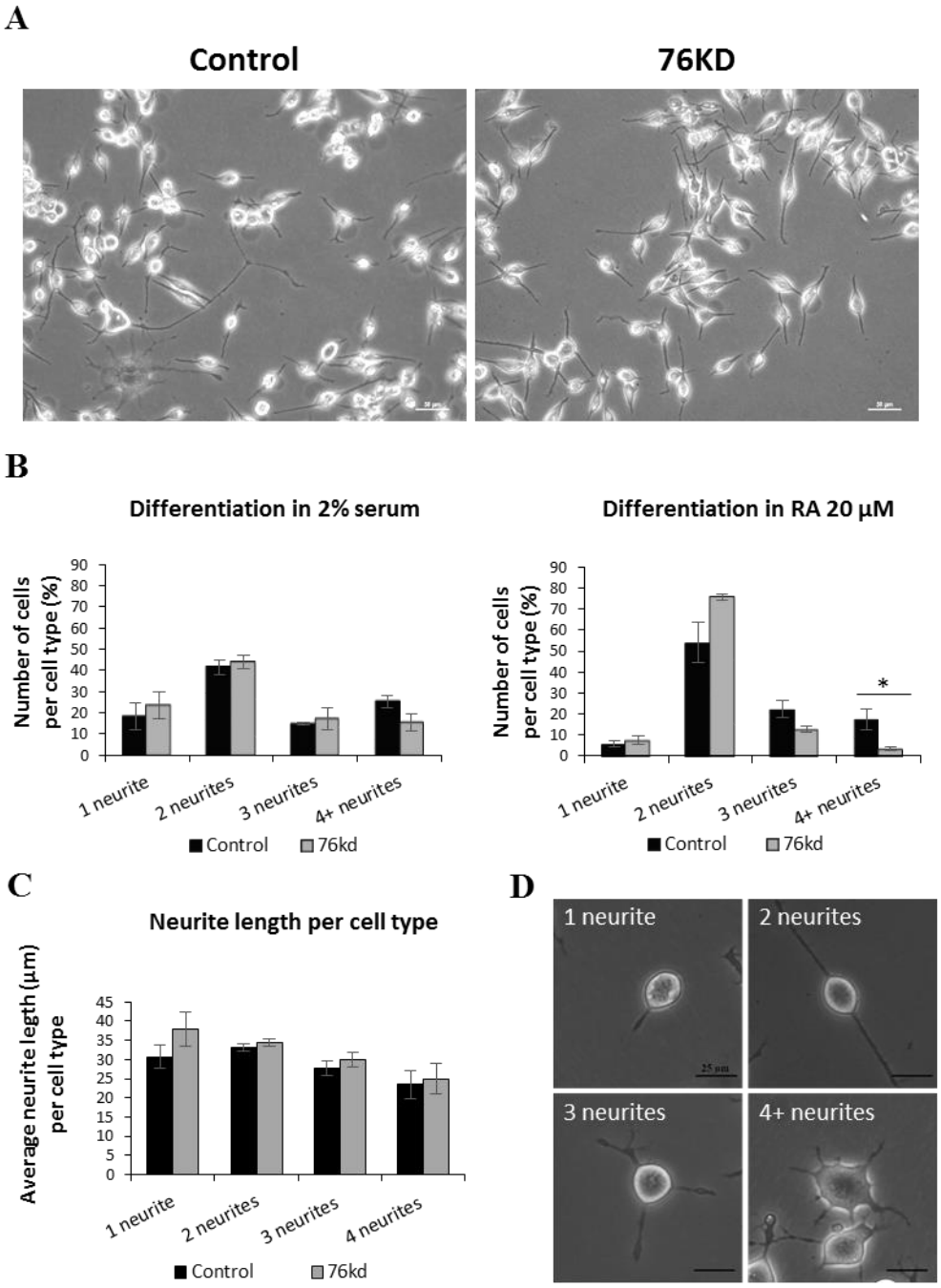

Figure 4. 5

76kd cells show a different response to RA treatment. A) Control and 76kd cells after 24h incubation with 20 µM RA. B) Analysis of the abundance of the different cell types within the population. 76kd preferentially differentiate into cells with one or two neurites in the presence of 20 µM RA + 2% serum but not in 2% serum only. C) The average neurite length per cell type of 76kd cells was not statistically different from control cells. The average neurite length was calculated by averaging measures from all the analysed neurites per cell type (e.g. every 10 3-neurite cells, 30 neurite measures). D) Differentiated cell types observed in culture. Scale bar 50 µm in A and 25 µm in D. Neurite length analysis: n=3, 548 control cells, 565 76kd cells. Differentiation analysis: 2% serum n=2, 1076 control cells, 1007 76kd cells; 20 µM RA n=3, 1114 control cells, 1017 76kd cells. Error bars show standard error.*p<0.05.

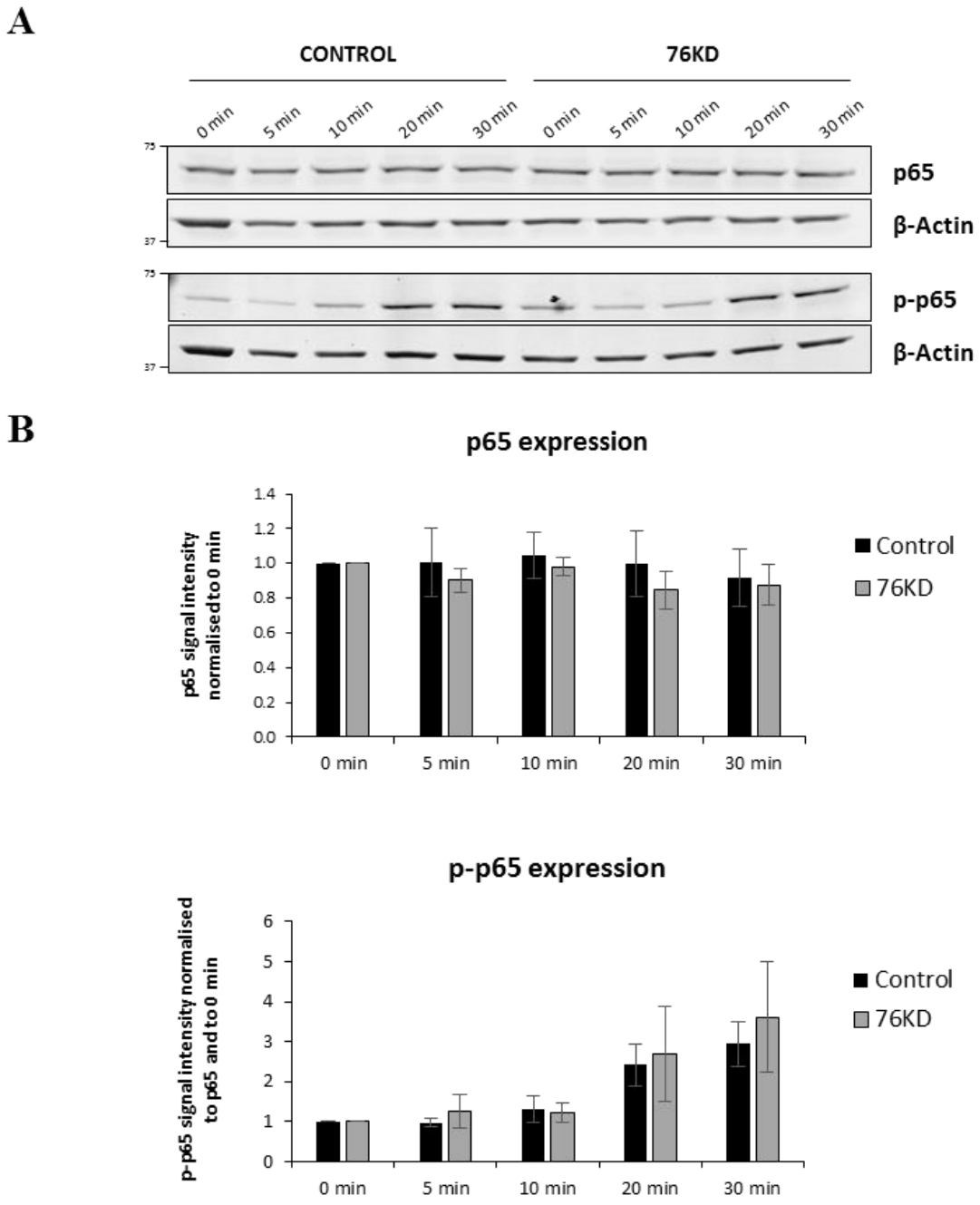

Figure 4. 6

p65 expression and phosphorylation in 76kd cells. A) Western blot representative images of p65 and p-p65 expression in control and 76kd cells following treatment with 10 ng/mL TNFα for 0, 5, 10, 20 and 30 min. While levels of p65 remain constant, p-p65 levels increase at 20 and 30 min of treatment in both control and 76kd. B) Quantification of p65 and p-p65 expression from western blots. No statistical difference was found between control and 76kd. p65 and p-p65 quantification was performed on separate blots but from the same cell lysate. p65 signal intensity levels were normalised to β-actin and to 0 min; p-p65 levels were normalised to β-actin first, then to p65 levels (normalised to β-actin) and finally to 0 min. n=4, error bars represent standard error calculated from normalised to 0 min values.

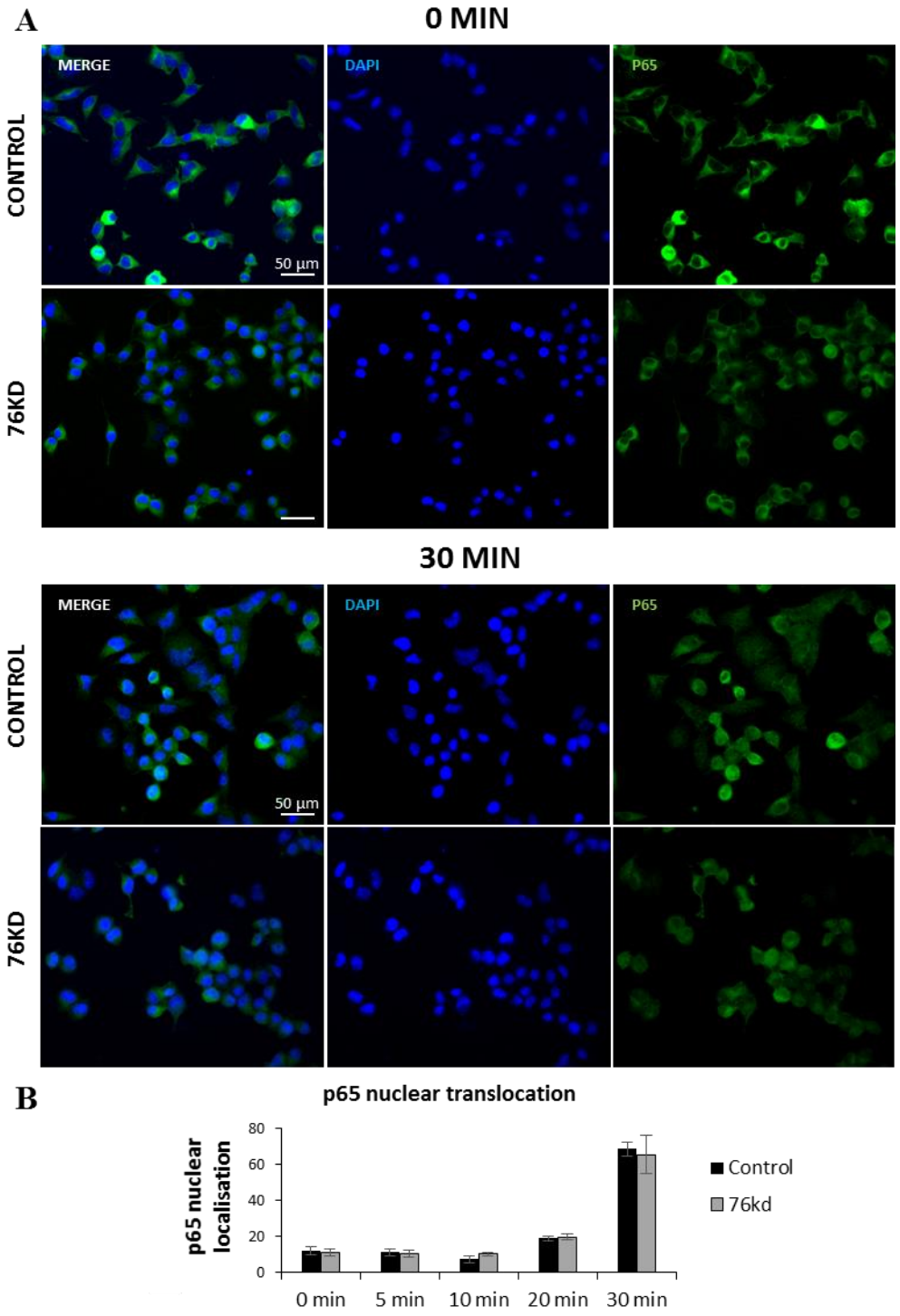

Figure 4. 7

p65 nuclear translocation after TNFα treatment. **A)** Control and 76kd cells were incubated with 10 ng/mL TNFα for 0, 5, 10, 20 and 30 minutes (only 0 and 30 min shown in the figure). At 30 min incubation both control and 76kd cells show expression of p65 in the nucleus. **B)** Quantification of cells expressing p65 in the nucleus. Cells were considered positive for nuclear translocation if p65 signal in the nucleus was equal or stronger than the signal in the cytoplasm. No significant difference was found between control and 76kd cells. The experiment was performed in n=3. Images are representative. Error bars show standard error. Scale bars: 50 µm.

Deficiency in Trappc9, however, does not appear to impair the transport of p65 into the nucleus, as no statistical difference between control and 76kd cells was found.

Similarly, Trappc9 has been reported to potentiate the TNFα-induced degradation of IκBα with peaks at 15-30 min (Hu et al., 2005).

I also isolated skin embryonic fibroblasts (EMFIs) from WT and KO Tm1a embryos at E13.5 (see Chapter 5 for details on the animal model) and treated them at p3 with 10 ng/mL TNFα for 0-120 min (Fig 4.8). The western blot analysis revealed that the degradation of IκBα induced by the TNFα reached a peak at 20-30 min to then restore normal levels at 120 min. No major differences were observed between WT and KO cells. However, a general trend was noticed towards higher expression levels for IκBα in KO cells compared to WT EMFIs, which will need to be confirmed with further experiments.

4.4 Discussion

4.4.1 Regulation of neurite outgrowth and neuronal differentiation

The role of Trappc9 within the cell and its contribution to brain development is still far from being elucidated. From subunit in a multiprotein complex involved in Golgi-trafficking to regulator of the NF-κB pathway to regulator of gene expression, it appears to be involved in many major pathways and systems that could justify the brain abnormalities observed in individuals with loss-of-function mutations in this gene. The lack of in depth studies in neurons, and the lack of consensus between data published from different groups, leaves us with uncertainties on the specific cellular mechanisms that underlie the human developmental brain symptoms. Individuals with homozygous mutations in *TRAPPC9* show a set of symptoms among which microcephaly and white matter abnormalities are consistently observed amongst the affected individuals. These

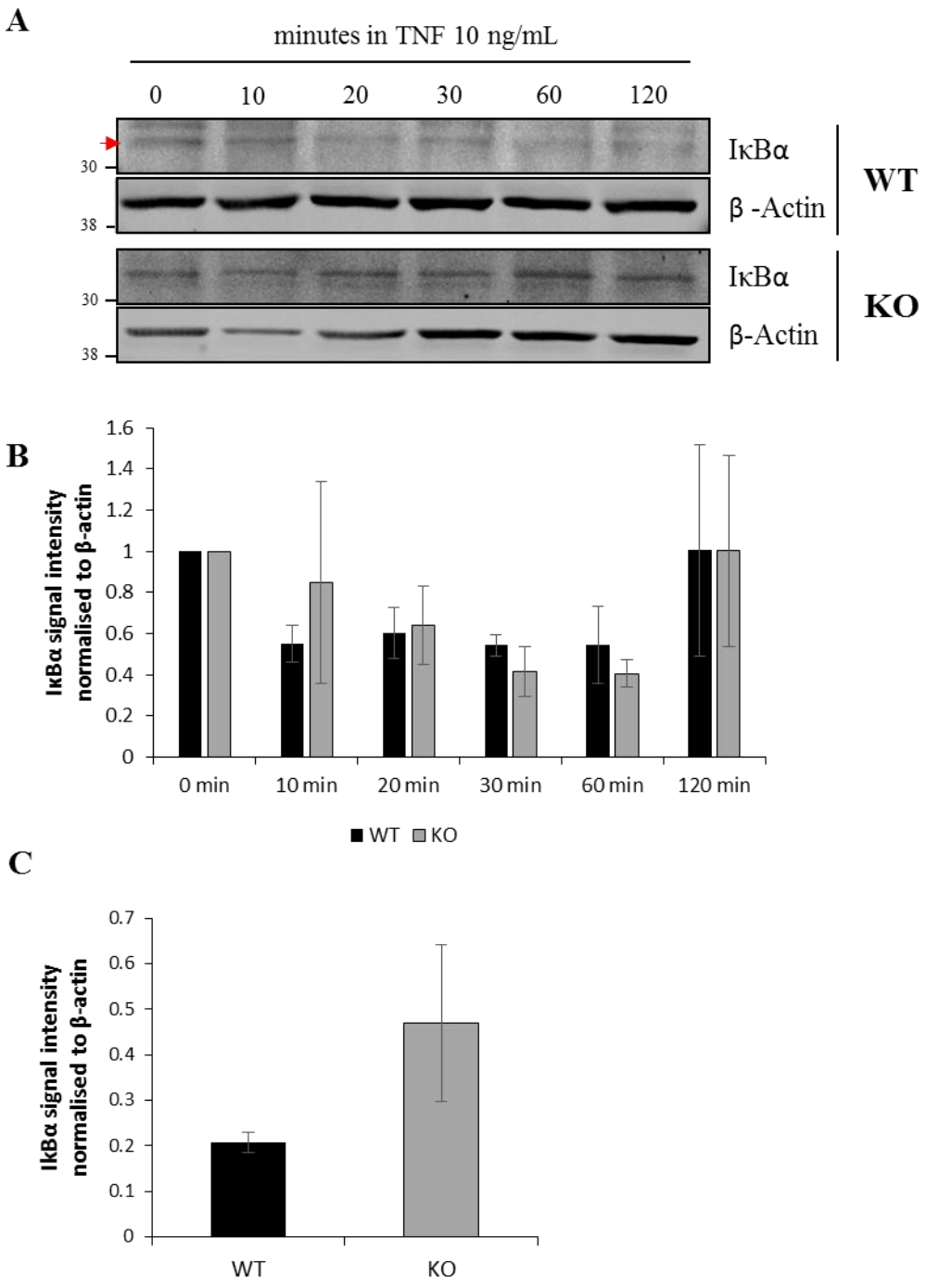

Figure 4. 8

IκBα expression in WT and KO mouse embryonic fibroblasts (EMFIs). **A)** Representative image of western blot for IκBα of EMFIs at p3 after treatment with 10 ng/mL TNFα for 0, 10, 20, 30, 60 and 120 min. **B)** Quantification of western blot for IκBα. Both WT and KO cells exhibit a decrease in IκBα expression after 10-20 min of exposure to TNFα, and a gradual restoration to baseline levels at 120 min. **C)** Baseline IκBα expression levels in WT and KO EMFIs. Although not statistically different, a general trend suggests KO EMFIs possess higher levels of IκBα. IκBα signal intensity levels were normalised to β-actin and to 0 min (A), n=3, error bars represent standard error.

abnormalities appear shortly after but not at birth, suggesting that TRAPPC9 might be more important in the postnatal maturation of the brain and/or in neuronal maintenance. In fact, a case has been reported in which an affected individual exhibited the brain abnormalities previously described (microcephaly, thinning of the corpus callosum, cerebellar atrophy), but also a degeneration of the frontal cortex and loss of cerebellar volume over time (Koifman et al., 2010). Unfortunately, the lack of follow up reports on the affected individuals prevents us from observing how this condition progresses with age and thus we can only speculate how Trappc9 is involved in the onset of these symptoms.

The expression of Trappc9 has been previously confirmed in neurons and not in glial cells (Hu et al., 2005). In light of the major effects on brain anatomy observed with the loss-of-function of this protein, I was interested in investigating how it is involved in regulating neuronal functions.

The multitude of systems it has been associated with leaves Trappc9's role within the cell unclear, as it is not known whether it is implicated in proliferation, differentiation and/or survival, as all of these processes could explain the microcephaly and brain abnormalities.

Possibly the most easily correlated with the observed phenotype would be the association with the NF-κB pathway and its involvement in neurite outgrowth. The earliest report of Trappc9 in mammalian cells showed that its depletion in PC12 cells impairs the NGF-induced neurite outgrowth (Hu et al., 2005), possibly by reducing the activation of the NF-κB inducing kinase (NIK), which has been shown to promote NGF-induced neurite formation in PC12 cells (Foehr et al., 2000). This effect, however, could also be mediated by a role in the endocytic transport of NGF-activated Trk receptors to the nucleus where they activate gene expression (Delcroix et al., 2003). Our first aim was to reproduce these findings using a transient siRNA silencing for Trappc9 in contrast to the stable shRNA used by Hu and colleagues. We obtained an average 46% reduction in Trappc9 expression but

the neurite elongation analysis did not reveal any statistical difference between control and knockdown cells (Fig 4.1). As this method was not designed to produce a stable knockdown, I hypothesised that the inability to confirm the results from Hu et al. (2005) was due to residual amount of Trappc9 left in the cytoplasm. For this reason, I decided to adopt a stable knockdown approach via shRNA lentivirus transduction using a more versatile mouse neuroblastoma cell line, N2A, widely used in neurite outgrowth and differentiation studies. Of the three different shRNA clones tested (Table 2.3), one (74kd) produced a high knockdown degree (70%) that however was not stable (possibly due to the depletion of Trappc9 not being tolerated by the cells), the second (78kd) produced a low degree of knockdown (30%) and the third produced a stable 50-60% knockdown. For subsequent analysis I therefore selected clone 76kd (Fig 4.4).

Hu et al. (2005) observed a high degree of knockdown in PC12 targeting the C-terminal but not the N-terminal or the middle part of rat *Trappc9* mRNA. The clones used in this thesis targeted the central part of mouse *Trappc9* mRNA.

N2A cells do not differentiate in response to NGF as the PC12 cells do. They differentiate instead in response to retinoic acid (RA) treatment and, to a lesser extent, to serum withdrawal. We measured the neurite length after 24 hr treatment with 20 μM RA + 2% serum and found no statistical difference between control and 76kd cells. We did, however, observe an abnormal differentiation response in 76kd cells, where the treatment with 20 μM RA + 2% serum (but not in 2% serum only) produced a population with more cells with two neurites and less with four or more neurites (Fig 4.5). However, the importance of this observation in a biological context *in vivo* remains uncertain.

In culture, N2A cells appear as a mixed population of cells with a variable number of neurites. To my knowledge, the number of neurites is not a commonly investigated parameter and, for this reason, the differentiation stages of N2A cells have not been

investigated. Thus, there is no available information regarding the distinct stages these cells go through and I cannot assert whether the cells undergo a specific type of differentiation (e.g. either two neurites or three from the beginning) or if the addition of an extra neurite corresponds to a further step in differentiation.

Nonetheless, the change in differentiation observed in these cells is worth considering, as it could be an indication that the differentiation proceeds more quickly in a Trappc9-depleted background, or that the differentiation pattern has been altered. This could have important repercussion in a stem cells' active environment during brain development or in the subgranular and subventricular zones in the adult brain.

RA is a vitamin A-derived lipophilic molecule that acts as a ligand for the nuclear retinoic acid receptor (RAR) superfamily, converting them from transcriptional repressor to activators (Rhinn & Dollé 2012). It enters the cell by diffusing through the plasma membrane and reaches the nucleus with the involvement of cellular retinoic acid-binding proteins (CRABPs) (Rhinn & Dollé 2012). RA has a crucial role in development as it regulates segmentation and patterning of the hindbrain and it influences forebrain development. It has been suggested that RA signalling may influence specific progenitor populations as it is produced from E13.5 to postnatal stages in the developing meningeal cell layer, from where it would diffuse to regulate progenitor cell proliferation/differentiation/migration along cortical layers (Rhinn & Dollé 2012). *In vitro*, treatment of rapidly proliferating ES cells (cultured in suspension as embryo bodies) with RA induces the differentiation into neural progenitors (Bibel et al., 2004; Plachta et al., 2004). These cells are capable of differentiating into neurons with electrophysiological properties similar to those of pyramidal neurons and with the ability of establishing synaptic contacts with other cells. Furthermore, *in vitro* RA can promote neurogenesis by enhancing proliferation and differentiation of adult forebrain neuroblasts and regulate *in*

vivo the proliferation of astrocytes in the subventricular zone (Haskell and LaMantia, 2005).

With the aim to investigate N2A differentiation capacity in a Trappc9-deprived environment, I found an unexpected association between Trappc9 and RA, which had not been previously investigated. This suggests that Trappc9's functions are not limited to the NF-κB pathway (as we already perceived) but are probably linked to a general mechanism communal to different pathways (e.g. vesicular transport).

Interestingly, it has been reported that several Rab family members are implicated in neurite outgrowth and, as mentioned earlier, Trappc9 binds Rab1, Rab18 and Rabin 8, a GEF for Rab8 and Rab11 (Westlake et al., 2011; Homma and Fukuda, 2016; Li et al., 2017). Rab8, Rab13, Rab35 and Rab36, for example, have been shown to localise on recycling endosomes and regulate membrane trafficking, while Rab10 is involved in post-Golgi trafficking of plasmalemmal precursor vesicles that are added to the neurite tip. Rab11 is implicated in targeting integrins and Trk receptors to the neurite tips and is required for adhesion and signal transduction during neurite outgrowth (Villarroel-Campos et al. 2014). Furthermore, both Rab8 and Rabin8 are required for NGF-dependent neurite outgrowth in PC12 cells (Homma and Fukuda, 2016).

Thus, it appears that Trappc9's involvement in neurite outgrowth and differentiation might be due to its activity as part of the TRAPPII complex, although the specific role of Trappc9 in relation to RA signalling in N2A is not clear yet. Trappc9 has been shown to interact with $p150^{glued}$ (Zong et al., 2012), a subunit of dynactin that independently binds to microtubules and to dynein, having a role in ER-Golgi and retrograde transport (Lazarus et al., 2013). The exact mechanisms of RA transport and signalling pathway have not been fully elucidated, but it is possible that Trappc9 is involved in the transport dynamics of factors participating in the RA response and/or differentiation.

The involvement of Trappc9 in neuronal differentiation has been demonstrated by Zhang and colleagues (2013), who showed that the differentiation of an enteric neuronal cell line (ENC) in Trappc9-deficient cells is attenuated. The knockdown of Trappc9 led to a reduction in baseline TNFα-induced neuronal protein (e.g. NSE) expression, as well as a reduction in mRNA expression of pan-neuronal markers (PG9.5, NSE and TUJ1) and well differentiated neuronal markers (e.g. NEFM) (Zhang et al., 2014b).

Thus, Trappc9 might have an important role in cell differentiation in the context of the microcephaly observed in human patients.

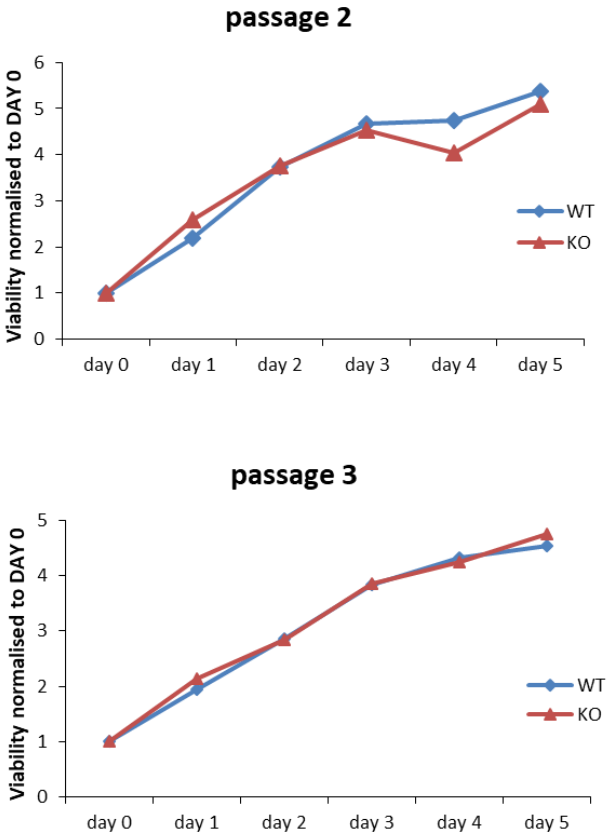

Figure 4. 9
Viability analysis of WT and KO (Tm1a) EMFIs at passage 2 and 3 over the course of 5 days with Prestoblue® viability reagent. n=1.

Cell proliferation might also be affected. Lentivirus knockdown of Trappc9 inhibited cell proliferation and viability in breast and colon cancer cell lines, and inhibited tumour formation in vivo (Zhang et al., 2015a). The stable knockdown in N2A cells presented in this thesis, however, did not inhibit cell proliferation/viability and, on the contrary, I observed a tendency of 76kd to replicate slightly faster than control cells. Furthermore, preliminary results on mouse KO EMFIs showed no difference in viability in comparison to WT cells (Fig 4.10). The involvement of Trappc9 in cell proliferation remains thus of uncertain nature, although it might be cell/tissue specific.

4.4.2 Regulation of NF-κB pathway

In the existing literature on Trappc9, its involvement in the regulation of the NF-κB pathway is a predominant theme in mammalian cells. The first report dates back to 2005, when Hu and colleagues co-immunoprecipitated the NF-κB inducing kinase (NIK) and the IκB kinase β (IKKβ) with a factor that they named NIK and IKKβ binding protein (NIBP) (Hu et al., 2005). NIBP was later identified as the mammalian orthologue of the TRAPPII complex yeast subunit trs120 and renamed Trappc9. Hu and colleagues discovered that Trappc9 potentiates the TNFα-induced NF-κB DNA binding activity with peaks at 15 and 30 min of treatment and that increases the degradation of the NF-κB inhibitor IκBα. The degradation of IκBα has also been observed in skin fibroblasts derived from patients with loss-of-function mutations of Trappc9. The treatment with TNFα induced the degradation of IκBα at 10 and 20 min in control cells while Trappc9-null fibroblasts showed a markedly reduced degradation (Philippe et al., 2009). I performed the same treatment of mouse WT and KO EMFIs but did not observe any statistical difference in IκBα degradation between the two groups (Fig 4.8). Among the factors that could have contributed to this discrepancy, should be noted the development stage difference and the species diversity and adaptability, in addition to the substantial level of remaining Trappc9 protein in our

knockdown cells. I did, however, observe higher IκBα basal levels (Fig 4.8) in KO EMFIs, as previously seen by Zhang et al. (2015a).

The NF-κB pathway is highly responsive to the environment and strictly regulated. Its functions are not limited to inflammation, but it is also involved in plasticity and learning and memory, as NF-κB p50 KO mice show impaired adult neurogenesis and memory defects (Denis-Donini et al., 2008). Furthermore, the NF-κB pathway is involved in synaptogenesis as it enhances dendritic spine and excitatory synapse density *in vitro* (Boersma et al., 2011). Moreover, NF-κB family members are expressed in specific cell populations of the neurogenic SVZ region of the adult brain (Denis-Donini et al., 2005).

Trappc9 is involved in both the canonical and non-canonical activation of the pathway by interacting with NIK and IKKβ. In the canonical activation, the cell receives external stimuli (e.g. TNFα) that trigger the activation of IKK heterodimers (composed of IKKα, IKKβ and IKKγ) that in turn phosphorylate the inhibitor IκBα, whose function is to bind NK-kB subunits in the cytoplasm preventing their migration to the nucleus. The phosphorylation of IκBα is the signal that leads to its ubiquitination and degradation, leaving NF-κB dimers free to translocate to the nucleus and activate NF-κB responsive genes. IκBα itself is a NF-κB responsive gene, and the activation of the pathway induces an auto feedback loop, where the expression of IκBα is induced to replenish baseline levels, thus generating oscillating levels of NF-κB activity (Ito et al., 1994). In the non-canonical activation of the pathway instead, the signal (e.g. lymphotoxin-β) induces the activation of NIK that phosphorylates IKKα homodimers, that in turn phosphorylate the NF-κB precursor p100, leading to its processing to p52/RelB dimers ready to translocate to the nucleus.

Although I could not replicate the results on IκBα degradation found in literature, Trappc9's role is supposedly to stimulate/regulate this degradation and its loss of function should inhibit the activation of the NF-κB pathway and the expression of its responsive

genes. The higher IκBα basal levels in Trappc9 KO cells are, therefore, more difficult to explain, although adaptation mechanisms could occur to overcome the lack of Trappc9 expression.

Trappc9 has also been shown to promote the phosphorylation of the NF-κB subunit p65 and IKKβ (Hu et al., 2005; Zhang et al., 2015a). We analysed our 76kd cells for TNFα-induced p65 phosphorylation and found no statistical difference in comparison with the control cells (Fig 4.6).

Interestingly, the knockdown of Trappc9 also inhibits the NGF-induced expression of the anti-apoptotic factor Bcl-xL, possibly by modulating the activity of the NF-κB pathway (Hu et al., 2005), and it increases the TNFα-induced apoptosis (Zhang et al., 2015a). Trappc9 might therefore modulate cell survival in response to external stimuli participating in brain development, although further studies should be performed in order to confirm its contribution.

4.4.3 Vesicle trafficking-related functions

Among the most interesting findings on Trappc9 is the interaction of this protein with the dynactin subunit p150^{glued} (Zong et al., 2012). Dynactin is involved in bidirectional organelle and vesicular transport by linking these particles to dynein and kinesin. In particular, p150^{glued} is the subunit responsible of the interaction with dynein and it binds COPII coated vesicles from ER to Golgi (Presley et al., 1997). It has been shown that Trappc9 binds the cargo-binding domain of p150^{glued} competing with COPII-coated vesicles. In addition, the overexpression of all TRAPP subunits can disrupt the architecture of microtubules and the localisation of p150^{glued} at the MTOC (Zong et al., 2012). This is probably due to the interaction between TRAPP subunits and microtubule-associated proteins, which would be competed away when TRAPP particles are overexpressed.

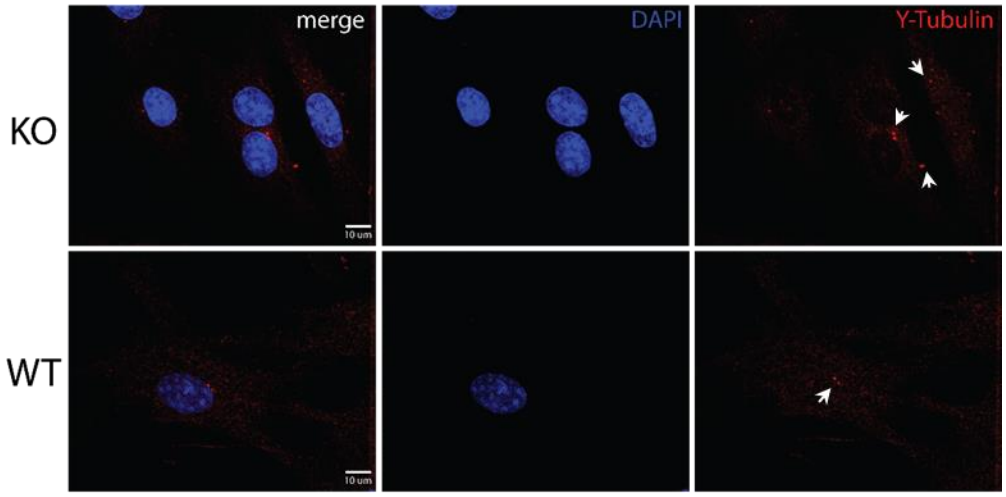

Number of MTOCs/cell	Number of cells	
	WT	KO
1	17	9
2	9	10
3	6	7
4	2	3
5	0	0
6	0	0
7	0	0
8	0	1
9	0	0
10	0	0

Figure 4. 10

A) Immunofluorescent staining for γ-tubulin (red) on WT and KO (Tm1a) EMFIs. **B)** Quantification of number of MTOCs/cell in WT and KO EMFI populations from staining in A. Total number of analysed cells WT: 34, KO: 30. Scale bar: 10µm.

It has recently been reported that skin fibroblasts from people harbouring *TRAPPC9* mutations exhibited multiple centrosomes per cell (Gan et al., 2014). I have analysed KO mouse EMFIs but preliminary data suggests the lack of difference in the number of MTOCs per cells compared to WT EMFIs (Fig 4.10), although such difference could be cell type and/or cell cycle specific.

Furthermore, in human retinal pigment epithelium cells TRAPPC9 is required for the localisation of Rabin8 at the centrosome where its GEF activity for Rab8 is required in primary cilia formation (Westlake et al., 2011). The available information on Trappc9 therefore suggests this protein plays an important role in microtubule organisation.

The disruption of the dynactin complex caused by the overexpression of p150glued inhibits TNFα-induced p65 nuclear translocation (Shrum et al., 2009). For this reason, I decided to investigate whether the TNFα-induced p65 translocation to the nucleus was affected in 76kd cells, where in theory the vesicular transport Trappc9-mediated by dynactin should be disrupted. I did not find any disruption in the translocation (Fig 4.7), however, this being a dynamic movement in and out of the nucleus, live imaging might be required to detect subtle differences in the dynamics of transport.

4.4.4 Concluding remarks

The analysis of the literature in combination with the results presented in this chapter have actually increased the amount of questions regarding Trappc9's role within cells and in regards to brain development. The picture appears still very complicated, with Trappc9 ranging from vesicle trafficking particle to regulator of gene expression. Trappc9 could therefore be defined as a moonlight protein, which by definition is <<a class of macromolecules that perform a large variety of functions>> (Huberts and Van Der Klei, 2010). Overall, in this chapter I have demonstrated that Trappc9's involvement in viability and neurite elongation remains unclear while preliminary results suggest an important role in neuronal differentiation. Progenitor cells might be affected by mutations in Trappc9 leading to defects in brain development or, considering the later onset of the brain abnormalities observed in humans, neuronal maintenance.

The multitude of roles for Trappc9 discussed in this chapter could be cell/tissue specific, thus explaining the reason why I could not replicate many of the results found in literature.

In addition, the lack of a full knockdown in PC12 and N2A cells might be the reason why I could not confirm the published results. However, differences in methods (including cell type) and techniques might be the basis of such discrepancies. In the next chapter I will describe a KO mouse line for Trappc9 and show how these animals present a phenotype that, in comparison to the human disorder, is much milder. Considering the difference in species and any adaptation mechanisms occurring in different organisms, it is logical to assume that the *in vitro* studies might also reveal subtle differences, which might be undetectable depending on the sensitivity of the method. Furthermore, in both *in vitro* and *in vivo* studies, it is not known how much is specifically mediated by Trappc9 and how much is mediated by the TRAPPII complex, which could still be partially functional and account for the lack of Trappc9.

Nevertheless, I have highlighted the importance of Trappc9 in the context of the TRAPPII complex, and the importance of this complex in many physiological functions. The fact that mutations in other TRAPPII subunits cause important phenotypes is another indication of that. In fact, mutations in TRAPPC11 have been associated with myopathy and intellectual disability, mutations in TRAPPC2 cause spondyloepiphyseal dysplasia tarda, a recessive disorder in bone formation, and TRAPPC4 has been associated with colorectal cancer (Brunet & Sacher 2014).

Further studies will need to be specifically designed to understand the role of Trappc9 with and without the involvement of the TRAPPII complex, in order to shed light upon the molecular basis of microcephaly and intellectual disability.

CHAPTER 5

Mouse model of Trappc9 knockout

5.1 Introduction

A set of loss-of-function mutations in the sequence of *TRAPPC9* have been associated with a type of autosomal non-syndromic intellectual disability. To date, only 21 affected individuals have been the subject of a thorough symptomatic description (Mir et al., 2009; Mochida et al., 2009; Philippe et al., 2009; Koifman et al., 2010; Abou Jamra et al., 2011; Kakar et al., 2012; Marangi et al., 2013). The occipitofrontal circumference measurements at birth are available for only three patients, showing a normal/borderline microcephaly head circumference (Mochida et al., 2009). All patients were examined during childhood except for three individuals that were adults at the time of the examination (Abou Jamra et al., 2011). They all presented moderate to severe intellectual disability and different degrees of microcephaly with head measurements ranging from -3 SD to -1 SD.

As mentioned in chapter 1, the definition of microcephaly is sometimes variable, generally defined as a head size of 3 SD or more below the appropriate mean and sometimes defined as 2 SD or more below the mean. In the second case, many intellectually normal individuals might actually fall within this description, making prenatal diagnosis particularly difficult.

The most common symptoms among the affected individuals are inability of speech or speech delay, dysmorphic facial features, inability to feed themselves and late start to walking. While the brain abnormalities included thinning of the corpus callosum, cerebellar hypoplasia and white matter abnormalities, Koifman et al. (2010) reported a

case with progressive loss of white matter and cerebellar volume over time, suggesting Trappc9's functions might not be limited only to early brain development.

Other symptoms are of a more variable nature, not being present in all the reported cases, such as epilepsy, bruxism, hand-flipping behaviour and weight gain.

The genes involved in brain development and cognitive capabilities belong to a highly heterogeneous group, encoding for proteins that play important roles in diverse processes. Microcephaly in particular can be caused by the epigenetic disregulation or by mutations in the sequence of transcription factors (FOXG1), ubiquitinases (UBE3A, Angelman syndrome), kinases (CDKL5), guanine nucleotide-binding proteins (Rab18) and proteins associated with centrosomes and microtubules (CDK5RAP, CENPJ, MCPH1) (Kuijpers and Hoogenraad, 2011; Seltzer and Paciorkowski, 2014).

Several animal models of microcephaly have been used in research, generated by mutations in specific genes usually associated with primary microcephaly and Rett-like syndromes.

The *Trappc9* gene has been targeted by the European Conditional Mouse Mutagenesis Program (EUCOMM) as part of the International Mouse Phenotyping Consortium (IMPC). We imported Trappc9 knockout (KO) mice that were generated in the Sanger Institute (Cambridge, UK) using the "KO-first" technology: the insertion of a gene trap within an intronic region of *Trappc9* causes a frameshift and the silencing of the host gene (Fig 5.1). Among the features of the gene trap, a *LacZ* reporter gene allows the investigation of Trappc9 expression in tissue. The presence of *loxP* and *FRT* sites also allows us, via crossing with *Cre* and *Flp* mice, to eliminate part or the entire gene trap and to create conditional KO mice.

The work described in this chapter was to analyse this animal model (named Tm1a in this thesis) and to describe any phenotype these animals might exhibit. I also investigated

Trappc9's expression within the mouse brain and used histological staining techniques to determine any possible causes underlying the brain abnormalities observed in individuals harbouring mutations in *TRAPPC9*.

5.2 Methods

Immunohistochemistry. Tissues were extracted and processed as described in chapter 2. Anti-Sox-2 goat primary antibody (R&D Systems #AF2018) was diluted 1:500 in rabbit normal serum. Vectastain goat kit (Vector Laboratories, goat kit #PK-6105) was used for the colour precipitation. Sox-2 positive cells were counted in a delimited area represented in Fig 5.8 in the anterior (Paxinos and Franklin atlas figure 45-49) and posterior (atlas figure 50-54) hippocampus. Student's T-test was performed between wild type (WT) and KO counts. Anti-GFAP (Glial Fibrillary Acidic Protein) rabbit primary antibody (Dako #Z0334) was diluted 1:2000 and incubated overnight. Vectastain rabbit kit (Vector Laboratories, rabbit kit #PL-6101) was used for the colour precipitation.

Western blot. Anti-Trappc9 rabbit primary antibody (Proteintech #16014-1-AP) and custom made R61_RVE_1.1 were diluted 1:1000, anti-β-Actin primary antibody (Abcam #ab13822) was diluted 1:8000.

5.3 Results

5.3.1 Animal phenotype

The Tm1a mice, both heterozygotes and homozygotes, do not show any immediately recognisable phenotype or motor defects. The animals are fertile and reproduce with a normal Mendelian distribution (Fig 5.1). Some developmental defects (hydrocephalus, right or left eye not fully formed) were randomly observed in the first 2-3 generations and were not associated with a particular genotype, suggesting it was due to mutations harboured by the C57BL/6N strain (see chapter 2 for details). Cross breeding with C57BL/6J mice, in fact, eliminated these malformations. I analysed the brain weight at 12 weeks of age and found that both females and males develop a mild microcephaly (8.9% reduction in brain weight in females and a 7.1% in male; WT females 0.44 g ± 0.03, KO females 0.40 g ± 0.20, $p<0.05$; WT males 0.43 g ± 0.01, KO males 0.40 g ± 0.11, $p<0.001$) compared to WT mice. A similar result was obtained by our laboratory via MRI volumetric analysis in which an average 6% reduction in brain volume was observed (analysis by Thomas Leather, see Supplementary Fig 2). Female KO mice also show a 16.7% body weight increase which is not observed in male KO mice (WT females 22.17 g ± 2.41, KO females 25.87 g ± 2.98; WT males 29.88 g ± 2.07, KO males 29.82 g ± 1.51, $p<0.01$)(Fig 5.1). I confirmed the KO status by western blot analysis of homozygous KO brain lysate with two different antibodies. The commercially available Proteintech antibody (#16014-1-AP) detected Trappc9 and an additional faint band that remained visible in the KO, while our custom-made antibody (R61_RVE_1.1) detected Trappc9 but not this faint additional band. Analyses of the mRNA expression via RT-PCR revealed that KO mice still express *Trappc9* mRNA downstream of the gene trap (Fig 5.2). A product was observed upstream of the gene trap (exon 2-5) as expected, although the expression appears to be lower in the KO

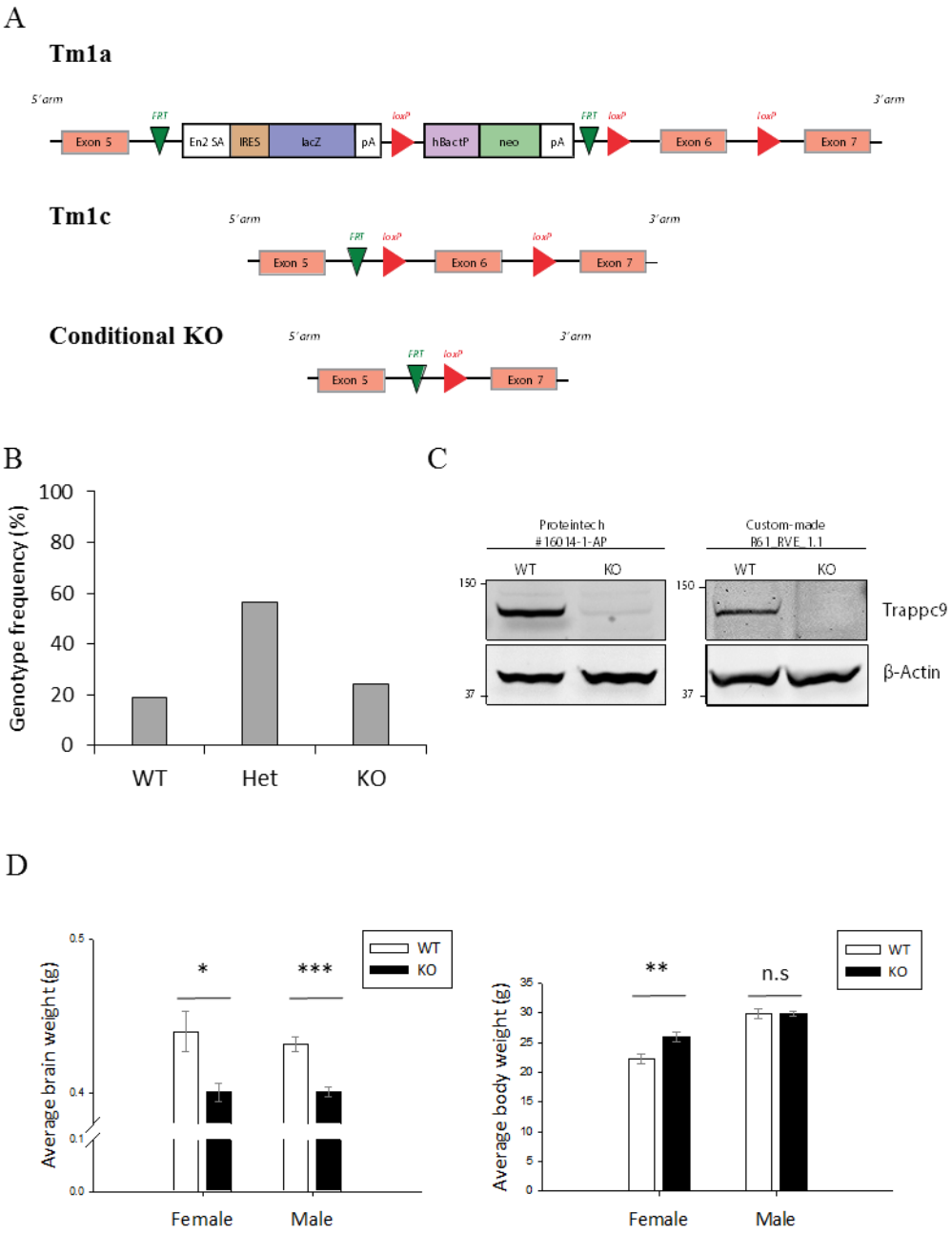

Figure 5. 1

A) Scheme of the gene trap used by the International Mouse Phenotyping Consortium (IMPC) for the "KO first" Tm1a mice. En2 SA: Engrailed 2 splice acceptor site; IRES: internal ribosomal entry site; pA: polyadenylation signal; hBactp: human β-Actin promoter; neo: neo cassette. B) Mendelian distribution of Tm1a pups per genotype (n. of animals 127). C) Western blot for Trappc9 in WT and homozygous KO (Tm1a) mouse brain with two different antibodies. D) WT and homozygous KO (Tm1a) brain and body weights of 12-week old mice. Both male and female homozygous KO mice show a 7-9% reduction in brain weight compared to WT counterparts. Female homozygous KO show a 16% increase in body weight compared to WT females. No statistical difference was observe in males. Females WT n=8, KO n=12. Males WT n=6, KO n=12. *p<0.05, **p<0.01, ***p<0.001.

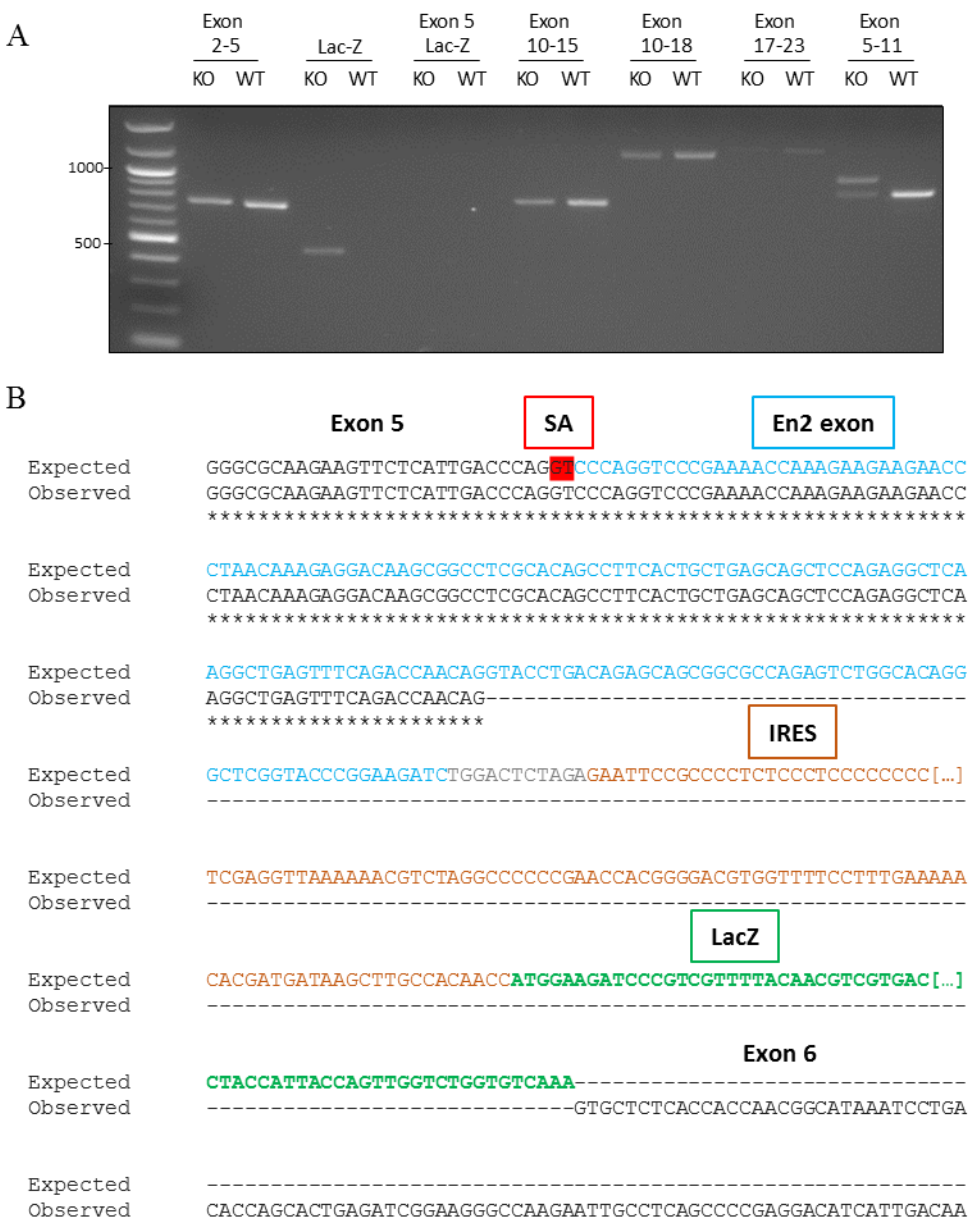

Figure 5. 2

A) RT-PCR from WT and homozygous KO total brain for different parts of *Trappc9* cDNA and the Tm1a allele. Despite the presence of the gene trap, *Trappc9* transcript downstream of exon 5 is still detectable in the KO brain. The double band in exon 5-11 KO has been confirmed using other primers targeting exon 3-7 (not shown). Expected products: exon 2-5 740 bp, LacZ 466 bp (KO), exon 5-LacZ 1044 bp (KO), exon 10-15 754 bp (WT), exon 10-18 1200 bp (WT), exon 17-23 1241 bp (WT), exon 5-11 844 bp (WT). Primers used: Pr_02FW in exon 2, Pr_04RV and Pr_04FW in exon 5, Trappc9F3 in exon 10, Pr_15RV in exon 11, Trappc9R3 in exon 18, Pr_06FW in exon 17, Trappc9R1 in exon 23, LacZ F4, LacZ R4 and Pr_025RV for LacZ. B) Sequencing of the KO allele (exon 5-11 upper band) revealed the absence of the *LacZ* sequence in the Tm1a allele. It also revealed an abnormal splicing, skipping the splice acceptor (SA) site, from the IRES element to exon 6.

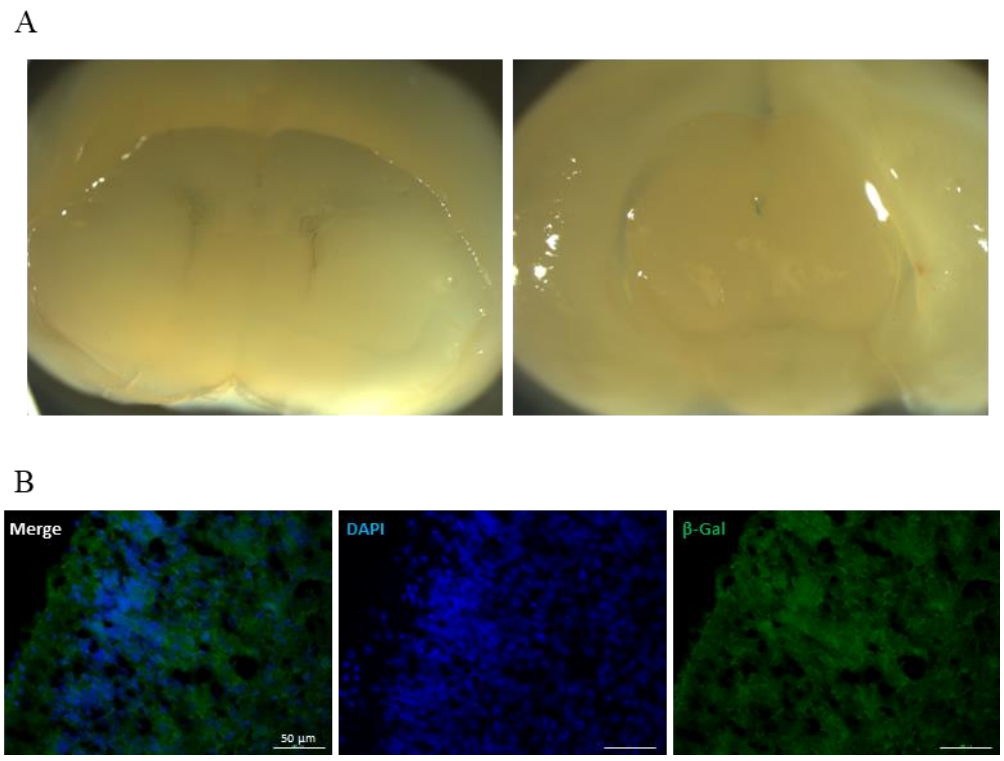

Figure 5. 3

A) X-Gal staining on homozygous KO (Tm1a) newborn brain. The expression of β-Galactosidase should cause the formation of a blue precipitate, absent in this case. B) β-Galactosidase fluorescent staining on the same tissues as in A (motor cortex). The signal from the anti-β-Gal green secondary antibody appears to be unspecific. Scale bars in B: 50µm.

sample, probably due to a reduced stability of the mRNA. I did observe the expression of *LacZ* cDNA in the KO but the β-galactosidase could not be detected in tissues either via antibody staining or X-Gal staining (Fig 5.3), suggesting the mRNA is not translated into a functional protein. Fragments were detected in the KO for exon 10-15, 10-18 and 17-23 downstream of the gene trap. The use of specific primers for exon 5-11 (from upstream to downstream the gene trap), revealed a faint WT band, suggesting splicing events are eliminating the entire gene trap, and a larger band in the KO sample, where there should not be any product. Sequencing analysis of the larger band revealed that a splicing event occurs at the splice acceptor (SA) site and inside the sequence of the En2 exon, producing a transcript comprising of exon 5, splice acceptor site, part of the En2 exon and exon 6 (Fig 5.4).

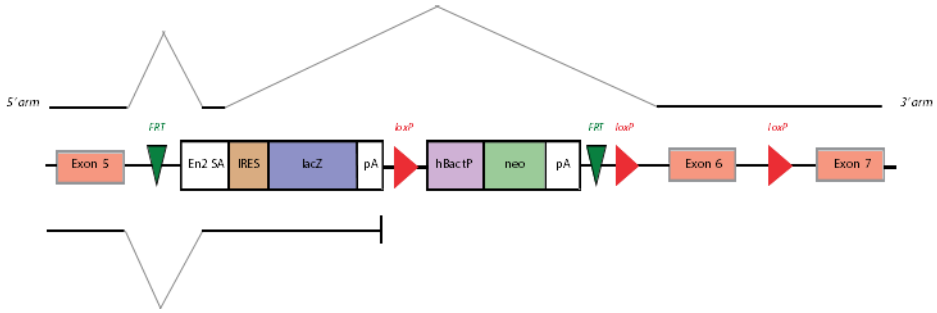

Figure 5. 4

Scheme of the alternative splicing observed in the Tm1a allele. The splicing should occur between exon 5 and the En2 SA site for the transcription of LacZ in association with Trappc9 mRNA (bottom part of the scheme). This event, however, does not occur correctly in some transcripts where an alternative splicing occurs so that exon 5 and exon 6 are still transcribed into a mRNA molecule with part of the sequence of the En2 site between them (top part of the scheme). The resulting mRNA would not be translated into a functional protein. Although LacZ cDNA is still being detected in the Tm1a allele (see Fig 5.2), it is expressed to a low degree as a single element (not in association with Trappc9), without being translated into a functional protein (see Fig 5.2).

This transcript would not give rise to a functional protein and the faint WT band observed in the KO sample might generate very low levels of Trappc9 protein, or these transcripts might contain further uncharacterised small, but disruptive mutations as no significant amount of protein was detectable in the Western blot (Fig 5.1). For this reason, the homozygous Tm1a is to be considered a real KO mouse model. However, the abnormal splicing observed within the gene trap sequence provides an explanation for the lack of detectable β-galactosidase where, even when *Lac-Z* is transcribed, the transcript is probably unstable or incomplete and thus not translated.

5.3.2 Progenitor cells and glial markers

The analysis of several commercially available antibodies on KO tissues revealed their lack of specificity for Trappc9 in immunohistochemistry, limiting considerably the range of experiments that could be performed on tissue. For this reason, the RNAscope® *in situ*

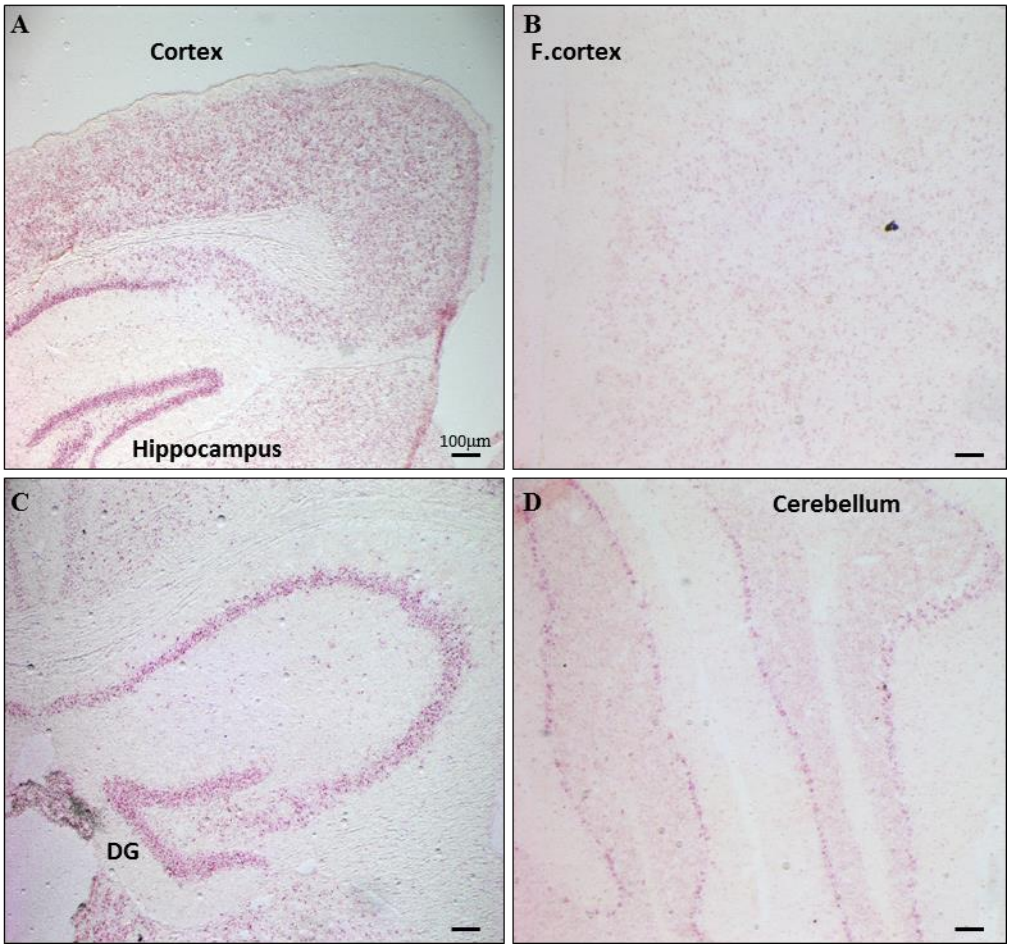

Figure 5. 5

A-D) *In situ* hybridisation for Trappc9 (pink signal) on WT brain shows a wide expression of Trappc9 throughout the brain, with a particularly strong expression in cerebral cortex, hippocampus, hypothalamus and cerebellum. F.cortex: frontal cortex, DG: dentate gyrus. Scale bars: 100 µm.

hybridisation method was adopted to detect mRNA levels of Trappc9 in the mouse brain (Fig 5.5-7). Neurons positive for Trappc9's expression were observed across the entire brain, with cortex (motor, sensory and piriform cortex), hippocampus, cerebellum and hypothalamus (paraventricular and arcuate nucleus) showing a particularly strong signal. Positive areas, although to a lower degree, were also frontal cortex, thalamus, periaqueductal grey, striatum and ventral tegmental area. No signal was detected in fibre structures such as the corpus callosum, consistent with the fact that Trappc9 mRNA is located in the cytoplasm of cell bodies.

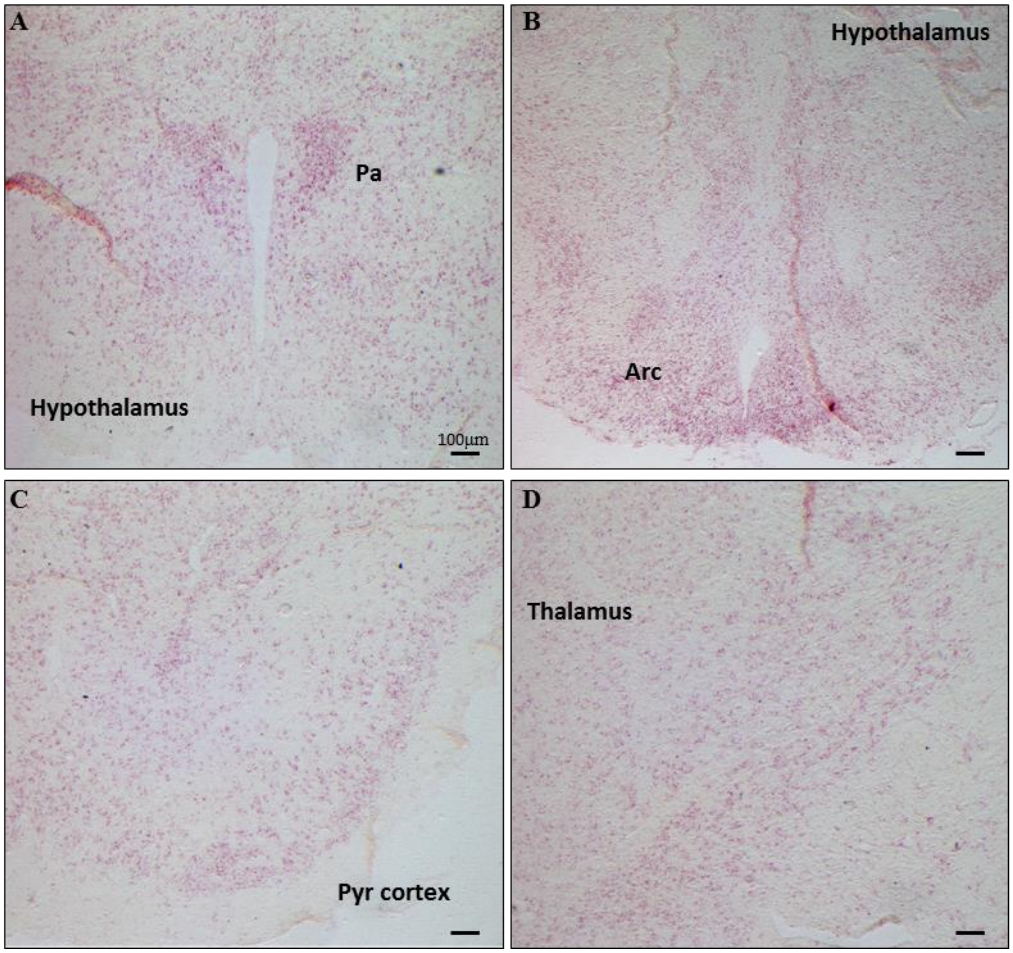

Figure 5. 6

A-D) *In situ* hybridisation for Trappc9 (pink signal) on WT brain shows a wide expression of Trappc9 throughout the brain, with a particularly strong expression in cerebral cortex, hippocampus, hypothalamus and cerebellum. Pa: paraventricular hypothalamic nucleus, Arc: Arcuate hypothalamic nucleus. Pyr cortex: pyriform cortex. Scale bars: 100 µm.

In order to analyse whether the microcephaly phenotype might be related to defects in neural progenitor cells, the dentate gyrus (known to contain a neurogenic niche in the adult brain) was analysed. A reduction in the population of cells expressing the stem cell marker Sox-2 was found in the dentate gyrus of the hippocampus of homozygous KO mice (anterior hippocampus: figure plates 45-49 from Paxinos and Franklin atlas, WT 206.89 ± 17.24 cells per section in the demarcated area, KO 179.48 ± 19.74 cells, $p<0.05$; no statistical difference found in posterior hippocampus - not shown) (Fig 5.8). A co-

localisation of Sox-2 and Trappc9 was observed in the subgranular layer of the dentate gyrus and a partial co-localisation was observed in the cerebral cortex (from Lucia Livoti). Preliminary results also highlighted a decrease in the astrocyte marker GFAP-positive cells in the KO corpus callosum and hypothalamus (Fig 5.9-10).

5.4 Discussion

5.4.1 A model for microcephaly

The available literature on people harbouring *TRAPPC9* mutations focuses on the description of the symptoms at the time of the examination and, in some cases, at birth. Although we have little or no information regarding the progression of the disorder, what transpires is that at birth the microcephaly is not established yet, although the head circumference of the affected individuals is reduced (from -0.3 SD to -2 SD) (Mochida et al., 2009).

The degree of microcephaly observed at older ages is variable across the different cases and also among different members of the same family. Marangi et al. (2013) reported two affected sisters that at 5 and 3.5 years of age presented with a reduction of head circumference

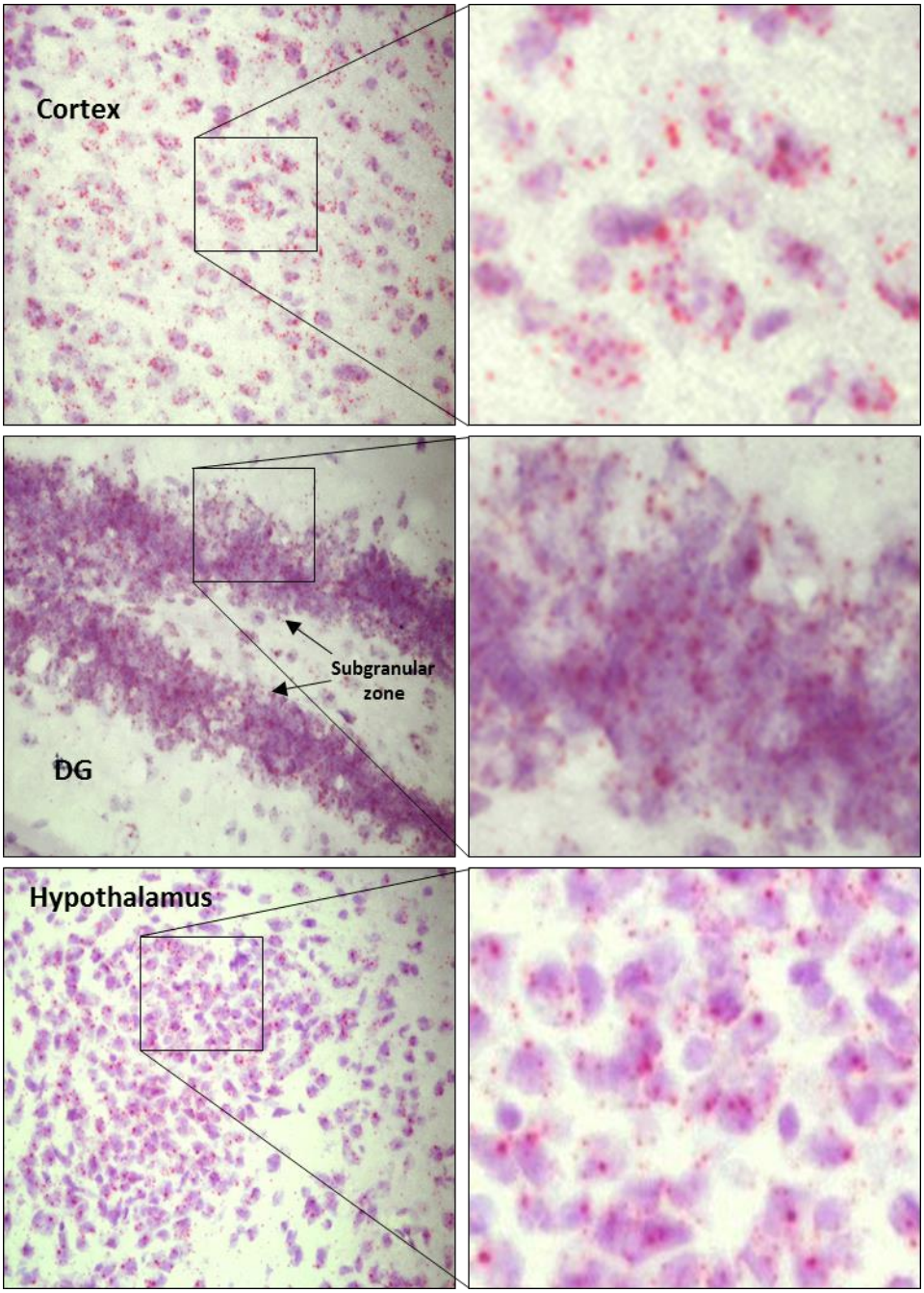

Figure 5. 7

In situ hybridisation for Trappc9 on WT brain with haematoxylin counterstaining (high magnification). The signal for Trappc9 (pink) is not present in all neurons, suggesting some sub-populations might be specific for its expression.

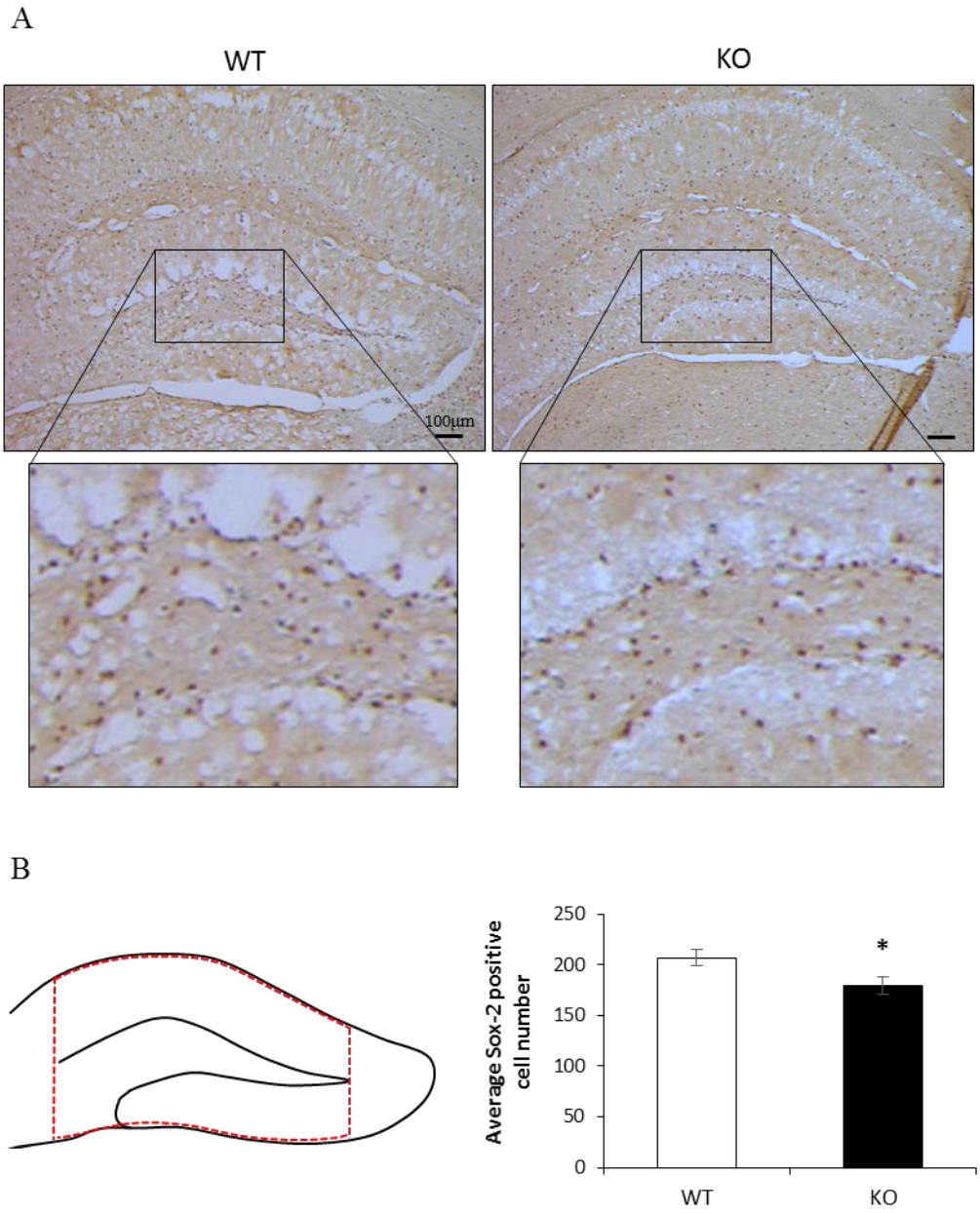

Figure 5. 8

Immunohistochemical staining for the progenitor cell nuclear marker Sox-2. **A)** Sox-2 positive cells in the dentate gyrus of WT and homozygous KO mouse brain. KO brains possess less Sox-2 positive cells in the dentate gyrus compared to WT brains. **B)** Scheme of the area analysed (delineated by the red dashed line) and quantification of Sox-2 positive cells in the highlighted area. WT n=3 animals (14 brain sections in total), KO n=3 animals (13 brain sections in total). Scale bars: 100 µm. *p<0.05

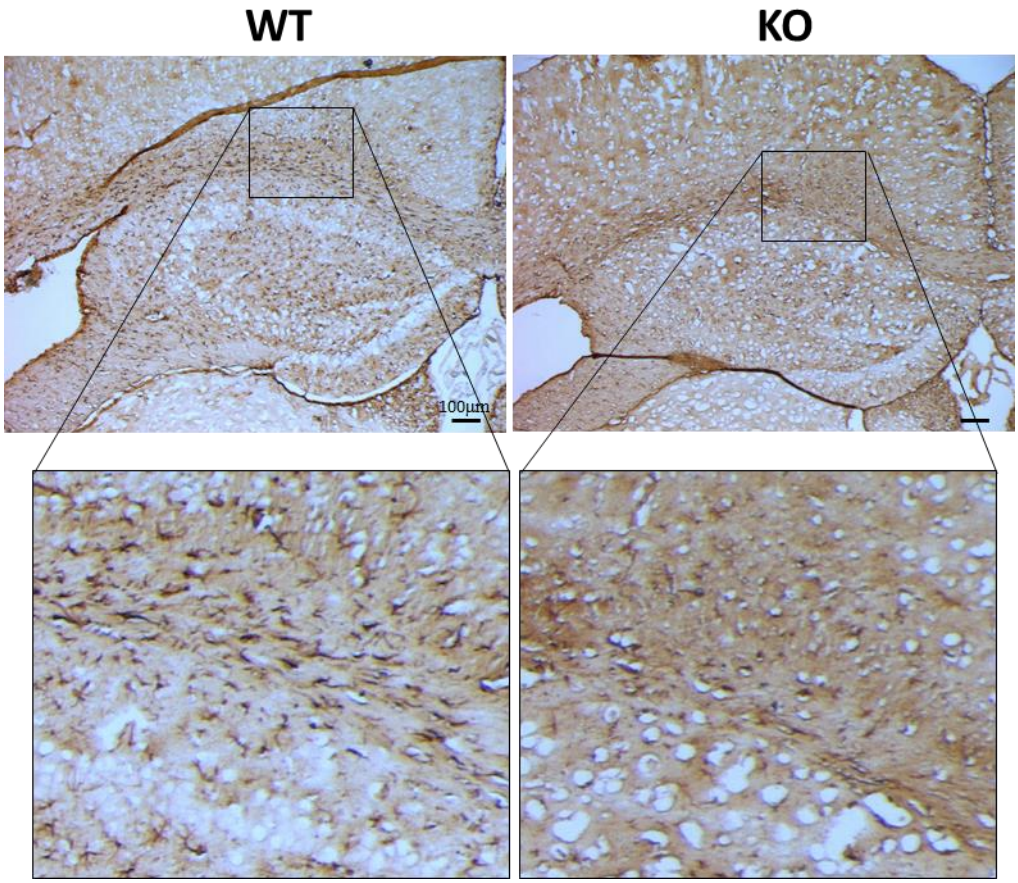

Figure 5. 9

Immunohistochemical staining for the glial marker GFAP on WT and homozygous KO mouse brain. A reduction of GFAP positive cells is visible in the KO corpus callosum (zoomed region). Scale bars: 100 µm

of -2 SD and -3 SD, respectively. Mir et al. (2009) reported instead three siblings carrying mutations in *TRAPPC9*, two of which presented with microcephaly while the third one had a normal head circumference.

As previously seen, many symptoms observed in affected individuals are often subjective or present to different degrees. Individual variability and genetic background are likely pivotal factors in determining the gravity of the symptoms, and considering the multitude of roles attributed to Trappc9 (see chapter 4), many factors could be contributing to the aetiology and severity of these symptoms.

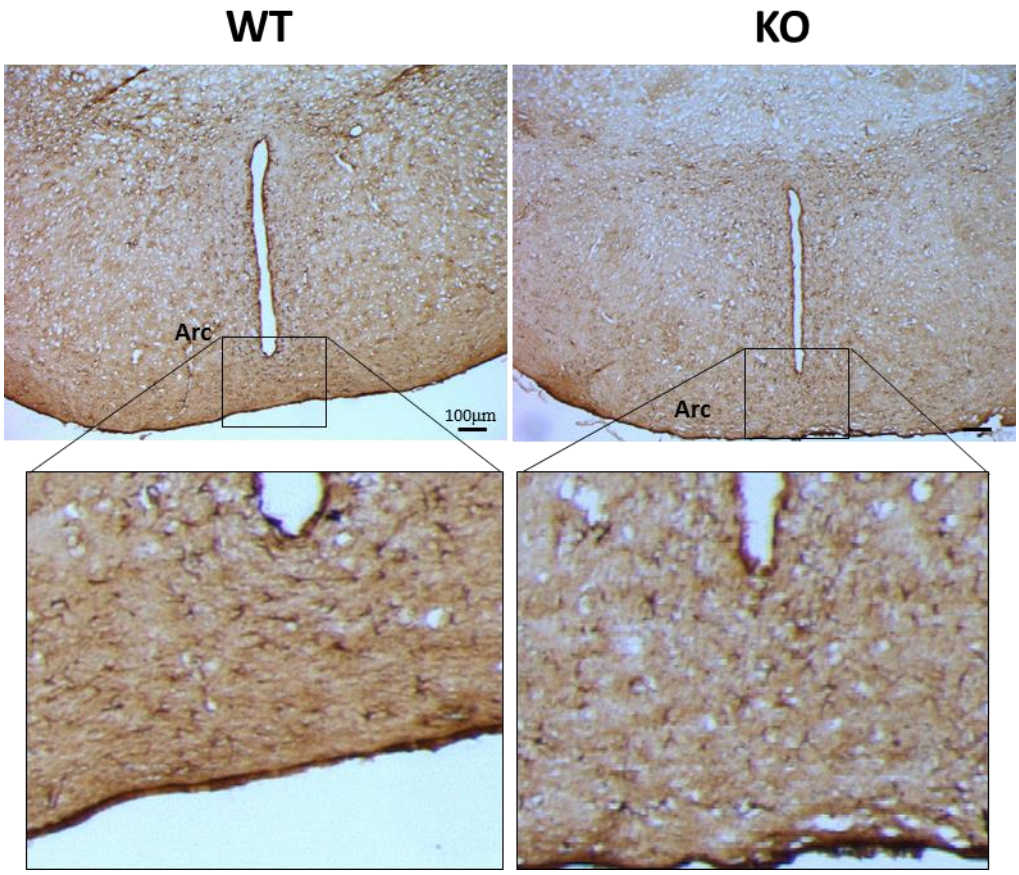

Figure 5. 10

Immunohistochemical staining for the glial marker GFAP on WT and homozygous KO mouse brain. A reduction of GFAP positive cells is visible in the KO arcuate nucleus (Arc, zoomed region). Scale bars: 100 µm.

If we add to this the species differences between human and mouse, it is therefore not surprising that the phenotype observed in mice is milder compared to the human condition. Mouse models often mirror symptoms of human disorders but with much milder phenotypes and in several cases, brain size reduction is less severe when compared to humans (Ribeiro et al., 2013; Homem et al., 2015; McGreevy et al., 2015; Lavelle et al., 2016).

What can be clearly observed in humans, though, is that the *TRAPPC9*-induced microcephaly has a postnatal occurrence.

Our group observed a reduction in brain weight and a reduction in brain volume (via MRI analysis) in homozygous KO mice consistent with a mild microcephaly phenotype. I also

observed a weight increase in female KO mice. Weight gain has been observed in only one male and one female human affected individuals (Mir et al., 2009; Philippe et al., 2009) but this parameter is probably biased by the inability of the majority of patients to feed themselves. It has recently been reported that both female and male homozygous Tm1a mice exhibit weight increase from 5 weeks of age, and that heterozygous m-/p+ mice exhibit a similar phenotype (Liang et al. unpublished).

Although I did not observe it in males at 12 weeks of age, it cannot be excluded that an obesity phenotype develops at older stages. However, the weight gain I observed in females might be an indication of a hypothalamic dysfunction. Interestingly, I observed a prominent expression of *Trappc9* in the paraventricular and arcuate nucleus, both important in regulating appetite and feeding behaviour. Preliminary results from our lab also hinted at a reduction in GFAP positive cells in the arcuate nucleus, where astrocytes play an important role in functioning as nutrient sensors for appetite controlling neurons (Chen et al., 2016).

It has recently been drawn to our attention that a group from the University of Philadelphia has generated similar Trappc9 KO-first (Tm1a) and Tm1c mouse lines, probably with the same gene trap. Crossbreeding Trappc9 Tm1c with universal *Cre* mice, they generated conditional Trappc9 KO mice and observed 15% reduction in brain weight at 10 weeks of age (Zhang et al., 2015b). They also observed a 5-10% residual expression of Trappc9 (both mRNA and protein) in the Tm1a line.

Intellectual disability being the major feature among individuals carrying mutations in *TRAPPC9*, it would be interesting to investigate the learning and memory capabilities of our KO mouse model. To date, it has only been reported that Tm1a homozygous KO mice show normal sociability when subjected to social recognition tests but they might show defects in a social discrimination test after 24 hours, suggesting defects in long-term

memory might be involved (Liang et al. unpublished). The defect in GFAP positive cells in several areas of the mouse brain could, however, impair many processes that might partially explain the human phenotype and should therefore be investigated.

5.4.2 Cellular basis for Trappc9 depletion-related microcephaly

As discussed in chapter 4, the mechanisms by which mutations in *TRAPPC9* affect brain development are still unknown. The processes involved might be numerous, including cell differentiation, proliferation or apoptosis.

It has been reported that the number and size of primary neurospheres derived from Trappc9 conditional KO mice was decreased in comparison to heterozygous littermates, and that Sox-2, GFAP and Ki67 positive cells are reduced in the subgranular zone of KO mice (Zhang et al., 2015b).

Parallel to these results, I have observed a decrease in Sox-2 positive cells in the dentate gyrus and a general reduction in GFAP positive cells, particularly in the corpus callosum (Fig 5.8-10).

Sox-2 is a transcription factor, part of the highly conserved Sox family of transcriptional regulators (Gubbay et al., 1990; Schepers et al., 2002; Wilson and Koopman, 2002), and included in the SoxB class of genes, that are expressed mainly in developing and adult central nervous system (Karnavas et al. 2013).

Sox-2 has been shown to have a role in epiblast formation, pluripotency and cell reprogramming (Masui et al., 2007; Mandalos et al., 2012; Polo et al., 2012; Sarkar and Hochedlinger, 2013).

During embryonic development, neuroepithelial cells undergo asymmetric cell division where they generate more progenitor cells and radial glial cells, which have the potential to differentiate into neurons, astrocytes or oligodendrocytes but also serve as scaffolding for migration (Deneen et al., 2006; Kang et al., 2012). It has been suggested that the

transcription factors Sox-1-3 prevent differentiation (Bylund et al., 2003; Holmberg et al., 2008; Oosterveen et al., 2013).

Recent experiments from our lab highlighted a co-localisation of Trappc9 and Sox-2 in the subgranular layer of the dentate gyrus and a partial co-localisation in the cortex, which is not surprising considering the neuronal expression of Trappc9 and the expression of Sox-2 outside the neurogenic niches. Sox-2 expression in the adult brain has been confirmed in the neuroepithelial and radial glial cells of the neurogenic niches, where it is important for the maintenance of their multipotency and where it is downregulated immediately before the differentiation (Favaro et al., 2009; Hutton and Pevny, 2011; Mandalos et al., 2012). However, Sox-2 is also expressed in the adult human brain in a glial progenitor cell population in the white matter and in the Bergmann glia, a subtype of radial glial cells present in the cerebellum (Alcock et al., 2009; Oliver-De La Cruz et al., 2014). Sox factor binding sites are present in the neural enhancer of the *Nestin* gene (neuronal precursor marker), and it has been shown that Sox-2 participates in promoting the differentiation of radial glial cells into oligodendrocytes (Tanaka et al., 2004).

A scenario with impaired neurogenesis would be consistent with the microcephaly observed in individuals and mice harbouring *TRAPPC9* mutations. Many other microcephaly models present defects in neurogenesis, with mutations in genes such as *NDE1* (*NudE development protein 1*), *ASPM* (*Abnormal Spindle Microtubule Assembly*) and *CDK5RAP2* (*CDK5 Regulatory Subunit Associated Protein 2*) being at the foundation of the phenotype (Gilmore and Walsh, 2013).

I also observed a reduction in GFAP positive cells in the KO brain, in particular in the corpus callosum region and hypothalamus (Fig. 5.9-10).

GFAP is an intermediate filament protein and a widely recognised marker for astrocytes and ependymal cells, but also radial glial cells (Molofsky and Deneen, 2015). It is also

expressed by neural stem cells in the subventricular and subgranular zone (Alvarez-Buylla and García-Verdugo, 2002).

Glial cells are responsible for the formation, plasticity and maintenance of neural circuits and play a pivotal role in neuronal survival and function (Allen and Barres, 2009).

Astrocytes in particular have been associated with blood brain barrier formation and maintenance, synaptogenesis, neurotransmission and metabolic regulation (Allen and Barres, 2009). They have also been implicated in numerous diseases and disorders, including multiple sclerosis, Alzheimer's disease, Huntington disease, Fragile X syndrome and Rett syndrome (Molofsky and Deneen, 2015). Specifically, Rett syndrome is a multi-genic X chromosome-linked autism spectrum disorder, in which the preponderant loss-of-function mutation is found in the sequence of the transcription factor methyl CpG-binding protein 2 (MeCP2)(Chahrour & Zoghbi 2007). The expression of MeCP2 in astrocytes supports normal neuronal morphology and influences neurons in a non-cell autonomous manner probably as a result of aberrant secretion of soluble factor(s). In fact, loss of function of MeCP2 in astrocytes induces significant abnormalities in brain-derived neurotrophic factor (BDNF) regulation, cytokine production, and neuronal dendritic induction (Ballas et al., 2009; Maezawa et al., 2009).

With Trappc9 being expressed in neurons but not in glial cells, this reduction in astrocytes in the adult brain could be explained either with the secretion of neuronal factors, similarly to MeCP2's regulation of astrocytes, or possibly by the expression (or lack thereof) of *Trappc9* in progenitor cells. These cells might be influenced in their differentiation to neurons or glial cells, therefore contributing to the observed phenotype. Such involvement of Trappc9, however, is still yet to be investigated.

Furthermore, recent studies have suggested the possibility that astrocytes might be able to reacquire stem cell properties by de-differentiating in response to reprogramming or brain

injury (Molofsky & Deneen 2015), a process that might be affected in individuals harbouring mutations in *TRAPPC*9.

A reduction in the astrocyte population might affect neuronal migration but also functioning. Neurotoxicity early in development might also be a key factor to be considered, as astrocytes are responsible for the scavenging of extracellular reactive oxygen species and for the clearance of glutamate in the synaptic cleft (Reemst et al., 2016).

It has also been shown that MeCP2-null microglia have a potent neurotoxic action due to high release of glutamate (Maezawa and Jin, 2010). Interestingly, microglia have been shown to regulate adult hippocampal and subventricular zone neurogenesis, providing trophic support to new cells, and to secrete several factors to stimulate astrocyte proliferation and/or differentiation (Reemst et al. 2016).

It would be interesting to investigate in our KO model whether the microglial population is impaired and to analyse the apoptotic rate in postnatal brain development.

Interestingly, lipid droplets (LD, see chapter 4) can accumulate in glial cells in response to mitochondrial dysfunction via a ROS-induced activation of Jun-N-terminal Kinase (JNK) in neighbouring neurons (Liu et al., 2015). Also, in drosophila the accumulation of LDs precedes neurodegeneration in adult photoreceptors (Yamamoto et al., 2014), suggesting that a reduced scavenging ability of glial cells might be an interesting factor to investigate in our model.

Another aspect that I have already mentioned in chapter 4 is the involvement of the microtubule organising centre (MTOC). The centrosome is responsible for microtubuli structure foundation but also for cell proliferation, migration and differentiation (Kuijpers & Hoogenraad 2011) and, although I have not analysed MTOC structure and function in this thesis, it is important to mention that several neurodevelopmental disorders are

caused by mutations in cytoskeletal protein-encoding genes (Thornton and Woods, 2009; Tischfield et al., 2011). Lissencephaly is caused by mutations in the gene *LIS1*, which causes defects in neuronal migration, severe intellectual disability and seizures. Mutations in *Disrupted-in-schizophrenia 1* (*DISC1*) cause mental and behavioural disorders by disrupting neurite outgrowth and neuronal migration (Palo et al., 2007). Mutations in several centrosomal proteins such as Microcephalin 1 (MCPH1), centromere-associated protein J (CENPJ) and CDK5RAP2 have been associated with autosomal recessive primary microcephaly (MCPH) (Thornton and Woods, 2009; Wu and Wang, 2012).

Mutations in *UBE3A*, the gene responsible for the onset of Angelman syndrome and its related postnatal microcephaly, cause many mitotic abnormalities including chromosome missegregation, abnormal cytokinesis and apoptosis (Singhmar and Kumar, 2011).

Furthermore, several centrosomal components are known to control neural progenitor self-renewal (Xie et al., 2007).

It has been hypothesised that the centrosome has a direct effect on Golgi-derived vesicle trafficking (Sütterlin and Colanzi, 2010). In fact, during and after neuronal migration, neurons polarise and develop an axon and several dendrites, with the centrosome as primary source for microtubule assembly (Stiess and Bradke, 2011). The centrosome would position the Golgi in front of the future axon directing the microtubule-dependent secretory transport (Kuijpers & Hoogenraad 2011).

As previously seen in chapter 4, human Trappc9 mutant fibroblasts present an abnormal MTOC number (Gan et al., 2014), although my preliminary results on KO mouse EMFIs did not recapitulate this phenomenon. For this reason, it would not be surprising if people with *TRAPPC9* mutations had defects in the MTOC as the basis of this condition.

5.4.3 Concluding remarks

In this chapter, I have demonstrated that Trappc9 KO mice exhibit a mild microcephaly phenotype, which has been observed independently by other groups.

The involvement of stem cells seems to be a key factor in the generation of this phenotype, but many other processes await to be investigated. Future studies will need to investigate the apoptotic rate in the developing brain but also the involvement of other cell types, such as the glia. When does the reduction in astrocytes occur? Is it affected during embryonic development or postnatally? Are other types of glial cells involved?

In addition, to date there is no record of the determination of specific neuronal subtypes expressing Trappc9. As it is widely expressed in the brain, this factor has been neglected so far but the involvement of a specific neuronal subpopulation should not be excluded, especially considering that this protein might have cell specific functions.

Furthermore, in the context of the mouse phenotype, it should not be forgotten that *Trappc9* is imprinted in the mouse brain (chapter 3). The imprinting in specific areas or cellular populations (e.g. progenitor cells), could be a determining factor in the recapitulation of the human symptoms in the mouse model.

CHAPTER 6

Variable number tandem repeat (VNTR) polymorphism in human TRAPPC9

6.1 Introduction

Human *TRAPPC9* is located on chromosome 8q24.3 and, similarly to the mouse gene, is flanked by *KCNK9*, *CHRAC1* and *AGO2* (Fig 3.1).

The mutations in this gene associated with intellectual disability and microcephaly disorder are located within exons and lead to the premature interruption of translation. The symptoms caused by such mutations are so severe that considerable emphasis has been placed upon investigating how *TRAPPC9* affects brain development and neuronal functions.

However, due to the cryptic nature of this gene and the diverse pathways and functions its protein has been associated with, it is surprising that the role of *TRAPPC9* and the regulation of its transcription in healthy individuals have not been investigated yet. The microcephaly and intellectual disability disorder observed in humans is caused by complete loss-of-function of TRAPPC9 but whether reduced levels of this protein lead to mild symptoms (e.g. mild cognitive impairment) is currently unknown.

Recently, mutations in the sequence of *TRAPPC9* have been linked with schizophrenia and multiple sclerosis (Gourraud et al., 2013; McCarthy et al., 2014), suggesting these conditions and the *TRAPPC9*-related intellectual disability disorder might share common causes. More importantly, these associations suggests that the functions of *TRAPPC9* might not be limited to brain development and intellectual disability, but also to neuronal functioning and maintenance in the adult brain.

I analysed the human sequence of this gene and observed two minisatellites located within exon 1 of transcript variant 001 and within the intronic region between exon 1 and the 5'-UTR of variant 002 (Fig 6.1).

These minisatellites, consisting of repeated sequences and for simplicity referred to as variable number tandem repeats (VNTRs) in this chapter, are located within a promoter region that has a strong enhancer activity (according to CHIP-seq data, see Fig 6.1).

Minisatellites have been implicated in gene regulation and chromatin organization (Li et al., 2007; Gymrek et al., 2016), and expansions of these sequences are often linked with diseases and disorders. A variation in the number of repeated copies can, in fact, alter gene expression as in Fragile X mental retardation syndrome where the expansion located in the 5′-UTR of the gene causes a dramatic reduction in gene expression (Garber et al., 2006). Furthermore, the position of the repeated sequence can also lead to disruption of the protein sequence when an expansion in copy number affects an exon (e.g. Huntington's disease) (Gusella and MacDonald, 2006).

The region I analysed is also rich in CCCTC-binding factor (CTCF) binding sites and it is a predicted G-quadruplex (G4) structure according to the Quadparser prediction tool (Huppert and Balasubramanian, 2005).

CTCF has been shown to act as a transcriptional regulator, as a regulator of RNA splicing and as an insulator by regulating the 3D structure of chromatin (Phillips and Corces, 2009), while G4s are four-dimensional secondary structures in DNA and RNA that are known regulators of gene expression (Bochman et al., 2012).

According to UCSC genome browser, there are more than 600,000 candidate VNTRs in the human genome and many occur in functional positions such as the first 50 bases of promoters as well as in enhancers and functional intronic regions (Breen et al., 2008).

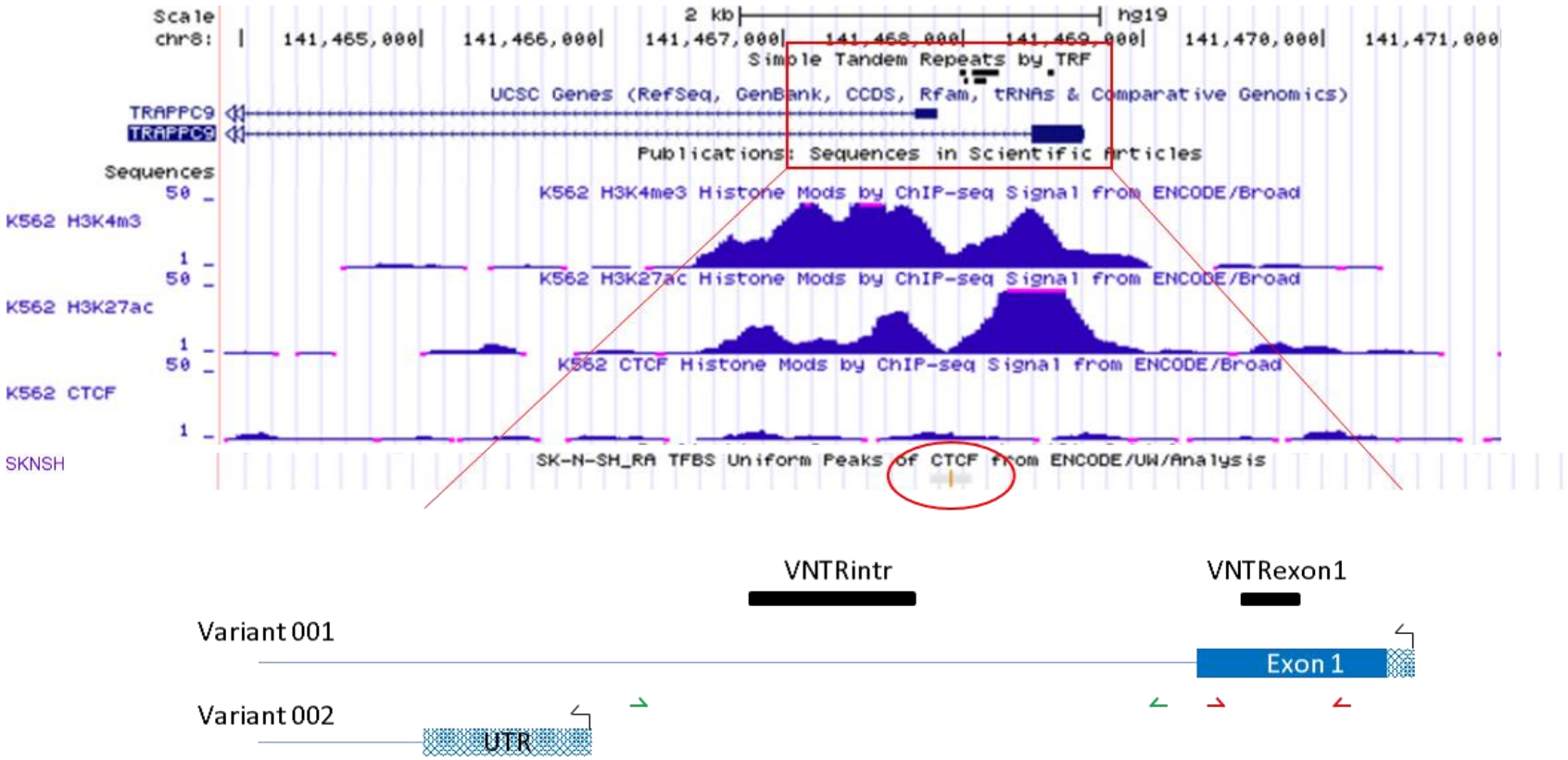

Figure 6. 1

Schematic representation of human *TRAPPC9* promoter region. TOP: Screenshot from UCSC genome browser showing the two main transcript variants for *TRAPPC9*, the VNTRs (black bars) and CHIP-seq from human immortalised myelogenous leukaemia cell line (K562) showing traces for H3K4m3 (promoter marker), H3K27ac (enhancer marker) and CTCF (enhancer blocker). Although this region does not show prominent CTCF binding in K562 cells, it does in the neuroblastoma cell line SKNSH. BOTTOM: close up of the promoter region and VNTRintr (green arrow for primers position) and VNTRexon (red arrows for primers position).

Considering the importance of VNTRs, G4s and CTCF binding sites for gene regulation, I aimed to analyse this region in order to determine whether it is polymorphic in human cell lines and human gDNA. After observing the existence of a polymorphism in the intronic VNTR, I aimed to determine whether this region and its variants have the ability to alter gene expression in a luciferase reporter gene assay.

6.2 Methods

PCR. For genotyping of the VNTR in the intron (VNTRintr) 30 cycles were performed at an annealing temperature of 60˚C using primers VNTRintr_Fw + VNTRintr_RV. For genotying of the VNTR in exon 1 (VNTRexon1) 30 cycles with an annealing temperature of 60˚C were performed using primers VNTRexon1_Fw + VNTRexon1_Rv. For this PCR, 4 μL of 5M Betaine (Sigma-Aldrich #B0300) were added to each PCR reaction.

Electrophoresis. PCR reactions for VNTRexon1 and VNTRintr on cell line DNA were run on 2.5% agarose gels. PCR reactions for human samples gDNA were run on the QIAxcel® (Qiagen) system for capillary electrophoresis using the QIAxcel® DNA High Resolution Gel Cartridge (designed for high-resolution genotyping, with an error margin of 3–5 bp).

6.3 Results

The genotyping of human immortalised cell lines (SH-SY5Y, SKNAS, HAP1, KELLY, M1184 and PO205) for the VNTR located in exon 1 of variant 001 (VNTRexon) did not show any polymorphism of this region (Fig 6.2). The genotyping for the VNTR located between exon 1 of *TRAPPC9* variant 001 and the 5′-UTR of variant 002 (VNTRintr) revealed instead a polymorphism with a product of ~460 bp and ~290 bp (Fig 6.2).

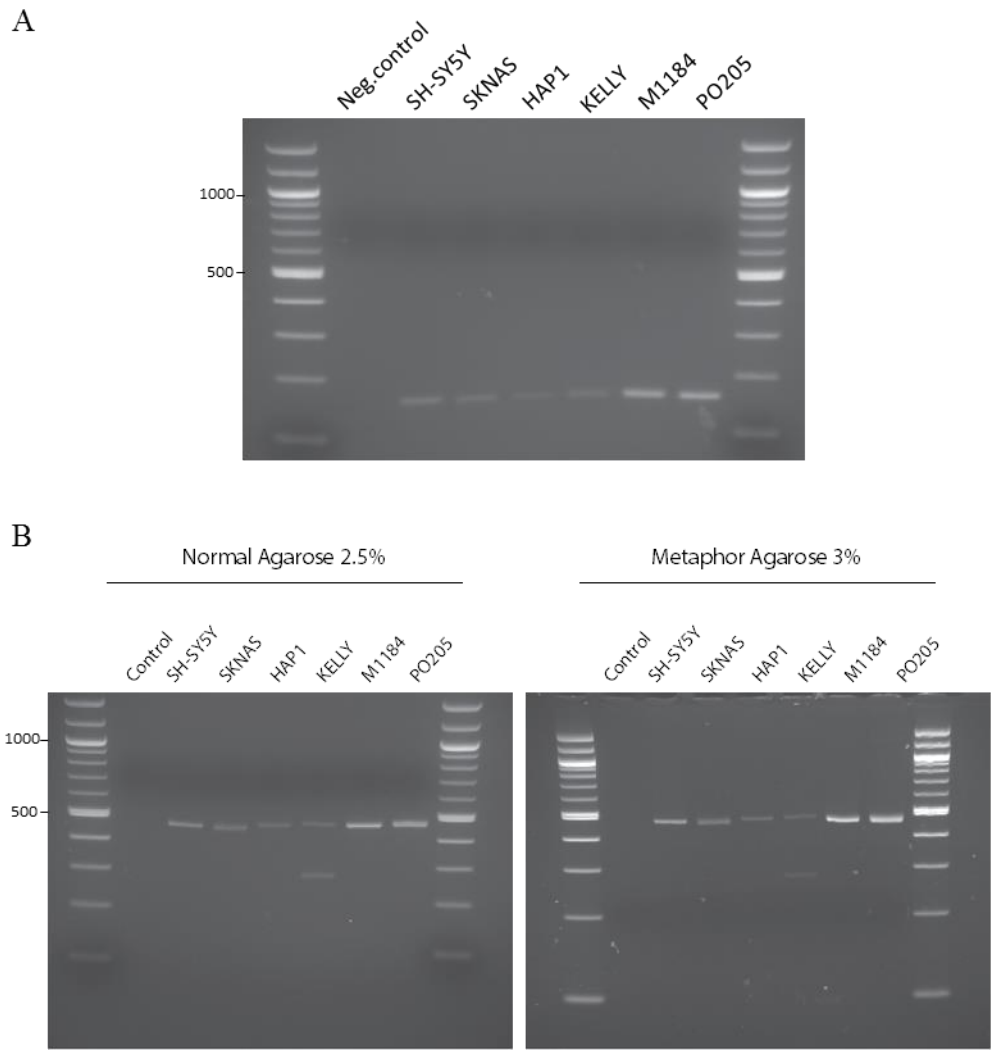

Figure 6. 2
Genotyping for VNTRs on human cell lines gDNA. **A)** PCR for VNTRexon. No polymorphisms were detected. Expected product 159 bp. **B)** PCR for VNTRintr on normal agarose (left) and on high-resolution agarose (right). A polymorphism was observed in gDNA from Kelly cell line. Expected product 464 bp. PCR primers are indicated in Fig 6.1.

To investigate whether this polymorphism exists within the general population, the same genotyping was performed on a small cohort of human gDNA samples from healthy individuals and from individuals with schizophrenia, as *TRAPPC9* has been associated with this disorder (McCarthy et al., 2014). The genotyping was performed on a high resolution capillary electrophoresis system (QIAxcel®) that confirmed the polymorphism of this

region and highlighted the existence of three variants, V1 of 464 bp, V2 of 454 bp and V3 of 290 bp (Fig 6.3).

The genotyping also revealed that the allele combination V1/1 is the most abundant while the others are less frequent. The allele combination V1/3 appears with a frequency of 16% in healthy individuals (14 individuals out of 87), while its frequency was 10% in individuals with schizophrenia (9 individuals out of 86) (Table 6.1).

Sequencing analysis of the three variants showed three copies of a repeated sequence of 10 bp (CTTTCACCCC), followed by a more variable sequence of 68-76 bp (Fig 6.4) in V1 and V2. V2 differs from V1 for a 10 bp sequence missing upstream of the VNTR, while V3 lacks part of the first copy of the VNTR, the second and part of the third (Fig 6.4).

The region is rich in CTCF binding sites and the use of the CTCFBSDB 2.0 database prediction tool revealed four main CTCF binding motifs, one of which is disrupted in V3 (for details on the database see Ziebarth et al. 2013).

In order to investigate the ability of these variants to influence gene transcription, the

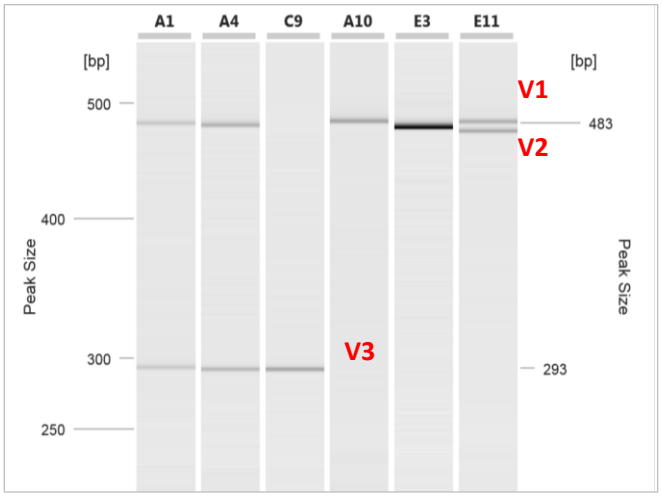

Figure 6. 3
Genotyping for VNTRintr. Virtual gel obtained with the Qiaxcel system for capillary electrophoresis for all the allelic variants on gDNA from healthy individuals obtained. V1: 464 bp; V2: 454 bp; V3: 290 bp.

three fragments were cloned into pGL3-P vector, that contains a minimal promoter (SV40) (Fig 6.5), and transfected into HEK293T and SH-SY5Y cells for luciferase reporter gene assays.

The analysis did not reveal any statistical difference between the three variants in either cell lines, but the three fragments had the ability to promote transcription in comparison to the empty pGL3-P vector in SH-SY5Y (Fig 6.6). Moreover, the assay proved to be highly cell line specific, with HEK293T and SH-SY5Y cells responding to different degrees to the control (pGL3-B) and enhancer (pGL3C) vectors.

Genotype	Controls		Schizo	
	prevalence	frequency	prevalence	frequency
1/1	68	78.16 %	74	86.04 %
1/2	2	2.3 %	3	3.48 %
1/3	14	16.09 %	9	10.46 %
2/2	1	1.15 %	0	0 %
2/3	0	0 %	0	0 %
3/3	1	1.15 %	0	0 %
Total	87		86	

Table 6. 1

Genotyping for VNTRintr on gDNA from a small cohort of healthy individuals (Controls) and individuals with schizophrenia (Schizo) obtained with the Qiaxcel system for capillary electrophoresis. The prevalence represents the number of individuals with that particular genotype, while the frequency represents the abundance within the entire group. The V1/3 allele is altogether found 14 times in controls vs 9 times in Schizo. V1: 464 bp; V2: 454 bp; V3: 290 bp.

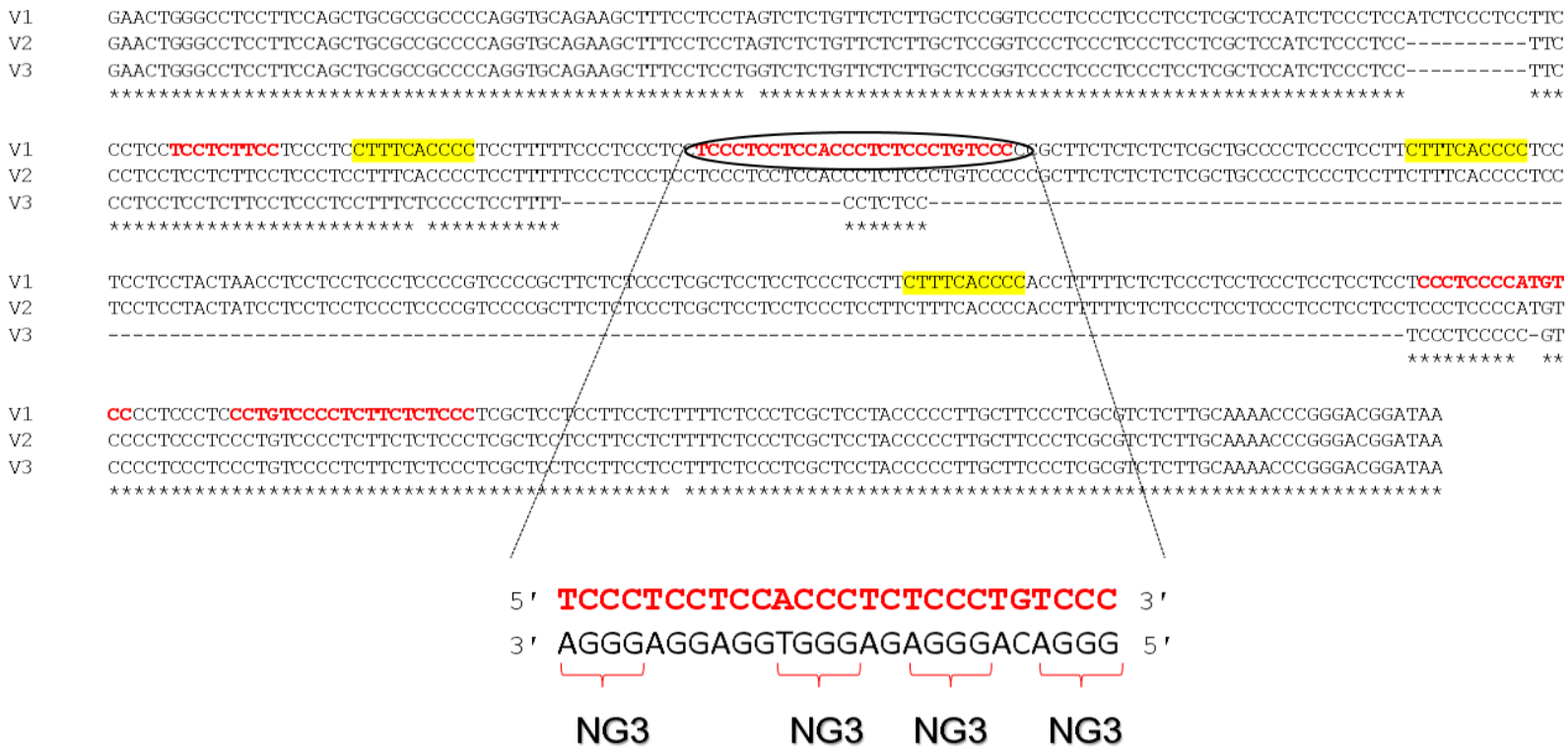

Figure 6. 4

Alignment of the sequencing results for the three different allele variants for *TRAPPC9* VNTRintr. TOP: Highlighted in yellow the constant 10 bp repeated sequence of the three repetitions that characterises this VNTR, followed by a less conserved region. In red CTCF binding motifs predicted by the CTCFBSBD 2.0 database prediction tool. BOTTOM: example of G4 predicted core sequence.

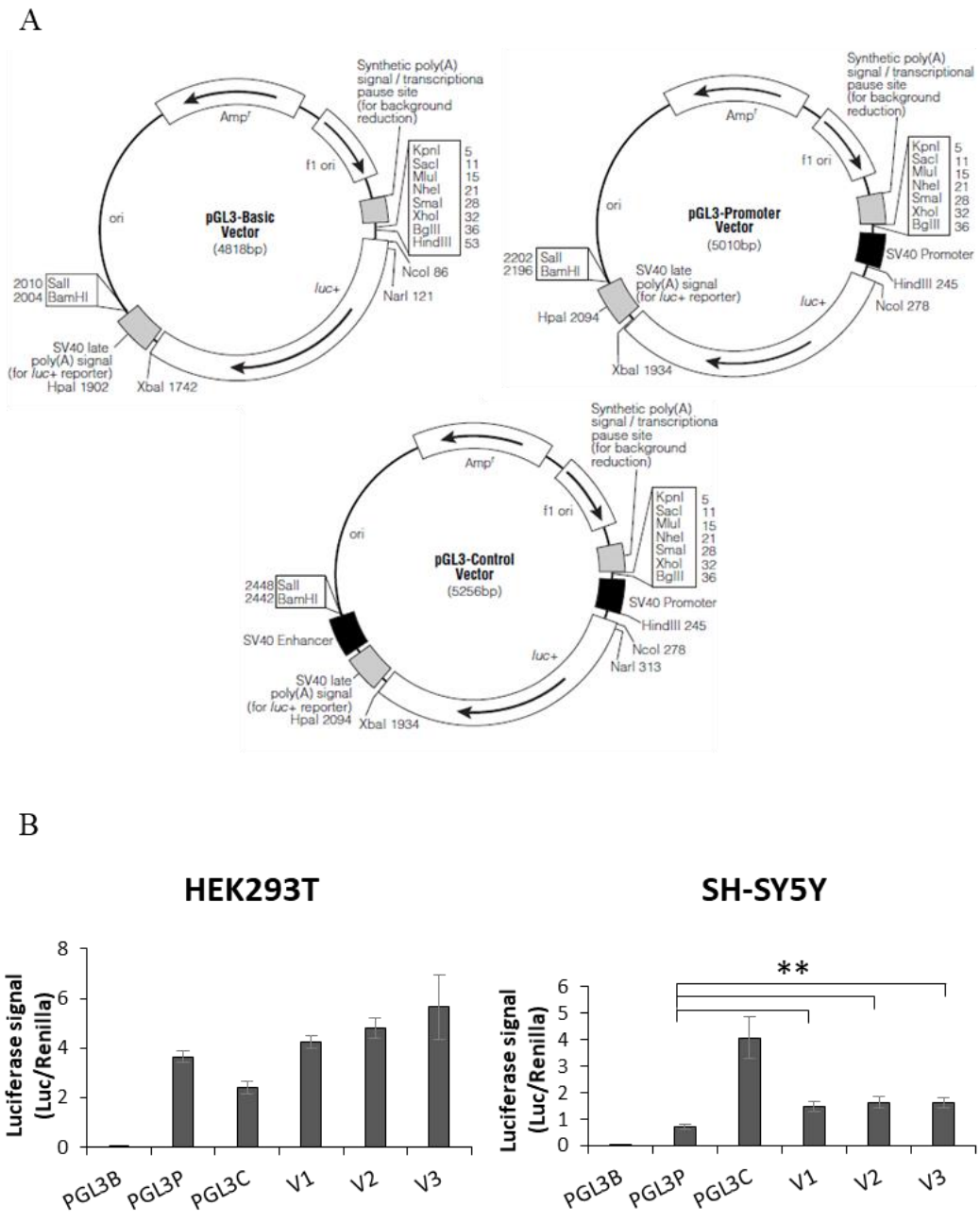

Figure 6. 5

Luciferase reporter gene assays. A) Scheme of pGL3 series of plasmids used for this analysis. The basic vector (PGL3B) was used as negative control as it does not possess any promoter sequence that could initiate transcription. The enhancer vector (PGL3C) was used as positive control as it contains a promoter and a strong enhancer that induce a high level of transcription. The allelic variants were cloned into PGL3P that contains a minimal promoter. B) Reporter gene assays with VNTRintr allelic variants V1-V3 in HEK293T (kidney) and SH-SY5Y (neuroblastoma) human cell lines. HEK293T cells were used for their non-neuronal background. While no statistical difference was observed between allelic variants in either cell lines, all three variants promote transcription in comparison to the empty PGL3P vector in SH-SY5Y. Furthermore, the activity of the enhancer vector was lower in HEK293T cells than in SH-SY5Y, suggesting a cell line specificity for this assay. HEK293T n=2, SH-SY5Y n=3. **p<0.01

6.4 Discussion

In addition to its role in microcephaly and intellectual disability, *TRAPPC*9 has also been linked with schizophrenia and multiple sclerosis, suggesting its contribution might be at the basis of several disorders (Gourraud et al., 2013; McCarthy et al., 2014).

To my knowledge, this is the first analysis of genetic variants in the human *TRAPPC9* promoter region and associated VNTR polymorphisms. As *TRAPPC9*'s molecular functions have not been fully elucidated yet, the physiological implications of these polymorphisms are currently unclear.

As mentioned before, this VNTR is located in the promoter region (Fig 6.1) and from the nature of its sequence it is predicted to generate a G4 conformation.

G4s are four-dimensional secondary structures that DNA and RNA form usually in correlation with a core sequence (called G4 motif), formed by four repetitions of at least three guanines separated by any other nucleotides ($G\geq3N_{1\text{-}7}G\geq3N_{1\text{-}7}G\geq3N_{1\text{-}7}G\geq3$) (Fig 1.3) (Bochman et al., 2012). These sequences fold to produce three parallel planes with the engagement of one or multiple DNA strands and have been known to incorporate structure-stabilising cations such as K^+ or Na^+ (Dapić et al., 2003).

G4s tend to cluster in telomeres and transcriptional start sites (often near promoters) but are also found in micro- and minisatellites (VNTRs) (Bochman et al. 2012). The high concentration of G4s near promoter regions suggests a potential role in gene regulation. In fact, the presence of a G4 motif on the template strand could block the transcription machinery or, if on the non-template strand, it could enhance transcription by maintaining the transcribed strand in a single stranded conformation. Furthermore, proteins bound to the G4 structures (transcriptional enhancers and/or repressors) could also regulate

transcription (Bochman et al. 2012). In addition, it has been suggested that G4 motifs might influence the epigenetic regulation of gene expression (Sarkies et al., 2010).

The structure and integrity of G4 motifs are therefore very important for gene regulation and expression.

As mentioned before, the analysis of *TRAPPC9*'s sequence on UCSC revealed a predicted G4 in the promoter region corresponding to the observed VNTR. The short variant I observed, V3, lacks a conspicuous portion of DNA sequence that most likely disrupts the formation of the G4. It could therefore be assumed that the short variant V3 lacks the ability to inhibit/promote *TRAPPC9* transcription and therefore would result in different levels of expression in comparison to the longer variant.

I performed luciferase reporter gene expression assays on the three variants and observed the ability of the constructs to promote transcription in SH-SY5Y but not in HEK293T, suggesting this regulatory region has cell-specific functions. However, I did not observe any difference in luciferase expression between the different constructs. The DNA fragment cloned into vectors for this analysis could be a small portion of the complete *TRAPPC9* promoter. Therefore, out of context, it might have lost its ability to fully regulate gene expression. A more intricate explanation, however, might be that the interaction between the promoter region and a distant enhancer, which would be affected by the polymorphism we observed, could not be investigated by the design of the assay.

The sequencing analysis of the three variants revealed that this region is rich in CTCF binding sites. The use of the CTCFBSBD 2.0 database prediction tool found 4 main CTCF binding motifs, one of which is disrupted in V3 (Fig 6.4). *In vitro*, CTCF binding activity has been confirmed in this region in SKNSH neuroblastoma cells (Fig 6.1) but not in a myelogenous leukaemia cell line (K562) or in total brain RNA (Court et al., 2014), suggesting this type of regulation might be cell specific.

CTCF is an ubiquitously expressed transcription factor with 11 zinc finger DNA-binding domains, able to bind a wide range of variant sequences and co-regulatory proteins through the use of different zinc fingers (Filippova et al., 1996; Kim et al., 2007; Phillips and Corces, 2009).

Two main CTCF binding motifs, composed of a set of non-palindromic CTCF binding sites, have been described. These motifs, named M1 and M2, consist of 20 and 10 bp cores respectively, and are responsible for the engagement of zinc fingers 4-7 and 9-11 (Kim et al., 2007; Schmidt et al., 2012; Nakahashi et al., 2013). Other motifs, with a different structure from M1 and M2, have been described but to date no consensus sequence of CTFC binding motifs has been reported, although it has been suggested that the binding may be partially stabilized by interactions between peripheral fingers and nucleotides surrounding the core consensus (Kim et al., 2007; Phillips and Corces, 2009).

As mentioned earlier in this chapter, CTCF has been shown to act as a transcriptional regulator, as a regulator of RNA splicing and as an insulator by regulating the 3D structure of chromatin (Phillips and Corces, 2009). CTCF can, in fact, form chromatin loops by interacting with other CTCF molecules or with other proteins to generate different classes of CTCF mediated contacts. It has been proposed that "during formation of a CTCF-DNA complex, both DNA and CTCF polypeptide allosterically 'customize' their conformation to engage different zinc fingers, either for making base contacts or to make a target-specific surface that determines interactions with other nuclear proteins" (Ohlsson et al., 2001). This differential conformation leads CTCF to interact with different zinc finger domains with different binding partners, leading to multiple functional roles.

Mutations in individual CTCF sites have been shown to lead to loss of binding and disruption of loop formation, and have been associated with intellectual disability, microcephaly and growth retardation (Gregor et al., 2013; Tang et al., 2015). The

difference in CTCF binding between V1-2 and V3 could therefore have important repercussions in the expression of *TRAPPC9*.

Interestingly, an example of CTCF insulator activity can be found at the imprinted *Igf2*/*H19* locus, where it blocks the interaction between the enhancer located downstream of *H19* and the *Igf2* promoter, resulting in the silencing of *Igf2* from the maternal allele (Bartolomei and Ferguson-Smith, 2011). The methylation of the imprinting control region (ICR) of the cluster in the paternal allele instead, prevents the binding of CTCF thus allowing the interaction of enhancer and promoter and the subsequent expression of *Igf2*.

In chapter 3 I discussed the imprinting status of human *TRAPPC9* that, similarly to the mouse orthologue, has a contradictory history of reports. Considering the technological advancement and the wider range of techniques used to study the epigenetic regulation of genes, it is possible that the studies that reported the maternal expression of *TRAPPC9* in the human (Garg et al., 2012; Babak et al., 2015) have actually detected what other studies could not. Although the ICR of the human locus is most likely to reside in *PEG13* as in the mouse, we cannot exclude that the regulation of the imprinting depends on the interaction between distant CTCF sites.

Furthermore, considering the strong enhancer marks in histone modifications observed in the same region (Fig 6.1) and the fact that CTCF is considered to be a marker for enhancer-blocker activity, it cannot be excluded that this polymorphism is affecting the expression or the epigenetic regulation of neighbouring genes. Interestingly, a missense SNP in the sequence of *TRAPPC9* exon 20 has been linked with schizophrenia, suggesting it might have a role in the onset of the disorder (McCarthy et al., 2014).

During the investigation of the VNTR polymorphism in *TRAPPC9*'s promoter, I genotyped gDNA samples from healthy individuals and from individuals with schizophrenia. Despite the small size of our cohort, preliminary results showed a 5.6% difference in allelic

frequency of the V1/3 genotype, with the healthy group carrying this variant more often than the schizophrenia group (Table 6.1).

As the role of G4s in regulating gene transcription are gene specific and considering our lack of knowledge regarding the G4 motif present in *TRAPPC9*'s promoter, any hypothesis on the role of this VNTR polymorphism would be, at this point, pure speculation.

However, considering the position of this VNTR and the importance of this region for both G4 formation and CTCF binding, it is logical to assume that different variants might influence gene expression levels and possibly cause varying protein levels with modest effects on brain functioning or association with different neurological disorders.

Considering the plethora of cellular functions and the brain disorders this gene has been associated with, it would be beneficial for the scientific community to further investigate its role in brain development and neuronal functioning in order to understand pathologies that might have a common aetiology.

CHAPTER 7

Conclusions

7.1 Where are we now?

In this thesis I have investigated a number of aspects of Trappc9, from its epigenetic regulation to its molecular function(s) in the cell and its physiological function *in vivo*.

I have analysed its structure in the mouse genome and, contrary to the information available in genomic databases (e.g. Ensembl), found only one transcript variant with an alternatively spliced exon of unknown significance. Exon 5 is highly conserved in human and mouse encoding for a 9 amino acid sequence (GAQEVLIDP) that could be important in regulating the interaction between Trappc9 and other factors (e.g. cargo proteins).

I have also confirmed *Trappc9* imprinting status in mouse brain, where it exhibits a preferential maternal expression in contrast to the biallelic expression found in peripheral tissues. It is currently unknown whether this preferential maternal expression is equal in every cell of the brain or if it is due to a mixture of cells with maternal expression and cells with biallelic expression.

What we know at the moment is that this imprinting status is not driven by hypermethylation of CpG islands at the start of *Trappc9*, but it is likely to be driven by the interaction between the DMR in *Peg13* and a distant enhancer, similarly to the *Igfr*/*H19* locus.

Regarding Trappc9's cellular functions, I have highlighted a role of this protein in cell differentiation in response to retinoic acid (RA) in N2A cells. Considering that RA needs to be transported into the nucleus in order to activate gene expression, and considering the

function of Trappc9 within the TRAPPII complex and its interaction with dynactin, the altered differentiation in Trappc9-depleted N2A cells could be due to defects in RA transport. This supposition is supported by the fact that lack of Bru/Trappc9 in Drosophila and of Trs120/Trappc9 in plants disrupts cytokinesis probably by causing defects in membrane and cytoskeleton components addition to the cell division plane. Thus, despite the emphasis that previous studies have placed on Trappc9's regulation of the NF-κB pathway, the basis for the brain abnormalities observed in affected individuals and in our KO mouse model could lie in defects of vesicular transport.

Interestingly, a recent report found that the TRAPPII Trappc9-mediated activation of Rab18 is necessary for the recruitment of Rab18 to the surface of lipid droplets (LD), cytosolic organelles involved in the storage, regulation of synthesis and metabolism of lipids (Li et al., 2017).

Rab18 is important in the regulation of lipid homeostasis, and mutations in this gene have been associated with the recessive autosomal Warburg micro syndrome (Liegel et al., 2013). Among the symptoms characteristic of this condition, there are some similar to the Trappc9-induced condition such as intellectual disability, postnatal microcephaly and brain abnormalities (hypogenesis of corpus callosum, cerebellar hypoplasia) and aberrantly large LDs (Liegel et al., 2013). In fact, fibroblasts from individuals with mutated Trappc9 showed similar aberrantly large LDs, a phenomenon which has been confirmed *in vitro* via siRNA and CRISPR-Cas silencing in HEK293 and HeLa cells (Li et al., 2017).

Although the role of LDs in neurons has only recently come under investigation, it is likely that their functions and defects play an important role in the nervous system. The stored lipids can be used to generate energy and to participate in many membrane functions and in different signalling events. Furthermore, they can sequester transcription factors, enzymes and chromatin components (nuclear LDs) and act as an isolator of toxic lipids.

The over-accumulation of free fatty acids and their break-down can generate toxic metabolites and oxidative damage. The abundant accumulation of LD is, in fact, common to several disease states such as obesity, atherosclerosis and fatty liver disease (Welte, 2015). LDs have been detected in cultured neurons and brain sections of Huntington's disease models and they were found bound to α-synuclein in Parkinson's disease models (Cole et al., 2002; Martinez-Vicente et al., 2010).

Rab18 itself has been reported to be a RA-responsive LD associated protein in hepatic stellate cells (O'Mahony et al., 2015), possibly providing a link between Trappc9's knockdown and the defects in differentiation observed in 76kd discussed in chapter 4.

In addition, Trappc9 has also been linked to cytokinesis. In *Drosophila*, mutants for the Trappc9 orthologue Brunelleschi show failure in spermatocyte meiotic cytokinesis where the formation of a contractile ring in mid anaphase is unaffected but its ability to contract is disrupted. Cytokinesis is dependent on the proper functioning of the Golgi membrane trafficking apparatus and Brunelleschi is required for the Rab11-mediated ring constriction (Robinett et al., 2009).

In plants, trs120/Trappc9 mutants show a defect in cell plate biogenesis while trs130/Trappc10 mutants have lost the ability to target membrane proteins to the cell plate during cytokinesis (Rybak et al., 2014).

It is possible that the lack of membrane addition and/or trafficking of actin-remodelling factors that fail to be transported to the cell midzone are responsible for the disruption of cytokinesis, which could be important in a progenitor cells background. Similarly, the same mechanisms could be the basis for the defects in cell differentiation. The TRAPPII complex could therefore regulate brain development and neuronal functioning via these systems.

With regards to the role of Trappc9 in vivo, I have confirmed that the analysed *Trappc9* KO Tm1a mouse line recapitulates the microcephaly observed in individuals harbouring mutations in *TRAPPC9*, and that the population of adult stem cells in the hippocampus is affected. Interestingly, preliminary results have shown a decrease in GFAP-positive cells (mainly astrocytes) in the corpus callosum and hypothalamus, but whether this is a cause of the phenotype or a consequence is still unknown.

I also observed a weight gain in female KO mice that mirrors the weight gain observed in two human patients, suggesting that a dysregulation at the hypothalamus level might be involved. An impairment in the astrocyte population in the hypothalamus might be the basis of the observed weight gain, as astrocytes exert a critical role in orchestrating the hypothalamic response to metabolic cues by participating in processes of synaptic transmission, synaptic plasticity and nutrient sensing (Chowen et al., 2016). However, since the depletion of TRAPPC9 causes defects in lipid homeostasis (Li et al., 2017), the weight gain could also be due to the lack of TRAPPC9 in peripheral tissues.

While the microcephaly and intellectual disability in humans are caused by recessive homozygous loss-of-function mutations, no clinical symptoms have been associated with abnormal levels of expression of *TRAPPC9* and, for this reason, not much thought has been given to the regulation of this gene in healthy individuals. In this thesis, I have described a VNTR polymorphism in the promoter region of human *TRAPPC9* and confirmed its activity as a promoter of expression in a luciferase reporter gene assay.

The functional significance of the three observed variants is still unknown. This appears to be an important regulatory region as it is rich in CTCF binding sites (specifically found in SKNSH neuroblastoma cells but not in peripheral cell types or whole brain lysates) and it is predicted to form a G4. Interestingly, while no difference was found between the different variants, all three sequences promote transcription in SH-SY5Y neuroblastoma cells but

not in the kidney-derived HEK293. This hints at *TRAPPC9* being differentially regulated in a cell specific manner and it could very well be linked to different roles of TRAPPC9 in different cell types. At this point we can only speculate how important this polymorphism is and what its function is. However, considering the strong clinical manifestations the lack of *TRAPPC9* causes in affected individuals, it seems possible that fine regulation of this gene may have important reverberations in brain physiology and development (e.g. reduced levels causing mild symptoms such as low IQ).

Furthermore, the imprinting status of *TRAPPC9* in the human brain is still unclear but a parental-specific expression of this gene in an individual carrying specific variants of this VNTR polymorphism could have important repercussions in the physiology of the brain.

7.2 Future directions

In this study I analysed a KO mouse model for Trappc9 focussing mainly on the microcephaly phenotype and the associated possible cellular basis. What I have not done, but would be interesting to do, is to investigate whether these mice exhibit any cognitive deficits that might be comparable to the intellectual disability observed in humans. A behavioural characterisation of this model would not only help to shed light on the progression of the human disorder but it would also validate a mouse model that could be useful to investigate other disorders as well, especially considering the number of complex multigenic conditions that exhibit microcephaly and intellectual disability. Furthermore, testing behavioural traits (e.g. locomotor activity, memory, anxiety and social interaction) at different ages (young vs aged mice) would be beneficial in order to study the development and progression of the disorder.

However, from a translational point of view, I believe it would be more beneficial to investigate the cellular basis of the microcephaly in order to develop therapeutic strategies aimed to prevent the progression of this disorder and other microcephaly/intellectual disability disorders related to trafficking processes.

New evidence suggests an important interaction between Trappc9 and centrosomes. Cell division could be affected, which would be particularly important in a progenitor cell environment. Furthermore, the involvement of Trappc9 in TRAPPII complex functions might be crucial for cell differentiation with regards to transport of cytoskeletal or membrane components. Response to growth factors and regulators could also be affected due to the interaction between Trappc9 and dynactin.

Regarding the imprinting in mouse, it would be of interest to investigate the interaction between the DMR in *Peg13* and the enhancer described in chapter 3. Moreover, it would be interesting to study the distribution of imprinting across the brain, whether it is uniform or cell specific, with particular reference to progenitor cells as an imprinted regulation could have important repercussions in such a scenario.

Last but not least, the human VNTR polymorphism described in chapter 6 is particularly intriguing. Investigating whether the three different promoter variants regulate *TRAPPC9*'s expression, possibly by interacting with distant enhancers, might help shed light on the functional role of this gene.

7.3 Limitations

What transpires from the results presented in this thesis, as well as from the published literature, is that Trappc9 may have cell specific functions and regulation. The lack of consensus in the literature (e.g. imprinting status, cellular functions), in combination with

the results presented in this thesis, might very well be a consequence of different methods and cell lines/tissues used for the different studies, especially since no studies have been conducted in primary neurons.

The lack of specific antibodies for Trappc9 appropriate for cytological and histological techniques is another important limitation. Our group has designed and generated a GFP-tagged Trappc9 expressing N2A cell line to overcome this problem. However, GFP-Trappc9 appears to have a wide and general localisation in the cytoplasm which has made it impossible to study specific interactions with other factors. The RNAscope® method of *in situ* hybridisation appears to be very specific and will be a useful tool to study the expression and function of Trappc9 at a histological level.

A similar limitation applies to the study of imprinting. The lack of specific cell isolation techniques in the past prevented the investigation of cell specific imprinting, leaving to questioning whether the parental bias really exists or if it is due to a mixture of cell specific biases. In the future, the recently developed SNP-FISH method of visualising allele-specific expression in single cells (Ginart et al., 2016) will be a key tool in the imprinting research.

Ultimately, the fact that animal models often exhibit milder symptoms of human disorders limits the amount of information that could be gathered from such tools and thus the development of therapeutic strategies.

Supplementary figures

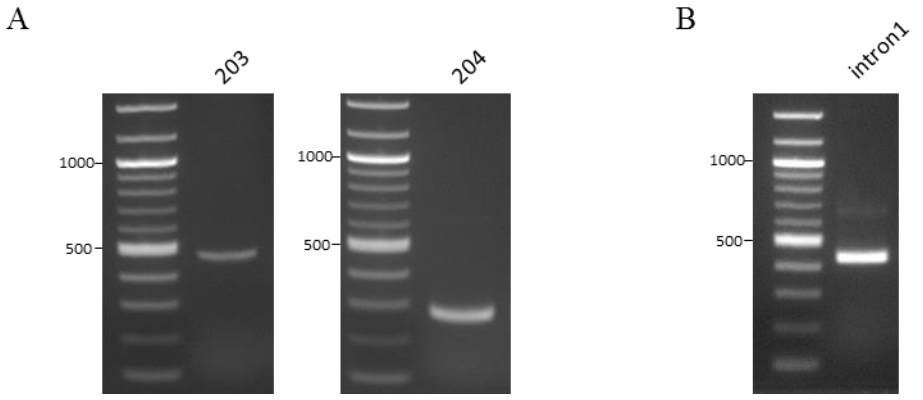

Supplementary Figure 1

A) PCR for *Trappc9* truncated variants on gDNA using Tr_203FW (intron before 203-UTR) + Tr_203RV (variant 203 UTR) and Tr_204FW (intron before 204-UTR) + Tr_204RV (variant 204 UTR). Expected products: 452 bp for 203, 272 bp for 204. B) PCR for *Trappc9* alternative start site on gDNA using Tr_upex2n1_Fw + Pr_02RV (exon 2). Expected product: 431 bp.

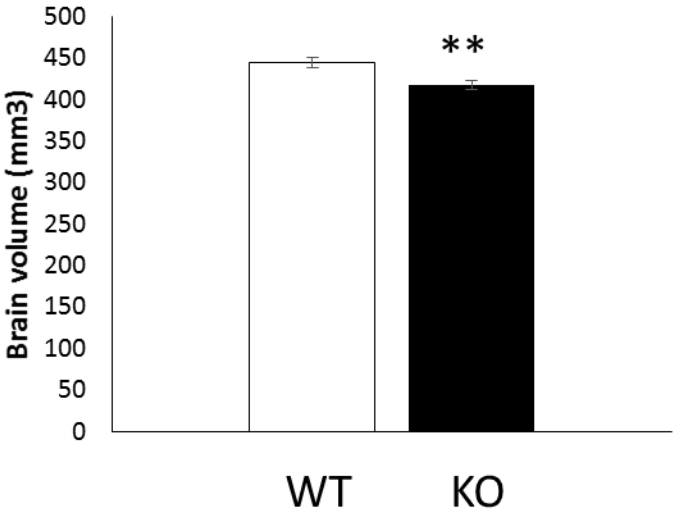

Supplementary Figure 2

Average brain volume of WT and homozygous KO Tm1a mice measured via MRI. For the analysis the measurements at 12 weeks of age of 8 WT females and 5 WT males were averaged and compared to the averaged measurements of 7 KO females and 8 KO males. No statistical difference was found between males and females within the two groups. Analysis by Thomas Leather. **p<0.001

Bibliography

Abou Jamra R, Wohlfart S, Zweier M, Uebe S, Priebe L, Ekici A, Giesebrecht S, Abboud A, Al Khateeb MA, Fakher M, Hamdan S, Ismael A, Muhammad S, Nöthen MM, Schumacher J, Reis A (2011) Homozygosity mapping in 64 Syrian consanguineous families with non-specific intellectual disability reveals 11 novel loci and high heterogeneity. Eur J Hum Genet 19:1161–1166.

Albensi BC, Mattson MP (2000) Evidence for the involvement of TNF and NF-kappaB in hippocampal synaptic plasticity. Synapse 35:151–159.

Albrecht U, Sutcliffe JS, Cattanach BM, Beechey C V., Armstrong D, Eichele G, Beaudet AL (1997) Imprinted expression of the murine Angelman syndrome gene, Ube3a, in hippocampal and Purkinje neurons. Nat Genet 17:75–78.

Alcock J, Lowe J, England T, Bath P, Sottile V (2009) Expression of Sox1, Sox2 and Sox9 is maintained in adult human cerebellar cortex. Neurosci Lett 450:114–116.

Allen NJ, Barres BA (2009) Neuroscience: Glia — more than just brain glue. Nature 457:675–677.

Almouzni G, Probst A V (2011) Heterochromatin maintenance and establishment: lessons from the mouse pericentromere. Nucleus 2:332–338.

Alvarez-Buylla A, García-Verdugo JM (2002) Neurogenesis in adult subventricular zone. J Neurosci 22:629–634.

Anderlid B-M, Lundin J, Malmgren H, Lehtihet M, Nordgren A (2014) Small mosaic deletion

encompassing the snoRNAs and SNURF-SNRPN results in an atypical Prader-Willi syndrome phenotype. Am J Med Genet A 164A:425–431.

Babak T, DeVeale B, Tsang EK, Zhou Y, Li X, Smith KS, Kukurba KR, Zhang R, Li JB, van der Kooy D, Montgomery SB, Fraser HB (2015) Genetic conflict reflected in tissue-specific maps of genomic imprinting in human and mouse. Nat Publ Gr 47:544–549.

Bahi-Buisson N, Bienvenu T (2012) CDKL5-Related Disorders: From Clinical Description to Molecular Genetics. Mol Syndromol 2:137–152.

Bahi-Buisson N, Nectoux J, Girard B, Van Esch H, De Ravel T, Boddaert N, Plouin P, Rio M, Fichou Y, Chelly J, Bienvenu T (2010) Revisiting the phenotype associated with FOXG1 mutations: two novel cases of congenital Rett variant. Neurogenetics 11:241–249.

Bahi-Buisson N, Nectoux J, Rosas-Vargas H, Milh M, Boddaert N, Girard B, Cances C, Ville D, Afenjar A, Rio M, Héron D, N'guyen Morel MA, Arzimanoglou A, Philippe C, Jonveaux P, Chelly J, Bienvenu T (2008) Key clinical features to identify girls with CDKL5 mutations. Brain 131:2647–2661.

Ballas N, Lioy DT, Grunseich C, Mandel G (2009) Non–cell autonomous influence of MeCP2-deficient glia on neuronal dendritic morphology. Nat Neurosci 12:311–317.

Bannister AJ, Kouzarides T (2011) Regulation of chromatin by histone modifications. Cell Res 21:381–395.

Barel O, Shalev SA, Ofir R, Cohen A, Zlotogora J, Shorer Z, Mazor G, Finer G, Khateeb S, Zilberberg N, Birk OS (2008) Maternally Inherited Birk Barel Mental Retardation Dysmorphism Syndrome Caused by a Mutation in the Genomically Imprinted Potassium Channel KCNK9. Am J Hum Genet 83:193–199.

Barlow DP, Stöger R, Herrmann BG, Saito K, Schweifer N (1991) The mouse insulin-like growth factor type-2 receptor is imprinted and closely linked to the Tme locus. Nature

349:84–87.

Barrowman J, Bhandari D, Reinisch K, Ferro-Novick S (2010) TRAPP complexes in membrane traffic: convergence through a common Rab. Nat Rev Mol Cell Biol 11:759–763.

Barski A, Cuddapah S, Cui K, Roh T-Y, Schones DE, Wang Z, Wei G, Chepelev I, Zhao K (2007) High-resolution profiling of histone methylations in the human genome. Cell 129:823–837.

Bartolomei MS, Ferguson-Smith AC (2011) Mammalian Genomic Imprinting. Cold Spring Harb Perspect Biol 3:1–18.

Bartolomei MS, Zemel S, Tilghman SM (1991) Parental imprinting of the mouse H19 gene. Nature 351:153–155.

Bassères DS, Baldwin AS (2006) Nuclear factor-kappaB and inhibitor of kappaB kinase pathways in oncogenic initiation and progression. Oncogene 25:6817–6830.

Beattie EC, Stellwagen D, Morishita W, Bresnahan JC, Ha BK, Von Zastrow M, Beattie MS, Malenka RC (2002) Control of synaptic strength by glial TNFalpha. Science 295:2282–2285.

Berger SL, Kouzarides T, Shiekhattar R, Shilatifard A (2009) An operational definition of epigenetics. Genes Dev 23:781–783.

Bian C, Xu C, Ruan J, Lee KK, Burke TL, Tempel W, Barsyte D, Li J, Wu M, Zhou BO, Fleharty BE, Paulson A, Allali-Hassani A, Zhou J-Q, Mer G, Grant PA, Workman JL, Zang J, Min J (2011) Sgf29 binds histone H3K4me2/3 and is required for SAGA complex recruitment and histone H3 acetylation. EMBO J 30:2829–2842.

Bibel M, Richter J, Schrenk K, Tucker KL, Staiger V, Korte M, Goetz M, Barde Y-A (2004)

Differentiation of mouse embryonic stem cells into a defined neuronal lineage. Nat Neurosci 7:1003–1009.

Bochman ML, Paeschke K, Zakian VA (2012) DNA secondary structures: stability and function of G-quadruplex structures. Nat Rev Genet 13:770–780.

Boersma MCH, Dresselhaus EC, De Biase LM, Mihalas AB, Bergles DE, Meffert MK (2011) A requirement for nuclear factor-kappaB in developmental and plasticity-associated synaptogenesis. J Neurosci 31:5414–5425.

Bögershausen N et al. (2013) Recessive TRAPPC11 Mutations Cause a Disease Spectrum of Limb Girdle Muscular Dystrophy and Myopathy with Movement Disorder and Intellectual Disability. Am J Hum Genet 93:181–190.

Bouschet T, Dubois E, Reynès C, Kota SK, Rialle S, Maupetit-Méhouas S, Pezet M, Le Digarcher A, Nidelet S, Demolombe V, Cavelier P, Meusnier C, Maurizy C, Sabatier R, Feil R, Arnaud P, Journot L, Varrault A (2016) In Vitro Corticogenesis from Embryonic Stem Cells Recapitulates the In Vivo Epigenetic Control of Imprinted Gene Expression. Cereb Cortex:bhw102.

Brancaccio M, Pivetta C, Granzotto M, Filippis C, Mallamaci A (2010) Emx2 and Foxg1 inhibit gliogenesis and promote neuronogenesis. Stem Cells 28:1206–1218.

Breen G, Collier D, Craig I, Quinn J (2008) Variable number tandem repeats as agents of functional regulation in the genome. IEEE Eng Genomics Biol:103–105.

Brioude F, Lacoste A, Netchine I, Vazquez M-P, Auber F, Audry G, Gauthier-Villars M, Brugieres L, Gicquel C, Le Bouc Y, Rossignol S (2013) Beckwith-Wiedemann syndrome: growth pattern and tumor risk according to molecular mechanism, and guidelines for tumor surveillance. Horm Res Paediatr 80:457–465.

Brookes KJ (2013) The VNTR in complex disorders: The forgotten polymorphisms? A

functional way forward? Genomics 101:273–281.

Brunet S, Sacher M (2014) in sickness and in health: The role of TRAPP and associated proteins in disease. Traffic 15:803–818.

Buiting K (2010) Prader-Willi syndrome and Angelman syndrome. Am J Med Genet C Semin Med Genet 154C:365–376.

Buiting K, Saitoh S, Gross S, Dittrich B, Schwartz S, Nicholls RD, Horsthemke B (1995) Inherited microdeletions in the Angelman and Prader-Willi syndromes define an imprinting centre on human chromosome 15. Nat Genet 9:395–400.

Buiting K, Williams C, Horsthemke B (2016) Angelman syndrome - insights into a rare neurogenetic disorder. Nat Rev Neurol 12:584–593.

Bylund M, Andersson E, Novitch BG, Muhr J (2003) Vertebrate neurogenesis is counteracted by Sox1-3 activity. Nat Neurosci 6:1162–1168.

Cai H, Zhang Y, Pypaert M, Walker L, Ferro-Novick S (2005) Mutants in trs120 disrupt traffic from the early endosome to the late Golgi. J Cell Biol 171:823–833.

Castiel A, Danieli MM, David A, Moshkovitz S, Aplan PD, Kirsch IR, Brandeis M, Krämer A, Izraeli S (2011) The Stil protein regulates centrosome integrity and mitosis through suppression of Chfr. J Cell Sci 124:532–539.

Chahrour M, Zoghbi HY (2007) The Story of Rett Syndrome: From Clinic to Neurobiology. Neuron 56:422–437.

Chen N, Sugihara H, Kim J, Fu Z, Barak B, Sur M, Feng G, Han W (2016) Direct modulation of GFAP-expressing glia in the arcuate nucleus bi-directionally regulates feeding. Elife 5:e18716.

Choudhary C, Kumar C, Gnad F, Nielsen ML, Rehman M, Walther TC, Olsen J V, Mann M

(2009) Lysine acetylation targets protein complexes and co-regulates major cellular functions. Science 325:834–840.

Chowen JA, Argente-Arizón P, Freire-Regatillo A, Frago LM, Horvath TL, Argente J (2016) The role of astrocytes in the hypothalamic response and adaptation to metabolic signals. Prog Neurobiol 144:68–87.

Coan PM, Burton GJ, Ferguson-Smith AC (2005) Imprinted genes in the placenta--a review. Placenta 26 Suppl A:S10-20.

Cogoi S, Xodo LE (2006) G-quadruplex formation within the promoter of the KRAS proto-oncogene and its effect on transcription. Nucleic Acids Res 34:2536–2549.

Cole NB, Murphy DD, Grider T, Rueter S, Brasaemle D, Nussbaum RL (2002) Lipid droplet binding and oligomerization properties of the Parkinson's disease protein alpha-synuclein. J Biol Chem 277:6344–6352.

Contente A, Dittmer A, Koch MC, Roth J, Dobbelstein M (2002) A polymorphic microsatellite that mediates induction of PIG3 by p53. Nat Genet 30:315–320.

Court F, Camprubi C, Vicente Garcia C, Guillaumet-Adkins A, Sparago A, Seruggia D, Sandoval J, Esteller M, Martin-Trujillo A, Riccio A, Montoliu L, Monk D (2014) The PEG13-DMR and brain-specific enhancers dictate imprinted expression within the 8q24 intellectual disability risk locus. Epigenetics Chromatin 7:1–13.

Courtois G, Gilmore TD (2006) Mutations in the NF-κB signaling pathway: implications for human disease. Oncogene 25:6831–6843.

Creyghton MP, Cheng AW, Welstead GG, Kooistra T, Carey BW, Steine EJ, Hanna J, Lodato MA, Frampton GM, Sharp PA, Boyer LA, Young RA, Jaenisch R (2010) Histone H3K27ac separates active from poised enhancers and predicts developmental state. Proc Natl Acad Sci U S A 107:21931–21936.

Crouse H V (1960) The Controlling Element in Sex Chromosome Behavior in Sciara. Genetics 45:1429–1443.

Dapić V, Abdomerović V, Marrington R, Peberdy J, Rodger A, Trent JO, Bates PJ (2003) Biophysical and biological properties of quadruplex oligodeoxyribonucleotides. Nucleic Acids Res 31:2097–2107.

Davis JT (2004) G-Quartets 40 Years Later: From 5'-GMP to Molecular Biology and Supramolecular Chemistry. Angew Chemie - Int Ed 43:668–698.

Davis TL, Yang GJ, McCarrey JR, Bartolomei MS (2000) The H19 methylation imprint is erased and re-established differentially on the parental alleles during male germ cell development. Hum Mol Genet 9:2885–2894.

DeChiara TM, Robertson EJ, Efstratiadis A (1991) Parental imprinting of the mouse insulin-like growth factor II gene. Cell 64:849–859.

Deckert J, Catalano M, Syagailo Y V, Bosi M, Okladnova O, Di Bella D, Nöthen MM, Maffei P, Franke P, Fritze J, Maier W, Propping P, Beckmann H, Bellodi L, Lesch KP (1999) Excess of high activity monoamine oxidase A gene promoter alleles in female patients with panic disorder. Hum Mol Genet 8:621–624.

Delcroix J-D, Valletta JS, Wu C, Hunt SJ, Kowal AS, Mobley WC (2003) NGF signaling in sensory neurons: evidence that early endosomes carry NGF retrograde signals. Neuron 39:69–84.

Delgado MS, Camprubí C, Tümer Z, Martínez F, Milà M, Monk D (2014) Screening individuals with intellectual disability, autism and Tourette's syndrome for KCNK9 mutations and aberrant DNA methylation within the 8q24 imprinted cluster. Am J Med Genet Part B Neuropsychiatr Genet 165:472–478.

Deneen B, Ho R, Lukaszewicz A, Hochstim CJ, Gronostajski RM, Anderson DJ (2006) The

transcription factor NFIA controls the onset of gliogenesis in the developing spinal cord. Neuron 52:953–968.

Denis-Donini S, Caprini A, Frassoni C, Grilli M (2005) Members of the NF-kappaB family expressed in zones of active neurogenesis in the postnatal and adult mouse brain. Brain Res Dev Brain Res 154:81–89.

Denis-Donini S, Dellarole A, Crociara P, Francese MT, Bortolotto V, Quadrato G, Canonico PL, Orsetti M, Ghi P, Memo M, Bonini SA, Ferrari-Toninelli G, Grilli M (2008) Impaired adult neurogenesis associated with short-term memory defects in NF-kappaB p50-deficient mice. J Neurosci 28:3911–3919.

Ding Y-C, Chi H-C, Grady DL, Morishima A, Kidd JR, Kidd KK, Flodman P, Spence MA, Schuck S, Swanson JM, Zhang Y-P, Moyzis RK (2002) Evidence of positive selection acting at the human dopamine receptor D4 gene locus. Proc Natl Acad Sci U S A 99:309–314.

Donlon TA (1988) Similar molecular deletions on chromosome 15q11.2 are encountered in both the Prader-Willi and Angelman syndromes. Hum Genet 80:322–328.

Eddy J, Maizels N (2006) Gene function correlates with potential for G4 DNA formation in the human genome. Nucleic Acids Res 34:3887–3896.

Edwards CA, Ferguson-Smith AC (2007) Mechanisms regulating imprinted genes in clusters. Curr Opin Cell Biol 19:281–289.

Ehlers MD (2003) Activity level controls postsynaptic composition and signaling via the ubiquitin-proteasome system. Nat Neurosci 6:231–242.

El Chehadeh S et al. (2016) Large national series of patients with Xq28 duplication involving MECP2 : Delineation of brain MRI abnormalities in 30 affected patients. Am J Med Genet Part A 170:116–129.

Elhamamsy AR (2016) DNA methylation dynamics in plants and mammals: overview of regulation and dysregulation. Cell Biochem Funct 34:289–298.

ENCODE Project Consortium et al. (2012) An integrated encyclopedia of DNA elements in the human genome. Nature 489:57–74.

Favaro R, Valotta M, Ferri ALM, Latorre E, Mariani J, Giachino C, Lancini C, Tosetti V, Ottolenghi S, Taylor V, Nicolis SK (2009) Hippocampal development and neural stem cell maintenance require Sox2-dependent regulation of Shh. Nat Neurosci 12:1248–1256.

Feng Y, Walsh CA (2004) Mitotic spindle regulation by Nde1 controls cerebral cortical size. Neuron 44:279–293.

Ferguson-Smith AC (2011) Genomic imprinting: the emergence of an epigenetic paradigm. Nat Rev Genet 12:565–575.

Ferrón SR, Charalambous M, Radford E, McEwen K, Wildner H, Hind E, Morante-Redolat JM, Laborda J, Guillemot F, Bauer SR, Fariñas I, Ferguson-Smith AC (2011) Postnatal loss of Dlk1 imprinting in stem cells and niche astrocytes regulates neurogenesis. Nature 475:381–385.

Filippova GN, Fagerlie S, Klenova EM, Myers C, Dehner Y, Goodwin G, Neiman PE, Collins SJ, Lobanenkov V V (1996) An exceptionally conserved transcriptional repressor, CTCF, employs different combinations of zinc fingers to bind diverged promoter sequences of avian and mammalian c-myc oncogenes. Mol Cell Biol 16:2802–2813.

Foehr ED, Bohuslav J, Chen LF, DeNoronha C, Geleziunas R, Lin X, O'Mahony a, Greene WC (2000) The NF-kappa B-inducing kinase induces PC12 cell differentiation and prevents apoptosis. J Biol Chem 275:34021–34024.

Fondon JW, Hammock EAD, Hannan AJ, King DG (2008) Simple sequence repeats: genetic

modulators of brain function and behavior. Trends Neurosci 31:328–334.

Gan W, Zong M, Satoh A, Chan H, Yu S (2014) p150Glued-interacting domains of TRAPPC9 reveal regulatory function of TRAPPC9 at the centrosome . In: American Society for Cell Biology, pp 959. American Society for Cell Biology.

Garber K, Smith KT, Reines D, Warren ST (2006) Transcription, translation and fragile X syndrome. Curr Opin Genet Dev 16:270–275.

Garg P, Borel C, Sharp AJ, Chadwick BP (2012) Detection of Parent-of-Origin Specific Expression Quantitative Trait Loci by Cis-Association Analysis of Gene Expression in Trios. PLoS One 7:e41695.

Gécz J, Gedeon ÁK, Colley A, Jamieson R, Thompson EM, Rogers J, Sillence D, Tiller GE, Mulley JC (1999) Identification of the gene (SEDL) causing X-linked spondyloepiphyseal dysplasia tarda. Nat Genet 22:400–404.

Gilmore EC, Walsh C a. (2013) Genetic causes of microcephaly and lessons for neuronal development. Wiley Interdiscip Rev Dev Biol 2:461–478.

Ginart P, Kalish JM, Jiang CL, Yu AC, Bartolomei MS, Raj A (2016) Visualizing allele-specific expression in single cells reveals epigenetic mosaicism in an H19 loss-of-imprinting mutant. Genes Dev 30:567–578.

Gourraud P-A, Sdika M, Khankhanian P, Henry RG, Beheshtian A, Matthews PM, Hauser SL, Oksenberg JR, Pelletier D, Baranzini SE (2013) A genome-wide association study of brain lesion distribution in multiple sclerosis. Brain 136:1012–1024.

Graham JM, Zadeh N, Kelley M, Tan ES, Liew W, Tan V, Deardorff MA, Wilson GN, Sagi-Dain L, Shalev SA (2016) KCNK9 imprinting syndrome-further delineation of a possible treatable disorder. Am J Med Genet Part A 170:2632–2637.

Gregg C, Zhang J, Weissbourd B, Luo S, Schroth GP, Haig D, Dulac C (2010) High-resolution analysis of parent-of-origin allelic expression in the mouse brain. Science 329:643–648.

Gregor A, Oti M, Kouwenhoven EN, Hoyer J, Sticht H, Ekici AB, Kjaergaard S, Rauch A, Stunnenberg HG, Uebe S, Vasileiou G, Reis A, Zhou H, Zweier C (2013) De novo mutations in the genome organizer CTCF cause intellectual disability. Am J Hum Genet 93:124–131.

Grewal SIS, Jia S (2007) Heterochromatin revisited. Nat Rev Genet 8:35–46.

Grilli M, Ribola M, Alberici A, Valerio A, Memo M, Spano P (1995) Identification and characterization of a kappa B/Rel binding site in the regulatory region of the amyloid precursor protein gene. J Biol Chem 270:26774–26777.

Gubbay J, Collignon J, Koopman P, Capel B, Economou A, Münsterberg A, Vivian N, Goodfellow P, Lovell-Badge R (1990) A gene mapping to the sex-determining region of the mouse Y chromosome is a member of a novel family of embryonically expressed genes. Nature 346:245–250.

Guenther MG, Levine SS, Boyer LA, Jaenisch R, Young RA (2007) A chromatin landmark and transcription initiation at most promoters in human cells. Cell 130:77–88.

Guerrini L, Blasi F, Denis-Donini S (1995) Synaptic activation of NF-kappa B by glutamate in cerebellar granule neurons in vitro. Proc Natl Acad Sci U S A 92:9077–9081.

Guerrini R, Parrini E (2012) Epilepsy in Rett syndrome, and CDKL5- and FOXG1-gene-related encephalopathies. Epilepsia 53:2067–2078.

Guschin D, Wolffe AP (1999) SWItched-on mobility. Curr Biol 9:R742-6.

Gusella JF, MacDonald ME (2006) Huntington's disease: seeing the pathogenic process

through a genetic lens. Trends Biochem Sci 31:533–540.

Gwynn B, Smith RS, Rowe LB, Taylor BA, Peters LL (2006) A mouse TRAPP-related protein is involved in pigmentation. Genomics 88:196–203.

Gymrek M, Willems T, Guilmatre A, Zeng H, Markus B, Georgiev S, Daly MJ, Price AL, Pritchard JK, Sharp AJ, Erlich Y (2016) Abundant contribution of short tandem repeats to gene expression variation in humans. Nat Genet 48:22–29.

Ha SC, Lowenhaupt K, Rich A, Kim Y-G, Kim KK (2005) Crystal structure of a junction between B-DNA and Z-DNA reveals two extruded bases. Nature 437:1183–1186.

Hansen KD, Brenner SE, Dudoit S (2010) Biases in Illumina transcriptome sequencing caused by random hexamer priming. Nucleic Acids Res 38:1–7.

Harding RM, Boyce AJ, Clegg JB (1992) The evolution of tandemly repetitive DNA: recombination rules. Genetics 132:847–859.

Haskell GT, LaMantia A-S (2005) Retinoic acid signaling identifies a distinct precursor population in the developing and adult forebrain. J Neurosci 25:7636–7647.

Hébert JM, Fishell G (2008) The genetics of early telencephalon patterning: some assembly required. Nat Rev Neurosci 9:678–685.

Heintzman ND, Stuart RK, Hon G, Fu Y, Ching CW, Hawkins RD, Barrera LO, Van Calcar S, Qu C, Ching KA, Wang W, Weng Z, Green RD, Crawford GE, Ren B (2007) Distinct and predictive chromatin signatures of transcriptional promoters and enhancers in the human genome. Nat Genet 39:311–318.

Herculano-Houzel S, Collins CE, Wong P, Kaas JH (2007) Cellular scaling rules for primate brains. Proc Natl Acad Sci 104:3562–3567.

Holland AJ, Treasure J, Coskeran P, Dallow J (1995) Characteristics of the eating disorder in

Prader-Willi syndrome: implications for treatment. J Intellect Disabil Res 39 (Pt 5):373–381.

Holm VA, Cassidy SB, Butler MG, Hanchett JM, Greenswag LR, Whitman BY, Greenberg F (1993) Prader-Willi syndrome: consensus diagnostic criteria. Pediatrics 91:398–402.

Holmberg J, Hansson E, Malewicz M, Sandberg M, Perlmann T, Lendahl U, Muhr J (2008) SoxB1 transcription factors and Notch signaling use distinct mechanisms to regulate proneural gene function and neural progenitor differentiation. Development 135:1843–1851.

Homem CCF, Repic M, Knoblich JA (2015) Proliferation control in neural stem and progenitor cells. Nat Rev Neurosci 16:647–659.

Homma Y, Fukuda M (2016) Rabin8 regulates neurite outgrowth in both a GEF-activity-dependent and -independent manner.

Horsthemke B, Wagstaff J (2008) Mechanisms of imprinting of the Prader-Willi/Angelman region. Am J Med Genet Part A 146A:2041–2052.

Hu W-H, Pendergast JS, Mo X-M, Brambilla R, Bracchi-Ricard V, Li F, Walters WM, Blits B, He L, Schaal SM, Bethea JR (2005) NIBP, a novel NIK and IKK(beta)-binding protein that enhances NF-(kappa)B activation. J Biol Chem 280:29233–29241.

Huang Y-Y, Cate SP, Battistuzzi C, Oquendo MA, Brent D, Mann JJ (2004) An association between a functional polymorphism in the monoamine oxidase a gene promoter, impulsive traits and early abuse experiences. Neuropsychopharmacology 29:1498–1505.

Huberts DHEW, Van Der Klei IJ (2010) Moonlighting proteins: An intriguing mode of multitasking. BBA - Mol Cell Res 1803:520–525.

Huppert JL, Balasubramanian S (2005) Prevalence of quadruplexes in the human genome. Nucleic Acids Res 33:2908–2916.

Huppert JL, Balasubramanian S (2006) G-quadruplexes in promoters throughout the human genome. Nucleic Acids Res 35:406–413.

Huppert JL, Bugaut A, Kumari S, Balasubramanian S (2008) G-quadruplexes: the beginning and end of UTRs. Nucleic Acids Res 36:6260–6268.

Hutton SR, Pevny LH (2011) SOX2 expression levels distinguish between neural progenitor populations of the developing dorsal telencephalon. Dev Biol 352:40–47.

Hutvagner G, Simard MJ (2008) Argonaute proteins: key players in RNA silencing. Nat Rev Mol Cell Biol 9:22–32.

Ito CY, Kazantsevl AG, Jr ASB (1994) Three NF-xB sites in the IxB-oa promoter induction of gene expression by TNFcg are required for. Nulceic Acids Res 22:3787–3792.

Jahn R, Scheller RH (2006) SNAREs — engines for membrane fusion. Nat Rev Mol Cell Biol 7:631–643.

Johnson DR (1974) Hairpin-tail: a case of post-reductional gene action in the mouse egg. Genetics 76:795–805.

Kakar N, Goebel I, Daud S, Nürnberg G, Agha N, Ahmad A, Nürnberg P, Kubisch C, Ahmad J, Borck G (2012) A homozygous splice site mutation in TRAPPC9 causes intellectual disability and microcephaly. Eur J Med Genet 55:727–731.

Kalay E et al. (2011) CEP152 is a genome maintenance protein disrupted in Seckel syndrome. Nat Genet 43:23–26.

Kaltschmidt C, Kaltschmidt B, Baeuerle PA (1993) Brain synapses contain inducible forms of the transcription factor NF-kappa B. Mech Dev 43:135–147.

Kang P, Lee HK, Glasgow SM, Finley M, Donti T, Gaber ZB, Graham BH, Foster AE, Novitch BG, Gronostajski RM, Deneen B (2012) Sox9 and NFIA coordinate a transcriptional regulatory cascade during the initiation of gliogenesis. Neuron 74:79–94.

Kaplan LC, Wharton R, Elias E, Mandell F, Donlon T, Latt SA, Opitz JM, Reynolds JF (1987) Clinical heterogeneity associated with deletions in the long arm of chromosome 15: report of 3 new cases and their possible genetic significance. Am J Med Genet 28:45–53.

Karnavas T, Mandalos N, Malas S, Remboutsika E (2013) SoxB, cell cycle and neurogenesis. Front Physiol 4:298.

Kerjan G, Gleeson JG (2007) Genetic mechanisms underlying abnormal neuronal migration in classical lissencephaly. Trends Genet 23:623–630.

Kermicle JL (1970) Dependence of the R-mottled aleurone phenotype in maize on mode of sexual transmission. Genetics 66:69–85.

Khuu P, Sandor M, DeYoung J, Ho PS (2007) Phylogenomic analysis of the emergence of GC-rich transcription elements. Proc Natl Acad Sci U S A 104:16528–16533.

Kim TH, Abdullaev ZK, Smith AD, Ching KA, Loukinov DI, Green RD, Zhang MQ, Lobanenkov V V, Ren B (2007) Analysis of the Vertebrate Insulator Protein CTCF-Binding Sites in the Human Genome. Cell 128:1231–1245.

Kimura H (2013) Histone modifications for human epigenome analysis. J Hum Genet 5866:439–445.

Kishore S, Stamm S (2006) The snoRNA HBII-52 Regulates Alternative Splicing of the Serotonin Receptor 2C. Science (80-) 311:230–232.

Knoll JH, Nicholls RD, Magenis RE, Graham JM, Lalande M, Latt SA, Opitz JM, Reynolds JF

(1989) Angelman and Prader-Willi syndromes share a common chromosome 15 deletion but differ in parental origin of the deletion. Am J Med Genet 32:285–290.

Koehler K, Milev MP, Prematilake K, Reschke F, Kutzner S, Jühlen R, Landgraf D, Utine E, Hazan F, Diniz G, Schuelke M, Huebner A, Sacher M (2016) A novel TRAPPC11 mutation in two Turkish families associated with cerebral atrophy, global retardation, scoliosis, achalasia and alacrima. J Med Genet:jmedgenet-2016-104108.

Koifman A, Feigenbaum A, Bi W, Shaffer LG, Rosenfeld J, Blaser S, Chitayat D (2010) A homozygous deletion of 8q24.3 including the NIBP gene associated with severe developmental delay, dysgenesis of the corpus callosum, and dysmorphic facial features. Am J Med Genet A 152A:1268–1272.

Kolesov G, Wunderlich Z, Laikova ON, Gelfand MS, Mirny LA (2007) How gene order is influenced by the biophysics of transcription regulation. Proc Natl Acad Sci U S A 104:13948–13953.

Kong X, Qian J, Chen L-S, Wang Y-C, Wang J-L, Chen H, Weng Y-R, Zhao S-L, Hong J, Chen Y-X, Zou W, Xu J, Fang J-Y (2013) Synbindin in extracellular signal-regulated protein kinase spatial regulation and gastric cancer aggressiveness. J Natl Cancer Inst 105:1738–1749.

Kraus J, Börner C, Giannini E, Höllt V (2003) The role of nuclear factor kappaB in tumor necrosis factor-regulated transcription of the human mu-opioid receptor gene. Mol Pharmacol 64:876–884.

Kuijpers M, Hoogenraad CC (2011) Centrosomes, microtubules and neuronal development. Mol Cell Neurosci 48:349–358.

Kumamoto T, Toma K, Gunadi, McKenna WL, Kasukawa T, Katzman S, Chen B, Hanashima C (2013) Foxg1 coordinates the switch from nonradially to radially migrating

glutamatergic subtypes in the neocortex through spatiotemporal repression. Cell Rep 3:931–945.

Lander ES et al. (2001) Initial sequencing and analysis of the human genome. Nature 409:860–921.

Latos PA, Pauler FM, Koerner M V, Şenergin HB, Hudson QJ, Stocsits RR, Allhoff W, Stricker SH, Klement RM, Warczok KE, Aumayr K, Pasierbek P, Barlow DP (2012) Airn transcriptional overlap, but not its lncRNA products, induces imprinted Igf2r silencing. Science 338:1469–1472.

Lavelle GM, White MM, Browne N, McElvaney NG, Reeves EP (2016) Animal Models of Cystic Fibrosis Pathology: Phenotypic Parallels and Divergences. Biomed Res Int 2016:1–14.

Lazarus JE, Moughamian AJ, Tokito MK, Holzbaur ELF (2013) Dynactin Subunit p150Glued Is a Neuron-Specific Anti-Catastrophe Factor. PLoS Biol 11.

Li B, Carey M, Workman JL (2007) The role of chromatin during transcription. Cell 128:707–719.

Li C, Luo X, Zhao S, Siu GK, Liang Y, Chan HC, Satoh A, Yu SS (2017) COPI–TRAPPII activates Rab18 and regulates its lipid droplet association. EMBO J 36:441–457.

Li X, Ito M, Zhou F, Youngson N, Zuo X, Leder P, Ferguson-Smith AC, Trono D, Nakano T, Surani MA, al. et (2008) A Maternal-Zygotic Effect Gene, Zfp57, Maintains Both Maternal and Paternal Imprints. Dev Cell 15:547–557.

Lian Y, Garner HR (2005) Evidence for the regulation of alternative splicing via complementary DNA sequence repeats. Bioinformatics 21:1358–1364.

Liang Zhengzheng S, Raghupathy Narayanan, Lelliott Christopher J, Cimino Irene, Coll

Anthony P, Munger Steven C LDW (n.d.) Brain-specific allelic imbalance of Trappc9 influences methabolism and behaviour. Unpublished.

Liegel RP et al. (2013) Loss-of-Function Mutations in TBC1D20 Cause Cataracts and Male Infertility in blind sterile Mice and Warburg Micro Syndrome in Humans. Am J Hum Genet 93:1001–1014.

Lim LC, Powell J, Sham P, Castle D, Hunt N, Murray R, Gill M (1995) Evidence for a genetic association between alleles of monoamine oxidase A gene and bipolar affective disorder. Am J Med Genet 60:325–331.

Lipsky RH, Xu K, Zhu D, Kelly C, Terhakopian A, Novelli A, Marini AM (2001) Nuclear factor kappaB is a critical determinant in N-methyl-D-aspartate receptor-mediated neuroprotection. J Neurochem 78:254–264.

Liu L, Zhang K, Sandoval H, Yamamoto S, Jaiswal M, Sanz E, Li Z, Hui J, Graham BH, Quintana A, Bellen HJ (2015) Glial lipid droplets and ROS induced by mitochondrial defects promote neurodegeneration. Cell 160:177–190.

Lucifero D, Mann MRW, Bartolomei MS, Trasler JM (2004) Gene-specific timing and epigenetic memory in oocyte imprinting. Hum Mol Genet 13:839–849.

Luger K, Dechassa ML, Tremethick DJ (2012) New insights into nucleosome and chromatin structure: an ordered state or a disordered affair? Nat Rev Mol Cell Biol 13:436–447.

Mackay DJG, Callaway JLA, Marks SM, White HE, Acerini CL, Boonen SE, Dayanikli P, Firth H V, Goodship JA, Haemers AP, Hahnemann JMD, Kordonouri O, Masoud AF, Oestergaard E, Storr J, Ellard S, Hattersley AT, Robinson DO, Temple IK (2008) Hypomethylation of multiple imprinted loci in individuals with transient neonatal diabetes is associated with mutations in ZFP57. Nat Genet 40:949–951.

Madrigal JL, Moro MA, Lizasoain I, Lorenzo P, Castrillo A, Boscá L, Leza JC (2001) Inducible

nitric oxide synthase expression in brain cortex after acute restraint stress is regulated by nuclear factor kappaB-mediated mechanisms. J Neurochem 76:532–538.

Maezawa I, Jin L-W (2010) Rett syndrome microglia damage dendrites and synapses by the elevated release of glutamate. J Neurosci 30:5346–5356.

Maezawa I, Swanberg S, Harvey D, LaSalle JM, Jin L-W (2009) Rett syndrome astrocytes are abnormal and spread MeCP2 deficiency through gap junctions. J Neurosci 29:5051–5061.

Mandalos N, Saridaki M, Harper JL, Kotsoni A, Yang P, Economides AN, Remboutsika E (2012) Application of a novel strategy of engineering conditional alleles to a single exon gene, Sox2. Androutsellis-Theotokis A, ed. PLoS One 7:e45768.

Manzini MC, Walsh CA (2011) What disorders of cortical development tell us about the cortex: one plus one does not always make two. Curr Opin Genet Dev 21:333–339.

Marangi G, Leuzzi V, Manti F, Lattante S, Orteschi D, Pecile V, Neri G, Zollino M (2013) TRAPPC9-related autosomal recessive intellectual disability: report of a new mutation and clinical phenotype. Eur J Hum Genet 21:229–232.

Martinez-Vicente M, Talloczy Z, Wong E, Tang G, Koga H, Kaushik S, de Vries R, Arias E, Harris S, Sulzer D, Cuervo AM (2010) Cargo recognition failure is responsible for inefficient autophagy in Huntington's disease. Nat Neurosci 13:567–576.

Martinez ME, Charalambous M, Saferali A, Fiering S, Naumova AK, St Germain D, Ferguson-Smith AC, Hernandez A (2014) Genomic imprinting variations in the mouse type 3 deiodinase gene between tissues and brain regions. Mol Endocrinol 28:1875–1886.

Masui S, Nakatake Y, Toyooka Y, Shimosato D, Yagi R, Takahashi K, Okochi H, Okuda A, Matoba R, Sharov AA, Ko MSH, Niwa H (2007) Pluripotency governed by Sox2 via regulation of Oct3/4 expression in mouse embryonic stem cells. Nat Cell Biol 9:625–

635.

McCarthy SE, Gillis J, Kramer M, Lihm J, Yoon S, Berstein Y, Mistry M, Pavlidis P, Solomon R, Ghiban E, Antoniou E, Kelleher E, O'Brien C, Donohoe G, Gill M, Morris DW, McCombie WR, Corvin A (2014) De novo mutations in schizophrenia implicate chromatin remodeling and support a genetic overlap with autism and intellectual disability. Mol Psychiatry 19:652–658.

McGrath J, Solter D (1984) Completion of mouse embryogenesis requires both the maternal and paternal genomes. Cell 37:179–183.

McGreevy JW, Hakim CH, McIntosh MA, Duan D (2015) Animal models of Duchenne muscular dystrophy: from basic mechanisms to gene therapy. Dis Model Mech 8:195–213.

Meffert MK, Baltimore D (2005) Physiological functions for brain NF-kappaB. Trends Neurosci 28:37–43.

Meffert MK, Chang JM, Wiltgen BJ, Fanselow MS, Baltimore D (2003) NF-kappa B functions in synaptic signaling and behavior. Nat Neurosci 6:1072–1078.

Meister G, Landthaler M, Patkaniowska A, Dorsett Y, Teng G, Tuschl T (2004) Human Argonaute2 Mediates RNA Cleavage Targeted by miRNAs and siRNAs. Mol Cell 15:185–197.

Mir A et al. (2009) Identification of mutations in TRAPPC9, which encodes the NIK- and IKK-beta-binding protein, in nonsyndromic autosomal-recessive mental retardation. Am J Hum Genet 85:909–915.

Mochida GH (2009) Genetics and Biology of Microcephaly and Lissencephaly. Semin Pediatr Neurol 16:120–126.

Mochida GH, Mahajnah M, Hill AD, Basel-Vanagaite L, Gleason D, Hill RS, Bodell A, Crosier M, Straussberg R, Walsh C a (2009) A truncating mutation of TRAPPC9 is associated with autosomal-recessive intellectual disability and postnatal microcephaly. Am J Hum Genet 85:897–902.

Molofsky AV, Deneen B (2015) Astrocyte development: A Guide for the Perplexed. Glia 63:1320–1329.

Morita S, Horii T, Kimura M, Goto Y, Ochiya T, Hatada I (2007) One Argonaute family member, Eif2c2 (Ago2), is essential for development and appears not to be involved in DNA methylation. Genomics 89:687–696.

Murrell A (2014) Cross-talk between imprinted loci in Prader-Willi syndrome. Nat Genet 46:528–530.

Nagano T, Fraser P (2009) Emerging similarities in epigenetic gene silencing by long noncoding RNAs. Mamm Genome 20:557–562.

Nakahashi H, Kwon K-RK, Resch W, Vian L, Dose M, Stavreva D, Hakim O, Pruett N, Nelson S, Yamane A, Qian J, Dubois W, Welsh S, Phair RD, Pugh BF, Lobanenkov V, Hager GL, Casellas R (2013) A genome-wide map of CTCF multivalency redefines the CTCF code. Cell Rep 3:1678–1689.

Nakamura T, Liu Y-J, Nakashima H, Umehara H, Inoue K, Matoba S, Tachibana M, Ogura A, Shinkai Y, Nakano T (2012) PGC7 binds histone H3K9me2 to protect against conversion of 5mC to 5hmC in early embryos. Nature 486:415–419.

Napetschnig J, Wu H (2013) Molecular basis of NF-κB signaling. Annu Rev Biophys 42:443–468.

Neitzel H, Neumann LM, Schindler D, Wirges A, Tönnies H, Trimborn M, Krebsova A, Richter R, Sperling K (2002) Premature chromosome condensation in humans

associated with microcephaly and mental retardation: a novel autosomal recessive condition. Am J Hum Genet 70:1015–1022.

Nestorov P, Tardat M, Peters AHFM (2013) H3K9/HP1 and Polycomb: two key epigenetic silencing pathways for gene regulation and embryo development. Curr Top Dev Biol 104:243–291.

Nicholls RD, Knepper JL (2001) Genome organization, function, and imprinting in Prader-Willi and Angelman syndromes. Annu Rev Genomics Hum Genet 2:153–175.

Nickols JC, Valentine W, Kanwal S, Carter BD (2003) Activation of the transcription factor NF-κB in Schwann cells is required for peripheral myelin formation. Nat Neurosci 6:161–167.

O'mahony F, Wroblewski K, O'byrne SM, Jiang H, Clerkin K, Benhammou J, Blaner WS, Beaven SW (2015) Liver X Receptors Balance Lipid Stores in Hepatic Stellate Cells via Rab18, a Retinoid Responsive Lipid Droplet Protein HHS Public Access. Hepatology 62:615–626.

Oganesian L, Graham ME, Robinson PJ, Bryan TM (2007) Telomerase recognizes G-quadruplex and linear DNA as distinct substrates. Biochemistry 46:11279–11290.

Ohlsson R, Renkawitz R, Lobanenkov V (2001) CTCF is a uniquely versatile transcription regulator linked to epigenetics and disease. Trends Genet 17:520–527.

Oliver-De La Cruz J, Carrión-Navarro J, García-Romeroí N, Gutiérrez-Martín A, Lázaro-Ibáñez E, Escobedo-Lucea C, Perona R, Belda-Iniesta C, Ayuso-Sacido A (2014) SOX2+ cell population from normal human brain white matter is able to generate mature oligodendrocytes. PLoS One 9:e99253.

Oosterveen T, Kurdija S, Ensterö M, Uhde CW, Bergsland M, Sandberg M, Sandberg R, Muhr J, Ericson J (2013) SoxB1-driven transcriptional network underlies neural-specific

interpretation of morphogen signals. Proc Natl Acad Sci U S A 110:7330–7335.

Palo OM, Antila M, Silander K, Hennah W, Kilpinen H, Soronen P, Tuulio-Henriksson A, Kieseppä T, Partonen T, Lönnqvist J, Peltonen L, Paunio T (2007) Association of distinct allelic haplotypes of DISC1 with psychotic and bipolar spectrum disorders and with underlying cognitive impairments. Hum Mol Genet 16:2517–2528.

Patrick GN, Bingol B, Weld HA, Schuman EM (2003) Ubiquitin-mediated proteasome activity is required for agonist-induced endocytosis of GluRs. Curr Biol 13:2073–2081.

Pearson CE, Zorbas H, Price GB, Zannis-Hadjopoulos M (1996) Inverted repeats, stem-loops, and cruciforms: significance for initiation of DNA replication. J Cell Biochem 63:1–22.

Percy AK (2002) Rett syndrome. Current status and new vistas. Neurol Clin 20:1125–1141.

Perez JD, Rubinstein ND, Fernandez DE, Santoro SW, Needleman L a, Ho-Shing O, Choi JJ, Zirlinger M, Chen S-K, Liu JS, Dulac C (2015) Quantitative and functional interrogation of parent-of-origin allelic expression biases in the brain. Elife 4:1–41.

Philippe O, Rio M, Carioux A, Plaza J-M, Guigue P, Molinari F, Boddaert N, Bole-Feysot C, Nitschke P, Smahi A, Munnich A, Colleaux L (2009) Combination of linkage mapping and microarray-expression analysis identifies NF-kappaB signaling defect as a cause of autosomal-recessive mental retardation. Am J Hum Genet 85:903–908.

Phillips JE, Corces VG (2009) CTCF: Master Weaver of the Genome. Cell 137:1194–1211.

Plachta N, Bibel M, Tucker KL, Barde Y-A (2004) Developmental potential of defined neural progenitors derived from mouse embryonic stem cells. Development 131:5449–5456.

Plasschaert RN, Bartolomei MS (2014) Genomic imprinting in development, growth, behavior and stem cells. Development 141:1805–1813.

Polo JM et al. (2012) A Molecular Roadmap of Reprogramming Somatic Cells into iPS Cells. Cell 151:1617–1632.

Presley JF, Cole NB, Schroer TA, Hirschberg K, Zaal KJ, Lippincott-Schwartz J (1997) ER-to-Golgi transport visualized in living cells. Nature 389:81–85.

Probst A V, Almouzni G (2011) Heterochromatin establishment in the context of genome-wide epigenetic reprogramming. Trends Genet 27:177–185.

Rada-Iglesias A, Bajpai R, Swigut T, Brugmann SA, Flynn RA, Wysocka J (2011) A unique chromatin signature uncovers early developmental enhancers in humans. Nature 470:279–283.

Reemst K, Noctor SC, Lucassen PJ, Hol EM (2016) The Indispensable Roles of Microglia and Astrocytes during Brain Development. Front Hum Neurosci 10:566.

Rett A (1966) On a unusual brain atrophy syndrome in hyperammonemia in childhood. Wien Med Wochenschr 116:723–726.

Rhinn M, Dollé P (2012) Retinoic acid signalling during development. Development 139:843–858.

Ribeiro FM, Camargos ER da S, Souza LC de, Teixeira AL, Ribeiro FM, Camargos ER da S, Souza LC de, Teixeira AL (2013) Animal models of neurodegenerative diseases. Rev Bras Psiquiatr 35:S82–S91.

Ricciardi S, Ungaro F, Hambrock M, Rademacher N, Stefanelli G, Brambilla D, Sessa A, Magagnotti C, Bachi A, Giarda E, Verpelli C, Kilstrup-Nielsen C, Sala C, Kalscheuer VM, Broccoli V (2012) CDKL5 ensures excitatory synapse stability by reinforcing NGL-1-PSD95 interaction in the postsynaptic compartment and is impaired in patient iPSC-derived neurons. Nat Cell Biol 14:911–923.

Robinett CC, Giansanti MG, Gatti M, Fuller MT (2009) TRAPPII is required for cleavage furrow ingression and localization of Rab11 in dividing male meiotic cells of Drosophila. J Cell Sci 122:4526–4534.

Rybak K, Steiner A, Synek L, Klaeger S, Kulich I, Facher E, Wanner G, Kuster B, Zarsky V, Persson S, Assaad FF (2014) Plant Cytokinesis Is Orchestrated by the Sequential Action of the TRAPPII and Exocyst Tethering Complexes. Dev Cell 29:607–620.

Sabol SZ, Hu S, Hamer D (1998) A functional polymorphism in the monoamine oxidase A gene promoter. Hum Genet 103:273–279.

Samochowiec J, Lesch KP, Rottmann M, Smolka M, Syagailo Y V, Okladnova O, Rommelspacher H, Winterer G, Schmidt LG, Sander T (1999) Association of a regulatory polymorphism in the promoter region of the monoamine oxidase A gene with antisocial alcoholism. Psychiatry Res 86:67–72.

Sanchez-Delgado M, Riccio A, Eggermann T, Maher ER, Lapunzina P, Mackay D, Monk D (2016) Causes and Consequences of Multi-Locus Imprinting Disturbances in Humans. Trends Genet 32:444–455.

Sarkar A, Hochedlinger K (2013) The sox family of transcription factors: versatile regulators of stem and progenitor cell fate. Cell Stem Cell 12:15–30.

Sarkies P, Reams C, Simpson LJ, Sale JE (2010) Epigenetic Instability due to Defective Replication of Structured DNA. Mol Cell 40:703–713.

Schaaf CP, Gonzalez-Garay ML, Xia F, Potocki L, Gripp KW, Zhang B, Peters BA, McElwain MA, Drmanac R, Beaudet AL, Caskey CT, Yang Y (2013) Truncating mutations of MAGEL2 cause Prader-Willi phenotypes and autism. Nat Genet 45:1405–1408.

Schepers GE, Teasdale RD, Koopman P (2002) Twenty pairs of sox: extent, homology, and nomenclature of the mouse and human sox transcription factor gene families. Dev Cell

3:167–170.

Schlötterer C (2004) The evolution of molecular markers--just a matter of fashion? Nat Rev Genet 5:63–69.

Schmidt D, Schwalie PC, Wilson MD, Ballester B, Gonçalves A, Kutter C, Brown GD, Marshall A, Flicek P, Odom DT (2012) Waves of retrotransposon expansion remodel genome organization and CTCF binding in multiple mammalian lineages. Cell 148:335–348.

Schuman EM, Madison D V (1994) Nitric oxide and synaptic function. Annu Rev Neurosci 17:153–183.

Seltzer LE, Paciorkowski AR (2014) Genetic disorders associated with postnatal microcephaly. Am J Med Genet Part C Semin Med Genet 166:140–155.

Sen R, Baltimore D (1986) Inducibility of kappa immunoglobulin enhancer-binding protein Nf-kappa B by a posttranslational mechanism. Cell 47:921–928.

Shekar PC, Naim A, Sarathi DP, Kumar S (2011) Argonaute-2-null embryonic stem cells are retarded in self-renewal and differentiation. J Biosci 36:649–657.

Shrum CK, Defrancisco D, Meffert MK (2009) Stimulated nuclear translocation of NF-kappaB and shuttling differentially depend on dynein and the dynactin complex. Proc Natl Acad Sci U S A 106:2647–2652.

Siddiqui-Jain A, Grand CL, Bearss DJ, Hurley LH (2002) Direct evidence for a G-quadruplex in a promoter region and its targeting with a small molecule to repress c-MYC transcription. Proc Natl Acad Sci U S A 99:11593–11598.

Simone R, Fratta P, Neidle S, Parkinson GN, Isaacs AM (2015) G-quadruplexes: Emerging roles in neurodegenerative diseases and the non-coding transcriptome. FEBS Lett 589:1653–1668.

Simpson CS, Morris BJ (2000) Regulation of neuronal cell adhesion molecule expression by NF-kappa B. J Biol Chem 275:16879–16884.

Singhmar P, Kumar A (2011) Angelman syndrome protein UBE3A interacts with primary microcephaly protein ASPM, localizes to centrosomes and regulates chromosome segregation. PLoS One 6:e20397.

Smith RJ, Dean W, Konfortova G, Kelsey G (2003) Identification of novel imprinted genes in a genome-wide screen for maternal methylation. Genome Res 13:558–569.

Smits G, Mungall AJ, Griffiths-Jones S, Smith P, Beury D, Matthews L, Rogers J, Pask AJ, Shaw G, VandeBerg JL, McCarrey JR, SAVOIR Consortium MB, Renfree MB, Reik W, Dunham I (2008) Conservation of the H19 noncoding RNA and H19-IGF2 imprinting mechanism in therians. Nat Genet 40:971–976.

Spalding KL, Bhardwaj RD, Buchholz BA, Druid H, Frisén J (2005) Retrospective Birth Dating of Cells in Humans. Cell 122:133–143.

Spicuglia S, Vanhille L (2012) Chromatin signatures of active enhancers. Nucleus 3:126–131.

Stiess M, Bradke F (2011) Neuronal polarization: the cytoskeleton leads the way. Dev Neurobiol 71:430–444.

Sun D, Hurley LH (2009) The importance of negative superhelicity in inducing the formation of G-quadruplex and i-motif structures in the c-Myc promoter: implications for drug targeting and control of gene expression. J Med Chem 52:2863–2874.

Surani MA, Barton SC, Norris ML (1984) Development of reconstituted mouse eggs suggests imprinting of the genome during gametogenesis. Nature 308:548–550.

Sutcliffe JS, Nakao M, Christian S, Orstavik KH, Tommerup N, Ledbetter DH, Beaudet AL

(1994) Deletions of a differentially methylated CpG island at the SNRPN gene define a putative imprinting control region. Nat Genet 8:52–58.

Sütterlin C, Colanzi A (2010) The Golgi and the centrosome: building a functional partnership. J Cell Biol 188:621–628.

Suzuki S, Shaw G, Kaneko-Ishino T, Ishino F, Renfree MB (2011) The evolution of mammalian genomic imprinting was accompanied by the acquisition of novel CpG islands. Genome Biol Evol 3:1276–1283.

Takai D, Jones PA (2002) Comprehensive analysis of CpG islands in human chromosomes 21 and 22. Proc Natl Acad Sci U S A 99:3740–3745.

Tanaka S, Kamachi Y, Tanouchi A, Hamada H, Jing N, Kondoh H (2004) Interplay of SOX and POU factors in regulation of the Nestin gene in neural primordial cells. Mol Cell Biol 24:8834–8846.

Tang Z et al. (2015) CTCF-Mediated Human 3D Genome Architecture Reveals Chromatin Topology for Transcription. Cell 163:1611–1627.

Thornton GK, Woods CG (2009) Primary microcephaly: do all roads lead to Rome? Trends Genet 25:501–510.

Tischfield MA, Cederquist GY, Gupta ML, Engle EC (2011) Phenotypic spectrum of the tubulin-related disorders and functional implications of disease-causing mutations. Curr Opin Genet Dev 21:286–294.

Toubi E, Shoenfeld Y (2004) Toll-like receptors and their role in the development of autoimmune diseases. Autoimmunity 37:183–188.

Trimborn M, Bell SM, Felix C, Rashid Y, Jafri H, Griffiths PD, Neumann LM, Krebs A, Reis A, Sperling K, Neitzel H, Jackson AP (2004) Mutations in microcephalin cause aberrant

regulation of chromosome condensation. Am J Hum Genet 75:261–266.

van Holde K, Zlatanova J (1994) Unusual DNA structures, chromatin and transcription. BioEssays 16:59–68.

Veale EL, Hassan M, Walsh Y, Al-Moubarak E, Mathie A (2014) Recovery of current through mutated TASK3 potassium channels underlying Birk Barel syndrome. Mol Pharmacol 85:397–407.

Vermeulen M, Mulder KW, Denissov S, Pijnappel WWMP, van Schaik FMA, Varier RA, Baltissen MPA, Stunnenberg HG, Mann M, Timmers HTM (2007) Selective anchoring of TFIID to nucleosomes by trimethylation of histone H3 lysine 4. Cell 131:58–69.

Villarroel-Campos D, Gastaldi L, Conde C, Caceres A, Gonzalez-Billault C (2014) Rab-mediated trafficking role in neurite formation. J Neurochem 129:240–248.

Waddington CH (2014) Epigenetics of birds. (Press CU, ed). Cambridge Univ Press.

Wang W, Ferro-Novick S (2002) A Ypt32p Exchange Factor Is a Putative Effector of Ypt1p. Mol Biol Cell 13:3336–3343.

Wang X, Sun Q, McGrath SD, Mardis ER, Soloway PD, Clark AG (2008) Transcriptome-wide identification of novel imprinted genes in neonatal mouse brain. PLoS One 3:e3839.

Weaving LS, Christodoulou J, Williamson SL, Friend KL, McKenzie OLD, Archer H, Evans J, Clarke A, Pelka GJ, Tam PPL, Watson C, Lahooti H, Ellaway CJ, Bennetts B, Leonard H, Gécz J (2004) Mutations of CDKL5 cause a severe neurodevelopmental disorder with infantile spasms and mental retardation. Am J Hum Genet 75:1079–1093.

Wellmann H, Kaltschmidt B, Kaltschmidt C (2001) Retrograde transport of transcription factor NF-kappa B in living neurons. J Biol Chem 276:11821–11829.

Welte MA (2015) Expanding Roles for Lipid Droplets. Curr Biol 25:R470–R481.

Westlake CJ, Baye LM, Nachury M V, Wright KJ, Ervin KE, Phu L, Chalouni C, Beck JS, Kirkpatrick DS, Slusarski DC, Sheffield VC, Scheller RH, Jackson PK (2011) Primary cilia membrane assembly is initiated by Rab11 and transport protein particle II (TRAPPII) complex-dependent trafficking of Rabin8 to the centrosome. Proc Natl Acad Sci U S A 108:2759–2764.

Wilkinson LS, Davies W, Isles AR (2007) Genomic imprinting effects on brain development and function. Nat Rev Neurosci 8:832–843.

Wilson M, Koopman P (2002) Matching SOX: partner proteins and co-factors of the SOX family of transcriptional regulators. Curr Opin Genet Dev 12:441–446.

Woodcock CL, Skoultchi AI, Fan Y (2006) Role of linker histone in chromatin structure and function: H1 stoichiometry and nucleosome repeat length. Chromosome Res 14:17–25.

Woods CG, Parker A (2013) Investigating microcephaly. Arch Dis Child 98:707–713.

Wu Q, Wang X (2012) Neuronal stem cells in the central nervous system and in human diseases. Protein Cell 3:262–270.

Wu Y-H, Fischer DF, Swaab DF (2007) A promoter polymorphism in the monoamine oxidase A gene is associated with the pineal MAOA activity in Alzheimer's disease patients. Brain Res 1167:13–19.

Xie Z, Moy LY, Sanada K, Zhou Y, Buchman JJ, Tsai L-H (2007) Cep120 and TACCs control interkinetic nuclear migration and the neural progenitor pool. Neuron 56:79–93.

Xu Y, Goodyer CG, Deal C, Polychronakos C (1993) Functional polymorphism in the parental imprinting of the human IGF2R gene. Biochem Biophys Res Commun 197:747–754.

Yamamoto S et al. (2014) A Drosophila Genetic Resource of Mutants to Study Mechanisms Underlying Human Genetic Diseases. Cell 159:200–214.

Yamasaki A, Menon S, Yu S, Barrowman J, Meerloo T, Oorschot V, Klumperman J, Satoh A, Ferro-novick S (2009) mTrs130 Is a Component of a Mammalian TRAPPII Complex , a Rab1 GEF That Binds to COPI-coated Vesicles. Mol Biol Cell 20:4205–4215.

Yazdi PG, Pedersen BA, Taylor JF, Khattab OS, Chen YH, Chen Y, Jacobsen SE, Wang PH, Imhof A (2015) Nucleosome organization in human embryonic stem cells. PLoS One 10.

Yin Q-F, Yang L, Zhang Y, Xiang J-F, Wu Y-W, Carmichael GG, Chen L-L (2012) Long Noncoding RNAs with snoRNA Ends. Mol Cell 48:219–230.

Young D, Nagarajan L, de Klerk N, Jacoby P, Ellaway C, Leonard H (2007) Sleep problems in Rett syndrome. Brain Dev 29:609–616.

Zahler AM, Williamson JR, Cech TR, Prescott DM (1991) Inhibition of telomerase by G-quartet DMA structures. Nature 350:718–720.

Zahoor MA, Yamane D, Mohamed YM, Suda Y, Kobayashi K, Kato K, Tohya Y, Akashi H (2010) Bovine viral diarrhea virus non-structural protein 5A interacts with NIK- and IKKbeta-binding protein. J Gen Virol 91:1939–1948.

Zhai L, Joo H-Y, Wang H (2009) In vitro and in vivo assays for studying histone ubiquitination and deubiquitination. Methods Mol Biol 523:295–309.

Zhang W, Peterson M, Beyer B, Frankel WN, Zhang Z (2014a) Loss of MeCP2 from forebrain excitatory neurons leads to cortical hyperexcitation and seizures. J Neurosci 34:2754–2763.

Zhang Y, Bitner D, Pontes Filho AA, Li F, Liu S, Wang H, Yang F, Adhikari S, Gordon J,

Srinivasan S, Hu W (2014b) Expression and function of NIK- and IKK2-binding protein (NIBP) in mouse enteric nervous system. Neurogastroenterol Motil 26:77–97.

Zhang Y, Liu S, Wang H, Yang W, Li F, Yang F, Yu D, Ramsey F V, Tuszyski GP, Hu W (2015a) Elevated NIBP/TRAPPC9 mediates tumorigenesis of cancer cells through NFκB signaling. Oncotarget 6:6160–6178.

Zhang YG, Yang F, Jones A, Li F, Hu WH (2015b) Conditional NIBP/TRAPPC9 knockout induced defects in adult neurogenesis. In: International Journal of Developmental Neuroscience, pp 113.

Zhao S-L, Hong J, Xie Z-Q, Tang J-T, Su W-Y, Du W, Chen Y-X, Lu R, Sun D-F, Fang J-Y (2011) TRAPPC4-ERK2 interaction activates ERK1/2, modulates its nuclear localization and regulates proliferation and apoptosis of colorectal cancer cells. Blagosklonny M V., ed. PLoS One 6:e23262.

Zhu Y-C, Li D, Wang L, Lu B, Zheng J, Zhao S-L, Zeng R, Xiong Z-Q (2013) Palmitoylation-dependent CDKL5-PSD-95 interaction regulates synaptic targeting of CDKL5 and dendritic spine development. Proc Natl Acad Sci U S A 110:9118–9123.

Ziebarth JD, Bhattacharya A, Cui Y (2013) CTCFBSDB 2.0: A database for CTCF-binding sites and genome organization. Nucleic Acids Res 41.

Zoghbi HY, Amir RE, Van den Veyver IB, Wan M, Tran CQ, Francke U (1999) Rett syndrome is caused by mutations in X-linked MECP2, encoding methyl-CpG-binding protein 2. Nat Genet 23:185–188.

Zong M, Satoh A, Yu MK, Siu KY, Ng WY, Chan HC, Tanner J a, Yu S (2012) TRAPPC9 mediates the interaction between p150 and COPII vesicles at the target membrane. PLoS One 7:e29995.

Zong M, Wu X, Chan CWL, Choi MY, Chan HC, Tanner J a, Yu S (2011) The adaptor function

of TRAPPC2 in mammalian TRAPPs explains TRAPPC2-associated SEDT and TRAPPC9-associated congenital intellectual disability. PLoS One 6:e23350.

Zwart R, Sleutels F, Wutz A, Schinkel AH, Barlow DP (2001) Bidirectional action of the Igf2r imprint control element on upstream and downstream imprinted genes. Genes Dev 15:2361–2366.

Acknowledgements

This is officially the third thesis I write. You would assume I knew how to do it by now but if there is something I can't put up with is the use of the pronoun 'I'. Although I have personally done the work presented in this thesis, I firmly believe there is no 'I' in science and every small result is achieved by team work. I have many people to thank, without whom this thesis would not be as it is now, and without whom I probably would not be here today.

The first THANK YOU goes to my supervisor Toni, who patiently taught me what it means to be a good scientist in the past four years and that guided me in every small step along the way. Despite my many questions and mistakes, his door has always been open to me. Thank you, really.

A great thanks goes also to our great collaborators, Dr Lakis Liloglou for the help in designing (and running) the pyrosequencing assays and to Dr Philippe Arnaud for kindly providing us with RNA samples for the imprinting analysis.

A special thanks goes to Prof John Quinn, not only for kindly providing human gDNA samples and for the use of the QIAxcel, but also for enduring me in those 10 weeks 5 years ago and during every lab meal and gathering since then. I am honoured I had the chance to work with you.

Next in line are the amazing people I had the chance to work with to produce the data presented in this thesis. Jade Sallis, the best undergraduate student I've ever worked with, helped me with the work on PC12 cells. Usman Anjum and David Hay helped me with N2A cells and brightened my days and Lucia Livoti, who continued with the *in situ* hybridisation after I left, has proven to be one of the best additions to the team. Thomas Leather and

Kirsty Ingram not only helped me with many things in the lab (too many to count) while they were MRes students, but they also became some of my best friends outside that grey building that is our department. Thank you!!!!

Not directly work related, but surely one of the reasons I survived the stress of the PhD, are the great friendships that developed in that office nobody wanted to move in to. Ilaria, for being a touch of home in a foreign country and a point of reference in science and in life, thank you. Sumaya, for always being there when I need you and for sharing beautiful embarrassing moments with me that neither of us necessarily wanted to make public, but that somehow ended up on Facebook anyway, thank you. Kelly, for making me laugh even when I was crying and for teaching me that if you don't stand up for yourself nobody will, thank you. Lauren, for being my favourite crazy cat lady and for being an example to follow, thank you. And the latest addition to the team, Sumita, for being an amazing and selfless person with the biggest heart, thank you.

A great thank you also goes to the other amazing members in the lab: Bettina, Thomas (Wilm), Trish, Chris, Jing, Isabel and all the MRes students past and present, it has been a pleasure getting to know you and thank you for the support, advice and the great chats.

I also need to thank Graeme Sills, for replying to that email one day a long time ago, accepting to supervise an international student who knew very little molecular biology and not much more English. I wouldn't be here today if it weren't for you.

At last the most important people of all. My parents, for always loving me and for providing me with the education they couldn't have. You taught me what the important things in life are and I am who I am today thanks to you. I love you!

And of course, Maurizio, who left everything behind without hesitation, including a PhD, to follow me to a country with very little sunshine, where he couldn't speak and where he

didn't have anyone but me. This has been the greatest adventure so far for the both us, and it goes without saying that without you I couldn't have done it. I love you.